



Universität für Bodenkultur Wien
University of Natural Resources
and Life Sciences, Vienna

Doctoral Dissertation

On the Discovery and Development of novel Enzymes

submitted by

DI Peter L. HERZOG

in partial fulfilment of the requirements for the academic degree

Doktor der Bodenkultur (Dr.nat.techn.)

Vienna, October 2021

Supervisor:

Univ. Prof. Dr. Clemens Peterbauer

Institute of Food Technology

Department of Food Science and Technology

Ich erkläre eidesstattlich, dass ich die Arbeit selbständig angefertigt, keine anderen als die angegebenen Hilfsmittel benutzt und alle aus ungedruckten Quellen, gedruckter Literatur oder aus dem Internet im Wortlaut oder im wesentlichen Inhalt übernommenen Formulierungen und Konzepte gemäß den Richtlinien wissenschaftlicher Arbeiten zitiert, durch Fußnoten gekennzeichnet bzw. mit genauer Quellenangabe kenntlich gemacht habe.

Peter Herzog

From my perspective, the English translation of “curiosity” does not do the meaning of “Neugier” full justice. It seemingly omits the sense of ravenousness that is incorporated into the German word, emphasizing the eagerness and ambition to discover something new or experiencing something unexpected. As researchers we are curious and thrive at pursuing the unexplored and novel. Yet with time we grow into appreciating the foreseen and resent the unexpected.

This work I dedicate to my 1-year-old son Jakob, who is a personification of natural “Neugier” and whose joyfulness for all that’s new and different is a heartwarming inspiration.

Table of Contents

Table of Contents.....	7
Acknowledgements	9
Abstract	I
Kurzfassung.....	III
Aims and outline	1
Aims	1
Outline	1
Chapter 1 – An Introduction into Enzymes	3
A) Enzymes - the biological catalysts:.....	3
B) Lignocellulose: its constituents and enzymatic degradation	14
C) The AA3 family of oxidoreductases.....	22
D) References (I).....	41
Chapter 2 – Discovering new enzymes	58
Chapter 3 – Introduction II.....	91
A) Enzyme engineering.....	91
B) Directed Evolution	93
C) Screening	103
D) References	124
Chapter 4 – Developing new Enzymes.....	134
Chapter 5 – Conclusion and Outlook	155
Appendix.....	159
Figure Index	159
List of publications.....	160
Curriculum vitae	161

Acknowledgements

Before expressing my sincere gratitude for the support, assistance and guidance that were offered to me during my PhD, I feel urged to emphasize that this work is the product of a vast number of encouraging interactions and that many more contributed to its successful outcome than I can acknowledge here.

First and foremost, I would like to acknowledge the financial support from universities and scientific funding agencies that I was lucky to receive. In particular, I want to express my gratitude for financing from the Austrian Science Fund (FWF) and BOKU University via the BioToP doctoral program (FWF: W1224) and for BOKU University especially, for receiving a research scholarship.

I wish to express my deepest gratitude to my supervisor **Prof. Clemens K. Peterbauer** for his guidance, unwavering support, the constructive discussions and for always being a pillar of positivity during the difficult parts of the project. I also want to express my heartfelt gratitude for his encouragement to pursue a scientific career outside academia and his patience that was needed as a consequence of it. I want to extend my thanks to my co-supervisor **Prof. Christian Obinger**, for his invaluable advice, support and for arranging scientific assistance on several occasions.

Similarly, I want to acknowledge **Prof. Dietmar Haltrich, Prof. Roland Ludwig, Dr. Thu Ha Nguyen and Prof. Clemens Peterbauer** for establishing and nourishing the supportive and encouraging environment that is our food biotechnology laboratory. I would also like to pay my special regards to my many lab mates: **Leander Sützl, Erik Breslmayr, Georg Schütz, Stefan Scheiblbrandner, Daniel Kracher, Marita Preims, Christian Leitner, Christophe Laurent, Florian Csarman** and **Lena Wohlschlager** whose assistance was a milestone in the completion of my projects. Also, I am indebted to my former master students **Beate Eisenhut, Enrico Borghi** and **Doris Abraham**. I would like to recognize the contribution that your ideas and thorough work had on the success of our projects. Special thanks to the BOKU core facility BmCA and its caring team, who were instrumental for assisting the technical aspects of my project.

My sincere appreciation is extended to the people that I met during my research collaborations abroad. Special thanks to **Prof. Ulrich Schwaneberg** for welcoming me in his lab, for his guidance and invaluable input during my research stay at the RWTH Aachen. Similarly, I want to acknowledge **Khalil Essani** and **Volkan Besirlioglu**, without your persistent help the screening project would have been a distant reality. I want to offer my special thanks to **Prof. Hadley Sikes** from the MIT, for giving me the opportunity to continue my research at her lab and for her insightful input, ingenious suggestions, and unrelenting support during the organization of my research stay in the US. I also had great pleasure working with **Eric Miller, Ki-Joo Sung, Emma Yee, Seunghyeon Kim, Yining Hao** and **Sun Jin Moon**, thank you for the wonderful time in- and outside the lab.

Last but not least I wish to acknowledge the deep love and support from my family and friends. To my friends **Sebastian, Rupi, Max, Lisa, Georg, Patrik, Alex, Laurenz, Stefan** and **Matthias**; to Martina's family, **Christl, Michi, Georg, Lisi, Valentin, Vinzent** and **Leopold** for their support and for being there for me. I want to thank my family: **Fritz, Roswitha** and **Martin**. Thanks for your unconditional love and comfort, for shaping me to becoming the happy person I am today, enjoying every little detail of my life and work.

Finally, I want to thank **Martina** and **Jakob**, my lovely wife and son. **Martina**, thank you for being my best friend and companion, my love, for helping me, understanding me, distracting me, helping me, cheering me up and being my supporter, and fan. Thank you two for brightening my world!

Abstract

Enzymes are the molecular machines orchestrating the chemical processes that define life. Following the powerful algorithm of evolution, nature generated a multihued palette of these catalysts performing an astonishing diversity of reactions. Their outstanding specificity, efficiency, and ability to catalyze reactions at moderate conditions encourages their adoption for technological processes.

As the interest in novel enzymes is surging, the development of tailored catalysts via engineering and discovery of adapted enzymes from natural sources both present viable options to meet this demand. In the case of oxidoreductases of the GMC family, tremendous effort was hitherto invested in the identification of suitable enzyme variants but predominantly relied on manual methodology. With the accelerated development of bioinformatic tools, screening platforms and DNA sequencing/synthesis in modern times, enormous opportunities arise for this family of enzymes that have not been addressed yet.

In this work, two enzymes of the GMC family, pyranose 2-oxidase (POx) and cellobiose dehydrogenase (CDH) were tackled in that regard. For POx, a straightforward bioinformatic approach involving a comprehensive database search and phylogenetic analysis allowed to discover a new bacterial POx from *Kitasatospora aureofaciens* and for the first time elucidated a gene transfer of POx between bacteria and fungi. This POx could be produced and characterized in great detail, which uncovered a synergistic effect with peroxidases and promising properties for applying this enzyme in synthetic lignin revalorization. The well-established fungal CDH from *Crassicarpon hotsonii* was utilized to develop novel high-throughput screening technology based on yeast surface display and the fluorescent H₂O₂ reporter protein roGFP2-Orp1. This screen could successfully resolve the small differences in peroxide formation of certain CDH variants and could be implemented in flow cytometry analysis, using cell numbers of around 10⁶. This technology is regarded as especially suited for directed evolution campaigns of industrially relevant oxidases.

With this novel technology for the high-throughput screening of oxidoreductases could be established that can aid to develop advanced biocatalysts via engineering. Additionally, it could be demonstrated how bioinformatic sequence analysis can help to discover new enzymes and resolve their origins.

Kurzfassung

Enzyme sind die molekularen Maschinen, welche die chemischen Prozesse des Lebens steuern. Basierend auf dem mächtigen Algorithmus der Evolution, hat die Natur eine bunte Palette dieser Katalysatoren hervorgebracht, die eine erstaunliche Vielfalt an Reaktionen ausführen. Ihre herausragende Spezifität, Effizienz und Fähigkeit, Reaktionen unter gemäßigten Bedingungen zu katalysieren, empfiehlt sie auch für die Anwendung in technologischen Prozessen.

Dem stets steigenden Bedarf an neuen Enzymen stehen die Entwicklung maßgeschneiderter Enzyme durch Engineering und die Entdeckung angepasster Enzyme aus natürlichen Quellen gegenüber. Im Falle der Oxidoreduktasen der GMC-Familie wurde bisher großer Aufwand in die Identifizierung verbesserter Enzymvarianten investiert, wobei man sich überwiegend auf manuelle Methodik stützte. Mit der rasanten Entwicklung von bioinformatischen Werkzeugen, Screening-Plattformen und beschleunigt durch moderne DNA-Sequenzierung und -synthese ergeben sich hier enorme Möglichkeiten, die bisher nicht genutzt wurden.

Diese Arbeit befasste sich dahingehend mit zwei Enzymen der GMC-Familie: Pyranose 2-Oxidase (POx) und Cellobiose-Dehydrogenase (CDH). Für POx konnte durch einen einfachen bioinformatischen Ansatz, bestehend aus einer umfassenden Datenbanksuche und phylogenetischer Analyse, eine neue bakterielle POx aus *Kitasatospora aureofaciens* entdeckt und erstmals ein Gentransfer von POx zwischen Bakterien und Pilzen aufgeklärt werden. Dieses POx wurde produziert und ausführlich charakterisiert, was einen synergistischen Effekt mit Peroxidasen und vielversprechende Eigenschaften für die Anwendung dieses Enzyms in der synthetischen Lignin Verwertung aufdeckte. Die etablierte CDH des Pilzes *Crassicarpon hotsonii* wurde genutzt, um neue Hochdurchsatz-Screening Technologie zu entwickeln, die auf Hefe-Oberflächendisplay und dem fluoreszierenden H₂O₂-Reporterprotein roGFP2-Orp1 basiert. Das so entwickelte Screening konnte erfolgreich verwendet werden, um die geringen Unterschiede in der Peroxidbildung bestimmter CDH-Varianten aufzulösen und konnte in der Durchflusszytometrie mit Zellzahlen von etwa 10⁶ umgesetzt werden. Diese Technologie wird als besonders geeignet für Directed Evolution Kampagnen von industriell relevanten Oxidasen angesehen.

Mit diesen Entwicklungen konnte eine neuartige Technologie für das Hochdurchsatz-Screening von Oxidoreduktasen etabliert werden, die helfen kann, maßgeschneiderte Enzyme durch Engineering zu entwickeln. Zusätzlich konnte gezeigt werden, wie die bioinformatische Sequenzanalyse helfen kann, neue Enzyme zu entdecken und deren Herkunft aufzuklären.

Aims and Outline

Aims

This work aimed at developing a novel high-throughput screening platform that enables single cell analysis and can be adopted for various H₂O₂ generating and consuming oxidoreductases. It was devised to utilize roGFP2-Orp1 as a reporter protein, translating the enzymatic H₂O₂ formation into a quantifiable fluorescent signal. This use of this fusion protein is regarded as superior to diffusible detection systems since - as a protein - it allows to be tethered to the cell surface which likely renders compartmentalization, a usually critical step, obsolete.

Pyranose 2-oxidase (Pox) was intended as a role model for the development of this screening, but established fungal representatives failed to express in the yeast cell surface format, likely due to their tetrameric occurrence. Instead of changing the expression format, we envisioned to identify a new POx from previously discovered bacterial representatives which reportedly disobey the tetrameric form. We thus focused on identifying a suitable bacterial POx candidate for display expression and carried out a comprehensive phylogenetic analysis of available sequences, inadvertently discovering a new clade of bacterial POx and elucidating the origins of this enzyme in a gene transfer between bacteria and fungi, *in silico*. Ensuing successful expression and characterization of a new POx from *K. aureofaciens*, we set out to unravel the biochemical function of this enzyme during lignin degradation and identified an intricate synergism with peroxidases.

In continuation of the screening project, cellobiose dehydrogenase (CDH) replaced POx as a surrogate since it could be efficiently expressed on the surface of the yeast cells. Our efforts then focused on realizing a system for the cell attachment of the roGFP2-Orp1 sensor and implementation into the flow cytometry platform. We later aimed at alleviating the roGFP2-Orp1 side reactivity with oxygen and establishing the screening system with different variants of CDH, showing differently pronounced oxidase character.

Outline

This thesis is separated into multiple chapters that guide through the topics of enzyme discovery and enzyme development.

In **Chapter 1 – Introducing Enzymes** an introduction into the topic is provided and guides through the various fundamental aspects of enzymes in a holistic view. This chapter is dedicated to discussing the role of cofactors in enzymatic catalysis, interaction between enzyme and substrate and enzyme

classification. Subsequently, the focus lies on lignocellulose and its degradation and how enzymes contribute to the microbial attack of this biopolymer. This part of the thesis then discusses the topic of oxidoreductases and introduces two members of the AA3 family, namely pyranose 2-oxidase and cellobiose dehydrogenase that were in the center of attention for the experiments and analyses of this work.

Ensuing to the introduction to the relevant background, **Chapter 2 – Discovering new Enzymes** resolves the phylogenetic whereabouts of the pyranose 2-oxidase enzyme and unravels the relations of fungal and bacterial representatives of this enzyme. Additionally, the successful expression and characterization of new pyranose 2-oxidase from the actinobacterium *Kitasatospora aureofaciens* is highlighted and the elucidation of a synergistic action when working in conjunction with manganese peroxidase could be unraveled. Following from that, a potential involvement in the enzymatic ligninolytic machinery and importance of the enzyme for bacterial litter degraders was debated.

Enzyme engineering, activity screening platforms and directed evolution were the subjects lined out in **Chapter 3 – Introducing Enzyme Engineering**. There, an introduction into the various aspects of enzyme engineering is provided in the beginning and discusses rational design approach and directed evolution in the subsequent section. Next, various screening methodologies are introduced, and recent advances described before providing a short outlook into future directions of screening technology for oxidoreductases.

Chapter 4 – Developing new Enzymes deals with the establishment of a screening system for oxidase activity employing a peroxide sensitive GFP variant as a fluorescent H₂O₂ reporter. In the beginning it is demonstrated how this roGFP2-Orp1 can be used to translate oxidase activity into fluorescent signals in solution. With the subsequent expression of cellobiose dehydrogenase variants in the yeast surface display format and tethering of roGFP2-Orp1 to yeast cell walls, utilizing a newly developed immobilization technique, a single cell screening could be designed and successfully employed in a proof-of-concept experiment.

In the last part of this thesis, **Chapter 5 – Conclusion and Outlook** the key results and most important findings from the mentioned studies are summarized and the relevance of this work is discussed. A perspective of future possibilities in the fields of discovering and engineering is also addressed and the importance of novel technology to guide its advancement is underlined.

Chapter 1 – Introducing Enzymes

A) Enzymes - the biological catalysts:

Enzymes constitute the many-splendored palette of fundamental processes that create and maintain life. They are the macromolecular catalysts that drive the great multitude of biochemical reactions and capacitate all organisms with the ability to grow, adapt, reproduce, organize, transform energy and interact with their environment (Koshland 2002). Their importance in life is also reflected in the human genome, where according to recent estimations an approximate quarter of human genes encode enzymes and upwards of 50 % of human genes contribute to one or more enzymatic reactions (Berg et al. 2015).

Nature apparently provides a sheer limitless reservoir of these biological catalysts and their diverse functionalities have promoted an equally diverse technological exploitation. Enabled by the rise of recombinant DNA technology, the utilization of enzymes from microbial sources has advanced as a common strategy to improve conventional processes in all fields of the (bio)chemical industry (Illanes 2008; Choi, Han, and Kim 2015; Rajendra Singh et al. 2016). Enzymatic reactions supporting technical processes have a long history in the food and beverage industry (Raveendran et al. 2018) and are well-established in the textile and paper industry (Maciel, Castro e Silva, and Ribeiro 2010). Tremendous effort has been invested recently in developing enzyme technology to assist the synthesis of fine chemicals and pharmaceutical compounds (Bornscheuer et al. 2012) and to include enzymatic catalysis in the valorization of lignocellulosic biomass (Himmel et al. 2007; Chundawat et al. 2011; Sheldon 2016). Success in these areas has also spurred the advancement of novel bioelectrochemical applications of enzymes in for example biofuel cells and diagnostic biosensors (Gonzalez-Solino and Di Lorenzo 2018; Rocchitta et al. 2016). Enzymatic catalysis additionally delivers an essential advantage in these industries as it boosts established processes by increasing yields and productivity whilst reducing waste and energy demands, as reviews highlighted a decade ago (Savile et al. 2010; Woodley 2008). Thus, enzyme technology should be understood as indispensable on the path towards greener chemistry and environmentally

compatible processes - a common aspect for future perspectives in these industries (Aldridge 2013).

A nice summary on the fundamentals and principles of enzymatic reactions in the biochemical context was compiled into the textbook “*Biochemistry*” by Berg JM, Tymoczko JL, Gatto GJ Jr. and Stryer L (Berg et al. 2015). Some of the most important paragraphs of its Part I, Chapter 8 were distilled into this introduction to provide a brief glance on the thermodynamic mechanistic of enzyme-catalyzed reactions and explain their mode of action.

1. The thermodynamic equilibrium

The exceptionality of enzyme catalyzed reactions is sourced in two key features of the biological catalysts: **specificity** and **catalytic power**.

Enzymatic reactions, as are all chemical reactions, are governed by a thermodynamic equilibrium of their reactants or “educts” (A, B) and products (C, D).



Dependent on the position of a specific equilibrium, on the present concentration of educts and products and external input of energy, forward and reverse reactions will proceed at different speeds until the equilibrium is reached. Once established, the forward and reverse reaction do not cease but rather progress at identical rates leading to an apparent stop of the reaction as there is no further net change of reactants. In order to delineate this equilibrium, an equilibrium constant K_{eq} is defined by the molar concentrations of educts and products.

$$K_{eq} = \frac{[C][D]}{[A][B]} \quad \{2\}$$

$$\Delta G = \Delta G^{\circ} + RT \ln \frac{[C][D]}{[A][B]} \quad \{3\}$$

Directly related to K_{eq} is the standard free energy change (ΔG), which characterizes the energy difference between educts and products. ΔG is derived from the standard free-energy change ΔG°

(reflecting ΔG at standard conditions, specific for the nature of the reaction) and additionally accounts for the temperature (T), the gas constant (R) and the concentration of reactants participating in the reaction. In a nutshell, a reaction is likely to occur if the free energy of products C, D in the final state is lower than the free energy of educts A, B and hence free energy conversion can proceed downhill. That means, provided that the ΔG for a reaction

- is negative, the reaction can take place spontaneously
- is zero, the reaction is in an equilibrium state
- is positive, the reaction cannot take place spontaneously but can be initiated if free energy is added on the educts side of the thermodynamic equilibrium.

Reactions that are catalyzed by enzymes are also governed by these thermodynamic fundamentals and obey the dictate of ΔG : the involvement of enzymes in (bio)chemical reactions leaves the position of the equilibrium unaltered. The fundamental ability of enzymes instead lies in lowering the energy of activation which tremendously accelerates reaching this particular equilibrium and hence increases the reaction rate of the conversion of educts to products. It is quite common that the degree of acceleration between the non-enzymatic reaction *versus* the enzyme-catalyzed reaction can differ by factors of 10^6 and higher. A good display of the catalytic power of enzymatic reactions can be deduced from the well-studied example of carbonic anhydrase, one of most efficient enzymes characterized. Carbon anhydrase, harboring a zinc prosthetic group, catalyzes the reversible formation of carbonic acid H_2CO_3 from CO_2 and H_2O at rates of $10^6 s^{-1}$, a reaction that would otherwise progress slowly at rates of $5 sec^{-1}$ when uncatalyzed (Lindskog 1997).

2. Interaction of substrate and the enzyme's active site

Enzymes were designed by nature to specialize in the interaction with their preferred substrates. Binding to the substrate is the root cause for lowering ΔG^\ddagger as the complex of substrate and enzyme can react via a catalyzed reaction pathway that is characterized by a lower energy transition state (X^\ddagger). Enzymes are capable of lowering this energetic barrier due to the association of the enzyme's active site residues with the substrate: external forces are imposed onto the substrate which results in certain configurational constraints in its movement, brings substrate and co-substrate into close vicinity or modifies local electron densities. This can then lead to the formation and

disruption of bonds, the transfer of hydrides or the abstraction of protons and electrons (Berg et al. 2015; Wongnate et al. 2019). Generally said, the enzyme's active site allows to hold the substrate in a configuration of higher energy (that is more prone to reaction) for an extended period of time, a state that would otherwise be short-lived in uncatalyzed reactions.

Hence, the compatible three-dimensional structure of the active site is what realized substrate specificity in a first step and concomitantly drives catalytic efficiently.

3. Cofactors

To even further multiply the possibilities to interact with their preferred substrates, enzymes have adopted the chemical diversity of cofactors. Protein chemists differentiate between cofactors, often synonymously referred to as “prosthetic groups” (remain associated with the enzyme, often metal ions or flavins) and co-substrates (are bound and released). Both components allow expanding possibilities for interaction with the substrate beyond the native set of 20 amino acids and often endow the enzyme with specific catalytic features that expand the catalytic repertoire and enhance the catalytic power of the enzyme.

In the case of a diverse group of enzymes, the catalysts employ the chemical power of flavins to mediate electron transfer reactions. Flavin mononucleotide (FMN) and flavin adenine dinucleotide (FAD) are chemical derivatives of riboflavin vitamin B2. In the majority of enzymes known to harbor flavonoid cofactors, the FAD or FMN molecule is inserted into the enzyme active site by electrostatic and hydrophobic interaction with certain amino acid sidechains only, more seldomly the cofactor is covalently attached to a His, Cys or Tyr residue of the protein backbone which was suggested to have positive impact on protein stability, cofactor economy and saturation and the redox properties amongst others (Joosten and van Berkel 2007).

These flavin cofactors, although chemically rather uniform, contribute to a wide array of diverse biological functions by catalyzing energetically intensive one- and two-electron electron transfer reactions. These reactions can span from the synergistic action on peroxidase-mediated lignin depolymerization in bacteria and fungi by pyranose 2-oxidase (Wang, Huang, and Ai 2019; Herzog et al. 2019) to the photo induced DNA repair of DNA damage during apoptosis by photolyase throughout the tree of life (Yamamoto et al. 2017). Flavin coenzymes are maybe most prominent

for their role in the oxidation of CH and C-OH groups in various substrates by dehydrogenases and the often concomitant activation of molecular oxygen when enzymes are thus referred to oxidases or oxygenases (Mansoorabadi, Thibodeaux, and Liu 2007).

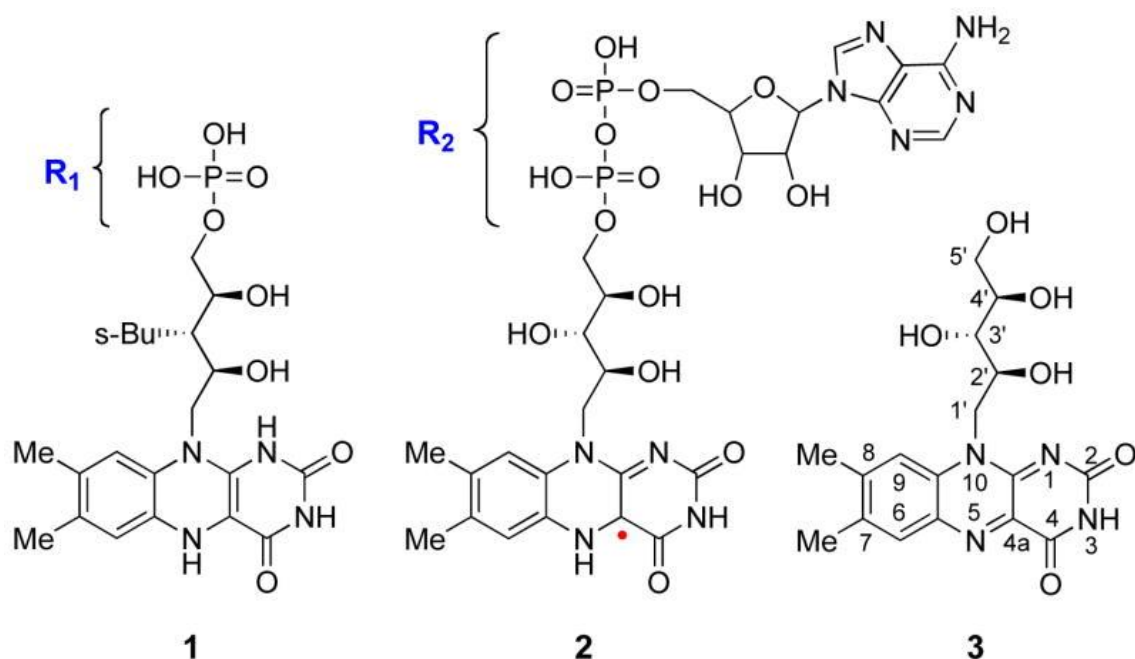


Figure 1 Structures of flavin coenzymes Flavin mononucleotide (FMN, 1), Flavin adenine dinucleotide (FAD, 2) and riboflavin (Vitamin B2, 3). FMN and FAD contain distinctive ribityl moieties: FMN contains a single phosphate (R1) where in contrast FAD contains an adenosine monophosphate instead. In all flavins, the isoalloxazine unit is the redox active center of the cofactor and occurs in three redox-states: FMN in the double reduced state (hydroquinone), FAD in the one-electron semiquinone state and riboflavin fully oxidized. Figure adapted from Mansoorabadi, Thibodeaux and Liu, 2007 (Mansoorabadi, Thibodeaux, and Liu 2007).

Generally, more than 25 organic cofactors (vitamins, vitamin derivatives and others) and 8 inorganic cofactors (metal ion, iron-sulfur clusters) are currently described, with the actual number varying depending on the terminological discrimination differing between cofactors and co-substrate. As different sources seem to be still discordant on the definition of “coenzymes”, “cofactors” and “prosthetic groups”, commonly those definitions are synonymously used.

In the case of so termed metalloenzymes, the biological catalysts have adopted metal ions from Cu, Fe, Mg, Mn, Md, Ni, Zn to assist their reactions. The utilization of metal ions to assist catalytic reactions is a common feature of enzymes in nature as close to one third of known enzymes either

contain a metal-ion cofactor or depend on it in another way. The association of metal ions in enzymes accompanies a set of chemical features that are more than desirable for the biological catalyst: the positive charge, the development of strong but volatile bonds and the possibility to shuttle electrons between usually more than one redox state (Berg et al. 2015). In the special case of *heme*, the cofactor is a combination of an inorganic Fe(II)/Fe(III) metal ion, which is coordinated by an organic porphyrin ring to center the metal ion. Also, Fe-S-cluster represent a specialty in cofactor chemistry where in prominent enzymes such as ferredoxins, the Fe₂-S₂ cluster is coordinated by cysteines in the active site and fulfills electron transfer reactions during photophosphorylation reactions in photosynthesis (Bugg 2009).

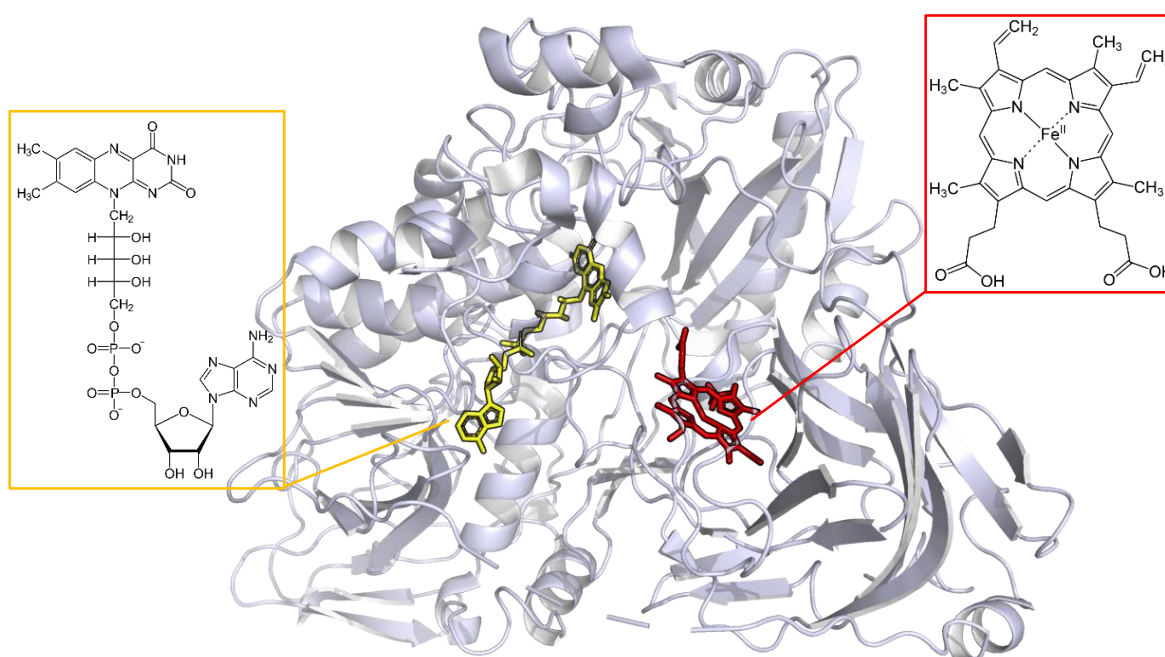


Figure 2 PyMOL protein model of cellobiose dehydrogenase (CDH) from *Crassicarpon hotsonii* (formerly *Myriococcum thermophilum*) harboring an organic FAD cofactor (yellow frame) in its dehydrogenase domain and a protoporphyrin IX partnered with an iron central ion (Heme b, red frame) in its cytochrome domain. When a suitable sugar substrate is oxidized at the CDH dehydrogenase domain electrons are withdrawn from the substrate by the oxidative power of the adjacent FAD. These electrons are then shuttled to the neighboring cytochrome domain one-by-one in a process that is not fully resolved yet. The CDH enzyme can make use of the electrons stored at the heme cofactor when supplying enzymes involved in the disintegration of crystalline cellulose (Kracher et al. 2016).

Contrasting to the group of metalloenzymes, enzymes is often associated a small, usually less than 1 kDa, organic compound serving the catalyst as a cofactor. Many of the known organic cofactors are derived from vitamins and need to be supplied through the human nutrition as they cannot be synthesized (in sufficient amounts) *de-novo*. Prominent examples include FMN/FAD which

participate in electron transfer reactions and are derived from riboflavin (Vitamin B₂), or Menaquinone (Vitamin K) which is described for its interaction with carbonyl groups. The case of dihydrofolate reductase represent a special case to underline the dependency of the human physiology on cofactor-dependent enzymatic catalysis: Dihydrofolate reductase is commonly known for its ability to transform folic acid (Vitamin B₉) into tetrahydrofolic acid (THFA) which is essential for the biosynthesis of nucleotides for DNA synthesis. For its catalysis, the enzyme relies on NADPH, a derivative of niacin (Vitamin B₃). The synthesized THFA is also further utilized in the formation of methionine, which is catalyzed by methionine synthetase, a cobalamin (Vitamin B₁₂) dependent enzyme (Lee et al. 2012).

4. Categorization and classification of enzymes

Enzymes can be categorized by their activity as they employ fundamentally different biochemical functionalities. This categorization is reflected in a nomenclature which is guided by the Committee of the International Union of Biochemistry and Molecular Biology (IUBMB) and establishes seven distinct classes of enzymes (Kennedy and Lloyd 1994; Tipton and Boyce 2000): Oxidoreductases (EC 1), Transferases (EC 2), Hydrolases (EC 3), Lyases (EC 4), Isomerases (EC 5), Ligases (EC 6) and Translocases (EC 7). These classes can be progressively sub-classified further defining the substrates and site of action. As an example, the class of Oxidoreductases EC 1 enzymes is principally subdivided according to their site of action, whether CH-OH (EC 1.1), aldehyde or oxo groups (EC 1.2) or one of the many others is acted on by the enzyme. As a ensuing sub-division, these categories are then further categorized according to the acceptor molecular used in the reaction. For EC 1.1 the oxidation reaction of CH-OH groups can be performed with a wide variety of electron acceptor molecules. Prominently, NAD(P)⁺ (EC 1.1.1), cytochrome (EC 1.1.2), oxygen (EC 1.1.3) or quinones (EC 1.1.5) amongst others should be stated here. The previously mentioned example of the FAD-containing pyranose 2-oxidase can be found within the EC 1.1.3 category since it utilized oxygen to oxidize sugars at their CH-OH group. Although quite similar in its oxidation reaction and most likely evolved from a not too distant common ancestor, the afore mentioned two-domain cellobiose dehydrogenase enzyme is categorized as EC 1.1.99. Subgroup 1.1.99 considers an unknown physiological electron acceptor. With more knowledge gained on the

physiological whereabouts of the CDH enzyme in recent times, this categorization seems to be up for debate (Kracher et al. 2016; Sützl et al. 2018).

Independent from this general and mechanistic categorization of enzymes by the UIBMB, enzymes can also be classified by their physiological function, as is the case for the renowned carbohydrate-active enzymes database (CAZy). This database archives data and describes enzymes that are involved in the creation, modification or degradation of glycosidic bonds and was initiated by researches from the field in 2013 (Levasseur et al. 2013; Lombard et al. 2014). The constituting enzymes in the CAZy database – the so-called CAZymes - are responsible for the biochemical generation and degradation of polysaccharides and hence play a vital role in the interplay of formation and break down of plant cell wall polysaccharides, the most abundant natural polymer. As such, these enzymes is also ascribed a great importance in the biotechnological industry; in biofuel processing applications especially since their utilization often allows to break the persistent polysaccharides into their commonly more valuable monosaccharide constituents. One of the key features of this collection of enzyme data is that the classification is rooted in the structure and molecular mechanism of its enzymes. Currently 300 different CAZyme families are organized in this collection where entries are separated into the classes Glycoside Hydrolases (GH), Glycodyl Transferases (GT), Polysaccharide Lyases (PL), Carbohydrate Esterases (CE) and Auxiliary Activity (AA) CAZymes which are redox enzymes working in conjunction with enzymes from the other classes. Generally, these classes are further subdivided into families that are structurally and functionally related.

5. Versatile Oxidoreductases

A mechanistic view

The class of EC 1 represents oxidoreductases and summarizes the various sub-classes of enzymes that are able to transfer hydrogen or electrons and oxygen atoms in balancing oxidation and reduction reactions. Generally, the class of oxidoreductases represents an astonishingly versatile class of enzymes that catalyze a wide multitude of redox reactions of an even wider array of substrates. In the exchange of electrons and redox equivalents the compound donating electrons is oxidized, electrons are transferred and concomitantly the compound receiving electrons is reduced.



The enzyme's tendency to receive or donate electrons from suitable substrates can be understood as an (electro)chemical equilibrium. Each functional redox center able to mediate electron transfers can be assigned a potential – usually given in milli volts (mV) and often referred to as electrochemical midpoint potential E_m . This potential is a means to describe the thermodynamic force to receive and donate electrons. In a series of electron transfer events, redox centers with a lower E_m will donate electrons whereas, vice versa, components with a high E_m will receive electrons. As is typical for a chemical equilibrium, the absolute difference in redox potentials between donor and acceptor molecular determines the rate of reaction, which in the case of many oxidoreductases, is the general energy barrier and contributes substantially to the ΔG of the reaction. (Christgen, Becker, and Becker 2019).

With the increase in atmospheric oxygen concentrations approximately 600 million years ago, enzyme evolution was challenged with the abundantly present electron acceptor O_2 , a molecule endowed with a soaring electrochemical force. For the enzyme catalysts that are oxidoreductases, harnessing this potent electron acceptor comes at the expense of needing to:

- adapt the enzyme architecture and active site to make O_2 accessible as co-substrate

- prevent or at least manage the often harmful byproducts generated during oxygen reduction (Romero et al. 2018).

Having evolved to utilize various oxygen species, oxidoreductases generally rely on the presence of cofactors (FMN, FAD, pterins, quinones and complexed metal ions) to tame the reductive power of O_2 and H_2O_2 and help orchestrating electron transfer processes (Xu 2005).

A prominent example to display the processes of electron transfer between oxygen and cofactor in oxidoreductases is presented here for the activation of O_2 by FAD. The majority of enzymes containing a flavin cofactor (FAD, FMN) is involved in electron transfer reactions. The difference in redox potentials between the O_2/H_2O_2 transition and the FAD^{ox}/FAD^{red} transition of free FAD accounts for nearly 500 mV and underlines the exceptional reactivity of this redox couple (Massey Vincent 1994). As is described in the following, FAD can directly interact with O_2 and mediate two subsequent electron transfers onto O_2 , establishing a short-lived superoxide anion radical and releasing H_2O_2 ultimately or introducing oxygen into molecules.

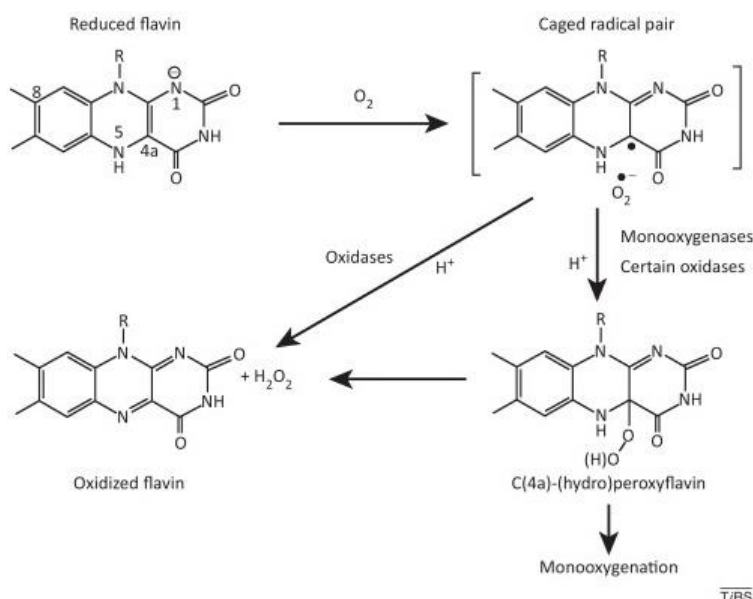


Figure 3 Catalytic pathways of the FAD cofactor with O_2 . In the reduced ground state, the N^5 of the isoalloxazine ring of the flavin is present as a N^5H . Upon association with O_2 , a single electron is abstracted from the FAD conjugated ring and transferred to O_2 to form a superoxide anion $O_2^{\bullet -}$, leaving the other electron in the now semiquinone FAD (radical) behind. In most oxidases, this radical couple is then resolved with H^+ proton transfer in a second oxidation step and causes the formation of H_2O_2 and an oxidized N^5 . In monooxygenases and few oxidases like pyranose 2-oxidase, a short-lived hydroperoxyflavin intermediate occurs when the radical pair collapses. This species can be stabilized and be spontaneously released as H_2O_2 or introduces oxygen establishing a hydroxy-flavin before returning to the reduced FAD. Figure from Chaiyen, Fraaije and Mattevi, 2012 (Chaiyen, Fraaije, and Mattevi 2012).

If this reaction cycle involves the formation of a ternary complex where the oxidized substrate is associated with the FAD cofactor, then the reaction is referred to as “ternary complex mechanism” whereas if the oxidized substrate is released prior the regeneration of the oxidized FAD the reaction mechanism is from the “ping-pong” type (Mattevi 2006).

The class of oxidoreductases can further be subdivided depending on the nature of the electron acceptor: enzymes endowed with the ability to activate oxygen are generally referred to as “oxidases” whereas those which prefer to reduce organic compounds or complexed ions instead are called “dehydrogenases” (Romero et al. 2018; McDonald et al. 2011).

- If O_2 is activated and receives electrons and H^+ to generate H_2O_2 , the oxidoreductase is termed “Oxidase”
- If O_2 is activated and introduced into an organic molecule, oxidoreductases are referred to as oxygenase or hydroxylase.
- If H_2O_2 is the primary electron acceptor and is reduced to water, oxidoreductases are called “peroxidases” wherein the special case of “catalases”, H_2O_2 is disproportionated rather than reduced and yields O_2 and water.

B) Lignocellulose: its constituents and enzymatic degradation

6. Lignocellulose

Plants have mastered the ability to convert sunlight into energy and with it amass the majority of terrestrial biomass. Feeding on CO₂ and H₂O, plants are able to fixate atmospheric carbon and have developed biochemical pathways to convert light energy into chemical energy, storing molecules of high energy such as sugars and phenols whilst forming O₂ is a byproduct. These molecules are commonly arranged into complex and recalcitrant polymers to ease energy storage, build mechanically stable scaffolds for growth, and prevent hostile attack on these energy dense structures by microorganisms. Still, the assimilation of light energy into organic compounds is the grand mechanism and vital origin for delivering the predominant carbon source for life on this planet and many enzymatic systems have evolved to make this packed energy available (Eastwood et al. 2011; Mäkelä, Donofrio, and De Vries 2014; de Gonzalo et al. 2016; Andlar et al. 2018) .

Although the cell wall composition of plants is subject to great variation, three major polymer constituents make up most of the plant biomass and are found in all plant tissues: cellulose, hemicellulose, and lignin. Based on the spatial organization of these polymers in the secondary cell wall, a network of chemically distinct compounds forms a biological superstructure - a composite material that is interconnected by a multitude of interactions. Glucose monomers that accumulate from photosynthesis are activated chemically and connected by synthetase enzymes to form long cellulose chains. Several of these chains then assemble into crystalline cellulose bundles called microfibrils, recalcitrant structures that are distributed laterally in the plant tissue to form a web providing the plant tissue with tenancy (Loix et al. 2017; Andlar et al. 2018).

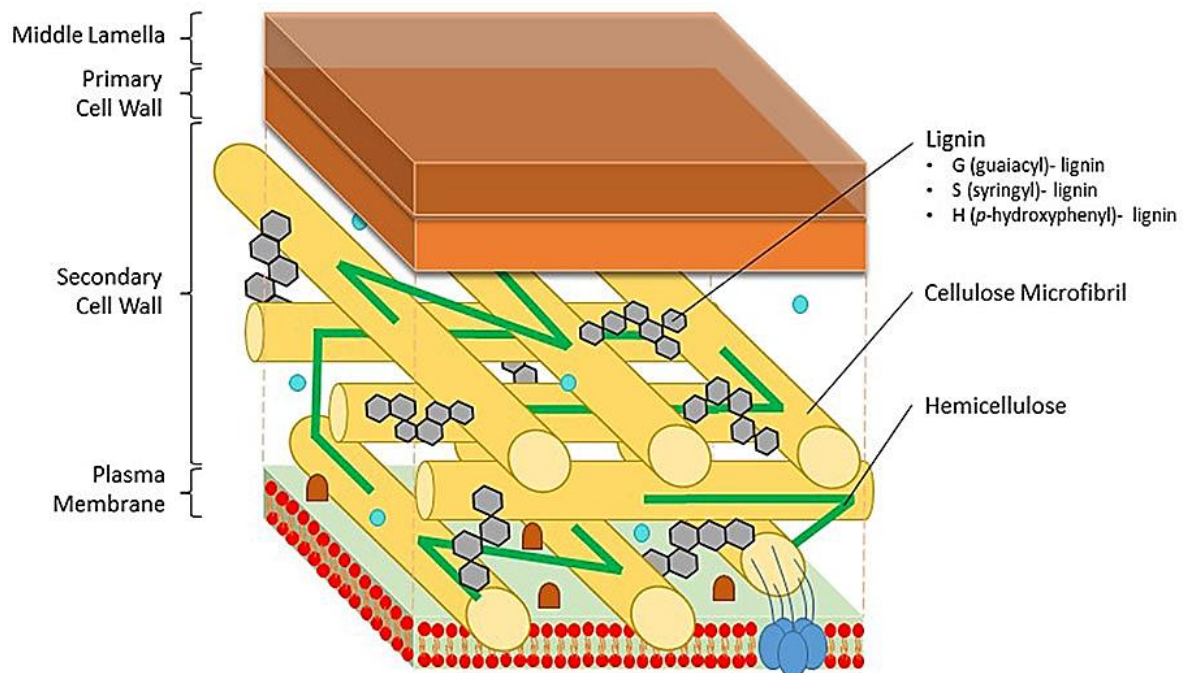


Figure 4 Scheme of the plant cell wall composition. The structure of a plant's cell can be categorized into two subgroups depending on the composition: the primary and secondary cell wall. The latter occurs mainly in plant tissue that provide mechanical robustness. The cell wall's major components are cellulose, which is arranged in microfibrils, hemicellulose and lignin. Figure modified from Loix et al. (Loix et al. 2017).

Hemicellulose is similar to cellulose in that it is composed of sugar monomers but generally, hemicellulose strings are shorter in length. As in the case of cellulose, glucose monomers are the sole constituents which are linearly connected via glycosidic bonds. In hemicellulose different pentose and hexose sugars are found including xylose, arabinose, galactose, glucose and mannose which are polymerized with at least partial glycosidic branching. The composition and the degree of branching are usually varying a lot depending on plant and tissue type (Scheller and Ulvskov 2010). Within the cellulose mesh, hemicellulose fibers are anchored to the cellulose microfibrils and establish a matrix of interconnections increasing the robustness of the cellulose network whilst simultaneously surrounding it in a protective manner (Loix et al. 2017).

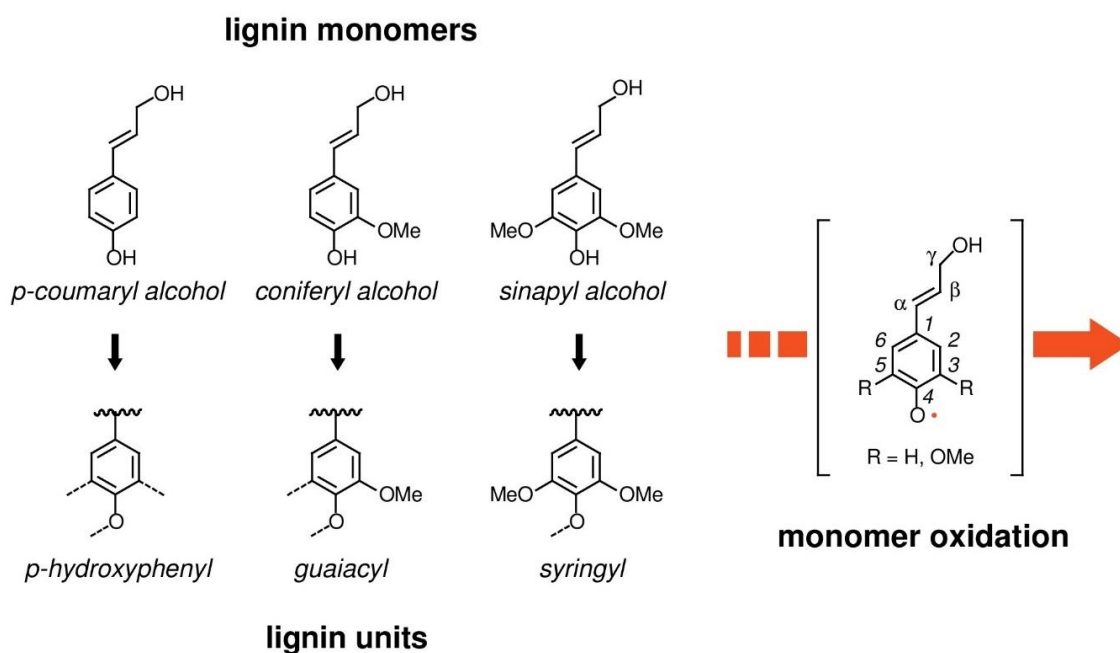


Figure 5 The lignin building blocks. Three major phenolpropanoid alcohols are differently derivatized with methoxy groups and referred to as *p*-coumaryl, coniferyl and sinapyl alcohol. Enzymes can mediate the oxidation of the C4' hydroxyl group to form a phenoxy radical which can be coupled to the growing lignin polymer in spontaneous reactions. Figure modified from Brown and Chang (Brown and Chang 2014).

In contrast to (hemi)cellulose, lignin does not occur as a linear polymer and is not polymerized from monosaccharides. Instead, lignin is polymerized from three different monolignol alcohol units: cumaryl, coniferyl and sinapyl alcohol, all being differently derivatized phenylpropanoids (Figure 5). The current theory to explain lignin formation is based on an enzymatic process which involves establishment of radical states of the three monolignol building blocks and successive docking of these activated to the growing lignin polymer as C-C or C-O bonds. It has been suggested that several plant oxidoreductases, laccases predominantly, drive this process (Liu, Luo, and Zheng 2018). As is thought, this process itself is not directed specifically and rather progresses wherever space and monomer activation (enzyme) is available. Sourced in this oxidative domino-effect mechanism, lignin is formed to fill the gaps between (hemi)cellulose bundles and is embedded into the polysaccharide mesh to create an amorphous, cross-linked hydrogel, increasing the mechanical resistance even further and protecting the energy rich polysaccharides from hostile degradation by its exceptional chemical resistance (Loix et al. 2017; Brown and Chang 2014).

As plants invest a lot of biochemical energy into building and maintaining these recalcitrant and dense structures that are wood, the plant cell wall has also evolved to be as resilient as possible to

hostile attack from microorganisms. The energy rich plant polymers are well-shielded from being harnessed by microorganisms, even when the plant dies. Bacteria and fungi have thus co-evolved enzymatic systems to facilitate the attack on lignocellulose polymers, to counteract the plant defense systems and to progressively make polysaccharides available whilst processing their constituents into building blocks suitable for assimilation.

7. Enzymatic lignocellulose degradation

The interaction of biochemical key players dedicated to the degradation of lignocellulose in itself is quite complex. This topic becomes even more complex when one regards the variation in enzymatic cocktail composition, the synergies between the enzymes involved and the variations in the way these enzymes operate in a timely fashion when fungi or bacteria employ different strategies of lignocellulose degradation. Sourced in this complexity, lignocellulose degradation is often described on the basis of well-described examples.

During the natural turnover of plant biomass, nature encounters a sheer endless supply of nutrients. As a result, a myriad of fungal and bacterial organisms has evolved to take part in the degradation process, responding to the variation in energy sources with equal phenotypic diversity. Within this forest biome, fungi are most vital for the ecosystem as they account for the majority of biomass decomposition and assimilation. Thus, most research so far has been conducted elucidating the fungal way of biomass degradation and the majority of characterized enzymes involved in the degradation or assimilation process are from fungal origin (Sánchez 2009; Andlar et al. 2018). In contrast, knowledge on the bacterial ways of lignocellulose degradation, lignin in particular is rather scarce (Brown and Chang 2014; de Gonzalo et al. 2016).

When it comes to efficient biomass degradation, white-rot fungi are arguably most specialized as they master the proficient hydrolysis of both cellulosic and lignin matter. Prominent white-rot representatives such as *Phanerochate chrysosporium*, *Irpex lacteus*, *Trametes versicolor* and others have evolved advanced enzymatic systems to disintegrate the recalcitrant and amorphous network that is lignin.

Great importance to the interaction with lignin is attributed to laccases (EC 1.10.3.2), which belong to the family of multi-copper oxidases and are commonly found in fungal, bacterial, and also plant proteomes. Laccases are endowed with an active site of four copper ions, coordinated into clusters in a characteristic brace of histidines. They are well-known to act on phenolic substrates by mediating single electron oxidations, generally causing the establishment of short-lived phenoxy radicals. In these reactions, O_2 serves as the sole co-substrate and terminal electron acceptor, water is released as a product alongside the phenoxy compound. (Mate and Alcalde 2017; de Gonzalo et al. 2016; Brown and Chang 2014). Multiple examples from modern research demonstrate that laccases are key to the efficient disruption of the lignin polymer (Cragg et al. 2015; Longe et al. 2018). In white-rot fungi, enzymatic lignin depolymerization also relies on secretory *heme*-dependent peroxidases (class II): lignin peroxidase (LiP, EC 1.11.1.14), manganese peroxidase (MnP, EC 1.11.1.13) and versatile peroxidase (VP, 1.11.1.16). These three peroxidases are all characterized by an extraordinary high redox potential which empowers them to oxidize - otherwise chemically resistant - phenolic lignin constituents. These ligninolytic extracellular peroxidases are fueled by H_2O_2 and accept a broad array of phenolic and non-phenolic substrates, such as lignin derived aryles, methoxylated aromatics (e.g. veratryl alcohol) and complexed metal ions. In their catalytic cycle, these peroxidases complete two distinct one-step electron oxidation reaction and transfer the two electrons gained onto H_2O_2 , releasing H_2O . In the case of MnP, most commonly employed in fungal delignification, complexed Mn^{2+} ions act as intermediate electron shuttle and can mediate two substrate oxidation reactions at site or be released as complexed Mn^{3+} for mediated action. (Wariishi, Valli, and Gold 1992; Nousiainen et al. 2014; Rahul Singh and Eltis 2015)

Recent research suggests that the direct interaction of laccases and peroxidases with lignin is unlikely, and reconstruction of the polymer is instead triggered by cascades of primary reaction products of these enzymatic reactions. As suggested, small (phenolic) reactants of high redox potential are generated by the enzymes and are able to penetrate the lignin polymer (Figure 6); diffusion of molecules larger than several kDa was demonstrated to be impossible given the dense structure of the polymer. The so formed “mediators” presumably directly interact with lignin at site and establish radical sites that lead to progressing bond scission in the polymer (Christopher, Yao, and Ji 2014; de Gonzalo et al. 2016; Brown and Chang 2014).

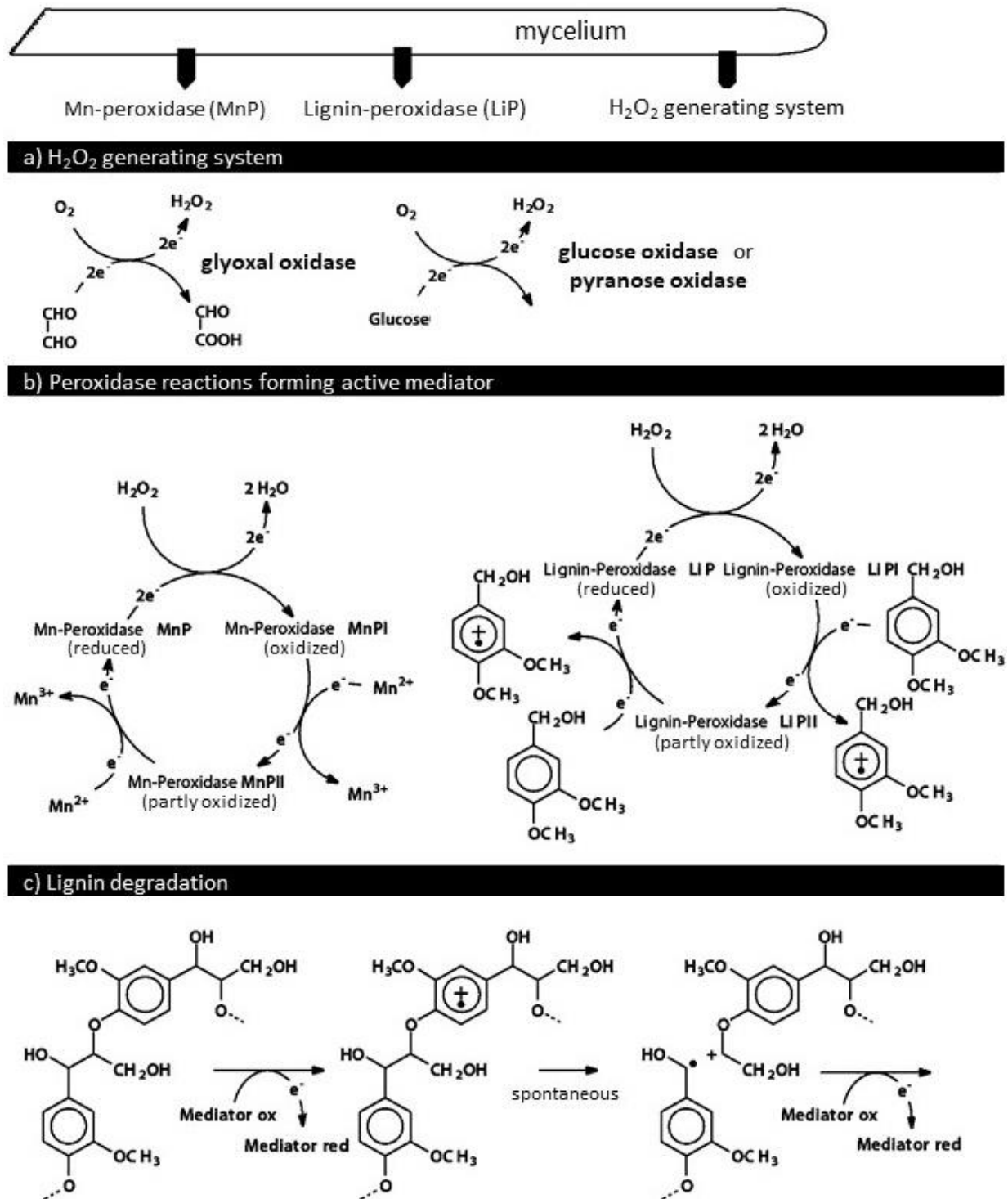


Figure 6 Lignin attack by mediated peroxidase catalysis. (a) The *heme*-dependent peroxidases are secreted by the microorganism and cooperate with a co-secreted system for H_2O_2 generation. These system, fueling the peroxidase reactions, are in return operating on reaction products from biomass degradation such as glyoxal and glucose. (b) During their catalytic cycle, the peroxidases undergo redox reaction from the reduced to the oxidized state whilst generating mediators (Mn^{3+} , veratryl alcohol radical) able to diffuse into the lignin (c) and trigger bond fission. Figure modified from Reineke W. et al., 2020 (Reineke et al. 2020).

8. Bacterial Systems

The situation in bacterial litter degraders seems to overlap with fungal systems when the types of employed enzymes are considered, but differs when their catalysis and synergies are, as a limited number of well-characterized examples points out. Strikingly, bacterial genomes generally harbor laccase and peroxidase genes comparable in sequence to fungal counterparts.

Although bacterial laccases are found in various bacterial genera (*Bacillus*, *Streptomyces*, *Klebsiella*, *Pseudomonas*, ...) as a recent review comprehensively summarizes (Arregui et al. 2019), the ability to modify lignin similarly to fungal relatives is only attributed so-called “small laccases” isolated from Actinomycetes (Bugg et al. 2011; Majumdar et al. 2014).

A different superfamily of peroxidase appears in fungi and bacteria and was first discovered in 1999 (Kim and Shoda 1999). This *heme*-peroxidase was isolated from the yeast *Geotrichum candidum* and reported for its ability to decolorize synthetic dyes and was thus termed “dye-decolorizing peroxidase” (DyP, EC 1.11.1.19). From genomic analyses it could also be shown that the occurrence of these DyP-type peroxidases is rare in fungi but quite prominent in bacteria, in litter degrader and soil bacteria of the actinomycetes genus especially. This reasons why often DyP are also referred to as bacterial peroxidases. A phylogenetic classification of DyP sequences into class A, B, C, and D revealed that only sequences from the A class harbor a bacterial Tat-dependent secretion signal and are suggested to occur extracellularly where they could be involved in degradation processes (Colpa, Fraaije, and Van Bloois 2014). Still, characterized DyP from class B were also shown to exhibit the fundamental catalytic features needed for lignin degradation, as the example from the *Rhodococcus jostii* DyP (Ahmad et al. 2011) and *Pseudomonas putida* (Santos A. et al. 2014) point out.

Although appearing in fungi and bacteria, DyP are of special interest in the scope of bacterial lignocellulose degradation since they are thought to represent the sole peroxidase potentially capable of oxidation of lignin constituents as no homolog of the classic fungal peroxidases (LiP, MnP and VP, Figure 6-b) were found in bacteria yet. More and more reports assess the biochemical properties of DyP and find evidence for the ability to oxidize lignin as such or its constituents (Ahmad et al. 2011; Brown, Barros, and Chang 2012; Santos et al. 2014; Qin et al. 2018). An interesting

addition to the catalytic repertoire of these peroxidases was reported by Brown, Barros and Chang (Brown, Barros, and Chang 2012) for the C-type DyP from *Amycolatopsis* sp. 75iv2. In their publication, the authors mention notable oxidase activity and an association with manganese ions, similar to fungal MnP (Figure 6-b). This implies, that either this DyP is able to fuel its own peroxidase activity by generating H₂O₂ when both O₂ and Mn²⁺ or this oxidase activity is an additional mode that the enzyme is able to utilize to access other substrates.

Generally, another difference between the fungal and bacterial way of approaching lignocellulose degradation is thought to lay within the oxidase system that provides H₂O₂ for the activity of the respective peroxidase (Figure 6-a). This supply of H₂O₂ fuel is covered by fungal oxidase systems employing enzymes such as glyoxal oxidase (EC 1.2.3.15) and the various peroxide-producing enzymes from the CAZy AA3 family of oxidoreductases feeding on a palette of different degradation products from lignocellulose disintegration (Qin et al. 2018; Sützl et al. 2018). The situation in bacterial biomass degraders seems to be a different proposition as - with the exception of pyranose 2-oxidase - no homologous oxidase genes were yet identified in bacteria (Mendes et al. 2016; Herzog et al. 2019). How bacterial lignocellulose degraders are able to fuel their oxidative, peroxidase-driven lignin attack with a comparably limited set of enzymatic functions and what role is attributed to the dehydrogenase activity of available enzymes is yet to be fully elucidated.

C) The AA3 family of oxidoreductases

As is explained above, enzymes are commonly categorized by matters of their fundamental catalytic functionality and structure - as is the case the EC classification of enzymes (page 3). But enzymes can also be assembled into families according to their enzymatic significance for a certain physiological role. The database on carbohydrate active enzymes (CAZy) defines families of “structurally-related catalytic modules and domains of enzymes that degrade, modify or create glycosidic bonds” as is described on www.cazy.org (Levasseur et al. 2013; Lombard et al. 2014). These so called CAZymes are accompanied by a set of oxidoreductase enzymes that do not directly interact with polysaccharides but act in conjunction with polysaccharide-active enzymes, the so-called class of “auxiliary activities” (AA). Given the biologically relevant association of plant polysaccharides and lignin, also enzymes such as the aforementioned laccases (class AA1) and heme-peroxidases (AA2) that are strictly acting on lignin were recently included in the “AA” class (Levasseur et al. 2013).

The class of auxiliary activity AA3 contains a set of functionally diverse enzymes which all belong to the glucose-methanol-choline (GMC) family of oxidoreductases. These enzymes all obey the canonical $\beta\alpha\beta$ -fold (Rossmann fold), a common structural motif found to be typical for the association with flavin nucleotide cofactors (Figure 1) (Cavener 1992). Although the domain architecture between the members of the AA3 group can vary, and some representatives are equipped with an additional cofactor-carrying domain, the common denominator in all of these GMC enzymes is the highly conserved N-terminal flavin-binding domain that harbors the nucleotide part of the FAD cofactor (Figure 2). The AA3 group comprises the enzymes: glucose oxidase (GOx, 1.1.3.4), Aryl-alcohol oxidases and dehydrogenases (AAO, 1.1.3.7), pyranose 2-oxidase (POx, 1.1.3.10), alcohol oxidase (AOX, 1.1.3.13), glucose dehydrogenase (GDH, 1.1.5.9), cellobiose dehydrogenase (CDH, 1.1.99.18) and pyranose dehydrogenase (PDH, 1.1.99.29).

The multiplicity of enzymatic function of the AA3 oxidoreductases was comprehensively discussed in a recent review (Sützl et al. 2018) and their phylogenetic relationships and sequence space subsequently analyzed in greater detail as is summarized in a follow-up publication (Sützl et al. 2019). There it was concluded that enzymes sharing a common substrate not necessarily share a

direct common ancestor and routes for enzyme evolution should not always be deduced from enzymatic function alone.

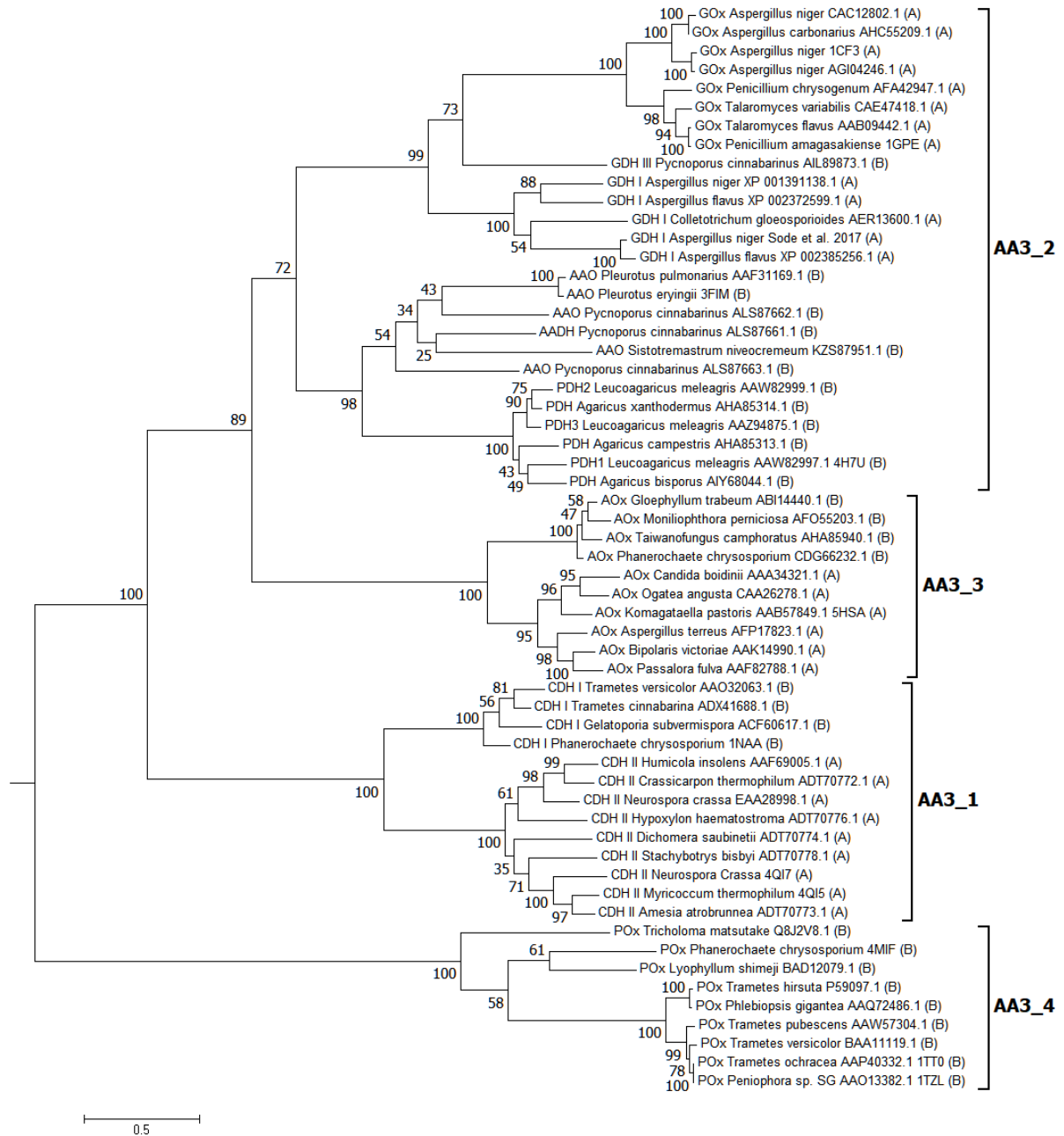


Figure 7 Phylogenetic tree of characterized enzymes from the AA3 family. The sequences of 58 biochemically characterized enzymes containing GOx, GDH, AAO (and aryl alcohol dehydrogenase, AADH), PDH, AOX, CDH and POx were subject to calculation of a phylogenetic tree based on the PhyML algorithm with statistical support of 500 bootstrap repetitions and the WAG amino acid substitution model. Sequences are annotated with species name, NCBI accession numbers and PDB code if available. The reference bar indicates the phylogenetic distance of 50 % substitutions per sequence. Figure kindly provided by L. Sützl (Sützl et al. 2018).

For instance, GOx and GDH are enzymes both extensively characterized for strictly acting on D-glucose as a substrate (Ferri, Kojima, and Sode 2011) seem to have evolved from a common ancestor as is observable in **Figure 7** (Sützl et al. 2019). The ability to accept oxygen as a terminal electron acceptor is inherent in GOx (oxidase activity) and specific to the fungal taxonomical class of Eurotiomycetes which are the sole fungal organisms carrying GOx genes. The oxidase activity is, in contrast, entirely absent in GDH enzymes, which seem to never have developed oxidase activity and evolved parallel to GOx in other fungal (sub)divisions. Still, the work by Sützl et al. demonstrates that large portions of the sequence space are still uncovered as of today and new enzymatic functions could be concealed in yet uncharacterized sequences (Sützl et al. 2019).

As their respective names potentially falsely imply, the relation between PDH and POx cannot be compared to the case of GOx and GDH. It was derived from the calculation of a phylogenetic tree of AA3 enzymes that PDH and POx do not share a common ancestor (Sützl et al. 2019) although both enzymes accept a similar set of pyranose sugars and electron acceptors as substrate (Sygmund et al. 2008; Peterbauer 2020; Leitner, Volc, and Haltrich 2001; Abrera, Sützl, and Haltrich 2020). Interestingly, the sequence space of PDH sequences shares more relation to that of AAO and both PDH and AAO enzymes appear in the same fungal class of Agaricomycetes. On the contrary POx genes can be found in Basidiomycetous and ascomycetous fungi as well as in bacteria and available sequences seem to be more diverse compared to other members of the AA3 family (Sützl et al. 2019).

9. Pyranose 2-oxidase

In the AA3 family the subfamily of AA3_4 accounts for pyranose oxidases (pyranose 2-oxidase, POx). The first description of a pyranose oxidase dates back to 1968 where researchers first isolated a novel enzyme from the mycelium of a basidiomycetous fungi which was able to oxidize various carbohydrates at the C2 position. This enzyme, initially termed carbohydrate oxidase, was given the name pyranose oxidase several years later when research confirmed that the enzyme specifically accepted pyranose sugars (monosaccharides of six-membered rings, five carbon one oxygen) only (F. W. Janssen and Ruelius 1968; F. Janssen and Ruelius 1975). Based on the particular mode of catalysis, oxidizing the C2 atom of pyranose sugars the enzyme is now commonly referred to as pyranose 2-oxidase. Its addition to the family of GMC oxidoreductases happened comparably

late. In 2003, a bioinformatic analysis of POx sequences via structure-based multiple sequence alignment confirmed the presence of conserved features of the predicted 3D structure before the crystal structure of the enzyme was solved. Similarities to enzymes such as glucose oxidase were highlighted in this work (Albrecht and Lengauer 2003). Progressively, many POx from various basidiomycetous and ascomycetous fungi were characterized biochemically and crystal structures for three basidiomycetous POx were solved: *Trametes ochracea* POx [PDB 1TT0] (M. Hallberg et al. 2004), *Peniophora sp.* POx [PDB 1TZL] (Bannwarth et al. 2004) and *Phanerochaete chrysosporium* POx [PDB 4MIF] (Hassan et al. 2013).

Phylogenetic distribution

Strikingly, putative POx genes are not only found in fungi but also occur in bacteria as a comprehensive phylogenetic analysis underscored (Herzog et al. 2019). First speculations that an early horizontal gene transfer between bacteria and fungi led to the distribution of POx genes in both kingdoms appeared in 2009 (Pisanelli et al. 2009). The first evidence of a functionally active bacterial POx was reported several years later when POx from the soil bacterium *Pseudoarthrobacter siccitolerans* (*PsPOx*) was expressed and biochemically characterized. Interestingly, this bacterial POx did not obey all of the the general POx hallmarks as it was reported to occur as a monomer; fungal POx uniformly occurs in a tetrameric fungal form. In addition, the FAD cofactor is covalently attached to the protein backbone in fungal POx which was not the case for the *PsPOx*. Notably, the biochemical characterization of the *PsPOx* catalysis highlighted that this enzyme does exhibit only minor oxidase activity whereas organic electron acceptors are generally well accepted (Mendes et al. 2016). Just recently thereafter, the characterization of a POx from the plant-pathogenic bacterium *Pantoea ananatis* was described. It needs to be stated that the true identity of the enzyme is doubtful since major POx characteristics – such as die classical C2-oxidation – were not confirmed in the original publication (Zhang et al. 2018). More so, this enzyme appeared as an outsider, distinct from bacterial POx in the aforementioned phylogenetic analysis and hence its identity should be reconsidered.

Structure

POx, like other GMC oxidoreductases, exhibits a two-domain architecture comprising the flavin-binding domain – of the typical Rossmann-fold - and a substrate-binding domain. As the FAD

harboring flavin-domain is well-conserved among all GMC enzymes, the substrate-binding domain in contrast is subject to greater variation, in POx especially. In fungal POx, the FAD cofactor is covalently anchored to the protein backbone via a histidyl-linkage of the isoalloxazine moiety of FAD which is otherwise unprecedented in AA3 enzymes (Halada et al. 2003). In addition, POx is unique among the AA3 family as it also contains a small sub-structure called the “head-domain”. This protruding sequence stretch contains a pair of short anti-parallel beta sheets that are connected via loops and develop a remarkably flat beta-hairpin fold of yet unknown function. It was speculated that this head-domain initiates or assists in the formation of the multimeric state of the enzyme (M. Hallberg et al. 2004; Hassan et al. 2013). Structure-wise, evidence for the multimeric state of POx is only available for fungal enzymes, which generally develop a tetrameric state from identical monomers. This association into a so-called “homo-tetramer” results in the formation of a central cavity or void that is the point of entry for the substrate channels of the individual monomers (M. Hallberg et al. 2004). Furthermore, the substrate’s access to the active is also controlled by a substrate-recognition loop acting as a structural gate-keeper in the active site. This element is subject to conformational change upon interaction with substrates and inhibitors and regulates turnover, another structural feature specific to POx (Spadiut et al. 2010).

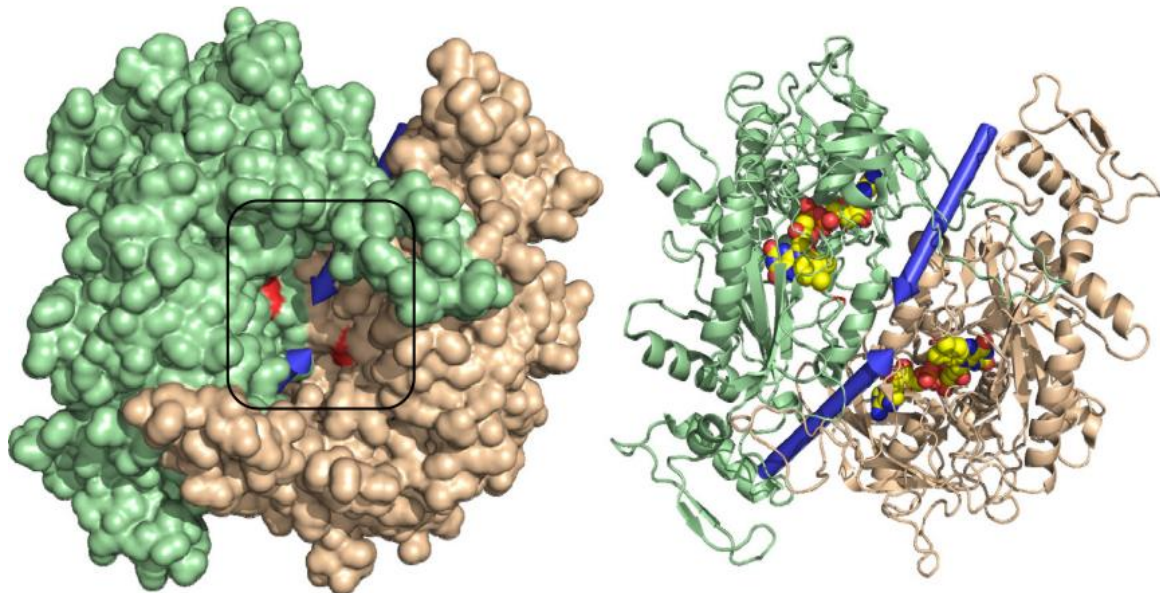


Figure 8 3D structure model of the POx from *T. ochracea* (PDB 1TT0) in cartoon representation. The central cavity (black frame) isolates the active site entrances from the exterior (left). The substrate channels are indicated with blue arrows and the FAD cofactor with colored spheres. Figure by courtesy of A.T. Abrera (Abrera, Sützl, and Haltrich 2020).

Catalysis and substrates

POx catalyze the oxidation of an alcohol moiety to the corresponding aldehyde or ketone, whilst transferring the gained electrons to a suitable electron acceptor that not necessarily needs to be O₂. The reaction mechanism of POx proceeds in two half-reaction, an initial reductive and subsequent oxidative one and employs the ping-pong bi-bi type (Wongnate and Chaiyen 2013). In the reductive reaction, catalysis is initiated when the sugar CH-OH group associates with the cofactor and two electrons are transferred to the FAD as a hydride (C-H bond breakage, no proton abstraction), reducing it consequently and leaving a protonated ketone sugar behind. In this early enzyme-substrate complex key catalytic residues contribute to stabilizing this transitional protonated state. The catalytic Histidine then scavenges the proton leaving the oxidized sugar behind as a recent study shed light on (Wongnate et al. 2019). Before the FAD is recovered, the oxidized sugar is released as a C2-keto form, which generally characterizes the ping-pong bi-bi type of the reaction. In the ensuing oxidative half reaction, the reduced FAD associates with O₂, transfers two electrons and forms a FAD-O-OH peroxy-flavin intermediate (Figure 3). This intermediate is not found in other AA3 family enzymes and it seems that only POx is competent to stabilize this peroxy intermediate in this group; certain flavin-monooxygenases also can establish this intermediate. In the last step of the reaction, H₂O₂ is eliminated from the FAD-O-OH hydroperoxyl-flavin intermediate leaving the FAD in the native oxidized form (Wongnate and Chaiyen 2013).

POx readily reacts with a small set of monosaccharides and for POx from various organisms, commonly a specific interaction with the pyranose sugars D-glucose, D-galactose and D-xylose is reported as a recent review summarized (Abrera, Sützl, and Haltrich 2020). As a reaction product, the enzyme releases the oxidized keto-sugar, where a C=O at the pyranose C2 is formed (2-dehydro sugar). Contrasting to other GMC enzymes accepting glucose as a substrate, POx specializes in oxidizing both anomeric glucose forms, α and β , (Nishimura, Okada, and Koyama 1996) and is thus sometimes preferred over other enzymes such as glucose oxidase for biosensing applications. As the physiological importance of the electron donor substrates is still debated, a pronounced affinity for the sugars glucose, xylose and galactose can be put into perspective when one regards the potential biomass feedstock. Although glucose appears ubiquitously incorporated into

cellulosic biomass, xylose and galactose appear predominantly in hemi-cellulose where they are major constituents of the biopolymer. One can therefore hypothesize that POx is involved in biomass breakdown what initial decomposition already progressed and these specific sugars are released from hemi-cellulose and available for the enzyme.

When it comes to the electron acceptor, a wide variety of accessible substrates are reported for POx and amongst others include oxygen, (chelated) metal ions as well as variably derivatized organic quinones (Leitner, Volc, and Haltrich 2001). The latter are believed to be structurally related to compounds that are released from lignin during the enzymatic degradation of the biopolymer. Although POx is rightfully referred to as an oxidase and reactivities with oxygen are generally high for almost all representatives of the enzyme, POx commonly accept the aforementioned “alternative” electron acceptors just as well as is indicated by the high specific activities and usually low K_m values, as the example of 1,4-benzoquinone highlights (Ai et al. 2014). The physiological role of an enzyme that is able to efficiently utilize O_2 to form H_2O_2 and simultaneously accept potential lignin degradation product might be of good use for a microorganism, be it from fungal or bacterial origin, that is involved in lignin degradation where a large proportion of the enzymatic attack is mediated by H_2O_2 -dependent peroxidases (Bugg et al. 2011). When concurrently acting with peroxidases, POx could potentially play a role in supporting these peroxidases in a threefold manner:

- H_2O_2 could be supplied for the peroxidase catalysis. This degradation might be fueled by sugars that are released from preliminary (hemi)-cellulose attack.
- Reactive lignin degradation products, such as quinones, that are released from the biopolymer could be inactivated by reduction.
- Metal ions that are embedded within the lignin mesh are utilized by enzymes such as MnP and DyP for their mode of action and often used as mediators in the degradation process. These complexed and often highly reactive ions could be regenerated by the POx enzyme since it is able to reduce them to their ground state.

Biotechnological applications

Starting in the late 1990s, several studies researched the application of pyranose 2-oxidase as a recognition element in biosensors, mainly due to its specificity for glucose. The enzymes reactivity with oxygen allows to simplify sensor architectures since the enzymes reaction product H_2O_2 is easily electrochemically detected itself or by a partnering enzyme such as horseradish peroxidase (Lidén et al. 1998). Given the broad substrate specificity of POx, several other sugars (xylose, galactose, mannose and maltose) could be detected in more advanced sensor developments and were successfully employed for analyses and monitoring in the food and beverage industry (Odaci, Telefoncu, and Timur 2008). Subsequent research approached the improvement of POx-based sensors by establishing mediated electron transfer systems which allowed reducing background reactions and simultaneously increasing analytical sensitivity (Gokoglan et al. 2015; Kurbanoglu et al. 2018). In addition, the combination with other enzymes helped to broaden the substrate spectrum of the analytical sensor. For instance, POx was combined with a glucosidase to estimated maltodextrin levels in beer (Odaci, Telefoncu, and Timur 2010).

POx can also be employed for point-of-care diagnostics as a recent example successfully underlines. 1,5-anhydroglucitol (1,5-AG) is a prominent marker for diabetes and reflects a patient's glycemic status. Elevated levels of 1,5-AG can be detected for up to weeks in the urine or saliva when blood glucose levels are pathological. Sourced in the promiscuity of the POx substrate acceptance, 1,5-AG can be oxidized by the enzyme and commercial "GlycoMark" detection kits are available and FDA approved (Nowatzke et al. 2004)

A different area of application of POx is the utilization of the enzyme as a catalyst in the biochemical synthesis of 2-keto sugars. The maybe most prominent example includes synthesis of the antibiotic agent corticosterone, a carbohydrate compound originally identified in cultures of the fungus *Corticium caeruleum* (Baute et al. 1976). In the synthesis process, two enzymes work in tandem to stepwise synthesize the antibiotic from D-glucose. POx is used in the initial oxidation step to generate the intermediate 2-keto glucose derivate, termed glucosone. This is then in return substrate for a fungal aldose 2-ulose dehydratase enzyme which catalyzes ring-opening and derivatization under the influence of assisting chemical catalysis. This synthesis process was protected under the patent US4569913A which expired in 2004. At that time, the corticosterone compound was researched for the application as an anti-cancer drug as antiproliferative activity

on human cancer cells could be shown (Koths, Halenbeck, and Moreland 1992).

10. Cellobiose dehydrogenase

Another member of the AA3 family is the hemoflavoenzyme cellobiose dehydrogenase (AA3_1, CDH) and was first identified and isolated from fungal cultures by Westermark and Eriksson in 1974, just some years after POx was first described. The quinone reducing activities of the CDH enzyme were confirmed after cultures of the basidiomycetous fungi *Trametes versicolor* and *Phanerochaete chrysosporium* (back then annotated differently) were grown with cellulose as sole carbon source. The researchers observed that the expressed activities of CDH aligned well with the activity of cellulases and glucosidase activity and rightfully attributed the enzyme an involvement in the degradation of the recalcitrant polymer that is cellulose. Furthermore, it could be shown that cellobiose is the preferred substrate for the enzyme and monosaccharides were not efficiently turned over. At the opposite enzymatic half-reaction, the CDH sample displayed quinone reducing activities, a reactivity which seemed ambiguous and was hypothesized to potentially assist laccase activity during lignin decomposition (Westermark and Eriksson 1974).

CDH is unique among the family of AA3 oxidoreductases as it comprises not only the conserved FAD-containing flavin domain but a cytochrome (cyt) domain in addition, which coordinates a heme cofactor of the *b* type serving the enzyme with the ability to shuttle electrons to a wide variety of suitable redox partners (Tan et al. 2015). It has been shown that, depending on the availability of the β 1-4 glucose-dimer cellobiose from cellulose degradation, CDH can assist in the action of the cellulose attacking enzyme lytic polysaccharide monooxygenase (LPMO) by supplying electrons for its monooxygenase (potentially peroxygenase) activity via direct contact to the enzyme (Kracher et al. 2016; 2019; Laurent et al. 2019). Further synergistic support for the LPMO catalysis by CDH is assumed to be sourced in the recycling of quinoid compounds by the CDH reductive activity and potentially by the supply of minimal amounts of H₂O₂ (Kracher et al. 2019). Still, it needs to be mentioned that the whereabouts of this catalysis, the involved oxygen species and the mode of interaction are not fully elucidated yet and subject to the ongoing scientific debate. Remaining unclarity in that regard is partly due to the lack of comprehensive data from real biological systems and scarcity of conclusive insights into the varying degradation strategies of

different fungi at the molecular level. Nevertheless, the holistic view on fungal lignocellulose decomposition improves steadily as secretome and proteome studies shed light on the relevancy of certain enzyme families during degradation of biomass of varying composition and the temporal orchestration of key enzymes within this process (Paës et al. 2019; Valadares et al. 2019; Gauna et al. 2020; Umezawa et al. 2020).

Phylogenetic distribution

Sützl and colleagues recently published their work on the phylogenetic distribution of cellobiose dehydrogenase sequences and drafted a classification of these sequence entries into four clusters (Sützl et al. 2019). The calculations on their phylogenetic relation were conducted using the dehydrogenase domain sequence as a template and results are generally consistent with the previous classification of characterized CDH and putative CDH genes based on their fungal origin, which separates CDH sequences into those from ascomycetes (class II and class III) and basidiomycetes (class I) as was described previously (Harreither et al. 2011; Zámocký et al. 2008). In the latest analysis, an additional CDH cluster IV was identified in sequences from Ascomycota and represents the evolutionary most distant clade. It disobeys the CDH’s canonical multi-domain architecture, a phenomenon not uncommon in sequence collections of putative CDH genes.

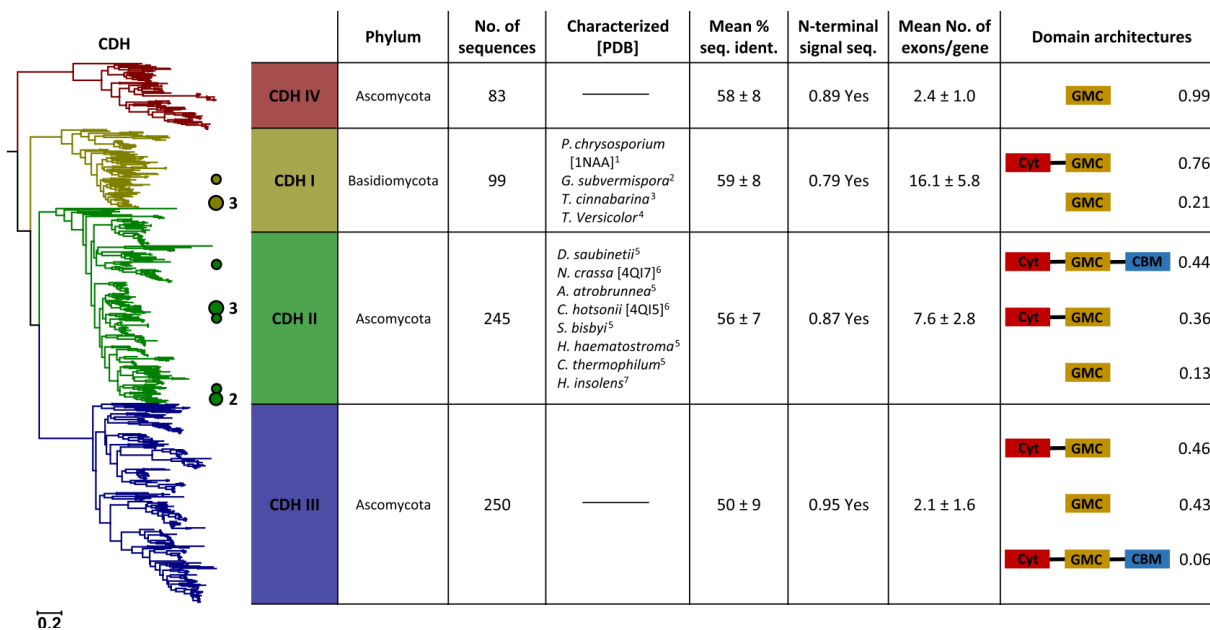


Figure 9 Phylogenetic tree of putative and characterized CDH sequences (flavin-domain only) based on the maximum-likelihood algorithm. Colored cycles and numbers indicate characterized members with biochemical evidence. Table by courtesy of L. Sützl (Sützl et al. 2019).

One should be careful with drawing assumptions on the physiological relevance of these dispersedly occurring sequences which constitute the dehydrogenase domain only. Until now, no comprehensive biochemical evidence could be gathered on these representatives and the whereabouts of enzymatic functions remain unclear. Thus, conclusion on their native biological role seem rather unmerited but can be supported by reports on the successful truncation of characterized CDH to the dehydrogenase domain. This allowed to elucidate substrate preferences and metrics of the enzymatic dehydrogenase activities, independent of any inter-domain electron transfer, as was described for the well-studied CDH of *Crassicarpon hotsonii* (Kracher et al. 2015; Tan et al. 2015); formerly referred to as *Myriococcum thermophilum*. Another study highlighted recently that CDH cyt and dehydrogenase domains from different organisms can be non-natively combined to form artificial chimeras, capable of efficient electron transfer between the partnering domains if electrostatic surface interactions are complementing (Felice et al. 2020). Following from that it has been reasonably hypothesized that the lack of a cytochrome domain coding sequence - as multiple examples across the phylogenetic tree underline - is indicative of the dehydrogenase domain being the underlying conserved part of the CDH enzyme. As such, fusion with an electron shuttling cyt domain happened as an independent event down the evolutionary path (Zámocký et al. 2004; Sützl et al. 2019) wherever it equipped the fungal host organisms with increased fitness, likely improving its biomass degrading capabilities via enzymatic synergisms.

Structure

CDH is a secretory enzyme and occurs in a monomeric form of approximately 100 kDa with glycosylation of the N- and O-type. CDH enzymes from 23 different fungal species are characterized as of today and several of the fungal host organisms account for the thermophilic or thermotolerant kind (Zámocký et al. 2008). Owing to the lifestyle of their host, some CDH enzymes display outstanding stability, withstanding temperatures of 70 °C or higher (Sigoillot et al. 2002; Langston et al. 2012) and resisting extreme pH (Bao, Usha, and Renganathan 1993), highlighting

the fitness required for enzymes to uphold activities in the demanding milieu of lignocellulose decomposition.

As is displayed in Figure 2, CDH comprises an N-terminal cytochrome (cyt) domain, embracing a *b*-type *heme* cofactor in the active site. This domain is around 25-30 kDa in molecular weight and bears N-linked glycosylation and usually several disulfide bonds. The cyt domain has a beta-sandwich fold resembling the immunoglobulin-like fold in its assembly of secondary structure elements (Martin Hallberg et al. 2002). The cyt domain is fused to the partnering dehydrogenase (DH) domain which holds an FAD cofactor non-covalently, contains two subdomains and is roughly 65 kDa in weight. Characteristically, the N-terminal part of the DH domain is formed from a meandering set of beta-sheets which is typical for nucleotide binding domains and observed frequently in FAD-binding proteins. It is commonly referred to as Rossmann fold or $\beta\alpha\beta$ motif, given the canonical assembly of beta-sheets, three alpha helices and more beta-sheets. The C-terminal moiety of the DH domain is known as substrate binding domain and contains the isoalloxazine ring system of the FAD in the active site (Martin Hallberg et al. 2002; Tan et al. 2015). The DH domain from the basidiomycetous CDH from *Phanerochaete chrysosporium* (PDB: 1KDG, 1NAA) was the first CDH to be partially resolved (Martin Hallberg et al. 2002). Later, crystal structures for the full-length enzyme were resolved for the ascomycetous CDHs from *C. hotsonii* (PDB: 4QI6) and *Neurospora crassa* (PDB: 4QI7), which proved to be bothersome initially owing to the dynamic nature of the enzyme.

The backbone of the multi-domain architecture of CDH is rooted in a flexible linker of around 25 amino acids (but often varying length), connecting the two domains at their respective posterior, thus allowing unaffected interaction of the FAD and *heme* reaction centers. One of the major takeaways from a study of chimeric CDH constructs was that the linker plays an important role in synchronizing the electron transfer from DH to cyt domain and that an exchange to a non-native tandem of linker and domains can have detrimental effects on this interaction, especially if a longer linker is inserted. Still, a complementary set of physicochemical properties is thought to be the key player in efficient electron transfer (Felice et al. 2020). A systematic analysis of the linker regions of basidiomycetous CDH sequence entries displays a fairly conserved set of rather charged residues at position 4-39 of the alignment and an ensuing segment rich in serine, threonine, glycine and

proline close to the beginning of the DH domain at Y/F/V-D-Y-I/V. It has often been discussed that this latter part of the linker serves in a protective manner with pronounced O-glycosylation preventing proteolytic cleavage of the individual domains (Sulej et al. 2013; 2015).

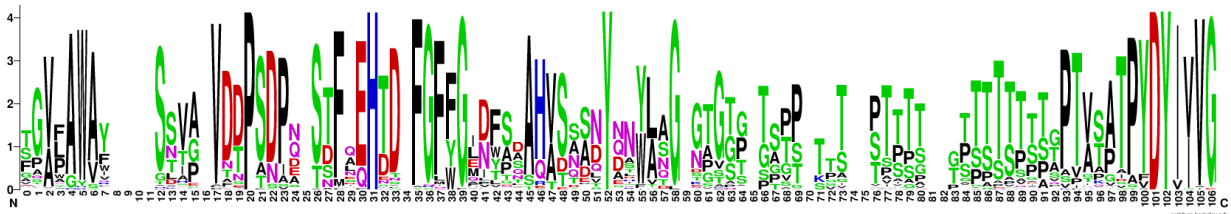


Figure 10 Weblogo illustration of a multiple sequence alignment of putative basidiomycetous CDH sequences of the linker region. The alignment was prepared from 82 sequence entries using the MAFFT algorithm with the G-INS-i accuracy-oriented presets. At the N-terminus, a conserved tryptophane (W) marks the end of the structural cyt domain and beginning of the linker region that stretches until a prloin (P), adjacent to the x-D-Y-I/V motif of the nucleotide binding domain.

Several representatives of CDH from ascomycetous origin is added a small additional non-catalytic domain to their bipartite architecture at the C-terminus, a carbohydrate-binding module (CBM). This domain was described to facilitate firm association of the enzyme with the cellulose polymer (Zámocký et al. 2006) thus increasing residence times at site and with it synergistic action with other enzymes such das LPMO (Sygmund et al. 2012). Interestingly, these CBM domains only occur in ascomycetous CDH of class II, allowing to sub-categorize these enzymes into Class II-A if a CBM is present. Even more interestingly, certain Ascomycetes like *Neurospora crassa* encode more than one CDH gene in their genome. Two functional *N. crassa* CDH were described, one of the class IIA equipped with a CBM and an additional CDH IIB lacking this extended module. The overall sequence identity of these enzymes is quite low (53 %) and rather dissimilar biochemical properties were reported (Harreither et al. 2011; Sygmund et al. 2012). It could be shown that a significant upregulation of the type IIA CDH expression is triggered by cellulolytic growth of the host whereas the IIB CDH expression is rather unaffected (Tian et al. 2009). The underlying physiological reason why the fungus benefits from two different CDH and why this peculiarity is specific to ascomycetous fungi is still to be solved.

Catalysis

CDH's substrate preference is generally biased towards β -(1,4)-linked sugars. Preferably, the enzyme accepts disaccharides and oligosaccharides that constitute a glucose moiety as the

terminal reducing end unit, such as β -D-cellobiose – its native substrate - and lactose, its closely related epimer. For these substrates a K_M around 0.1 mM and k_{cat} of 10-100 s⁻¹ is common. Basidiomycetous CDH are more restrictive in their substrate spectrum and commonly do not accept monosaccharides, or disaccharides with differing glycosidic connection (maltose). This is in contrast the case for CDH of certain ascomycetous fungi as was summarized (Kracher and Ludwig 2016; Scheiblbrandner and Ludwig 2020). In fact, a double digit K_M for D-glucose was reported for the ascomycetous CDH from *Thelavia terrestris* (Langston et al. 2012), *Hypoxylon haematostroma*, *Dichomera saubinetti* (Harreither et al. 2011) and *Corynascus thermophilus* (Harreither et al. 2012) whereas a K_M around 1000 mM is common for basidiomycetous CDHs (Kracher and Ludwig 2016).

During substrate oxidation, CDH acts on the C1 atom of the reducing end sugar. It has been proposed that the catalytic cycle is initiated with the attack of a catalytic histidine at the O1, ensuing abstraction of a (hydroxyl) proton and subsequently proceeds via a hydride transfer to the isoalloxazine N5, establishing FADH₂. In summary, the 2e⁻/2H⁺ type oxidation gains two electrons from the sugar conversion which are received by the FAD reducing it to its hydroquinone state concomitantly, in what is called the reductive half reaction (B. M. Hallberg et al. 2003). A comprehensive analysis on active side residues and their interaction with the substrate was carried out by Hallberg and colleagues with the DH domain of the *P. chrysosporium* CDH in complex with the cellobiono-1,5-lactam inhibitor (B. M. Hallberg et al. 2003). One will notice that this reaction mechanism is similar to the aforementioned mechanism of POx, which was described in greater detail in **part 9**. This is unsurprising when the shared ancestral background, comparable cofactor utilization and physiological involvement in biomass degradation of both enzymes are regarded (Sützl et al. 2018). From the fully reduced state, the flavin cofactor can then recover its quinone ground state by transferring electrons to a variety of electron acceptors during what is referred to as the oxidative half reaction.

Aside from suitable low molecular weight compounds such as quinones and phenols, or even oxygen, CDH is most prominent for the electron shuttling route from the DH to the partnering cyt domain. This transfer is thought to progress in a sequential exchange, shuttling only one electron at a time. Although a number of recent publications contributed to shed light on the enigmatic process that used to be the intra- and interdomain electron transfer, several of the molecular

configurations key to explaining the proposed shuttling mechanism are not confirmed to date. Most notably, presence of the intermediate FAD semiquinone state, harboring only a single electron could not confidently be determined; indications for its existence were found in experiments though (Igarashi et al. 2002). Still, it was observed that CDH undergoes a structural rearrangement during the transfer of single electrons from the DH to the cyt domain, a phenomenon which is potentially triggered by electrostatic repulsion of the respective domains resulting from the change of net charge during transfer (Igarashi et al. 2005; Kracher et al. 2015). This rearrangement is reflected in an “open” and “closed” conformation of the two-domain enzyme and could be confirmed in crystal structures (Tan et al. 2015). From a thermodynamic perspective, a sequential flux of electrons from the DH to the cyt domain (and onto a terminal acceptor) seems to be reasonable. It was shown that the redox potentials of the cyt domain - in both the reduced and oxidized state – can favor electron shuttling from the FAD since the electrochemical driving force is sufficiently high in both conditions (Vasile Coman et al. 2007; Tasca et al. 2011; Scheiblbrandner and Ludwig 2020). Just some years ago, the role of the cyt domain as a built-in electron relay was added another chapter when a specific electrochemical synergism with LPMO was described, which broadened the array of molecular considerations even wider (Kracher et al. 2016).

Bioelectrochemical applications

Owed to its unique ability to transfer electrons to artificial metallized and carbonous surfaces directly, CDH is in the spotlight for bioelectronic applications such enzymatic biosensors and biofuel cells. It is the electron-mediating nature of the enzyme together with its set of desirable biochemical properties (thermal stability, chemical resistance, high solubility, protein mobility, substrate specificity, high production yields) that make it exclusively well-suited and led to early developments almost 30 years ago (Elmgren, Lindquist, and Henriksson 1992). For modern biosensors, a direct interaction between electrode surface and enzyme is regarded as profoundly desirable as it permits to omit electron mediating compounds from the sensor setup, establishing what is called a 3rd generation biosensor depending on “direct electron transfer” (DET) (Felice et al. 2013). Mediators employed in 2nd generation sensor normally are redox active compounds bridging electron transfer between enzyme and electrode, which generally increases measurement signals sensitivity. Still, these molecules are oftentimes unsafe and interfere with

the physiological environment if incorporated into life tissue (Tasca et al. 2011; Harreither et al. 2012; Scheiblbrandner and Ludwig 2020).

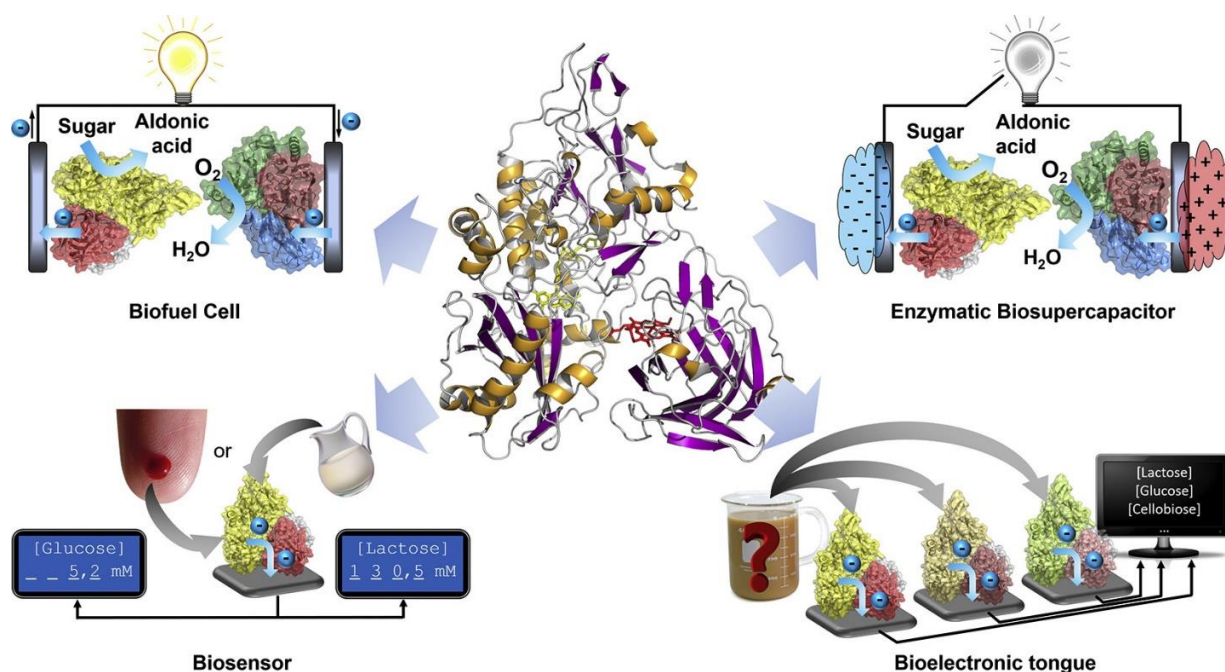


Figure 11 Graphical abstract summarizing the current and emerging bio-electrochemical applications of CDH: As bioanode element in biofuel cells (A) and in enzymatic biosupercapacitors (B); As recognition element in biosensors (C) and in bioelectronic tongues (D). The CDH enzyme is represented in a three-dimensional structure model in the middle. Graphic by courtesy of S. Scheiblbrandner (Scheiblbrandner and Ludwig 2020).

A holistic review on CDH from a bioelectrochemical perspective was assembled in 2020 by Scheiblbrandner and Ludwig and highlighted the utilization of CDH in four different bioelectronic applications: biosensors, biofuel cells, bio-supercapacitors and bioelectronic tongues as is summarized in Figure 11 (Scheiblbrandner and Ludwig 2020).

Enzymatic biosensors employ oxidoreductases like CDH to detect their preferred substrates as an analyte usually a complex solution (food, body fluids, environmental samples etc.). In architectures of the third generation, the enzyme performs its redox reaction and exchanges electrons with an artificial electrode surface directly. This creates an electrical current that is proportional to the turnover rate of the enzyme, and the analyte concentration consequently. When regarding the mono- and disaccharide substrates of CDH such as glucose, lactose, maltose a potential application in the food industry is rather obvious and research was strongly directed at it. Following from

academic research, the company DirectSens GmbH developed a CDH based biosensor for the detection of lactose in dairy products which is marketed globally under the name “lactosens”. Since several ascomycetous CDH were reported to accept glucose at least partially, a potential application of the enzyme in blood sugar monitoring and diabetic care was envisioned early. Later advancements led to the improvement of glucose acceptance and reduction of maltose interferences for the CDH of *Corynascus thermophilus* when two mutations were introduced into the active site (Ortiz et al. 2017). Additionally, the oxidative half reaction of the CDH catalysis was employed for sensing uses as well, and examples showed the biosensing capabilities for phenolic analytes such as catechol, dopamine, noradrenalin (Stoica et al. 2006) and others but efforts did not lead to a mature commercial product yet. A detailed summary on analytes, enzyme and detection limits can be found in a review from Ludwig and colleagues (Ludwig et al. 2013).

Contrasting to biosensors, the purpose of enzymatic biofuel cells is understood as generating as much electrical current as possible from substrates that are abundantly available **Figure 11**. This principle can be realized by the enzymatic conversion of physiologically relevant molecules such as glucose, lactate, oxygen, and others. Thus, these cells can operate locally isolated in tissue, which is envisioned to be ideal for powering bionic implants (González-Arribas et al. 2017). In that regard, CDH is a desirable candidate for the bioanodic element, oxidizing glucose or lactose *in-situ* and delivering the gained electrons to a suitable electrode at low potential. Trials have been conducted where the enzyme was partnered with a multicopper oxidase at the cathodic site, drawing electrons from the circuit that have previously been generated by CDH and transferring them on O₂ in its catalysis at a high electrochemical potential. This allows to generate power that is proportional to the electrochemical potential difference between the two enzymes and the reaction rates of converting the respective substrates as was highlighted in a study with the CDH from *Dichomera saubinetti* (Vasile Coman et al. 2008). In this application again CDH is favored over other enzymes which is rooted in its ability to transfer electrons directly which allows to minimize interference from mediators or electrochemically active compounds such as ascorbic acid (V. Coman et al. 2009). For the application under physiological conditions, CDH enzymes are desired that operate efficiently under neutral pH and convert glucose well, requirements that are generally fulfilled by ascomycetous CDH from class II (Scheiblbrandner and Ludwig 2020).

Parallel to providing power constantly, enzymes can also be used in combination with supercapacitors, charging the energy storage device from constant turnover. This generally allows to yield higher momentary power output, something that is often required in modern day miniaturized electronics. The functionality of a biosupercapacitors is comparable to biofuel cells and can in certain cases also just be a biofuel cell coupled to a supercapacitor to realize storage of electrons (or charge). In the simplest design, enzymes such as CDH are employed as the capacitive element, depending on their redox active cofactors to accommodate electron storage. In the perspective of energy density, the true three-dimensional structures that are proteins can help to store more energy in lower volumes. Other biosupercapacitor designs depend on self-charging and harvest electrons from progressing oxidation of a suitable substrate. These electrons can then be stored in the capacitor, trapped by an accumulating opposing charge that neutralizes the polarized electrode surface (Shleev, González-Arribas, and Falk 2017).

Another emerging field of bioelectrochemical applications that exploits CDH as a recognition element can be seen as an evolved form of biosensor array and is commonly referred to as “bioelectronic tongue” (BioET). There, the sensing principle lies in the combination of enzymes or enzyme variants in a biosensor setting, detecting multiple analytes from a complex solution simultaneously without pre-treatment to remove or digest certain analytes. Bioelectronic tongues have been developed for CDH before and exploit the fact, that enzymes from different host organisms display varying preferences for glucose and lactose. If a multiplexing electrode setup with multiple working electrodes is used, interferences in the measurement can be nicely eliminated and the general accuracy of analyte detection increases, as pioneering work from Cipri and colleagues underlined (Cipri et al. 2016).

In that regard, there are ample cases where CDH would benefit from improved enzymatic properties and advanced adaptation to the reaction conditions. As such, rooted in the outstanding stability and built-in electron array that is the cytochrome domain, CDH may represent an extraordinarily well-adapted enzyme for biosensing applications but could potentially see improvement in terms of substrate specificity or a substantially wider substrate palette, even. Certainly, an improved specificity towards certain mono- or disaccharides whilst excluding other

interfering, structurally related molecules would be undoubtedly valuable for any bioelectrochemical application and could broaden the palette for sensing applications. As the above-mentioned example of the CDH from *C. thermophilus*, harboring two active site mutations highlighted, substrate discrimination can be adapted with enzyme engineering, but takes considerable effort if rational design approaches reach their limits (Ortiz et al. 2017). When comparing substrate engineering endeavors of CDH to other redox enzymes such as laccase, it becomes evident that future focus in CDH engineering might better be directed towards evolutionary design, especially if it can be supported by computational methods, as recent success stories with laccase underline (Mate and Alcalde 2015; 2017; Santiago et al. 2016). Although the prerequisites might differ, a lack of high-throughput technology for CDH seems to currently hamper attempts for more sophisticated engineering of the enzyme. Methodologies that would be able to boost screening regimes (agar plate pre-screening, liquid handling automatization, display technology, microfluidics, cell sorting) are developed in part but only few examples show successful implementation in directed evolution and enzyme engineering and are almost never combined. Still, more advanced technologies and an even larger contribution from computational methods are expected in the upcoming years, together with a more radical utilization of established techniques, there is plenty of room for CDH success stories in the near future.

D) References (I)

- Abrera, Annabelle T., Leander Sützl, and Dietmar Haltrich. 2020. "Pyranose Oxidase: A Versatile Sugar Oxidoreductase for Bioelectrochemical Applications." *Bioelectrochemistry*. Elsevier B.V. <https://doi.org/10.1016/j.bioelechem.2019.107409>.
- Ahmad, Mark, Joseph N. Roberts, Elizabeth M. Hardiman, Rahul Singh, Lindsay D. Eltis, and Timothy D.H. Bugg. 2011. "Identification of DypB from *Rhodococcus Jostii* RHA1 as a Lignin Peroxidase." *Biochemistry* 50 (23): 5096–5107. <https://doi.org/10.1021/bi101892z>.
- Ai, Ming-Qiang, Fang-Fang Wang, Yu-Zhong Zhang, and Feng Huang. 2014. "Purification of Pyranose Oxidase from the White Rot Fungus *Irpex Lacteus* and Its Cooperation with Laccase in Lignin Degradation." *Process Biochemistry* 49 (12): 2191–98. <https://doi.org/10.1016/J.PROCBIO.2014.10.001>.
- Albrecht, Mario, and Thomas Lengauer. 2003. "Pyranose Oxidase Identified as a Member of the GMC Oxidoreductase Family." *Bioinformatics* 19 (10): 1216–20. <https://doi.org/10.1093/bioinformatics/btg140>.
- Aldridge, Susan. 2013. "Industry Backs Biocatalysis for Greener Manufacturing." *Nature Biotechnology*. <https://doi.org/10.1038/nbt0213-95>.
- Andlar, Martina, Tonči Rezić, Nenad Marđetko, Daniel Kracher, Roland Ludwig, and Božidar Šantek. 2018. "Lignocellulose Degradation: An Overview of Fungi and Fungal Enzymes Involved in Lignocellulose Degradation." *Engineering in Life Sciences* 18 (11): 768–78. <https://doi.org/10.1002/elsc.201800039>.
- Arregui, Leticia, Marcela Ayala, Ximena Gómez-Gil, Guadalupe Gutiérrez-Soto, Carlos Eduardo Hernández-Luna, Mayra Herrera De Los Santos, Laura Levin, et al. 2019. "Laccases: Structure, Function, and Potential Application in Water Bioremediation." *Microbial Cell Factories*. BioMed Central Ltd. <https://doi.org/10.1186/s12934-019-1248-0>.
- Bannwarth, Michael, Sabine Bastian, Dorothee Heckmann-Pohl, Friedrich Giffhorn, and Georg E. Schulz. 2004. "Crystal Structure of Pyranose 2-Oxidase from the White-Rot Fungus *Peniophora* Sp." *Biochemistry* 43 (37): 11683–90. <https://doi.org/10.1021/bi048609q>.
- Bao, Wenjun, S. N. Usha, and V. Renganathan. 1993. "Purification and Characterization of Cellobiose Dehydrogenase, a Novel Extracellular Hemoflavoenzyme from the White-Rot

- Fungus *Phanerochaete chrysosporium*." *Archives of Biochemistry and Biophysics* 300 (2): 705–13. <https://doi.org/10.1006/abbi.1993.1098>.
- Baute, Robert, Marie Antoinette Baute, Gérard Deffieux, and Marie José Filleau. 1976. "Corticalcerone, a New Antibiotic Induced by External Agents in *Corticium caeruleum*." *Phytochemistry* 15 (11): 1753–55. [https://doi.org/10.1016/S0031-9422\(00\)97471-5](https://doi.org/10.1016/S0031-9422(00)97471-5).
- Berg, Jeremy M., John L. Tymoczko, Gregory J. Gatto, and Lubert Stryer. 2015. *Biochemistry-W.H. Freeman*. 8th ed. New York : W.H. Freeman. <https://doi.org/10.1360/zd-2013-43-6-1064>.
- Bornscheuer, U. T., G. W. Huisman, R. J. Kazlauskas, S. Lutz, J. C. Moore, and K. Robins. 2012. "Engineering the Third Wave of Biocatalysis." *Nature* 485 (7397): 185–94. <https://doi.org/10.1038/nature11117>.
- Brown, Margaret E., Tiago Barros, and Michelle C Y Chang. 2012. "Identification and Characterization of a Multifunctional Dye Peroxidase from a Lignin-Reactive Bacterium." *ACS Chemical Biology* 7 (12): 2074–81. <https://doi.org/10.1021/cb300383y>.
- Brown, Margaret E., and Michelle C Y Chang. 2014. "Exploring Bacterial Lignin Degradation." *Current Opinion in Chemical Biology* 19 (1): 1–7. <https://doi.org/10.1016/j.cbpa.2013.11.015>.
- Bugg, Timothy D.H. 2009. *Introduction to Enzyme and Coenzyme Chemistry: Second Edition*. *Introduction to Enzyme and Coenzyme Chemistry: Second Edition*. Wiley. <https://doi.org/10.1002/9781444305364>.
- Bugg, Timothy D.H., Mark Ahmad, Elizabeth M. Hardiman, and Rahman Rahmanpour. 2011. "Pathways for Degradation of Lignin in Bacteria and Fungi." *Natural Product Reports* 28 (12): 1883–96. <https://doi.org/10.1039/c1np00042j>.
- Cavener, Douglas R. 1992. "GMC Oxidoreductases: A Newly Defined Family of Homologous Proteins with Diverse Catalytic Activities." *Journal of Molecular Biology* 223 (3): 811–14. [https://doi.org/10.1016/0022-2836\(92\)90992-S](https://doi.org/10.1016/0022-2836(92)90992-S).
- Chaiyen, Pimchai, Marco W. Fraaije, and Andrea Mattevi. 2012. "The Enigmatic Reaction of Flavins with Oxygen." *Trends in Biochemical Sciences*. Elsevier Current Trends. <https://doi.org/10.1016/j.tibs.2012.06.005>.
- Choi, Jung Min, Sang Soo Han, and Hak Sung Kim. 2015. "Industrial Applications of Enzyme Biocatalysis: Current Status and Future Aspects." *Biotechnology Advances*. Elsevier Inc.

- <https://doi.org/10.1016/j.biotechadv.2015.02.014>.
- Christgen, Shelbi L., Sophia M. Becker, and Donald F. Becker. 2019. "Methods for Determining the Reduction Potentials of Flavin Enzymes." In *Methods in Enzymology*, 620:1–25. Academic Press Inc. <https://doi.org/10.1016/bs.mie.2019.03.004>.
- Christopher, Lew Paul, Bin Yao, and Yun Ji. 2014. "Lignin Biodegradation with Laccase-Mediator Systems." *Frontiers in Energy Research*. Frontiers Media S.A. <https://doi.org/10.3389/fenrg.2014.00012>.
- Chundawat, Shishir P.S., Gregg T. Beckham, Michael E. Himmel, and Bruce E. Dale. 2011. "Deconstruction of Lignocellulosic Biomass to Fuels and Chemicals." *Annual Review of Chemical and Biomolecular Engineering* 2 (1): 121–45. <https://doi.org/10.1146/annurev-chembioeng-061010-114205>.
- Cipri, Andrea, Christopher Schulz, Roland Ludwig, Lo Gorton, and Manel del Valle. 2016. "A Novel Bio-Electronic Tongue Using Different Cellobiose Dehydrogenases to Resolve Mixtures of Various Sugars and Interfering Analytes." *Biosensors and Bioelectronics* 79: 515–21. <https://doi.org/10.1016/j.bios.2015.12.069>.
- Colpa, Dana I., Marco W. Fraaije, and Edwin Van Bloois. 2014. "DyP-Type Peroxidases: A Promising and Versatile Class of Enzymes." *Journal of Industrial Microbiology and Biotechnology*. Springer Berlin Heidelberg. <https://doi.org/10.1007/s10295-013-1371-6>.
- Coman, V., R. Ludwig, W. Harreither, D. Haltrich, L. Gorton, T. Ruzgas, and S. Shleev. 2009. "A Direct Electron Transfer-Based Glucose/Oxygen Biofuel Cell Operating in Human Serum." *Fuel Cells* 10 (1): NA-NA. <https://doi.org/10.1002/fuce.200900121>.
- Coman, Vasile, Wolfgang Harreither, Roland Ludwig, Dietmar Haltrich, and Lo Gorton. 2007. "Investigation of Electron Transfer between Cellobiose Dehydrogenase from *Myriococcum Thermophilum* and Gold Electrodes." *Chemical Analysis* 52 (6): 945–60. [https://portal.research.lu.se/portal/en/publications/investigation-of-electron-transfer-between-cellobiose-dehydrogenase-from-myriococcum-thermophilum-and-gold-electrodes\(c1b7558a-f7e0-4fb9-9d6c-f73fd9a6fa4c\).html](https://portal.research.lu.se/portal/en/publications/investigation-of-electron-transfer-between-cellobiose-dehydrogenase-from-myriococcum-thermophilum-and-gold-electrodes(c1b7558a-f7e0-4fb9-9d6c-f73fd9a6fa4c).html).
- Coman, Vasile, Cristina Vaz-Domínguez, Roland Ludwig, Wolfgang Harreither, Dietmar Haltrich, Antonio L. De Lacey, Tautgirdas Ruzgas, Lo Gorton, and Sergey Shleev. 2008. "A Membrane-, Mediator-, Cofactor-Less Glucose/Oxygen Biofuel Cell." *Physical Chemistry Chemical Physics*

- 10 (40): 6093–96. <https://doi.org/10.1039/b808859d>.
- Cragg, Simon M., Gregg T. Beckham, Neil C. Bruce, Timothy D.H. Bugg, Daniel L. Distel, Paul Dupree, Amaia Green Etxabe, et al. 2015. “Lignocellulose Degradation Mechanisms across the Tree of Life.” *Current Opinion in Chemical Biology* 29: 108–19. <https://doi.org/10.1016/j.cbpa.2015.10.018>.
- Eastwood, Daniel C, Dimitrios Floudas, Manfred Binder, Andrzej Majcherczyk, Patrick Schneider, Andrea Aerts, Fred O Asiegbu, et al. 2011. “The Plant Cell Wall-Decomposing Machinery Underlies the Functional Diversity of Forest Fungi.” *Science* 333 (6043): 762–65. <https://doi.org/10.1126/science.1205411>.
- Elmgren, Maja, Sten Eric Lindquist, and Gunnar Henriksson. 1992. “Cellobiose Oxidase Crosslinked in a Redox Polymer Matrix at an Electrode Surface—a New Biosensor.” *Journal of Electroanalytical Chemistry* 341 (1–2): 257–73. [https://doi.org/10.1016/0022-0728\(92\)80487-O](https://doi.org/10.1016/0022-0728(92)80487-O).
- Felice, Alfons K. G., Christian Schuster, Alan Kadek, Frantisek Filandr, Christophe V. F. P. Laurent, Stefan Scheiblbrandner, Lorenz Schwaiger, et al. 2020. “Chimeric Cellobiose Dehydrogenases Reveal the Function of Cytochrome Domain Mobility for the Electron Transfer to Lytic Polysaccharide Monooxygenase.” *ACS Catalysis* 28: 517–32. <https://doi.org/10.1021/acscatal.0c05294>.
- Felice, Alfons K.G., Christoph Sygmund, Wolfgang Harreither, Roman Kittl, Lo Gorton, and Roland Ludwig. 2013. “Substrate Specificity and Interferences of a Direct-Electron-Transfer-Based Glucose Biosensor.” *Journal of Diabetes Science and Technology* 7 (3): 669–77. <https://doi.org/10.1177/193229681300700312>.
- Ferri, Stefano, Katsuhiko Kojima, and Koji Sode. 2011. “Review of Glucose Oxidases and Glucose Dehydrogenases: A Bird’s Eye View of Glucose Sensing Enzymes.” In *Journal of Diabetes Science and Technology*, 5:1068–76. Diabetes Technology Society. <https://doi.org/10.1177/193229681100500507>.
- Gauna, Albertina, Alvaro S Larran, Susana R Feldman, Hugo R Permingeat, and Valeria E Perotti. 2020. “Secretome Characterization of the Lignocellulose-Degrading Fungi *Pycnoporus Sanguineus* and *Ganoderma Applanatum*.” *BioRxiv*, September, 2020.09.22.308908. <https://doi.org/10.1101/2020.09.22.308908>.

- Gokoglan, Tugba Ceren, Saniye Soylemez, Melis Kesik, Sinem Toksabay, and Levent Toppare. 2015. "Selenium Containing Conducting Polymer Based Pyranose Oxidase Biosensor for Glucose Detection." *Food Chemistry* 172 (April): 219–24. <https://doi.org/10.1016/j.foodchem.2014.09.065>.
- González-Arribas, Elena, Tim Bobrowski, Chiara Di Bari, Kirill Sliozberg, Roland Ludwig, Miguel D. Toscano, Antonio L. De Lacey, Marcos Pita, Wolfgang Schuhmann, and Sergey Shleev. 2017. "Transparent, Mediator- and Membrane-Free Enzymatic Fuel Cell Based on Nanostructured Chemically Modified Indium Tin Oxide Electrodes." *Biosensors and Bioelectronics* 97: 46–52. <https://doi.org/10.1016/j.bios.2017.05.040>.
- Gonzalez-Solino, Carla, and Mirella Di Lorenzo. 2018. "Enzymatic Fuel Cells: Towards Self-Powered Implantable and Wearable Diagnostics." *Biosensors*. MDPI AG. <https://doi.org/10.3390/bios8010011>.
- Gonzalo, Gonzalo de, Dana I. Colpa, Mohamed H.M. Habib, and Marco W. Fraaije. 2016. "Bacterial Enzymes Involved in Lignin Degradation." *Journal of Biotechnology* 236: 110–19. <https://doi.org/10.1016/j.jbiotec.2016.08.011>.
- Halada, Petr, Christian Leitner, Petr Sedmera, Dietmar Haltrich, and Jindřich Volc. 2003. "Identification of the Covalent Flavin Adenine Dinucleotide-Binding Region in Pyranose 2-Oxidase from *Trametes Multicolor*." *Analytical Biochemistry* 314 (2): 235–42. [https://doi.org/10.1016/S0003-2697\(02\)00661-9](https://doi.org/10.1016/S0003-2697(02)00661-9).
- Hallberg, B. Martin, Gunnar Henriksson, Göran Pettersson, Andrea Vasella, and Christina Divne. 2003. "Mechanism of the Reductive Half-Reaction in Cellobiose Dehydrogenase." *Journal of Biological Chemistry* 278 (9): 7160–66. <https://doi.org/10.1074/jbc.M210961200>.
- Hallberg, Martin, Christian Leitner, Dietmar Haltrich, and Christina Divne. 2004. "Crystal Structure of the 270 KDa Homotetrameric Lignin-Degrading Enzyme Pyranose 2-Oxidase." *Journal of Molecular Biology* 341 (3): 781–96. <https://doi.org/10.1016/j.jmb.2004.06.033>.
- Harreither, Wolfgang, Alfons K. G. Felice, Regina Paukner, Lo Gorton, Roland Ludwig, and Christoph Sygmund. 2012. "Recombinantly Produced Cellobiose Dehydrogenase from *Corynascus Thermophilus* for Glucose Biosensors and Biofuel Cells." *Biotechnology Journal* 7 (11): 1359–66. <https://doi.org/10.1002/biot.201200049>.
- Harreither, Wolfgang, Christoph Sygmund, Manfred Augustin, Melanie Narciso, Mikhail L.

- Rabinovich, Lo Gorton, Dietmar Haltrich, and Roland Ludwig. 2011. "Catalytic Properties and Classification of Cellobiose Dehydrogenases from Ascomycetes." *Applied and Environmental Microbiology* 77 (5): 1804–15. <https://doi.org/10.1128/AEM.02052-10>.
- Hassan, Noor, Tien Chye Tan, Oliver Spadiut, Ines Pisanelli, Laura Fusco, Dietmar Haltrich, Clemens K. Peterbauer, and Christina Divne. 2013. "Crystal Structures of Phanerochaete Chrysosporium Pyranose 2-Oxidase Suggest That the N-Terminus Acts as a Propeptide That Assists in Homotetramer Assembly." *FEBS Open Bio* 3 (1): 496–504. <https://doi.org/10.1016/j.fob.2013.10.010>.
- Herzog, Peter L, Leander Sützl, Beate Eisenhut, Daniel Maresch, Dietmar Haltrich, Christian Obinger, and Clemens K Peterbauer. 2019. "Versatile Oxidase and Dehydrogenase Activities of Bacterial Pyranose 2-Oxidase Facilitate Redox Cycling with Manganese Peroxidase In Vitro." *Applied and Environmental Microbiology* 85 (13): e00390-19. <https://doi.org/10.1128/AEM.00390-19>.
- Himmel, Michael E., Shi You Ding, David K. Johnson, William S. Adney, Mark R. Nimlos, John W. Brady, and Thomas D. Foust. 2007. "Biomass Recalcitrance: Engineering Plants and Enzymes for Biofuels Production." *Science*. <https://doi.org/10.1126/science.1137016>.
- Igarashi, Kiyohiko, Ikuo Momohara, Takeshi Nishino, and Masahiro Samejima. 2002. "Kinetics of Inter-Domain Electron Transfer in Flavocytochrome Cellobiose Dehydrogenase from the White-Rot Fungus Phanerochaete Chrysosporium." *Biochemical Journal* 365 (2): 521–26. <https://doi.org/10.1042/BJ20011809>.
- Igarashi, Kiyohiko, Makoto Yoshida, Hirotoishi Matsumura, Nobuhumi Nakamura, Hiroyuki Ohno, Masahiro Samejima, Takeshi Nishino, and Correspondence K Igarashi. 2005. "Electron Transfer Chain Reaction of the Extracellular Flavocytochrome Cellobiose Dehydrogenase from the Basidiomycete Phanerochaete Chrysosporium." *FEBS Journal* 272: 2869–77. <https://doi.org/10.1111/j.1742-4658.2005.04707.x>.
- Illanes, Andrés. 2008. *Enzyme Biocatalysis: Principles and Applications*. *Enzyme Biocatalysis: Principles and Applications*. Springer Netherlands. <https://doi.org/10.1007/978-1-4020-8361-7>.
- Janssen, Frank, and Hans W. Ruelius. 1975. "Pyranose Oxidase from Polyporus Obtusus." *Methods in Enzymology* 41 (C): 170–73. [https://doi.org/10.1016/S0076-6879\(75\)41041-2](https://doi.org/10.1016/S0076-6879(75)41041-2).

- Janssen, Frank W., and Hans W. Ruelius. 1968. "Carbohydrate Oxidase, a Novel Enzyme from *Polyporus Obtusus*." *Biochimica et Biophysica Acta (BBA) - Enzymology* 167 (3): 501–10. [https://doi.org/10.1016/0005-2744\(68\)90040-5](https://doi.org/10.1016/0005-2744(68)90040-5).
- Joosten, Vivi, and Willem JH van Berkel. 2007. "Flavoenzymes." *Current Opinion in Chemical Biology*. Elsevier Current Trends. <https://doi.org/10.1016/j.cbpa.2007.01.010>.
- Kennedy, J.F., and L.L. Lloyd. 1994. "Enzyme Nomenclature — Recommendations of the Nomenclature Committee of the International Union of Biochemistry and Molecular Biology." *Carbohydrate Polymers* 23 (4): 291–92. [https://doi.org/10.1016/0144-8617\(94\)90194-5](https://doi.org/10.1016/0144-8617(94)90194-5).
- Kim, Seong Jun, and Makoto Shoda. 1999. "Purification and Characterization of a Novel Peroxidase from *Geotrichum Candidum* Dec 1 Involved in Decolorization of Dyes." *Applied and Environmental Microbiology* 65 (3): 1029–35. <https://doi.org/10.1128/aem.65.3.1029-1035.1999>.
- Koshland, Daniel E. 2002. "The Seven Pillars of Life." *Science*. <https://doi.org/10.1126/science.1068489>.
- Kothes, Kirston, Robert Halenbeck, and Margaret Moreland. 1992. "Synthesis of the Antibiotic Cortalcerone from D-Glucose Using Pyranose 2-Oxidase and a Novel Fungal Enzyme, Aldos-2-Ulose Dehydratase." *Carbohydrate Research* 232 (1): 59–75. [https://doi.org/10.1016/S0008-6215\(00\)90994-7](https://doi.org/10.1016/S0008-6215(00)90994-7).
- Kracher, Daniel, Zarah Forsberg, Bastien Bissaro, Sonja Gangl, Marita Preims, Christoph Sygmund, Vincent G.H. Eijsink, and Roland Ludwig. 2019. "Polysaccharide Oxidation by Lytic Polysaccharide Monooxygenase Is Enhanced by Engineered Cellobiose Dehydrogenase." *FEBS Journal*, October, febs.15067. <https://doi.org/10.1111/febs.15067>.
- Kracher, Daniel, and Roland Ludwig. 2016. "Cellobiose Dehydrogenase: An Essential Enzyme for Lignocellulose Degradation in Nature - A Review." *Bodenkultur*. Sciendo. <https://doi.org/10.1515/boku-2016-0013>.
- Kracher, Daniel, Stefan Scheiblbrandner, Alfons K.G. Felice, Erik Breslmayr, Marita Preims, Karolina Ludwicka, Dietmar Haltrich, Vincent G.H. Eijsink, and Roland Ludwig. 2016. "Extracellular Electron Transfer Systems Fuel Cellulose Oxidative Degradation." *Science* 352 (6289): 1098–1101. <https://doi.org/10.1126/science.aaf3165>.

- Kracher, Daniel, Kawah Zahma, Christopher Schulz, Christoph Sygmund, Lo Gorton, and Roland Ludwig. 2015. "Inter-Domain Electron Transfer in Cellobiose Dehydrogenase: Modulation by PH and Divalent Cations." *The FEBS Journal* 282 (16): 3136–48.
<https://doi.org/10.1111/febs.13310>.
- Kurbanoglu, Sevinc, Muhammed Nadeem Zafar, Federico Tasca, Iqra Aslam, Oliver Spadiut, Dónal Leech, Dietmar Haltrich, and Lo Gorton. 2018. "Amperometric Flow Injection Analysis of Glucose and Galactose Based on Engineered Pyranose 2-Oxidases and Osmium Polymers for Biosensor Applications." *Electroanalysis* 30 (7): 1496–1504.
<https://doi.org/10.1002/elan.201800096>.
- Langston, James A., Kimberly Brown, Feng Xu, Kim Borch, Ashley Garner, and Matt D. Sweeney. 2012. "Cloning, Expression, and Characterization of a Cellobiose Dehydrogenase from *Thielavia Terrestris* Induced under Cellulose Growth Conditions." *Biochimica et Biophysica Acta - Proteins and Proteomics* 1824 (6): 802–12.
<https://doi.org/10.1016/j.bbapap.2012.03.009>.
- Laurent, Christophe V.F.P., Erik Breslmayr, Daniel Tunega, Roland Ludwig, and Chris Oostenbrink. 2019. "Interaction between Cellobiose Dehydrogenase and Lytic Polysaccharide Monooxygenase." *Biochemistry* 58 (9): 1226–35.
<https://doi.org/10.1021/acs.biochem.8b01178>.
- Lee, Marina S., Jenna R. Bonner, David J. Bernard, Erica L. Sanchez, Eric T. Sause, R. Reid Prentice, Shawn M. Burgess, and Lawrence C. Brody. 2012. "Disruption of the Folate Pathway in Zebrafish Causes Developmental Defects." *BMC Developmental Biology* 12.
<https://doi.org/10.1186/1471-213X-12-12>.
- Leitner, Christian, Jindrich Volc, and Dietmar Haltrich. 2001. "Purification and Characterization of Pyranose Oxidase from the White Rot Fungus *Trametes Multicolor* Purification and Characterization of Pyranose Oxidase from the White Rot Fungus *Trametes Multicolor*" 67 (8): 3636–44. <https://doi.org/10.1128/AEM.67.8.3636>.
- Levasseur, Anthony, Elodie Drula, Vincent Lombard, Pedro M Coutinho, and Bernard Henrissat. 2013. "Expansion of the Enzymatic Repertoire of the CAZy Database to Integrate Auxiliary Redox Enzymes." *Biotechnology for Biofuels* 6 (1): 41. <https://doi.org/10.1186/1754-6834-6-41>.

- Lidén, Helena, Jindrich Volc, György Marko-Varga, and Lo Gorton. 1998. "Pyranose Oxidase Modified Carbon Paste Electrodes for Monosaccharide Determination." *Electroanalysis* 10 (4): 223–30. [https://doi.org/10.1002/\(SICI\)1521-4109\(199804\)10:4<223::AID-ELAN223>3.0.CO;2-7](https://doi.org/10.1002/(SICI)1521-4109(199804)10:4<223::AID-ELAN223>3.0.CO;2-7).
- Lindskog, Sven. 1997. "Structure and Mechanism of Carbonic Anhydrase." *Pharmacology and Therapeutics*. Elsevier Inc. [https://doi.org/10.1016/S0163-7258\(96\)00198-2](https://doi.org/10.1016/S0163-7258(96)00198-2).
- Liu, Qingquan, Le Luo, and Luqing Zheng. 2018. "Lignins: Biosynthesis and Biological Functions in Plants." *International Journal of Molecular Sciences* 19 (2): 335. <https://doi.org/10.3390/ijms19020335>.
- Loix, Christophe, Michiel Huybrechts, Jaco Vangronsveld, Marijke Gielen, Els Keunen, and Ann Cuypers. 2017. "Reciprocal Interactions between Cadmium-Induced Cell Wall Responses and Oxidative Stress in Plants." *Frontiers in Plant Science*. Frontiers Media S.A. <https://doi.org/10.3389/fpls.2017.01867>.
- Lombard, Vincent, Hemalatha Golaconda Ramulu, Elodie Drula, Pedro M Coutinho, and Bernard Henrissat. 2014. "The Carbohydrate-Active Enzymes Database (CAZy) in 2013." *Nucleic Acids Research* 42 (Database issue): D490–95. <https://doi.org/10.1093/nar/gkt1178>.
- Longe, Lionel F., Julien Couvreur, Mathilde Leriche Grandchamp, Gil Garnier, Florent Allais, and Kei Saito. 2018. "Importance of Mediators for Lignin Degradation by Fungal Laccase." *ACS Sustainable Chemistry and Engineering* 6 (8): 10097–107. <https://doi.org/10.1021/acssuschemeng.8b01426>.
- Ludwig, Roland, Roberto Ortiz, Christopher Schulz, Wolfgang Harreither, Christoph Sygmund, and Lo Gorton. 2013. "Cellobiose Dehydrogenase Modified Electrodes: Advances by Materials Science and Biochemical Engineering." *Analytical and Bioanalytical Chemistry*. Springer. <https://doi.org/10.1007/s00216-012-6627-x>.
- Maciel, Márcia Jaqueline Mendonça, Ademir Castro e Silva, and Helena Camarão Telles Ribeiro. 2010. "Industrial and Biotechnological Applications of Ligninolytic Enzymes of the Basidiomycota: A Review." *Electronic Journal of Biotechnology*. <https://doi.org/10.2225/vol13-issue6-fulltext-2>.
- Majumdar, Sudipta, Tiit Lukk, Jose O. Solbiati, Stefan Bauer, Satish K. Nair, John E. Cronan, and John A. Gerlt. 2014. "Roles of Small Laccases from *Streptomyces* in Lignin Degradation."

- Biochemistry* 53 (24): 4047–58. <https://doi.org/10.1021/bi500285t>.
- Mäkelä, Miia R., Nicole Donofrio, and Ronald P. De Vries. 2014. “Plant Biomass Degradation by Fungi.” *Fungal Genetics and Biology* 72 (November): 2–9. <https://doi.org/10.1016/j.fgb.2014.08.010>.
- Mansoorabadi, Steven O., Christopher J. Thibodeaux, and Hung Wen Liu. 2007. “The Diverse Roles of Flavin Coenzymes - Nature’s Most Versatile Thespians.” *Journal of Organic Chemistry*. NIH Public Access. <https://doi.org/10.1021/jo0703092>.
- Martin Hallberg, B., Gunnar Henriksson, Göran Pettersson, and Christina Divne. 2002. “Crystal Structure of the Flavoprotein Domain of the Extracellular Flavocytochrome Cellobiose Dehydrogenase.” *Journal of Molecular Biology* 315 (3): 421–34. <https://doi.org/10.1006/jmbi.2001.5246>.
- Massey Vincent. 1994. “Activation of Molecular Oxygen by Flavins and Flavoproteins.” *Journal of Biological Chemistry* 269 (36): 22459–62. <https://doi.org/10.1017/CBO9781107415324.004>.
- Mate, Diana M., and Miguel Alcalde. 2015. “Laccase Engineering: From Rational Design to Directed Evolution.” *Biotechnology Advances*. Elsevier Inc. <https://doi.org/10.1016/j.biotechadv.2014.12.007>.
- Mate, Diana M., and Miguel Alcalde. 2017. “Laccase: A Multi-Purpose Biocatalyst at the Forefront of Biotechnology.” *Microbial Biotechnology*. John Wiley and Sons Ltd. <https://doi.org/10.1111/1751-7915.12422>.
- Mattevi, Andrea. 2006. “To Be or Not to Be an Oxidase: Challenging the Oxygen Reactivity of Flavoenzymes.” *Trends in Biochemical Sciences*. Elsevier Current Trends. <https://doi.org/10.1016/j.tibs.2006.03.003>.
- McDonald, Claudia A., Rebecca L. Fagan, François Collard, Vincent M. Monnier, and Bruce A. Palfey. 2011. “Oxygen Reactivity in Flavoenzymes: Context Matters.” *Journal of the American Chemical Society* 133 (42): 16809–11. <https://doi.org/10.1021/ja2081873>.
- Mendes, Sónia, Catarina Banha, Joaquim Madeira, Diana Santos, Vanessa Miranda, Maximino Manzanera, M. Rita Ventura, Willem J.H. van Berkel, and Lúcia O. Martins. 2016. “Characterization of a Bacterial Pyranose 2-Oxidase from *Arthrobacter Siccitolerans*.” *Journal of Molecular Catalysis B: Enzymatic* 133: S34–43. <https://doi.org/10.1016/j.molcatb.2016.11.005>.

- Nishimura, Ikuko, Kimiharu Okada, and Yasuji Koyama. 1996. "Cloning and Expression of Pyranose Oxidase cDNA from *Coriolus Versicolor* in *Escherichia Coli*." *Journal of Biotechnology* 52 (1): 11–20. [https://doi.org/10.1016/S0168-1656\(96\)01618-5](https://doi.org/10.1016/S0168-1656(96)01618-5).
- Nousiainen, Paula, Jussi Kontro, Helmiina Manner, Annele Hatakka, and Jussi Sipilä. 2014. "Phenolic Mediators Enhance the Manganese Peroxidase Catalyzed Oxidation of Recalcitrant Lignin Model Compounds and Synthetic Lignin." *Fungal Genetics and Biology* 72 (November): 137–49. <https://doi.org/10.1016/J.FGB.2014.07.008>.
- Nowatzke, William, Mark J. Sarno, Nathan C. Birch, Douglas F. Stickle, Tanya Eden, and Thomas G. Cole. 2004. "Evaluation of an Assay for Serum 1,5-Anhydroglucitol (GlycoMark™) and Determination of Reference Intervals on the Hitachi 917 Analyzer." *Clinica Chimica Acta* 350 (1–2): 201–9. <https://doi.org/10.1016/j.cccn.2004.08.013>.
- Odaci, Dilek, Azmi Telefoncu, and Suna Timur. 2008. "Pyranose Oxidase Biosensor Based on Carbon Nanotube (CNT)-Modified Carbon Paste Electrodes." *Sensors and Actuators, B: Chemical* 132 (1): 159–65. <https://doi.org/10.1016/j.snb.2008.01.020>.
- Odaci, Dilek, Azmi Telefoncu, and Suná Timur. 2010. "Maltose Biosensing Based on Co-Immobilization of α -Glucosidase and Pyranose Oxidase." *Bioelectrochemistry* 79 (1): 108–13. <https://doi.org/10.1016/j.bioelechem.2009.12.010>.
- Ortiz, Roberto, Mahbubur Rahman, Beatrice Zangrilli, Christoph Sygmund, Pernille O. Micheelsen, Maria Silow, Miguel D. Toscano, Roland Ludwig, and Lo Gorton. 2017. "Engineering of Cellobiose Dehydrogenases for Improved Glucose Sensitivity and Reduced Maltose Affinity." *ChemElectroChem* 4 (4): 846–55. <https://doi.org/10.1002/celc.201600781>.
- Paës, Gabriel, David Navarro, Yves Benoit, Senta Blanquet, Brigitte Chabbert, Bernard Chaussepied, Pedro M. Coutinho, et al. 2019. "Tracking of Enzymatic Biomass Deconstruction by Fungal Secretomes Highlights Markers of Lignocellulose Recalcitrance." *Biotechnology for Biofuels* 12 (1): 76. <https://doi.org/10.1186/s13068-019-1417-8>.
- Peterbauer, Clemens K. 2020. "Pyranose Dehydrogenases: Rare Enzymes for Electrochemistry and Biocatalysis." *Bioelectrochemistry*. Elsevier B.V. <https://doi.org/10.1016/j.bioelechem.2019.107399>.
- Pisanelli, Ines, Magdalena Kujawa, Oliver Spadiut, Roman Kittl, Petr Halada, Jindrich Volc, Michael D. Mozuch, Philip Kersten, Dietmar Haltrich, and Clemens Peterbauer. 2009. "Pyranose 2-

- Oxidase from *Phanerochaete Chrysosporium*—Expression in *E. Coli* and Biochemical Characterization.” *Journal of Biotechnology* 142 (2): 97–106.
<https://doi.org/10.1016/J.JBIOTEC.2009.03.019>.
- Qin, Xing, Huiying Luo, Xiaoyu Zhang, Bin Yao, Fuying Ma, and Xiaoyun Su. 2018. “Dye-Decolorizing Peroxidases in *Irpex Lacteus* Combining the Catalytic Properties of Heme Peroxidases and Laccase Play Important Roles in Ligninolytic System.” *Biotechnology for Biofuels* 11 (1): 302. <https://doi.org/10.1186/s13068-018-1303-9>.
- Raveendran, Sindhu, Binod Parameswaran, Sabeela Beevi Ummalyima, Amith Abraham, Anil Kuruvilla Mathew, Aravind Madhavan, Sharrel Rebello, and Ashok Pandey. 2018. “Applications of Microbial Enzymes in Food Industry.” *Food Technology and Biotechnology*. University of Zagreb. <https://doi.org/10.17113/ftb.56.01.18.5491>.
- Reineke, Walter, Michael Schlömann, Walter Reineke, and Michael Schlömann. 2020. “Kohlenstoffkreislauf.” In *Umweltmikrobiologie*, 77–135. Springer Berlin Heidelberg. https://doi.org/10.1007/978-3-662-59655-5_4.
- Rocchitta, Gaia, Angela Spanu, Sergio Babudieri, Gavinella Latte, Giordano Madeddu, Grazia Galleri, Susanna Nuvoli, et al. 2016. “Enzyme Biosensors for Biomedical Applications: Strategies for Safeguarding Analytical Performances in Biological Fluids.” *Sensors (Switzerland)*. MDPI AG. <https://doi.org/10.3390/s16060780>.
- Romero, Elvira, J. Rubén Gómez Castellanos, Giovanni Gadda, Marco W. Fraaije, and Andrea Mattevi. 2018. “Same Substrate, Many Reactions: Oxygen Activation in Flavoenzymes.” *Chemical Reviews*. American Chemical Society. <https://doi.org/10.1021/acs.chemrev.7b00650>.
- Sánchez, Carmen. 2009. “Lignocellulosic Residues: Biodegradation and Bioconversion by Fungi.” *Biotechnology Advances*. Elsevier. <https://doi.org/10.1016/j.biotechadv.2008.11.001>.
- Santiago, Gerard, Felipe De Salas, M. Fátima Lucas, Emanuele Monza, Sandra Acebes, Ángel T. Martínez, Susana Camarero, and Víctor Guallar. 2016. “Computer-Aided Laccase Engineering: Toward Biological Oxidation of Arylamines.” *ACS Catalysis* 6 (8): 5415–23. <https://doi.org/10.1021/acscatal.6b01460>.
- Santos, Ana, Sónia Mendes, Vânia Brissos, and Lígia O Martins. 2014. “New Dye-Decolorizing Peroxidases from *Bacillus Subtilis* and *Pseudomonas Putida* MET94: Towards

- Biotechnological Applications.” *Applied Microbiology and Biotechnology* 98 (5): 2053–65.
<https://doi.org/10.1007/s00253-013-5041-4>.
- Savile, Christopher K., Jacob M. Janey, Emily C. Mundorff, Jeffrey C. Moore, Sarena Tam, William R. Jarvis, Jeffrey C. Colbeck, et al. 2010. “Biocatalytic Asymmetric Synthesis of Chiral Amines from Ketones Applied to Sitagliptin Manufacture.” *Science* 329 (5989): 305–9.
<https://doi.org/10.1126/science.1188934>.
- Scheiblbrandner, Stefan, and Roland Ludwig. 2020. “Cellobiose Dehydrogenase: Bioelectrochemical Insights and Applications.” *Bioelectrochemistry*. Elsevier.
<https://doi.org/10.1016/j.bioelechem.2019.107345>.
- Scheller, Henrik Vibe, and Peter Ulvskov. 2010. “Hemicelluloses.” *Annual Review of Plant Biology* 61 (1): 263–89. <https://doi.org/10.1146/annurev-arplant-042809-112315>.
- Sheldon, Roger A. 2016. “Green Chemistry, Catalysis and Valorization of Waste Biomass.” *Journal of Molecular Catalysis A: Chemical* 422 (October): 3–12.
<https://doi.org/10.1016/j.molcata.2016.01.013>.
- Shleev, Sergey, Elena González-Arribas, and Magnus Falk. 2017. “Biosupercapacitors.” *Current Opinion in Electrochemistry*. Elsevier B.V. <https://doi.org/10.1016/j.coelec.2017.09.023>.
- Sigoillot, C., A. Lomascolo, E. Record, J. L. Robert, M. Asther, and J. C. Sigoillot. 2002. “Lignocellulolytic and Hemicellulolytic System of *Pycnoporus Cinnabarinus*: Isolation and Characterization of a Cellobiose Dehydrogenase and a New Xylanase.” *Enzyme and Microbial Technology* 31 (6): 876–83. [https://doi.org/10.1016/S0141-0229\(02\)00208-9](https://doi.org/10.1016/S0141-0229(02)00208-9).
- Singh, Rahul, and Lindsay D. Eltis. 2015. “The Multihued Palette of Dye-Decolorizing Peroxidases.” *Archives of Biochemistry and Biophysics* 574 (May): 56–65.
<https://doi.org/10.1016/J.ABB.2015.01.014>.
- Singh, Rajendra, Manoj Kumar, Anshumali Mittal, and Praveen Kumar Mehta. 2016. “Microbial Enzymes: Industrial Progress in 21st Century.” *3 Biotech*. Springer Verlag.
<https://doi.org/10.1007/s13205-016-0485-8>.
- Spadiut, Oliver, Tien-Chye Tan, Ines Pisanelli, Dietmar Haltrich, and Christina Divne. 2010. “Importance of the Gating Segment in the Substrate-Recognition Loop of Pyranose 2-Oxidase.” *FEBS Journal* 277 (13): 2892–2909. <https://doi.org/10.1111/j.1742-4658.2010.07705.x>.

- Stoica, Leonard, Roland Ludwig, Dietmar Haltrich, and Lo Gorton. 2006. "Third-Generation Biosensor for Lactose Based on Newly Discovered Cellobiose Dehydrogenase." *Analytical Chemistry* 78 (2): 393–98. <https://doi.org/10.1021/ac050327o>.
- Sulej, Justyna, Grzegorz Janusz, Monika Osińska-Jaroszuk, Paweł Małek, Andrzej Mazur, Iwona Komaniecka, Adam Choma, and Jerzy Rogalski. 2013. "Characterization of Cellobiose Dehydrogenase and Its FAD-Domain from the Ligninolytic Basidiomycete *Pycnoporus Sanguineus*." *Enzyme and Microbial Technology* 53 (6–7): 427–37. <https://doi.org/10.1016/j.enzmictec.2013.09.007>.
- Sulej, Justyna, Grzegorz Janusz, Monika Osińska-Jaroszuk, Patrycja Rachubik, Andrzej Mazur, Iwona Komaniecka, Adam Choma, and Jerzy Rogalski. 2015. "Characterization of Cellobiose Dehydrogenase from a Biotechnologically Important *Cerrena Unicolor* Strain." *Applied Biochemistry and Biotechnology* 176 (6): 1638–58. <https://doi.org/10.1007/s12010-015-1667-2>.
- Sützl, Leander, Gabriel Foley, Elizabeth M.J. Gillam, Mikael Bodén, and Dietmar Haltrich. 2019. "The GMC Superfamily of Oxidoreductases Revisited: Analysis and Evolution of Fungal GMC Oxidoreductases." *Biotechnology for Biofuels* 12 (1): 118. <https://doi.org/10.1186/s13068-019-1457-0>.
- Sützl, Leander, Christophe V.F.P. Laurent, Annabelle T. Abrera, Georg Schütz, Roland Ludwig, and Dietmar Haltrich. 2018. "Multiplicity of Enzymatic Functions in the CAZy AA3 Family." *Applied Microbiology and Biotechnology* 102 (6): 2477–92. <https://doi.org/10.1007/s00253-018-8784-0>.
- Sygmund, Christoph, Roman Kittl, Jindřich Volc, Petr Halada, Elena Kubátová, Dietmar Haltrich, and Clemens K. Peterbauer. 2008. "Characterization of Pyranose Dehydrogenase from *Agaricus Meleagris* and Its Application in the C-2 Specific Conversion of d-Galactose." *Journal of Biotechnology* 133 (3): 334–42. <https://doi.org/10.1016/j.jbiotec.2007.10.013>.
- Sygmund, Christoph, Daniel Kracher, Stefan Scheiblbrandner, Kawah Zahma, Alfons K.G. Felice, Wolfgang Harreither, Roman Kittl, and Roland Ludwig. 2012. "Characterization of the Two *Neurospora Crassa* Cellobiose Dehydrogenases and Their Connection to Oxidative Cellulose Degradation." *Applied and Environmental Microbiology* 78 (17): 6161–71. <https://doi.org/10.1128/AEM.01503-12>.

- Tan, Tien-Chye, Daniel Kracher, Rosaria Gandini, Christoph Sygmund, Roman Kittl, Dietmar Haltrich, B. Martin Hällberg, Roland Ludwig, and Christina Divne. 2015. "Structural Basis for Cellobiose Dehydrogenase Action during Oxidative Cellulose Degradation." *Nature Communications* 6 (1): 7542. <https://doi.org/10.1038/ncomms8542>.
- Tasca, Federico, Muhammad Nadeem Zafar, Wolfgang Harreither, Gilbert Nöll, Roland Ludwig, and Lo Gorton. 2011. "A Third Generation Glucose Biosensor Based on Cellobiose Dehydrogenase from *Corynascus Thermophilus* and Single-Walled Carbon Nanotubes." *Analyst* 136 (10): 2033–36. <https://doi.org/10.1039/c0an00311e>.
- Tian, Chaoguang, William T. Beeson, Anthony T. Iavarone, Jianping Sun, Michael A. Marletta, Jamie H.D. Cate, and N. Louise Glass. 2009. "Systems Analysis of Plant Cell Wall Degradation by the Model Filamentous Fungus *Neurospora Crassa*." *Proceedings of the National Academy of Sciences of the United States of America* 106 (52): 22157–62. <https://doi.org/10.1073/pnas.0906810106>.
- Tipton, Keith, and Sinéad Boyce. 2000. "History of the Enzyme Nomenclature System." *Bioinformatics*. <https://doi.org/10.1093/bioinformatics/16.1.34>.
- Umezawa, Kiwamu, Mai Niikura, Yuka Kojima, Barry Goodell, and Makoto Yoshida. 2020. "Transcriptome Analysis of the Brown Rot Fungus *Gloeophyllum Trabeum* during Lignocellulose Degradation." Edited by Monika Schmoll. *PLOS ONE* 15 (12): e0243984. <https://doi.org/10.1371/journal.pone.0243984>.
- Valadares, Fernanda, Thiago A. Gonçalves, André Damasio, Adriane MF Milagres, Fabio M. Squina, Fernando Segato, and André Ferraz. 2019. "The Secretome of Two Representative Lignocellulose-Decay Basidiomycetes Growing on Sugarcane Bagasse Solid-State Cultures." *Enzyme and Microbial Technology* 130 (November): 109370. <https://doi.org/10.1016/j.enzmictec.2019.109370>.
- Wang, Fangfang, Feng Huang, and Mingqiang Ai. 2019. "Synergetic Depolymerization of Aspen CEL by Pyranose 2-Oxidase and Lignin-Degrading Peroxidases." *BioResources* 14 (2): 3481–94. <https://doi.org/10.15376/biores.14.2.3481-3494>.
- Wariishi, H, K Valli, and M H Gold. 1992. "Manganese(II) Oxidation by Manganese Peroxidase from the Basidiomycete *Phanerochaete Chrysosporium*. Kinetic Mechanism and Role of Chelators." *The Journal of Biological Chemistry* 267 (33): 23688–95.

- <http://www.ncbi.nlm.nih.gov/pubmed/1429709>.
- Westermark, Ulla, and Karl-Erik Eriksson. 1974. "Cellobiose: Quinone Oxidoreductase, a New Wood-Degrading Enzyme from White-Rot Fungi." *Acta Chem Scand Ser B Org Chem Biochem*. <https://agris.fao.org/agris-search/search.do?recordID=US201303188754>.
- Wongnate, Thanyaporn, and Pimchai Chaiyen. 2013. "The Substrate Oxidation Mechanism of Pyranose 2-Oxidase and Other Related Enzymes in the Glucose-Methanol-Choline Superfamily." *FEBS Journal* 280 (13): 3009–27. <https://doi.org/10.1111/febs.12280>.
- Wongnate, Thanyaporn, Panida Surawatanawong, Litavadee Chuaboon, Narin Lawan, and Pimchai Chaiyen. 2019. "The Mechanism of Sugar C-H Bond Oxidation by a Flavoprotein Oxidase Occurs by a Hydride Transfer before Proton Abstraction." *Chemistry - A European Journal*, January. <https://doi.org/10.1002/chem.201806078>.
- Woodley, John M. 2008. "New Opportunities for Biocatalysis: Making Pharmaceutical Processes Greener." *Trends in Biotechnology*. <https://doi.org/10.1016/j.tibtech.2008.03.004>.
- Xu, Feng. 2005. "Applications of Oxidoreductases: Recent Progress." *Industrial Biotechnology* 1 (1): 38–50. <https://doi.org/10.1089/ind.2005.1.38>.
- Yamamoto, Junpei, Kohei Shimizu, Takahiro Kanda, Yuhei Hosokawa, Shigenori Iwai, Pascal Plaza, and Pavel Müller. 2017. "Loss of Fourth Electron-Transferring Tryptophan in Animal (6-4) Photolyase Impairs DNA Repair Activity in Bacterial Cells." *Biochemistry* 56 (40): 5356–64. <https://doi.org/10.1021/acs.biochem.7b00366>.
- Zámocký, Marcel, Martin Hallberg, Roland Ludwig, Christina Divne, and Dietmar Haltrich. 2004. "Ancestral Gene Fusion in Cellobiose Dehydrogenases Reflects a Specific Evolution of GMC Oxidoreductases in Fungi." *Gene* 338 (1): 1–14. <https://doi.org/10.1016/j.gene.2004.04.025>.
- Zámocký, Marcel, R. Ludwig, C. Peterbauer, B. Hallberg, C. Divne, P. Nicholls, and D. Haltrich. 2006. "Cellobiose Dehydrogenase – A Flavocytochrome from Wood-Degrading, Phytopathogenic and Saprotropic Fungi." *Current Protein & Peptide Science* 7 (3): 255–80. <https://doi.org/10.2174/138920306777452367>.
- Zámocký, Marcel, Christina Schümann, Christoph Sigmund, John O'Callaghan, Alan D.W. Dobson, Roland Ludwig, Dietmar Haltrich, and Clemens K. Peterbauer. 2008. "Cloning, Sequence Analysis and Heterologous Expression in *Pichia Pastoris* of a Gene Encoding a Thermostable Cellobiose Dehydrogenase from *Myriococcum Thermophilum*." *Protein Expression and*

Purification 59 (2): 258–65. <https://doi.org/10.1016/j.pep.2008.02.007>.

Zhang, Keke, Mei Huang, Jiangshan Ma, Zeyi Liu, Jiarui Zeng, Xuanming Liu, Ting Xu, et al. 2018. "Identification and Characterization of a Novel Bacterial Pyranose 2-Oxidase from the Lignocellulolytic Bacterium *Pantoea Ananatis* Sd-1." *Biotechnology Letters* 40 (5): 871–80. <https://doi.org/10.1007/s10529-018-2538-z>.

Chapter 2 – Discovering new Enzymes

Appl Environ Microbiol. 2019 Jun 17;85(13):e00390-19. doi: 10.1128/AEM.00390-19. Print 2019 Jul 1.

Versatile Oxidase and Dehydrogenase Activities of Bacterial Pyranose 2-Oxidase Facilitate Redox Cycling with Manganese Peroxidase In Vitro

Peter L Herzog^{#1}, Leander Sützl^{#1}, Beate Eisenhut¹, Daniel Maresch², Dietmar Haltrich¹, Christian Obinger², Clemens K Peterbauer³

PMID: 31028028 PMCID: PMC6581175 DOI: 10.1128/AEM.00390-19

ABSTRACT:Pyranose 2-oxidase (POx) has long been accredited a physiological role in lignin degradation, but evidence to provide insights into the biochemical mechanisms and interactions is insufficient. There are ample data in the literature on the oxidase and dehydrogenase activities of POx, yet the biological relevance of this duality could not be established conclusively. Here we present a comprehensive biochemical and phylogenetic characterization of a novel pyranose 2-oxidase from the actinomycetous bacterium *Kitasatospora aureofaciens* (KaPOx) as well as a possible biomolecular synergism of this enzyme with peroxidases using phenolic model substrates in vitro. A phylogenetic analysis of both fungal and bacterial putative POx-encoding sequences revealed their close evolutionary relationship and supports a late horizontal gene transfer of ancestral POx sequences. We successfully expressed and characterized a novel bacterial POx gene from *K. aureofaciens*, one of the putative POx genes closely related to well-known fungal POx genes. Its biochemical characteristics comply with most of the classical hallmarks of known fungal pyranose 2-oxidases, i.e., reactivity with a range of different monosaccharides as electron donors as well as activity with oxygen, various quinones, and complexed metal ions as electron acceptors. Thus, KaPOx shows the pronounced duality of oxidase and dehydrogenase similar to that of fungal POx. We further performed efficient redox cycling of aromatic lignin model compounds between KaPOx and manganese peroxidase (MnP). In addition, we found a Mn(III) reduction activity in KaPOx, which, in combination with its ability to provide H₂O₂, implies this and potentially other POx as complementary enzymatic tools for oxidative lignin degradation by specialized peroxidases.

IMPORTANCE: Establishment of a mechanistic synergism between pyranose oxidase and (manganese) peroxidases represents a vital step in the course of elucidating microbial lignin degradation. Here, the comprehensive characterization of a bacterial pyranose 2-oxidase from *Kitasatospora aureofaciens* is of particular interest for several reasons. First, the phylogenetic analysis of putative pyranose oxidase genes reveals a widespread occurrence of highly similar enzymes in bacteria. Still, there is only a single report on a bacterial pyranose oxidase, stressing the need of closing this gap in the scientific literature. In addition, the relatively small *K. aureofaciens* proteome supposedly supplies a limited set of enzymatic functions to realize lignocellulosic biomass degradation. Both enzyme and organism therefore present a viable model to study the mechanisms of bacterial lignin decomposition, elucidate physiologically relevant interactions with specialized peroxidases, and potentially realize biotechnological applications.

Keywords: actinobacteria; lignin degradation; manganese peroxidase; phylogeny; pyranose oxidase.



Versatile Oxidase and Dehydrogenase Activities of Bacterial Pyranose 2-Oxidase Facilitate Redox Cycling with Manganese Peroxidase *In Vitro*

Peter L. Herzog,^a Leander Sützl,^a Beate Eisenhut,^a Daniel Maresch,^b Dietmar Haltrich,^a Christian Obinger,^b Clemens K. Peterbauer^a

^aDepartment of Food Science and Technology, BOKU—University of Natural Resources and Life Sciences, Vienna, Austria

^bDepartment of Chemistry, BOKU—University of Natural Resources and Life Sciences, Vienna, Austria

ABSTRACT Pyranose 2-oxidase (POx) has long been accredited a physiological role in lignin degradation, but evidence to provide insights into the biochemical mechanisms and interactions is insufficient. There are ample data in the literature on the oxidase and dehydrogenase activities of POx, yet the biological relevance of this duality could not be established conclusively. Here we present a comprehensive biochemical and phylogenetic characterization of a novel pyranose 2-oxidase from the actinomycetous bacterium *Kitasatospora aureofaciens* (*KaPOx*) as well as a possible biomolecular synergism of this enzyme with peroxidases using phenolic model substrates *in vitro*. A phylogenetic analysis of both fungal and bacterial putative POx-encoding sequences revealed their close evolutionary relationship and supports a late horizontal gene transfer of ancestral POx sequences. We successfully expressed and characterized a novel bacterial POx gene from *K. aureofaciens*, one of the putative POx genes closely related to well-known fungal POx genes. Its biochemical characteristics comply with most of the classical hallmarks of known fungal pyranose 2-oxidases, i.e., reactivity with a range of different monosaccharides as electron donors as well as activity with oxygen, various quinones, and complexed metal ions as electron acceptors. Thus, *KaPOx* shows the pronounced duality of oxidase and dehydrogenase similar to that of fungal POx. We further performed efficient redox cycling of aromatic lignin model compounds between *KaPOx* and manganese peroxidase (MnP). In addition, we found a Mn(III) reduction activity in *KaPOx*, which, in combination with its ability to provide H₂O₂, implies this and potentially other POx as complementary enzymatic tools for oxidative lignin degradation by specialized peroxidases.

IMPORTANCE Establishment of a mechanistic synergism between pyranose oxidase and (manganese) peroxidases represents a vital step in the course of elucidating microbial lignin degradation. Here, the comprehensive characterization of a bacterial pyranose 2-oxidase from *Kitasatospora aureofaciens* is of particular interest for several reasons. First, the phylogenetic analysis of putative pyranose oxidase genes reveals a widespread occurrence of highly similar enzymes in bacteria. Still, there is only a single report on a bacterial pyranose oxidase, stressing the need of closing this gap in the scientific literature. In addition, the relatively small *K. aureofaciens* proteome supposedly supplies a limited set of enzymatic functions to realize lignocellulosic biomass degradation. Both enzyme and organism therefore present a viable model to study the mechanisms of bacterial lignin decomposition, elucidate physiologically relevant interactions with specialized peroxidases, and potentially realize biotechnological applications.

KEYWORDS actinobacteria, lignin degradation, manganese peroxidase, phylogeny, pyranose oxidase

Citation Herzog PL, Sützl L, Eisenhut B, Maresch D, Haltrich D, Obinger C, Peterbauer CK. 2019. Versatile oxidase and dehydrogenase activities of bacterial pyranose 2-oxidase facilitate redox cycling with manganese peroxidase *in vitro*. *Appl Environ Microbiol* 85:e00390-19. <https://doi.org/10.1128/AEM.00390-19>.

Editor Emma R. Master, University of Toronto

Copyright © 2019 Herzog et al. This is an open-access article distributed under the terms of the [Creative Commons Attribution 4.0 International license](https://creativecommons.org/licenses/by/4.0/).

Address correspondence to Clemens K. Peterbauer, clemens.peterbauer@boku.ac.at. P.L.H. and L.S. contributed equally to this article.

Received 15 February 2019

Accepted 19 April 2019

Accepted manuscript posted online 26 April 2019

Published 17 June 2019

Auxiliary activity family 3 (AA3) of the Carbohydrate-Active enZymes Database (CAZy) (<http://www.cazy.org/>) comprises redox enzymes, which assist other AA family oxidoreductases or support the activity of glucoside hydrolases in lignocellulose degradation. All AA3 members belong to the glucose-methanol-choline (GMC) family of flavin-dependent oxidoreductases, and they typically are multidomain enzymes composed of a flavin-binding domain of the canonical Rossmann fold and a less preserved substrate-binding domain (1, 2). Subfamily AA3_4 comprises pyranose oxidases (POx [EC 1.1.3.10]), the phylogenetically most distantly related AA3 subfamily, which is also the most diverse with respect to structural features. POx oxidizes various monosaccharides, with glucose being preferred, but its substrate specificity is less strict than that of other members of the AA3 family.

The reaction mechanism of POx generally involves a hydride transfer from the sugar substrate, resulting in the reduction of its flavin adenine dinucleotide (FAD) cofactor to its hydroquinone form (FADH₂), referred to as the reductive half-reaction. FADH₂ is subsequently reoxidized in the oxidative half-reaction by a suitable electron acceptor (3). For POx, this electron acceptor can be molecular oxygen (which is reduced to hydrogen peroxide), a range of (substituted) quinones, (complexed) metal ions, or even various radicals (4). The role of POx has previously been seen in the provision of H₂O₂ to different peroxidases (5), yet these nonoxygen electron acceptors are often used with much higher catalytic efficiencies by POx, which points toward a potential physiological significance of reactions with such molecules (6).

The biological function of AA3-family redox enzymes—as defined by CAZy—is to act in conjunction with CAZymes during lignocellulose degradation. White-rot wood-degrading basidiomycetes employ a number of lignin-modifying enzymes (LMEs), extracellular heme-containing lignin, manganese, or versatile peroxidases as well as laccases. Hydrogen peroxide mediates the formation of the reactive peroxidase intermediate compound I [oxoiron(IV) porphyrin radical], which then—depending on the enzyme—generates various small oxidants, including the veratryl alcohol cation radical or Mn(III) coordination complexes. These diffusible mediators subsequently react with lignin in a nonspecific way, generating radical sites and thereby initiating a cascade of bond scission, which eventually results in lignin depolymerization (7–10).

Pyranose oxidase and certain other AA3 oxidases can also show a very pronounced dehydrogenase activity. Dehydrogenases involved in lignocellulose degradation are implicated in maintaining a quinone/hydroquinone redox cycle as well as in the provision of reduced metals for diverse radical-based depolymerization reactions (11). Recently, POx from the white-rot basidiomycete *Irpex lacteus* was shown to reduce quinoid intermediates produced by laccase from phenolic compounds and lignosulfonate *in vitro* and thus prevent their (re)polymerization (12). The same effect was also observed for this fungal POx when acting on extracted lignin with peroxidases (13). This is consistent with a proposed biological function of detoxifying lignin degradation products or phenolic compounds that are part of plant defense mechanisms (14).

Research on the enzymology of lignin depolymerization and oxidative polysaccharide degradation has largely focused on fungal systems; thus, the majority of characterized enzymes are from fungal sources (10, 15, 16), whereas knowledge on respective bacterial enzyme systems is comparably scarce. However, the capability for lignin oxidation was observed in a number of soil bacteria, the majority of which fall into the taxonomic groups of actinobacteria, alphaproteobacteria, and gammaproteobacteria (10). Recent studies implicate dye-decolorizing peroxidases (DyP) as key enzymes in bacterial lignin depolymerization (9, 17), and genome data suggest that these enzymes, while present in some fungi and higher eukaryotes, are most prominent in bacteria (18). Even though biochemical data on these bacterial enzymes are limited, it was shown that certain bacterial DyP possess a peroxidase activity comparable to those of fungal DyP and manganese peroxidases (19). Additionally, an H₂O₂-independent but Mn(II)- and O₂-dependent oxidase activity was demonstrated for DyP2 from *Amycolatopsis* sp. strain 75iv2 (17).

These observations suggest that bacteria utilize mechanisms for lignin depolymer-

ization that are more basic and “minimalistic” but similar to those used by fungi. This consequently poses several questions regarding the enzymatic equipment of these bacteria: what activities accessory to lignin and lignocellulose degradation exist and are employed in bacteria? How can lignin-modifying bacteria provide H₂O₂ for their peroxidases: do they possess a proprietary oxidase system for that purpose? Do bacteria utilize dehydrogenases for quinone/hydroquinone redox cycling and provision of reduced metals?

We searched for putative AA3 family enzymes in bacterial genomes by comparison with fungal AA3 sequences and established phylogenetic relationships between fungal and bacterial AA3 sequences. We further expressed, purified, and characterized a novel bacterial pyranose oxidase that demonstrates oxidase as well as dehydrogenase activities and may be involved in lignocellulose depolymerization via interaction with peroxidases, as was determined *in vitro* in this study.

RESULTS

Phylogenetic analysis. In order to evaluate which well-known fungal AA3 enzymes have close relatives in bacteria, we BLAST searched representative fungal enzyme sequences for their respective most similar sequences in the bacterial domain. Subsequently, their most probable phylogenetic relation was calculated and summarized in a phylogenetic tree (see Fig. S1 in the supplemental material). We found that POx is the only AA3 enzyme that is shared among fungi and bacteria. This is evident from the close relationship of identified bacterial POx hits with the clade of fungal POx sequences and a maximal (100%) bootstrap support for this relation. All other fungal AA3 enzymes, aryl-alcohol oxidase (AAO), alcohol oxidase (AOx), cellobiose dehydrogenase (CDH), glucose dehydrogenase (GDH), glucose oxidase (GOx), and pyranose dehydrogenase (PDH), have sequence hits in bacteria that cluster among or closely with characterized bacterial choline dehydrogenases (ChDH) rather than with their fungal query sequences. None of the bacterial hits were found to cluster with bacterial cholesterol oxidases (ChOx). Two bacterial sequences from the BLAST search clustered closest to fungal CDH. Still, they displayed a high degree of difference, given a branch length of 1.7 amino acid substitutions per site and sequence identities of 26% with fungal CDH. In addition, these bacterial sequences lack a cytochrome domain and therefore cannot be considered a bacterial equivalent of fungal CDH.

In the subsequent analysis of POx distribution in bacteria, we found the putative POx genes to occur mainly in *Actinobacteria* and *Proteobacteria* but also in *Bacilli* (Fig. 1). Putative POx sequences of *Proteobacteria* separated into two main clades of *Alpha-proteobacteria* and *Gammaproteobacteria*, and few sequences occurred in nonspecific clades, while sequences of actinobacterial origin separated mainly into four different clades. The smallest of these four clades was found closely associated with the fungal POx sequences. Again, a small number of actinobacterial sequences were found in nonspecific clades. Finding one separate clade of sequences from *Actinobacteria* this closely related to fungal POx sequences is of high interest, especially since no sequence of this clade has been characterized so far. The putative POx sequences occurring in *Bacilli* form a single and completely separate clade.

Sequence and structural model of pyranose oxidase from *Kitasatospora aureofaciens*. We selected the putative POx from *Kitasatospora aureofaciens* (formerly *Streptomyces aureofaciens*), for which complete high-quality genome data (20) are accessible in the NCBI genome database (txid1894), for further analysis, as this sequence (KaPOx) was the most similar one to that from *Trametes ochracea* (ToPOx), the most thoroughly characterized fungal POx to date. The sequences show an identity of 38.7%, a query match of 545 out of 623 ToPOx residues, and only limited gaps in the alignment of the two sequences (Fig. S2). Assessment of potential N-terminal signal peptides in both POx sequences yielded negative outcomes for eukaryotic and Gram-positive signal predictions. Surprisingly, prediction of a bacterial twin-arginine signal peptide was positive in the fungal ToPOx sequence, comprising the initial 27 residues (Fig. S3).

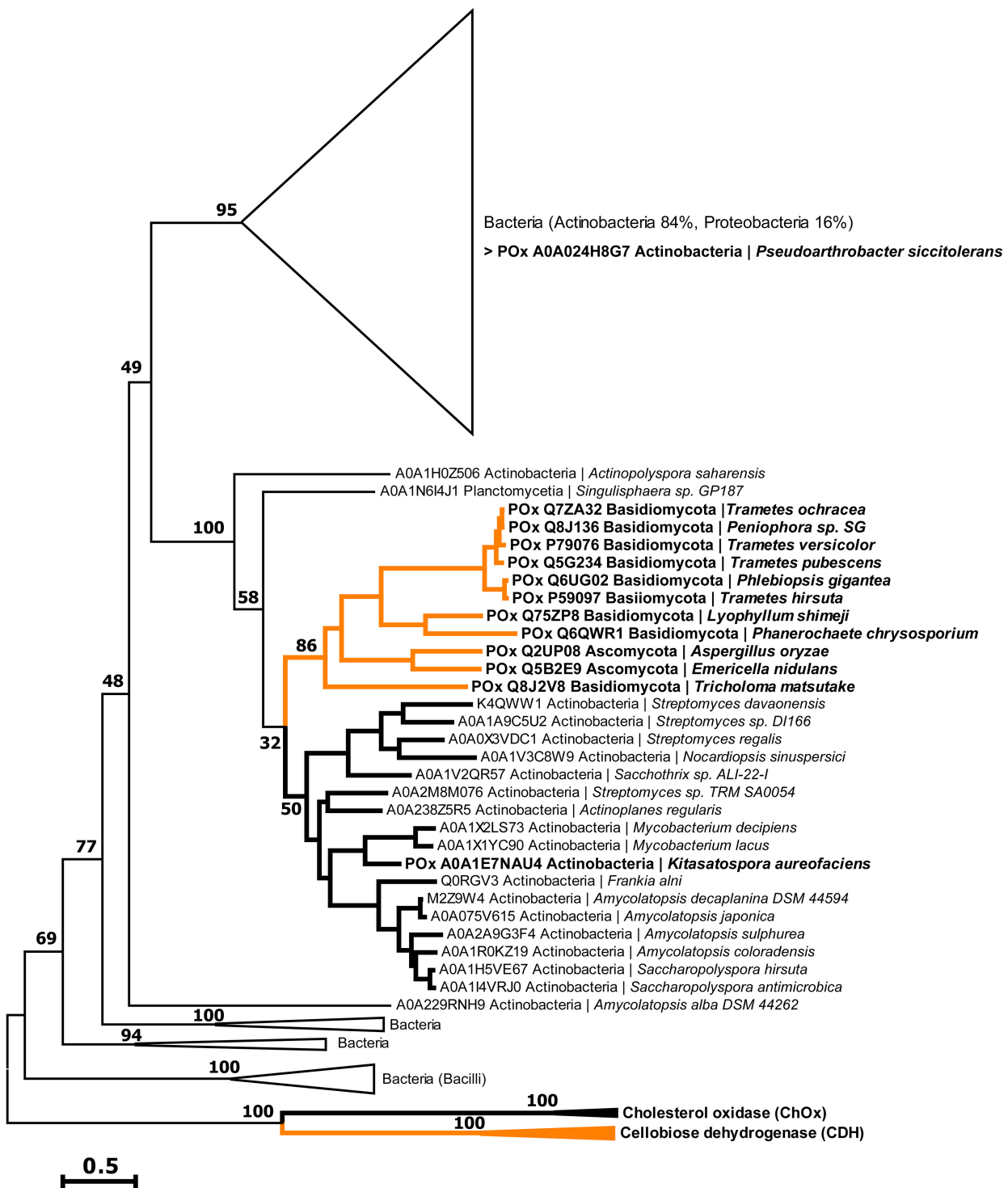


FIG 1 Phylogenetic tree of putative pyranose oxidase genes. The phylogenetic relation of bacterial (black) and fungal (orange) sequences based on maximum likelihood was assessed using 1,020 bootstrap repetitions as statistical support. Numbers in the graph represent bootstraps coefficients, expressed as percentages. Sequences from characterized fungal CDH and bacterial ChOx were used as outgroups. Sequences from characterized enzymes are indicated in bold letters. Most clades of closely related sequences were collapsed in triangles to reduce the complexity of the cladogram.

The correlation of the *KaPOx* sequence alignment and a homology model (Fig. S4) showed that *KaPOx* lacks a designated presequence at the N terminus, as its first residues (starting from Y5) are already part of the canonical Rossmann fold. In contrast to that, *ToPOx* contains approximately 40 N-terminal residues that are not part of the

Rossmann fold. A general complete match was obtained for most parts of the N-terminal Rossmann fold in *KaPOx*, the most notable difference being a missing sequence stretch (T385 to E410) corresponding to the *ToPOx* head domain and the absence of a loop (L337 to L349) on the opposite side of the enzyme. In addition, the *KaPOx* model displays minor deviations in the secondary-structure arrangements. Contrasting to *ToPOx*, the *KaPOx* homology model contains a short alpha-helix in the multimerization arm (P86 to L92).

We observed good agreement when aligning the active sites of the two POx homologues. The FAD-coordinating catalytic residues H548 and T169 in *ToPOx* (21) corresponded to H464 and T130 in *KaPOx*, respectively. Histidine 167, which is known to establish the covalent 8α -(N3)-histidyl link to FAD in *ToPOx* (22), corresponded to homologue H128 in the *KaPOx* model, presumably realizing a covalently attached FAD in the bacterial POx as well. Comparable motifs were also found for the FAD-coordinating *si*-side helix and loop, where 122-VGGMGTHWTGAT-133 is nearly identical to the corresponding *ToPOx* sequence (161-VGGMSTHWTCAT-172) (differences underlined). A notable dissimilarity was found in the gating segment of the substrate recognition loop (23), where T367 (H450) and H372 (S455) were identified in the *KaPOx* model (corresponding *ToPOx* amino acids are in parentheses).

Production and purification of recombinant *KaPOx*. Shake flask cultivation of 2.5 liters *E. coli* suspension, carrying the *KaPOx* gene with a C-terminal 6×His tag under the control of the T7 promoter, yielded 56 g of wet cell pellet. After resuspension and cell disruption, 450 ml of crude extract (CE) was obtained and subjected to immobilized-metal affinity chromatography (IMAC) purification. Active fractions were pooled to yield 33.2 mg of purified protein, with a specific activity of 6.9 U mg^{-1} using the 2,2'-azino-bis-3-ethylbenzothiazoline-6-sulfonic acid (ABTS) assay (pH 7.5). A subsequent dialysis step buffered the protein at pH 6.0 and caused the formation of an intensely yellow precipitate. This precipitation was reversible and did not affect enzymatic activities. The presence of the 61.2-kDa *KaPOx* band could be confirmed before and after the dialysis step via SDS-PAGE (Fig. S5A). Subsequent washing of the enzyme aggregate by gentle centrifugation allowed removal of soluble impurities to yield a >95% pure *KaPOx* preparation as determined by software-aided analysis of the SDS-PAGE. Analysis by liquid chromatography-electrospray ionization mass spectrometry (LC-ESI-MS) of the washed and dialyzed enzyme confirmed its complete sequence and the absence of host cell-derived protein impurities.

***KaPOx* is a homodimeric enzyme with covalently bound FAD.** Polyacrylamide gel electrophoresis under nondenaturing conditions displayed band sizes at approximately 120 kDa, indicating a 2×61.2 *KaPOx* dimer before and after dialysis (Fig. S5B). We observed complete resolubilization of dialyzed *KaPOx* aggregates when dissolving it in buffer at alkaline pH. Analysis of particle sizes via dynamic light scattering (DLS) revealed the pH dependence of aggregation of the purified enzyme. In accordance with native PAGE results, a dimeric state of *KaPOx* was confirmed by DLS measurements at pH 8.5. Analysis of 100 measurements yielded an estimated size distribution of 8.5 ± 1.9 nm, equaling an estimated protein size of 121 ± 13 kDa for 99.7% of the monodisperse mass (Fig. 2A). Titration of the soluble sample from pH 9.0 to 5.0 revealed initiation of aggregation at a pH below 7.5 (Fig. 2B).

Histidine 128, as was suggested by the *KaPOx* homology model, was confirmed to be covalently modified by FAD via LC-ESI-MS analysis of the chymotryptic digest of the enzyme. The covalently bound FAD moiety was identified on the peptide 121-AVGGM GTHW-129 containing the proposed H128. In the sample, a total of 91% of this peptide was conjugated with a FAD, leaving a respective 9% unmodified (Fig. S6). The same ratio was calculated by MS analysis of intact (undigested) recombinant *KaPOx* protein (data not shown).

***KaPOx* performs C-2 site oxidation in D-glucose.** High-performance liquid chromatography (HPLC) analysis of *KaPOx* oxidation products from batch conversion experiments confirmed the characteristic oxidation of sugar substrates at the C-2 position.

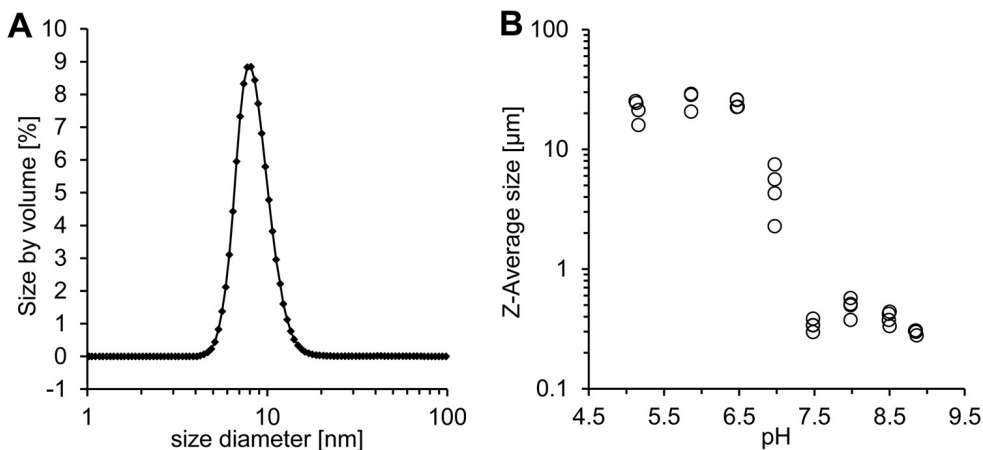


FIG 2 Dynamic light scattering (DLS) experiments to investigate *KaPOx* multimerization and pH-dependent aggregation. (A) Back scattering analysis of *KaPOx*. One hundred repeats were fitted to yield an average particle size (peak) of 8.5 nm for 99.7% of the mass, which estimated a protein size of 121 ± 13 kDa for the *KaPOx* at pH 8.5. (B) Protein aggregation observed during the titration of the *KaPOx* sample toward pH 5.0 was recorded by means of particle size.

A mixture of D-glucose and 2-keto-D-glucose (both 25 mM) was used as a measurement standard, and retention times (R_t) of 12.8 min and 15.3 min were determined, respectively. We detected a gradual increase in 2-keto-D-glucose signals and concomitant decrease of D-glucose signals (Fig. S7): after an initial lag phase, the oxidation proceeded almost linearly until the reaction was stopped at 84% D-glucose conversion after 20 h (data not shown).

Catalytic properties of *KaPOx*. Steady-state measurements with ambient oxygen as the electron acceptor yielded the Michaelis-Menten parameters presented in Table 1. These kinetic data display a pronounced preference for monosaccharides in general and for D-glucose and D-galactose in particular. This is predominantly reflected in the low K_m values of 1.5 ± 0.1 mM and 2.7 ± 0.5 mM, respectively. Efficient turnover of L-sorbose, D-xylose, D-glucono-1,5-lactone, and D-mannose, but no specific reactivity with any of the tested disaccharides, was observed.

We assessed the kinetic parameters of oxygen reduction with the help of a luminescent microsensor. This was approached by following the kinetics of consumption of dissolved oxygen by *KaPOx* from an initial concentration of $800 \mu\text{M}$ to $1 \mu\text{M}$. However, saturation of the reaction could not be observed at these concentrations, indicating the K_m for O_2 to be close to or above the maximal soluble O_2 concentration in this setup. Thus, it was decided to fit dissolved-oxygen curves to the integrated Michaelis-Menten equation as an estimation, which yielded an apparent K_m (O_2) of 1.1 ± 0.1 mM and a k_{cat} of $32.4 \pm 0.7 \text{ s}^{-1}$.

TABLE 1 Apparent kinetic constants of POx from *K. aureofaciens* for various electron donors^a

Substrate	V_{max} (U mg^{-1})	Activity ^b (%)	K_m (mM)	k_{cat} (s^{-1})	k_{cat}/K_m ($\text{mM}^{-1} \text{ s}^{-1}$)
D-Glucose	7.6 ± 0.0	100	1.5 ± 0.1	15.4 ± 0.0	10.0
D-Galactose	5.8 ± 0.2	77	2.7 ± 0.5	11.9 ± 0.5	4.40
L-Sorbose	5.0 ± 0.2	66	13.6 ± 1.3	10.2 ± 0.5	0.75
D-Xylose	3.3 ± 0.2	44	32.4 ± 3.9	6.8 ± 0.3	0.21
D-Glucono-1,5-lactone	0.8 ± 0.0	10	28.7 ± 2.4	1.8 ± 0.1	0.06
D-Mannose	1.1 ± 0.1	14	201.0 ± 60.1	2.2 ± 0.3	0.01

^aData were obtained from the standard ABTS assay under standard conditions with oxygen as electron acceptor (air saturation). Values represent averages and standard deviations of 3 technical replicates. For D-glucose-1-phosphate, D-ribose, D-sorbitol, maltose, cellobiose, lactose, and sucrose, substrate observed reaction rates under assay conditions (V_{obs}) values were <2% those for saturated D-glucose.

^bValues are expressed as relative activities with respect to the V_{max} of D-glucose (100%).

TABLE 2 Apparent kinetic constants of POx from *K. aureofaciens* for various electron acceptors^a

Substrate	V_{\max} ($\mu\text{M mg}^{-1}$)	Activity ^b (%)	K_m (mM)	k_{cat} (s^{-1})	k_{cat}/K_m ($\text{s}^{-1} \text{mM}^{-1}$)
Oxygen	15.9 ± 3.1	100	1.07 ± 0.1	32.4 ± 0.7	30
1,4-Benzoquinone	12.2 ± 0.3	77	0.08 ± 0.1	24.9 ± 7.1	311
DCIP	4.4 ± 0.5	28	0.03 ± 0.0	9.4 ± 1.1	313
Ferrocenium ion	105.0 ± 9.5	660	1.03 ± 1.0	214 ± 19	208
ABTS radical ^c	6.1 ± 0.2	38	0.04 ± 0.0	12.4 ± 0.3	309
Mn(III) ^d	226.0 ± 2.8				

^aData were obtained under standard conditions (unless indicated otherwise) using D-glucose as saturating substrate with nitrogen bubbled solutions. Values represent averages and standard deviations for 3 technical replicates.

^bValues are expressed as relative activities with respect to the V_{\max} of oxygen (100%).

^cLaccase was used to prepare the ABTS cationic radical and was removed by ultrafiltration. The ABTS radical concentration was determined photometrically.

^dFor Mn(III), no saturation could be reached; V_{\max} represents a V_{obs} reaction rate at the apparent solubility limit of the Mn(III) complex at 1 mM.

In addition to oxygen, various compounds were assessed as possible electron acceptors of *KaPOx*. Catalytic efficiencies for the two-electron acceptors 1,4-benzoquinone (1,4-BQ) and dichloroindophenol (DCIP) of 311 ± 44 and $313 \pm 36 \text{ mM}^{-1} \text{ s}^{-1}$, respectively, exceeded that for oxygen ($30 \pm 0.8 \text{ mM}^{-1} \text{ s}^{-1}$) by approximately 1 order of magnitude, which is mainly attributed to the substantially lower K_m value. The one-electron reduction reactions evaluated for the ferrocenium ion ($208 \pm 19 \text{ mM}^{-1} \text{ s}^{-1}$) and the ABTS radical ($309 \pm 8.5 \text{ mM}^{-1} \text{ s}^{-1}$) are equally pronounced in *KaPOx* (Table 2). In addition, we found complexed Mn(III) to be a one-electron acceptor for *KaPOx*. Although the measurements did not allow the estimation of kinetic parameters—due to limitations of Mn(III) complex solubility, saturation of the reaction could not be reached—the apparent activities for Mn(III) reduction were the highest among the measured compounds. We successfully verified the specific Mn(III) reduction reaction by *KaPOx* in a separate experiment (Fig. S8).

Analysis of the pH dependence of *KaPOx* activity revealed overlapping pH dependencies for the electron acceptors O_2 and BQ (maximal activities at pH 8.0 to 8.5) and a shifted pH curve for DCIP toward a more acidic pH (maximal activities at pH 6.5 to 7.0) (Fig. S9). In general, the enzyme displayed effective turnover at pH 5.0 to 9.5. Still, reactions at pH 9.0 and higher could partially not be maintained for longer than 150 s under the given conditions. As progressive aggregation was observed for pure *KaPOx* samples below pH 7.5, the pH-dependent activities in this experiments could have been subject to decreased activity due to the comparably lower soluble concentrations of *KaPOx* in the activity assays.

Oxidoreductive coupling between *KaPOx* and manganese peroxidase. Enzymatic redox cycling of model compounds between POx and manganese peroxidase (MnP) could be established for the methoxy-substituted phenols 2,6-dimethoxyphenol (DMP), guaiacol, acetosyringone, and sinapic acid. With the addition of hydrogen peroxide, MnP catalyzed the oxidation of these phenols to their respective quinoids, which was monitored spectrophotometrically at the respective characteristic wavelengths (Fig. 3 and Fig. S10). For 2,6-DMP and guaiacol, the subsequent addition of *KaPOx* to the assay mixture (containing the electron donor D-glucose) caused a sudden stop in oxidation and a full reversion of the reaction to base level absorbances after 5 to 7 min. For acetosyringone and sinapic acid, the addition of *KaPOx* facilitated partial reversion of the reaction, as the preceding formation of oxidation products was stopped at a certain level after >12 min. These results indicate that the tested phenols are oxidized by MnP and are then subject to reduction by *KaPOx*.

In contrast, the *KaPOx*-mediated reduction of 1,4-benzoquinone to its reduced hydroquinone state was monitored spectrophotometrically. Upon addition of MnP a decrease in the reduction reaction was observed, clearly demonstrating that MnP catalyzed the partial reoxidation of hydroquinone, thus competing with the proceeding

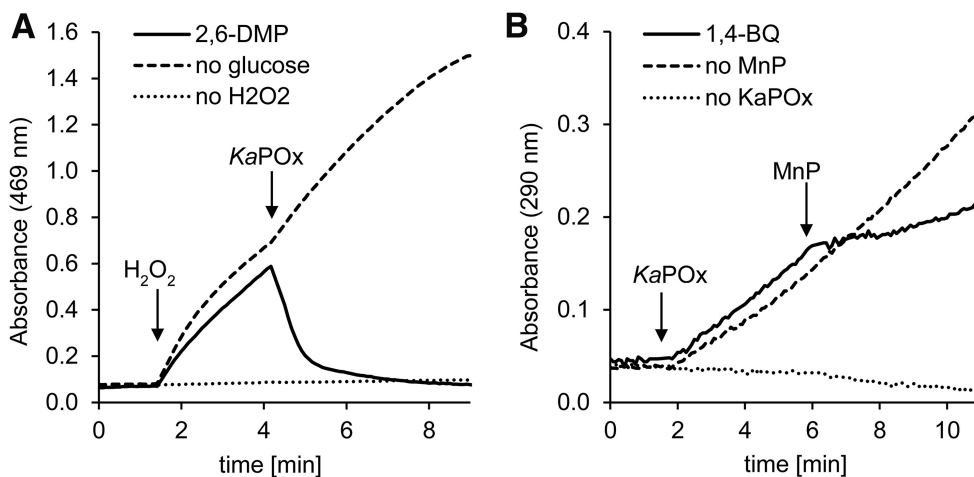


FIG 3 Cooperative redox cycling of substituted phenols between *KaPOx* and MnP. The qualitative photometric assays were started with phenol oxidation (A) or quinone reduction (B). (A) Assay mixtures contained manganese peroxidase (MnP), 2,6-dimethoxyphenol (2,6-DMP), and D-glucose. Reactions were started by the addition of H₂O₂. Four minutes into the reaction, *KaPOx* was added. (B) Assay mixtures contained 1,4-benzoquinone (1,4-BQ) and D-glucose. Reactions were started by addition of *KaPOx*; 6 min into the reaction, MnP was added.

reduction reaction. Here, MnP catalysis is driven by H₂O₂ derived from the *KaPOx* reaction with D-glucose and ambient O₂.

DISCUSSION

In this report, we provide the biochemical characterization of a pyranose 2-oxidase from the actinomycetous, Gram-positive soil bacterium *Kitasatospora aureofaciens* and show a possible interaction with peroxidases using lignin model compounds as substrates *in vitro*. Since POx has been characterized from prokaryotic and eukaryotic organisms, these results will aid to compare fungal and bacterial systems for biomass degradation.

The phylogenetic analysis of sets of fungal GMC enzymes with their most similar bacterial sequences highlights the close relation between fungal and bacterial POx, as was indicated by high sequence similarities reported previously (24). In the analyzed set of GMC enzymes, the resulting putative bacterial POx sequences are more closely related to fungal POx sequences than to their most similar bacterial sequences, which is the opposite for all other GMC enzymes (Fig. S1). This strongly suggests that fungal and bacterial POxs share an ancestor. A mutual origin for bacterial and fungal POxs is also supported by the phylogenetic analysis of assembled POx sequences, where characterized fungal POx genes cluster among putative bacterial POx sequences to form a distinct clade (Fig. 1). Within this clade, bacterial actinomycetous POxs are gathered alongside their fungal homologues. POxs from *Tricholoma matsutake*, *Aspergillus oryzae*, and *Aspergillus nidulans* (*Emericella nidulans*) are the most closely related biochemically characterized fungal enzymes, with sequence similarities of >40% with respect to *KaPOx*. This supports the proposed horizontal gene transfer of bacterial POx genes into the kingdom of fungi (25). This relationship furthermore explains the often described peculiar features of fungal POx, such as the overall structural diversity and unique combination of structural motifs (14), the general lack of glycosylation (4, 26, 27), and the prediction of bacterial signal peptides (28) that separate them from other fungal GMCs.

As is observable in the phylogenetic tree of POx sequences, putative pyranose 2-oxidase-encoding genes are widely distributed in the phylum of *Firmicutes* and particularly in *Actinobacteria* (Fig. 1). In these organisms, POx would be expected to fulfill physiological roles similar to those in biomass-degrading fungi. These bacteria and fungi often share a habitat, are comparable regarding their lifestyles, and contribute to lignocellulosic biomass degradation in a synergistic manner (29–32). Hence, gene transfer between different species should be regarded as beneficial for the organisms.

The comparison of putative active-site residues of *KaPOx* with the corresponding residues of characterized fungal *ToPOx* shows an excellent agreement. It is therefore not surprising that the determined *KaPOx* substrate preferences are quite comparable to those of fungal *POx* for electron donors as well as electron acceptors. Still, *KaPOx* exhibits a pronounced reactivity with D-galactose and a distinctively high K_m value for O_2 in the low millimolar range. The ability to use oxygen as an electron acceptor seems to be less developed in bacterial *POx*, as was also shown for the bacterial *POx* from *Pseudoarthrobacter siccitolerans* (24). Furthermore, the kinetic characterization of *KaPOx* revealed universally reduced turnover numbers (and narrower pH dependencies) in comparison to those of fungal *POx* (4, 12, 33). We hypothesize that this is caused partly by differences in the gating segment of *KaPOx*, a distinct loop in the active site that was reported to be influential for the catalytic rates in fungal *POx* (23, 34). In *KaPOx*, the comparably bulky H372 (S455 in *ToPOx*) could restrict flexibility of the loop due to increased (pH-dependent) interactions with its surroundings.

Similar to other *POx*, *KaPOx* exhibits substantial capacity to reduce one-electron acceptors such as the ferrocenium ion and the ABTS radical. Most strikingly, we additionally confirmed the enzymatic one-electron reduction of complexed Mn(III), a reactive by-product of peroxidase activity. For *KaPOx*, turnover rates for Mn(III) and ferrocenium were the highest measured but a K_m value for the reduction of Mn(III) to Mn(II) could not be resolved.

Surprisingly, we could not identify a signal peptide or targeting sequence for *KaPOx* with the available trained algorithms. As bacterial secretion systems are diverse and not entirely understood (35), an export of *KaPOx* from the cytoplasm can still be considered possible. A previous report on the actinomycetous *Streptomyces olivaceoviridis* documented the secretion of large cellulolytic enzyme complexes via the calcium-dependent dockerin-scaffoldin interaction, in which catalytically inactive scaffoldins bind various lytic enzymes at their dockerin domain (36). Studies of DyP from various actinobacteria describe the association of these enzymes with encapsulin to facilitate targeting of proteins via a C-terminal recognition sequence (37). Similar mechanisms could serve as means to translocate *KaPOx* and synergistic enzymes to the extracellular space in its native host. Interestingly, we found a dockerin-like motif and putative calcium-binding aspartate patches in the *KaPOx* homology model head domain, a domain which has not been ascribed a specific functionality in fungal *POxs* yet (38). We would like to stress at this point that *KaPOx* was selected for expression and characterization from a number of sequences from *Streptomyces* spp. and related species primarily based on sequence similarity. We cannot claim experimental evidence of actual growth on lignin of this bacterium.

As experiments with manganese peroxidase underlined, redox cycling occurs when DMP and other substituted phenols are oxidized by MnP and subsequently rereduced by *KaPOx*. We cannot experimentally verify if *POx* participates in the initial reduction of short-lived DMP phenoxy radicals or exclusively reduces the spontaneously formed quinoid DMP-dimer coerulignone (39, 40). Given the fact that *POx* efficiently mediates single-electron reductions with other substrates, we propose that aromatic radicals generally are subject to *POx* reduction, too. With this, the (re)polymerization of aromatic lignin constituent radicals (7–10) can be shifted toward depolymerization, as was confirmed for *POx* and laccase (12). The interaction of *POx* with manganese, and with (bacterial) DyP in particular (17, 41–43), may be even more complex. Here, the oxidase activity of *POx* can supply H_2O_2 to fuel peroxidase-mediated lignin decomposition, whereas the dehydrogenase activity recycles aromatic lignin compounds (radicals), decreases repolymerization, and scavenges highly reactive Mn(III) ions that are produced by the peroxidase (Fig. 4). A synergistic interaction between *POx* and peroxidases was recently demonstrated to effect lignin depolymerization *in vitro* (13).

Assuming at least limited hemicellulose degradation prior to delignification, small amounts of the major monosaccharide constituents D-glucose, D-galactose, D-xylose, L-arabinose, and D-mannose, which are all substrates for pyranose 2-oxidases, would be available at the early stage of lignocellulose deconstruction. Several reports on bacteria

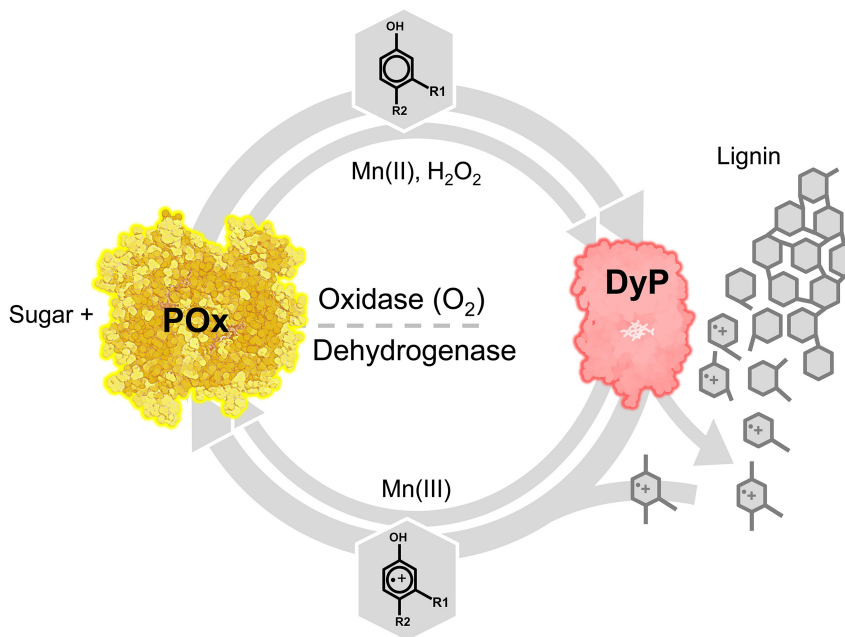


FIG 4 Proposed model of the physiological role of POx as a redox partner of specialized peroxidases. POx utilizes monosaccharides (D-glucose, D-galactose, D-xylose, etc.) potentially derived from (hemi)cellulose degradation. POx oxidase activity can supply diffusible H₂O₂ to fuel (dye-decolorizing) peroxidases (DyP). These peroxidases are known to produce aromatic radicals from lignin-derived phenols, mediating bond fission in the biopolymer. These radicals usually readily repolymerize but could be prevented from doing so if reduced by POx dehydrogenase activity as suggested. This would shift the balance toward depolymerization and additionally protect against cellular damage. For some peroxidases, Mn(III) is a by-product of their reaction. Like phenolic radicals, it can be seen as a potential mediator in depolymerization. Mn(III) can be reduced to Mn(II) and thus detoxified and recycled by POx.

of the *Streptomyces* genus provide data that these organisms possess the enzymatic equipment for at least partial extracellular polysaccharide degradation down to the monosaccharide level (44–47). These monosaccharide electron donors could be oxidized by POxs with concomitant H₂O₂ production, while other potential electron acceptors, like lignin-derived radicals (with their higher affinity for POxs), are expected to be largely absent at this stage. Transcriptome analysis in the white-rot fungus *Irpex lacteus* grown on lignin indicates a role for POx in the early stages of lignin degradation as well (43). In later stages, POx may preferentially reduce the increasingly present lignin-derived radicals (thereby preventing repolymerization) and reactive Mn(III)-complexes close to the cell, where such intermediates could cause damage to cellular constituents. The “switch” between oxidase and dehydrogenase activities could simply be dictated by the concentration of the available (dehydrogenase) acceptors and the high affinity of POx for those acceptors. Based on recently reported results, however, it is also conceivable that POx-supplied H₂O₂ activates lytic polysaccharide monooxygenases (LPMOs) in the presence of a reductant, as was shown for the cellulose-active ScLPMO10C from *Streptomyces coelicolor* (48). Additionally, phenols from plants and fungi were implicated in the reductive activation of LPMOs (11). This could suggest an intricate interplay of POx, peroxidase(s), and LPMO in the depolymerization of ligno-cellulosic substrates, particularly in the absence of a functional CDH, as we showed for bacteria.

Analysis of the *K. aureofaciens* genome revealed the presence of a set of genes encoding putative cellulolytic and ligninolytic enzymes. Our analysis identified five genes coding for putative laccases (26 to 27% identity to query; homologous laccase sequences are usually less conserved), six genes coding for putative DyP (42 to 61% identity to query), and five genes coding for putative LPMOs (41 to 74% identity to query). No genes with significant similarity to CAZy AA3 oxidoreductases besides POx (AOx, AAO, GOx, GDH, CDH, and PDH) could be found. Five putative choline dehydro-

TABLE 3 NCBI accession numbers of *K. aureofaciens* genes that were identified from genome mining to encode putative enzyme functionalities in biomass degradation^a

Category	Accession no. (sequence identity; E value)
AA3	
ChDH	WP_003983688.1 (40%; 2e-105) WP_003979475.1 (37%; 1e-101) WP_003981588.1 (36%; 4e-80) WP_003980634.1 (32%; 1e-75) WP_003983194.1 (31%; 1e-71)
ChOx	KOG78271.1 (82%; 0.0) WP_078575894.1 (83%; 0.0)
POx	WP_046385855.1 (38%; 6e-117)
DyP	WP_033347900.1 (60%; 7e-157) WP_050498772.1 (61%; 9e-157) WP_030278611.1 (60%; 1e-156) WP_030552786.1 (46%; 2e-95) WP_033348331.1 (46%; 5e-94) WP_003978980.1 (42%; 1e-88)
LPMO	WP_003983705.1 (74%; 2e-91) WP_003979198.1 (65%; 2e-83) WP_003986797.1 (51%; 2e-46) WP_033347003.1 (43%; 5e-39) WP_003986796.1 (41%; 1e-45)
Laccase	WP_033347195.1 (27%; 2e-42) WP_030552568.1 (27%; 1e-41) WP_003982845.1 (26%; 1e-26) WP_063736155.1 (26%; 2e-39) WP_030279851.1 (27%; 2e-38)

^aUsed query sequences (UniProtKB): AA3 (individual set), DyP (Q05415 and K7N5M8), LPMO (Q9RJC1, Q9RJJ2, B3PJ79, B3PDT6, Q838S1, Q2SNS3, C7R4I0, O83009, Q47QG3, Q47PB9, Q62YN7, and Q65N87), and laccase (J9PBQ8 and J9PBR2). No significantly similar sequence could be identified for queries of AAO, Aox, CDH, GDH, Gox, and PDH in the genome.

genes (ChDH) and two putative cholesterol oxidases (ChOx) represent the most closely related sequences to the AA3 queries (Table 3). Thus, *KaPOx* most likely represents the only AA3 family enzyme in this bacterium. Given the limited bacterial genome size (the *K. aureofaciens* genome is 7.1 Mb and the *I. lacteus* genome is 44.4 Mb), versatile oxidase and dehydrogenase activities for different purposes performed by one enzyme, POx, represent a vital advantage.

In summary, a comprehensive biochemical characterization of a novel pyranose 2-oxidase from the Gram-positive bacterium *K. aureofaciens* stresses the close biochemical similarity of this enzyme to previously reported POx from fungi. These data strongly support the close phylogenetic relation of bacterial and fungal POx established *in silico* and support the hypothesis of a late horizontal gene transfer of an ancestral POx gene from bacteria into the kingdom of fungi. The reported ability to reduce (complexed) manganese ions and the synergistic redox cycling with peroxidase by POx suggest a role in lignin degradation in bacteria.

MATERIALS AND METHODS

Phylogenetic analysis. Representative sequences of characterized GMC enzymes found on the UniProtKB Protein Knowledgebase (49) and in the literature were selected to create a phylogenetic tree compiling fungal and bacterial GMC enzymes. A protein search with the Basic Local Alignment Search Tool (BLAST) in bacteria (taxid: 2) was conducted on the nonredundant NCBI protein database (50) using the following characterized fungal enzymes as query sequences: AOx (GenBank accession numbers AAB57849.1 and ABI14440.1), AAO (AMW87253.1 and ALS87663.1), PDH (AAW82997.1 and AHA85314.1), GDH (XP_002372599.1 and AIL89873.1), GOx (AGI04246.1 and AAB09442.1), CDH (ADX41688.1 and EAA27355.1), and POx (AAO13382.1 and EAA62441.1). The 10 best hits for each fungal enzyme were combined in a tree of fungal and bacterial GMC enzymes. The selections were aligned in MAFFT v7.402 (51) using the E-INS-i algorithm, and maximum likelihood trees were calculated with PhyML (52) under the LG (53) substitution model, as determined by Smart Model Selection (54) under the Akaike information criterion (AIC) selection criterion. The tree topology was optimized using nearest neighbor

interchange (NNI) and subtree pruning and regrafting (SPR), and node support was assessed by performing 500 bootstrap replications.

To collect additional POx sequences occurring in bacteria we combined multiple searches on the UniProtKB, using either BLAST or HMMsearch (55). Queries for the HMMsearch were alignments of characterized fungal POx sequences and of the 10 best bacterial BLAST hits from the search described above. Queries for the BLAST search were characterized fungal POx sequences with GenBank accession numbers [AAO13382](#) and [EAA62441.1](#) (28, 33), characterized bacterial POx sequences with GenBank accession numbers [CCQ48064.1](#) and [A0A1E7NAU4](#) (6; this work), and the putative bacterial POx sequences with NCBI Reference Sequence numbers [WP_028814754.1](#) and [WP_035850787.1](#). All searches were restricted to E values of $<1.0e-30$, and duplicates were removed. Sequence names were renamed using SeqScrub (71), and the two most closely related GMC enzymes cholesterol oxidase (ChOx) and cellobiose dehydrogenase (CDH) were added as outgroups. Sequences not showing the flavin-binding GxGxxG motif (56) were removed from the selection. Sequences were aligned by MAFFT v7.402 using the FFT-NS-2 algorithm and a maximum likelihood tree was calculated with PhyML and the LG substitution model, as determined by Prottest 3.4.2 (57) under the AIC selection criterion. Tree topology was optimized using NNI and SPR and node support was assessed by performing 1,020 bootstrap replications.

Homology model and sequence analysis of KaPOx. We used the Protein Homology/Analogy Recognition Engine Phyre2 (58) to calculate the most probable homology model of the KaPOx based on the POx sequence from *Trametes ochracea* (formerly *Trametes multicolor*). For this pair, a sequence identity of 38.7% is reported for a covered sequence of 545 of 623 residues. The UniProtKB protein BLAST and PyMOL 1.3 were used for analyzing both the bacterial KaPOx sequence (A0A1E7NAU4) and the homology model with respect to ToPOx (Q7ZA32). The SignalP online tool (59) and the TatP online tool (60) were used for predicting the presence and identity of N-terminal signal peptides.

Recombinant expression and purification. The full-length KaPOx gene was synthesized with a C-terminal 6×His tag and inserted into the pET-21b(+) expression vector, in which the standard N-terminal T7-tag was excluded (BioCat). This plasmid was then transformed into chemically competent *E. coli* T7 Express cells (New England Biolabs) according to the standard 5-min transformation protocol. Sequencing (Microsynth) confirmed the identity of the plasmid. The cultivation of *E. coli* cultures was carried out routinely in terrific broth (TB) Amp⁺ buffered at pH 7.5 and supplemented with ampicillin ($100 \mu\text{g ml}^{-1}$) at 37°C. Cultures were incubated at 20°C for 20 h in the presence of 1.0% (wt/wt) lactose to induce expression of KaPOx. Cell disruption and immobilized metal affinity chromatography were carried out as previously described (61), with the adaptation of using 50 mM Tris-HCl based buffers at pH 8.0. Active fractions were pooled and dialyzed at 4°C against 50 mM potassium phosphate buffer (PPB; pH 6.5) using 7-kDa-cutoff Membra-Cel (Serva) dialysis tubing. After dialysis, the yellow KaPOx precipitate was harvested from the tube and washed twice with 50 mM PPB (pH 6.5) by centrifugation at $1,000 \times g$ and 4°C for 120 s. Homogeneity of the purified protein was confirmed by SDS-PAGE and LC-ESI-MS peptide mapping.

Protein concentration and purity. Protein concentrations of purification fractions and pure samples were analyzed using the Bio-Rad protein assay kit according to Bradford's method (62). For this, dilutions of bovine serum albumin were used as a standard. SDS-PAGE was carried out using Mini-PROTEAN TGX gels; Precision Plus unstained mass ladders served as a standard (both Bio-Rad). Purified protein samples were diluted to 0.5 mg ml^{-1} in 2× Laemmli buffer and incubated at 95°C for 5 min unless stated otherwise.

PAGE under nondenaturing conditions. Purified KaPOx was diluted to 1.5 mg ml^{-1} in nondenaturing sample buffer (25 mM Tris-HCl, 200 mM glycine, 10% [wt/wt] glycerol, 0.25% [wt/wt] bromophenol blue [pH 8.5]) and loaded onto a Mini-PROTEAN TGX stain-free gel (Bio-Rad) before being run at 150 V (25 to 50 mA) for 50 min. The results of the native PAGE were visualized using fluorescence imaging in a Gel Doc XR system (Bio-Rad).

DLS analysis of KaPOx multimerization and aggregation. Samples for dynamic light scattering (DLS) were prepared by diluting KaPOx to 1.0 mg ml^{-1} in 50 mM Tris-HCl and 100 mM NaCl (pH 8.5). Subsequently, the soluble protein solution was filtered through a 0.22- μm filter and centrifuged at $20,000 \times g$ for 5 min to remove remaining aggregates. Supernatants were analyzed in a Zetasizer Nano ZSP autotitrator system (Malvern) at 633 nm, and with back scattering at an angle of 173°. Size distribution models were fitted based on data obtained from 10-s integrations of the sample (Mark-Houwink parameters: $A = 0.428$ and $k = 7.67 \times 10^{-5} \text{ cm}^2 \text{ s}^{-1}$) with data processing optimized for protein sample by the supplier's software. Measurements of POx from *T. ochracea* and cellobiose dehydrogenase from *Myceliophthora thermophila* served as standards. Analysis of the pH-dependent aggregation of KaPOx was realized via pH titration with 0.5 M HCl from pH 9.0 to 5.0.

Peptide profiling of KaPOx H128 by LC-ESI-MS. LC-ESI-MS analysis was based on the previously described method (22) and was adapted to the given instrumentation. For localization of the covalently bound FAD, the same instruments were used as for protein identification. To this end, a total of 30 μg of KaPOx was S-alkylated with iodoacetamide and further digested with sequencing-grade chymotrypsin (Roche). The peptide mixture was analyzed using a Dionex Ultimate 3000 system directly linked to a quadrupole time of flight (Q-TOF) MS instrument (maXis 4G ETD; Bruker) equipped with the standard ESI source in the positive ion, data-dependent acquisition (DDA) mode (=switching to MS/MS mode for eluting peaks). MS scans were recorded (range, 150 to 2,200 m/z ; spectrum rate, 1.0 Hz) and the six highest peaks were selected for fragmentation (collision-induced dissociation [CID] mode). Instrument calibration was performed using ESI calibration mixture (Agilent). For separation of the peptides, a Thermo BioBasic C₁₈ separation column (5- μm particle size, 150 by 0.320 mm) was used. A gradient from 97% solvent A and 3% solvent B (solvent A, 65 mM ammonium formate buffer, pH 3.0 [formic acid

supplied by Carl Roth; ammonia supplied by VWR BDH Prolabo); solvent B, 80% acetonitrile [ACN; VWR BDH Prolabo] and 20% solvent A) to 40% solvent B in 45 min was applied, followed by a 15-min gradient from 40% solvent B to 95% solvent B at a flow rate of $6 \mu\text{l min}^{-1}$ at 32°C . DataAnalysis 4.0 (Bruker) was used for peptide evaluation.

Confirmation of C-2 glucose oxidation with HPLC. Twenty-milliliter enzymatic conversion mixes were prepared, containing 20 nM purified *KaPOx* (0.4 U), 20,000 U of washed *Corynebacterium glutamicum* catalase (Sigma) and 25 mM D-glucose, in 50 mM PPB (pH 7.5). Reaction mixtures were incubated at 30°C with 200 rpm shaking for 20 h; ambient oxygen served as the electron acceptor. Samples were drawn after 0, 20, 60, 180, 500, and 1,200 min, inactivated at 80°C for 20 min, and filtered through a 10-kDa spin filter prior to chromatographic analysis. 25 mM standards of D-glucose and 2-keto-D-glucose (both from Sigma) were used as analysis standards. High-performance liquid chromatography (HPLC) was carried out on a Dionex DX-500 system (Thermo Fisher) equipped with an Aminex HPX-87K column and an RI-101 refractive index detector (Shodex). Isocratic separations were run with H_2O at 0.5 ml min^{-1} (80°C) and data were processed with Chromleon 6.5 software.

Determination of kinetic constants. Assessments of the catalytic properties of the *KaPOx* were commonly carried out as 300- μl colorimetric reactions in the 96 well-plate format. Britton-Robinson buffer (63) (50 mM, pH 7.5) was the standard buffer system in all measurements unless stated otherwise. Kinetic slopes were recorded at 30°C for 1,200 s using an EnSpire multimode plate reader (PerkinElmer), with measurements being performed as triplicates.

We used the established peroxidase-coupled ABTS assay (64, 65) to determine the steady-state catalytic parameters of the *KaPOx* enzyme regarding its electron-donating substrates. Assay mixes contained 0.1 μM purified *KaPOx*, 1.0 mM ABTS ($\epsilon_{420} = 36.0 \text{ mM}^{-1} \text{ cm}^{-1}$; Amresco), horseradish peroxidase at 7.0 U ml^{-1} (181 U mg^{-1} ; Sigma) and 0.1 to 512 mM the respective electron donors. O_2 at ambient concentrations (approximately 250 μM) served as the electron acceptor.

Kinetic parameters were assessed for the electron acceptors 1,4-benzoquinone (1,4-BQ), 2,6-dichloroindophenol (DCIP), the ferrocenium ion, and the cationic ABTS radical with reported wavelengths and extinction coefficients (61). Enzymatic manganese(III) reduction was carried out using 50 mM sodium malonate buffer (pH 5.5) and Mn(III) acetate to facilitate formation of a stable Mn(III)-malonate complex. Reduction of the complexed Mn(III) cation ($\epsilon_{270} = 0.0116 \text{ mM}^{-1} \text{ cm}^{-1}$) was tracked at 270 nm (66) and reactions were run at 18°C to minimize autolytic dissociation. Colorimetric assay mixes contained 30 mM D-glucose, 0.5 μM purified *KaPOx*, and a 0.001 to 4 mM concentration of the respective electron acceptor and were buffered at pH 7.5 unless stated otherwise. To minimize the interference with ambient oxygen, all solutions used in the electron acceptor kinetic experiments were bubbled with nitrogen before use. Apparent kinetic constants were estimated by nonlinear least-square regression fitting using the Microsoft Excel Solver plugin. Catalytic turnover rates are stated with respect to the dimeric form of *KaPOx* of approximately 122 kDa.

pH-dependent enzyme activities for DCIP, 1,4-BQ, and O_2 (ABTS assay) were carried out under the aforementioned conditions and concentrations using 50 mM Britton-Robinson buffer at a pH range between 4.0 and 9.5, with increments of 0.5 unit.

We assessed the temperature-dependent inactivation of the *KaPOx* enzyme with respect to time and temperature. Buffered enzyme aliquots were incubated at 30, 36, 39, 45, 50, 56, 60, and 65°C in a C1000 thermocycler (Bio-Rad) for 20 min to evaluate temperature dependency. In contrast, a single buffered *KaPOx* sample was incubated at constant 50°C , and aliquots were drawn after 1, 2, 4, 8, 15, 20, 30, and 60 min to determine the influence of incubation times (at constant temperature) on thermal inactivation. Before measurement with the standard peroxidase/ABTS assay, samples were diluted to yield concentrations of 0.1 μM *KaPOx* in the assay mix.

Oxygen as the electron acceptor. The determination of apparent Michaelis-Menten parameters was realized using the luminescent oxygen microsensor Microx TX3 (PreSens), as has been described previously (67). In this way, the gradual consumption of O_2 from the sealed reaction vial was detected. Dissolved oxygen concentrations were tracked by the sensor for 10 min (30°C) in the stirred reaction mix, which contained 1.0 μM purified *KaPOx*. Initial substrate concentrations were 100 mM and 0.850 mM for D-glucose and O_2 , respectively. The obtained oxygen consumption curves were fitted to the Runge-Kutta integration of the Michaelis-Menten equation by minimizing least-mean square errors as described previously (68).

Quinone-hydroquinone redox cycling with manganese peroxidase. Redox-recycling assays were carried out in 50 mM tartrate buffer (pH 5.5) and contained 0.5 mM MnCl_2 , 30 mM D-glucose, and 0.1 μM *Nematoloma frowardii* manganese peroxidase (MnP; Sigma), alongside 10 mM 2,6-dimethoxyphenol (DMP), 10 mM guaiacol, 0.2 mM acetosyringone, or 0.4 mM sinapic acid. Peroxidase-mediated oxidation of phenols was started by adding 0.1 mM H_2O_2 , and reactions were run for 180 s before 1.0 μM *KaPOx* was added. In contrast, the 1,4-BQ (1 mM) reaction was started with 0.5 μM *KaPOx* before 1 μM MnP was added. Absorbance was tracked at 470 nm, 465 nm, 300 nm, 510 nm, and 290 nm, as was reported in the literature (12, 69, 70). All reactions were performed at 30°C with buffers and solutions exposed to ambient oxygen.

SUPPLEMENTAL MATERIAL

Supplemental material for this article may be found at <https://doi.org/10.1128/AEM.00390-19>.

SUPPLEMENTAL FILE 1, PDF file, 1 MB.

ACKNOWLEDGMENTS

This work was supported by the Austrian Science Fund (FWF) Doctoral Program BioToP—Biomolecular Technology of Proteins (FWF W1224). Experimental analysis and data processing were supported by EQ-BOKU VIBT GmbH and the BOKU Core Facility for Biomolecular and Cellular Analysis.

We thank Roland Ludwig for his scientific advice and Christian Leitner for critical reading of the manuscript. Also, we acknowledge Erik Breslmayr for helping to establish our infrastructure for phylogenetic analyses.

There are no conflicts of interest to declare.

REFERENCES

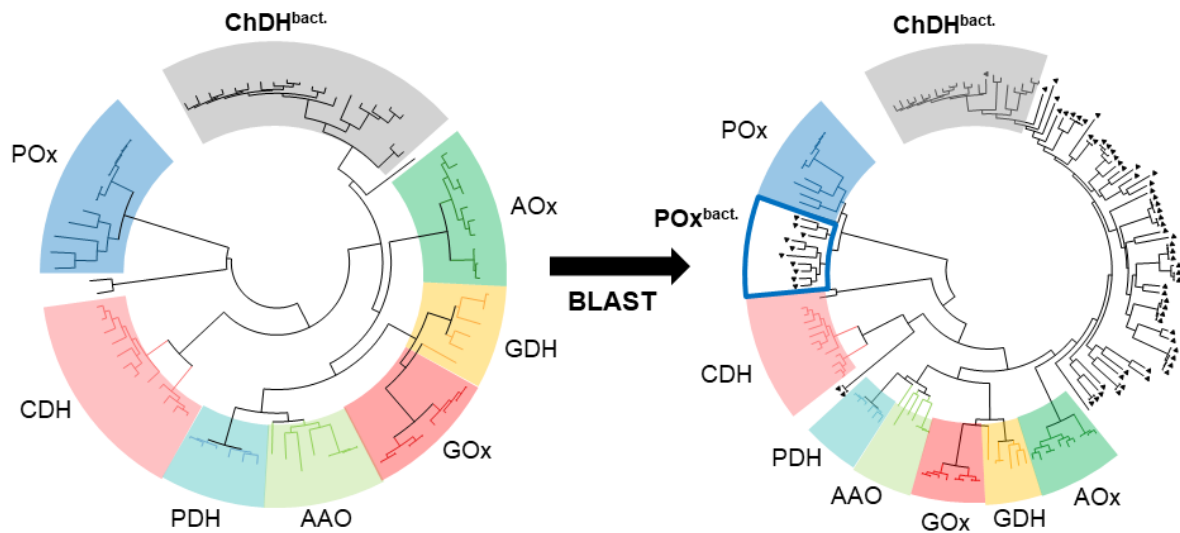
- Cavener DR. 1992. GMC oxidoreductases: a newly defined family of homologous proteins with diverse catalytic activities. *J Mol Biol* 223: 811–814. [https://doi.org/10.1016/0022-2836\(92\)90992-5](https://doi.org/10.1016/0022-2836(92)90992-5).
- Kiess M, Hecht H-J, Kalisz HM. 1998. Glucose oxidase from *Penicillium amagasakiense*. Primary structure and comparison with other glucose-methanol-choline (GMC) oxidoreductases. *Eur J Biochem* 252:90–99. <https://doi.org/10.1046/j.1432-1327.1998.2520090.x>.
- Wongnate T, Chaiyen P. 2013. The substrate oxidation mechanism of pyranose 2-oxidase and other related enzymes in the glucose-methanol-choline superfamily. *FEBS J* 280:3009–3027. <https://doi.org/10.1111/febs.12280>.
- Leitner C, Volc J, Haltrich D. 2001. Purification and characterization of pyranose oxidase from the white rot fungus *Trametes multicolor*. *Appl Environ Microbiol* 67:3636–3644. <https://doi.org/10.1128/AEM.67.8.3636-3644.2001>.
- Daniel G, Volc J, Kubatova E. 1994. Pyranose oxidase, a major source of H(2)O(2) during wood degradation by *Phanerochaete chrysosporium*, *Trametes versicolor*, and *Oudemansiella mucida*. *Appl Environ Microbiol* 60:2524–2532.
- Pisanelli I, Kujawa M, Spadiut O, Kittl R, Halada P, Volc J, Mozuch MD, Kersten P, Haltrich D, Peterbauer C. 2009. Pyranose 2-oxidase from *Phanerochaete chrysosporium*—expression in *E. coli* and biochemical characterization. *J Biotechnol* 142:97–106. <https://doi.org/10.1016/j.jbiotec.2009.03.019>.
- Bugg TDH, Ahmad M, Hardiman EM, Rahmanpour R. 2011. Pathways for degradation of lignin in bacteria and fungi. *Nat Prod Rep* 28:1883–1896. <https://doi.org/10.1039/c1np00042j>.
- Eastwood DC, Floudas D, Binder M, Majcherczyk A, Schneider P, Aerts A, Asiegbu FO, Baker SE, Barry K, Bendixby M, Blumentritt M, Coutinho PM, Cullen D, de Vries RP, Gathman A, Goodell B, Henrissat B, Ihrmark K, Kauserud H, Kohler A, LaButti K, Lapidus A, Lavin JL, Lee Y-H, Lindquist E, Lilly W, Lucas S, Morin E, Murat C, Oguiza JA, Park J, Pisabarro AG, Riley R, Rosling A, Salamov A, Schmidt O, Schmutz J, Skrede I, Stenlid J, Wiebenga A, Xie X, Kues U, Hibbett DS, Hoffmeister D, Höglberg N, Martin F, Grigoriev IV, Watkinson SC. 2011. The plant cell wall-decomposing machinery underlies the functional diversity of forest fungi. *Science* 333:762–765. <https://doi.org/10.1126/science.1205411>.
- Brown ME, Chang M. 2014. Exploring bacterial lignin degradation. *Curr Opin Chem Biol* 19:1–7. <https://doi.org/10.1016/j.cbpa.2013.11.015>.
- Cragg SM, Beckham GT, Bruce NC, Bugg TDH, Distel DL, Dupree P, Etxabe AG, Goodell BS, Jellison J, McGeehan JE, McQueen-Mason SJ, Schnorr K, Walton PH, Watts JEM, Zimmer M. 2015. Lignocellulose degradation mechanisms across the Tree of Life. *Curr Opin Chem Biol* 29:108–119. <https://doi.org/10.1016/j.cbpa.2015.10.018>.
- Kracher D, Scheiblbrandner S, Felice AKG, Breslmayr E, Preims M, Ludwig K, Haltrich D, Eijsink VGH, Ludwig R. 2016. Extracellular electron transfer systems fuel cellulose oxidative degradation. *Science* 352:1098. <https://doi.org/10.1126/science.aaf3165>.
- Ai M-Q, Wang F-F, Zhang Y-Z, Huang F. 2014. Purification of pyranose oxidase from the white rot fungus *Irpex lacteus* and its cooperation with laccase in lignin degradation. *Process Biochem* 49:2191–2198. <https://doi.org/10.1016/j.procbio.2014.10.001>.
- Wang F, Huang F, Ai M. 2019. Synergetic depolymerization of aspen CEL by pyranose 2-oxidase and lignin-degrading peroxidases. *BioResources* 14:3481–3494.
- Sützl L, Laurent C, Abrera AT, Schütz G, Ludwig R, Haltrich D. 2018. Multiplicity of enzymatic functions in the CAZy AA3 family. *Appl Microbiol Biotechnol* 102:2477–2492. <https://doi.org/10.1007/s00253-018-8784-0>.
- Pollegioni L, Tonin F, Rosini E. 2015. Lignin-degrading enzymes. *FEBS J* 282:1190–1213. <https://doi.org/10.1111/febs.13224>.
- Janusz G, Pawlik A, Sulej J, Swiderska-Burek U, Jarosz-Wilkolazka A, Paszczynski A. 2017. Lignin degradation: microorganisms, enzymes involved, genomes analysis and evolution. *FEMS Microbiol Rev* 41: 941–962. <https://doi.org/10.1093/femsre/fux049>.
- Brown ME, Barros T, Chang M. 2012. Identification and characterization of a multifunctional dye peroxidase from a lignin-reactive bacterium. *ACS Chem Biol* 7:2074–2081. <https://doi.org/10.1021/cb300383y>.
- Colpa DI, Fraaije MW, van Bloois E. 2014. DyP-type peroxidases: a promising and versatile class of enzymes. *J Ind Microbiol Biotechnol* 41:1–7. <https://doi.org/10.1007/s10295-013-1371-6>.
- Min K, Gong G, Woo HM, Kim Y, Um Y. 2015. A dye-decolorizing peroxidase from *Bacillus subtilis* exhibiting substrate-dependent optimum temperature for dyes and β -ether lignin dimer. *Sci Rep* 5:8245. <https://doi.org/10.1038/srep08245>.
- Ju K-S, Gao J, Doroghazi JR, Wang K-K, Thibodeaux CJ, Li S, Metzger E, Fudala J, Su J, Zhang JK, Lee J, Cioni JP, Evans BS, Hirota R, Labeda DP, van der Donk WA, Metcalf WW. 2015. Discovery of phosphonic acid natural products by mining the genomes of 10,000 actinomycetes. *Proc Natl Acad Sci U S A* 112:12175–12180. <https://doi.org/10.1073/pnas.1500873112>.
- Tan T-C, Pitsawong W, Wongnate T, Spadiut O, Haltrich D, Chaiyen P, Divne C. 2010. H-bonding and positive charge at the N(5)/O(4) locus are critical for covalent flavin attachment in *Trametes* pyranose 2-oxidase. *J Mol Biol* 402:578–594. <https://doi.org/10.1016/j.jmb.2010.08.011>.
- Halada P, Leitner C, Sedmera P, Haltrich D, Volc J. 2003. Identification of the covalent flavin adenine dinucleotide-binding region in pyranose 2-oxidase from *Trametes multicolor*. *Anal Biochem* 314:235–242. [https://doi.org/10.1016/S0003-2697\(02\)00661-9](https://doi.org/10.1016/S0003-2697(02)00661-9).
- Spadiut O, Tan T-C, Pisanelli I, Haltrich D, Divne C. 2010. Importance of the gating segment in the substrate-recognition loop of pyranose 2-oxidase. *FEBS J* 277:2892–2909. <https://doi.org/10.1111/j.1742-4658.2010.07705.x>.
- Mendes S, Banha C, Madeira J, Santos D, Miranda V, Manzanera M, Ventura MR, van Berkel WJH, Martins LO. 2016. Characterization of a bacterial pyranose 2-oxidase from *Arthrobacter siccitolerans*. *J Mol Catal B Enzym* 133:534–543. <https://doi.org/10.1016/j.molcatb.2016.11.005>.
- Kittl R, Sygmund C, Halada P, Volc J, Divne C, Haltrich D, Peterbauer CK. 2008. Molecular cloning of three pyranose dehydrogenase-encoding genes from *Agaricus meleagris* and analysis of their expression by real-time RT-PCR. *Curr Genet* 53:117–127. <https://doi.org/10.1007/s00294-007-0171-9>.
- Schafer A, Bieg S, Huwig A, Kohring G, Giffhorn F. 1996. Purification by immunoaffinity chromatography, characterization, and structural analysis of a thermostable pyranose oxidase from the white rot fungus *Phlebiopsis gigantea*. *Appl Environ Microbiol* 62:2586–2592.
- de Koker TH, Mozuch MD, Cullen D, Gaskell J, Kersten PJ. 2004. Isolation and purification of pyranose 2-oxidase from *Phanerochaete chrysosporium* and characterization of gene structure and regulation. *Appl Environ Microbiol* 60:5794–5800. <https://doi.org/10.1128/AEM.70.10.5794-5800.2004>.
- Bannwarth M, Bastian S, Heckmann-Pohl D, Giffhorn F, Schulz GE. 2004. Crystal structure of pyranose 2-oxidase from the white-rot fungus *Peniophora* sp. *Biochemistry* 43:11683–11690. <https://doi.org/10.1021/bi048609q>.
- Lynd LR, Weimer PJ, van Zyl WH, Pretorius IS. 2002. Microbial cellulose

- utilization: fundamentals and biotechnology. *Microbiol Mol Biol Rev* 66:506–577. <https://doi.org/10.1128/MMBR.66.3.506-577.2002>.
30. Prewitt L, Kang Y, Kakumanu ML, Williams M. 2014. Fungal and bacterial community succession differs for three wood types during decay in a forest soil. *Microb Ecol* 68:212–221. <https://doi.org/10.1007/s00248-014-0396-3>.
 31. Cortes-Tolalpa L, Jiménez DJ, de Lima Bossi MJ, Salles JF, van Elsas JD. 2016. Different inocula produce distinctive microbial consortia with similar lignocellulose degradation capacity. *Appl Microbiol Biotechnol* 100:7713–7725. <https://doi.org/10.1007/s00253-016-7516-6>.
 32. Wei H, Xu Q, Taylor LE, Baker JO, Tucker MP, Ding S-Y. 2009. Natural paradigms of plant cell wall degradation. *Curr Opin Biotechnol* 20: 330–338. <https://doi.org/10.1016/j.copbio.2009.05.008>.
 33. Pisanelli I, Wührer P, Reyes-Dominguez Y, Spadiut O, Haltrich D, Peterbauer C. 2012. Heterologous expression and biochemical characterization of novel pyranose 2-oxidases from the ascomycetes *Aspergillus nidulans* and *Aspergillus oryzae*. *Appl Microbiol Biotechnol* 93: 1157–1166. <https://doi.org/10.1007/s00253-011-3568-9>.
 34. Halada P, Brugger D, Volc J, Peterbauer CK, Leitner C, Haltrich D. 2016. Oxidation of Phe454 in the gating segment inactivates *Trametes multicolor* pyranose oxidase during substrate turnover. *PLoS One* 11: e0148108. <https://doi.org/10.1371/journal.pone.0148108>.
 35. Green ER, Meccas J. 2016. Bacterial secretion systems: an overview. *Microbiol Spectr* 4:VMBF-0012-2015. <https://doi.org/10.1128/microbiolspec.VMBF-0012-2015>.
 36. Jiang Z, Deng W, Yan Q, Zhai Q, Li L, Kusakabe I. 2006. Subunit composition of a large xylanolytic complex (xylanosome) from *Streptomyces olivaceoviridis* E-86. *J Biotechnol* 126:304–312. <https://doi.org/10.1016/j.jbiotec.2006.05.006>.
 37. Singh R, Eltis LD. 2015. The multihued palette of dye-decolorizing peroxidases. *Arch Biochem Biophys* 574:56–65. <https://doi.org/10.1016/j.abb.2015.01.014>.
 38. Hallberg M, Leitner C, Haltrich D, Divne C. 2004. Crystal structure of the 270 kDa homotetrameric lignin-degrading enzyme pyranose 2-oxidase. *J Mol Biol* 341:781–796. <https://doi.org/10.1016/j.jmb.2004.06.033>.
 39. Wariishi H, Valli K, Gold MH. 1992. Manganese(II) oxidation by manganese peroxidase from the basidiomycete *Phanerochaete chrysosporium*. Kinetic mechanism and role of chelators. *J Biol Chem* 267:23688–23695.
 40. Breslmayr E, Hanžek M, Hanrahan A, Leitner C, Kittl R, Šantek B, Oostenbrink C, Ludwig R. 2018. A fast and sensitive activity assay for lytic polysaccharide monoxygenase. *Biotechnol Biofuels* 11:79. <https://doi.org/10.1186/s13068-018-1063-6>.
 41. Santos A, Mendes S, Brissos V, Martins LO. 2014. New dye-decolorizing peroxidases from *Bacillus subtilis* and *Pseudomonas putida* MET94: towards biotechnological applications. *Appl Microbiol Biotechnol* 98: 2053–2065. <https://doi.org/10.1007/s00253-013-5041-4>.
 42. de Gonzalo G, Colpa DI, Habib MHM, Fraaije MW. 2016. Bacterial enzymes involved in lignin degradation. *J Biotechnol* 236:110–119. <https://doi.org/10.1016/j.jbiotec.2016.08.011>.
 43. Qin X, Luo H, Zhang X, Yao B, Ma F, Su X. 2018. Dye-decolorizing peroxidases in *Irpex lacteus* combining the catalytic properties of heme peroxidases and laccase play important roles in ligninolytic system. *Biotechnol Biofuels* 11:302. <https://doi.org/10.1186/s13068-018-1303-9>.
 44. Flores ME, Perez R, Huitron C. 1997. β -Xylosidase and xylanase characterization and production by *Streptomyces* sp. CH-M-1035. *Lett Appl Microbiol* 24:410–416. <https://doi.org/10.1046/j.1472-765X.1997.00149.x>.
 45. Arora A, Nain L, Gupta JK. 2005. Solid-state fermentation of wood residues by *Streptomyces griseus* B1, a soil isolate, and solubilization of lignins. *World J Microbiol Biotechnol* 21:303–308. <https://doi.org/10.1007/s11274-004-3827-3>.
 46. Takasuka TE, Book AJ, Lewin GR, Currie CR, Fox BG. 2013. Aerobic deconstruction of cellulosic biomass by an insect-associated *Streptomyces*. *Sci Rep* 3:1030. <https://doi.org/10.1038/srep01030>.
 47. Lee K-S, Kim C-J, Yoon K-H. 2003. Characterization of the β -galactosidase produced by *Streptomyces* sp. *Korean J Microbiol Biotechnol* 31:151–156.
 48. Bissaro B, Röhr ÅK, Müller G, Chylenski P, Skaugen M, Forsberg Z, Horn SJ, Vaaje-Kolstad G, Eijsink V. 2017. Oxidative cleavage of polysaccharides by monocopper enzymes depends on H₂O₂. *Nat Chem Biol* 13: 1123–1128. <https://doi.org/10.1038/nchembio.2470>.
 49. Pundir S, Martin MJ, O'Donovan C. 2017. UniProt Protein Knowledgebase. *Methods Mol Biol* 1558:41–55. https://doi.org/10.1007/978-1-4939-6783-4_2.
 50. Johnson M, Zaretskaya I, Raytselis Y, Merezuk Y, McGinnis S, Madden TL. 2008. NCBI BLAST: a better web interface. *Nucleic Acids Res* 36: W5–W9. <https://doi.org/10.1093/nar/gkn201>.
 51. Katoh K, Standley DM. 2013. MAFFT multiple sequence alignment software version 7: improvements in performance and usability. *Mol Biol Evol* 30:772–780. <https://doi.org/10.1093/molbev/mst010>.
 52. Guindon S, Dufayard J-F, Lefort V, Anisimova M, Hordijk W, Gascuel O. 2010. New algorithms and methods to estimate maximum-likelihood phylogenies: assessing the performance of PhyML 3.0. *Syst Biol* 59: 307–321. <https://doi.org/10.1093/sysbio/syq010>.
 53. Le SQ, Gascuel O. 2008. An improved general amino acid replacement matrix. *Mol Biol Evol* 25:1307–1320. <https://doi.org/10.1093/molbev/msn067>.
 54. Lefort V, Longueville J-E, Gascuel O. 2017. SMS: Smart Model Selection in PhyML. *Mol Biol Evol* 34:2422–2424. <https://doi.org/10.1093/molbev/msx149>.
 55. Eddy SR. 2011. Accelerated profile HMM searches. *PLoS Comput Biol* 7:e1002195. <https://doi.org/10.1371/journal.pcbi.1002195>.
 56. Dym O, Eisenberg D. 2001. Sequence-structure analysis of FAD-containing proteins. *Protein Sci* 10:1712–1728. <https://doi.org/10.1110/ps.12801>.
 57. Darriba D, Taboada GL, Doallo R, Posada D. 2011. ProtTest 3: fast selection of best-fit models of protein evolution. *Bioinformatics* 27: 1164–1165. <https://doi.org/10.1093/bioinformatics/btr088>.
 58. Kelley LA, Mezulis S, Yates CM, Sternberg M. 2015. The Phyre2 web portal for protein modeling, prediction and analysis. *Nat Protoc* 10:845–858. <https://doi.org/10.1038/nprot.2015.053>.
 59. Petersen TN, Brunak S, von Heijne G, Nielsen H. 2011. SignalP 4.0: discriminating signal peptides from transmembrane regions. *Nat Methods* 8:785–786. <https://doi.org/10.1038/nmeth.1701>.
 60. Bendtsen J, Nielsen H, Widdick D, Palmer T, Brunak S. 2005. Prediction of twin-arginine signal peptides. *BMC Bioinformatics* 6:167. <https://doi.org/10.1186/1471-2105-6-167>.
 61. Brugger D, Krondorfer I, Shelswell C, Huber-Dittes B, Haltrich D, Peterbauer CK. 2014. Engineering pyranose 2-oxidase for modified oxygen reactivity. *PLoS One* 9:e109242. <https://doi.org/10.1371/journal.pone.0109242>.
 62. Bradford MM. 1976. A rapid and sensitive method for the quantitation of microgram quantities of protein utilizing the principle of protein-dye binding. *Anal Biochem* 72:248–254. [https://doi.org/10.1016/0003-2697\(76\)90527-3](https://doi.org/10.1016/0003-2697(76)90527-3).
 63. Britton HTS, Robinson RA. 1931. CXC VIII. Universal buffer solutions and the dissociation constant of veronal. *J Chem Soc* 0:1456–1462. <https://doi.org/10.1039/JR9310001456>.
 64. Danneel HJ, Rössner E, Zeek A, Giffhorn F. 1993. Purification and characterization of a pyranose oxidase from the basidiomycete *Peniophora gigantea* and chemical analyses of its reaction products. *Eur J Biochem* 214: 795–802. <https://doi.org/10.1111/j.1432-1033.1993.tb17982.x>.
 65. Spadiut O, Leitner C, Tan T-C, Ludwig R, Divne C, Haltrich D. 2008. Mutations of Thr169 affect substrate specificity of pyranose 2-oxidase from *Trametes multicolor*. *Biocatal Biotransformation* 26:120–127. <https://doi.org/10.1080/10242420701789320>.
 66. Hofrichter M, Ziegenhagen D, Vares T, Friedrich M, Jäger MG, Fritsche W, Hatakka A. 1998. Oxidative decomposition of malonic acid as basis for the action of manganese peroxidase in the absence of hydrogen peroxide. *FEBS Lett* 434:362–366. [https://doi.org/10.1016/S0014-5793\(98\)01023-0](https://doi.org/10.1016/S0014-5793(98)01023-0).
 67. Sygmund C, Santner P, Krondorfer I, Peterbauer CK, Alcalde M, Nyanhongo GS, Guebitz GM, Ludwig R. 2013. Semi-rational engineering of cellobiose dehydrogenase for improved hydrogen peroxide production. *Microb Cell Fact* 12:38. <https://doi.org/10.1186/1475-2859-12-38>.
 68. Claassen N, Barber SA. 1974. A method for characterizing the relation between nutrient concentration and flux into roots of intact plants. *Plant Physiol* 54:564–568. <https://doi.org/10.1104/pp.54.4.564>.
 69. Pardo I, Chanagá X, Vicente A, Alcalde M, Camarero S. 2013. New colorimetric screening assays for the directed evolution of fungal laccases to improve the conversion of plant biomass. *BMC Biotechnol* 13:90. <https://doi.org/10.1186/1472-6750-13-90>.
 70. Brugger D, Krondorfer I, Zahma K, Stoisser T, Bolivar JM, Nidetzky B, Peterbauer CK, Haltrich D. 2014. Convenient microtiter plate-based, oxygen-independent activity assays for flavin-dependent oxidoreductases based on different redox dyes. *Biotechnol J* 9:474–482. <https://doi.org/10.1002/biot.201300336>.
 71. Foley G, Sützl L, D' Cunha S, Gillam EMJ, Bodén M. SeqScrub: a web tool for automatic cleaning and annotation of FASTA file headers for bioinformatic applications. *BioTechniques*, in press.

1 **SUPPLEMENTAL INFORMATION**

2 **Supplemental figures**

3 **Figure S1.**



4

5 **Phylogenetic indications for a horizontal gene transfer of POx.**

6 (Left) Phylogenetic tree of characterized fungal GMC_AA3 family enzyme sequences:

7 pyranose oxidase (POx), cellobiose dehydrogenase (CDH), pyranose dehydrogenase

8 (PDH), aryl-alcohol oxidase (AAO), glucose oxidase (GOx), glucose dehydrogenase

9 (GDH), alcohol oxidase (AOx) and bacterial choline dehydrogenase (ChDH). (Right)

10 Phylogenetic tree of the same collection of sequences with most similar bacterial

11 sequences from BLAST search added.

12 **Figure S2.**

```

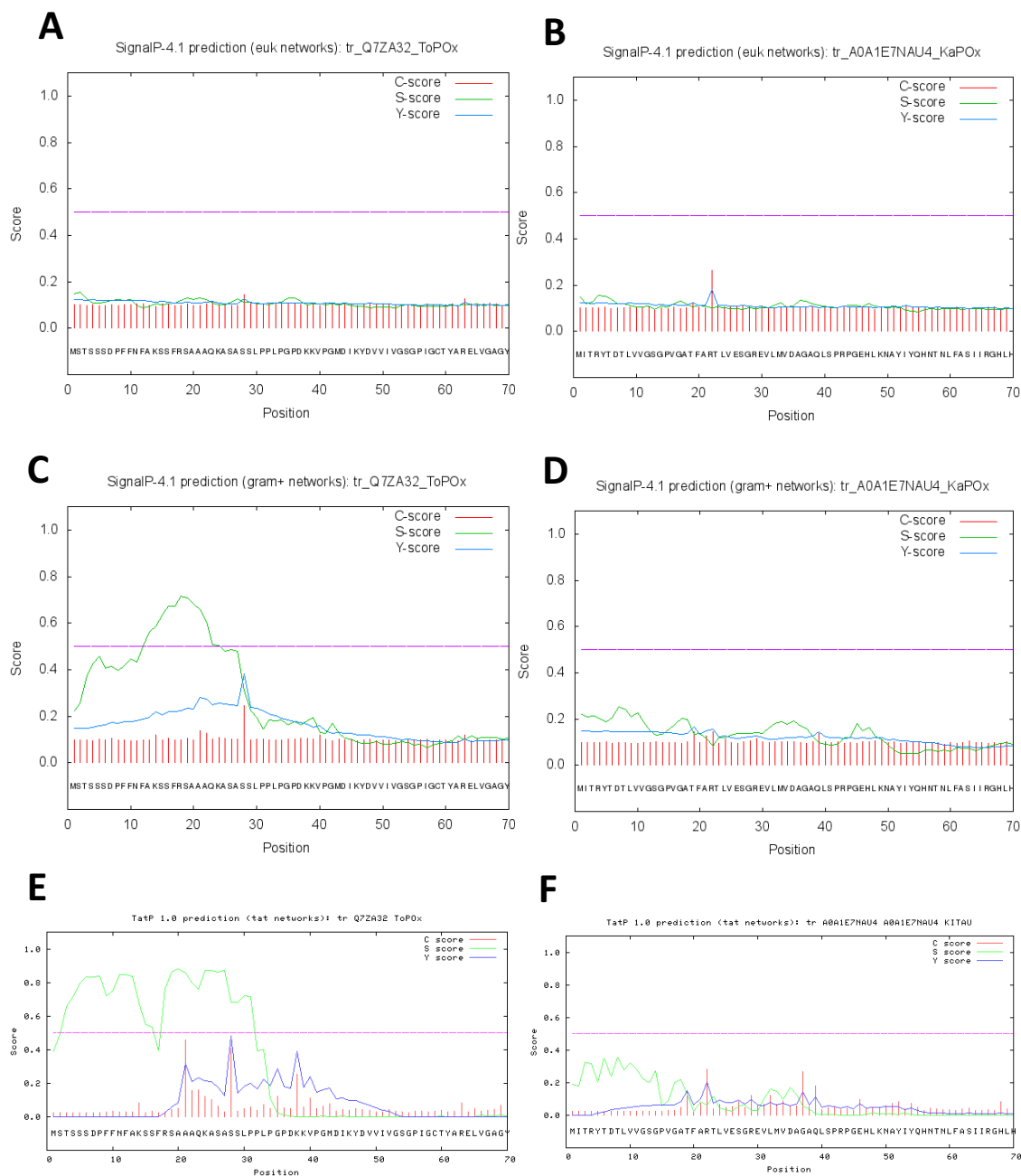
13
14 TR|Q7ZA32|TOPOX MSTSSSDPFFNFAKSSFRSAAAQKASASSLPLPGPKKVPGMDDIKYDVVIVGSGPIGCT 60
15 TR|A0A1E7NAU4|KAPOX -----MITRYTDTLVVGSVPVGT 19
16 : *.:*****:*.
17
18 TR|Q7ZA32|TOPOX YARELVGAGYKVMFMDIGEIDSGLKI GAHKNTVEYQKNIDKFNVIQQLMSVSVPVNT 120
19 TR|A0A1E7NAU4|KAPOX FARTLVESGREVLMDVMDAGAQL-SPRPGEHLKNAYIYQHNTNLFASII RGHLLHLSVPTSA 78
20 :** ** :* :* *.* * . : * * ** : ** * : *.:**:* :***.:
21
22 TR|Q7ZA32|TOPOX LVVDTLSP---TSWQASTFFVRNGSNPEQDPLRNLSGQAVTRVVGGMSTHWTGATPRFDR 177
23 TR|A0A1E7NAU4|KAPOX RAELAVDPAAMAELGNSRNSARNAENPDQDPYRNLSAAAACYAVGGMGTHWTGATPRHHP 138
24 . :.* :. :. .**..**:* ***. * . *****.***** ***.
25
26 TR|Q7ZA32|TOPOX EQRPLLKDDADADDAEWDRLYTKAESYFQGTGDFKESIRHNLVNLKLTTEEYKQR--- 234
27 TR|A0A1E7NAU4|KAPOX ----VL-ERYDGISDQEWGGLYGEAERLLRVSAREFDFSIRQHVLTEALRREFSELDPGY 193
28 :* : . * ** * * : * : : : : * . ** : * * : * . * : .
29
30 TR|Q7ZA32|TOPOX DFQQIPLAAT--RRSPTFVWSSANTVFDLQNRPNTPAPEERFNLFPAVACERVVRNALN 292
31 TR|A0A1E7NAU4|KAPOX VQVSLPLAARRRDNRPNMNVHVTGVDTVLGDL----ADGHPLFSLLPQLHCTRLVLDLDRG 248
32 :.*.:***** * . * :*.:**.:**.:
33 . *.:* * * : .
34
35 TR|Q7ZA32|TOPOX SEIESLHIHDLISGDRFEIKADVYVLTAGAVHNTQLLVNSGFGQLGRPNPANPELLPSL 352
36 TR|A0A1E7NAU4|KAPOX TRIAYAEVRDLNRSETVRVVDNYVVAAGAVLAPQLLHASGIRP-----AAL 295
37 :.* :.:** :. :. : * * :.:** * * * * : * :
38
39 TR|Q7ZA32|TOPOX GSYITEQSLVFCQTVMSTELIDSVKSDMTIRGTPGELTYSVTYTPGASTNKHPDWWNEKV 412
40 TR|A0A1E7NAU4|KAPOX GRYLTEHPMAFCQVILLKDLVEQARTDQRFGG-----QV 329
41 * *.:** : . ** : : . : : : : * : * : *
42
43 TR|Q7ZA32|TOPOX KNHMMQHQEDPLPIPEDPEPQVTTLFQPSHPWHTQIHRDAFSYGAVQQSIDSRLIVDWR 472
44 TR|A0A1E7NAU4|KAPOX ARHTTLFPDDDLPIPVDDPEPNVWIPVSEGRPWHAQITRDAFHYGDVPPHVDGRLIVDLR 389
45 . * . : * ** * : ** * * . . : ** * * * * * * * : * . ** * * *
46
47 TR|Q7ZA32|TOPOX FFGRTPEKKEENLWFSKITDAYNMPQPTFDFRFPAGRTSKEAEDMMTDMCVMSAKIGGF 532
48 TR|A0A1E7NAU4|KAPOX WFGIVEPRPDNRVTFSDTRTDVGMGPQPTFEYALSPQDAE-RQHAMMAEMMRAATALGGF 448
49 :** .** : : : * * . ** . ***** : : : . . . * : * : : * **
50
51 TR|Q7ZA32|TOPOX LPGSLPQFMPEGLVVLHGGTHRMGFDEKEDNCCVNTDSRVFGFKNLFLGCGNIPTAYGA 592
52 TR|A0A1E7NAU4|KAPOX LPGSEPRFTAPGLPLHIAGTIRMDDFPQ--SSVVDTDSRVWGLENLVYLGNGVIPTGTAC 506
53 **** *:* ** * * : . * ** * * : . . * : ** * : : * : ** * * * * . .
54
55 TR|Q7ZA32|TOPOX NPTLTAMSLAIKSEYIKQNFPTSPFTSEAQ----- 623
56 TR|A0A1E7NAU4|KAPOX NPTLTSVAMALKAHHLAGSREARERRRTGADEVLAVERS 545
57 ***** : : : * : : : . .

```

58 **Clustal Omega sequence alignment of bacterial *KaPOx* to fungal *ToPOx*.** The 623
59 amino acid long sequence of *T. ochracea* POx (TOPOX, top) was aligned to the 545
60 amino acid long sequence of *K. aureofaciens* POx (KAPOX, bottom) using the UniProtKB
61 alignment tool (Clustal Omega). Identical residues at aligned positions are indicated with
62 an asterisk (*).

63

64 **Figure S3.**



65

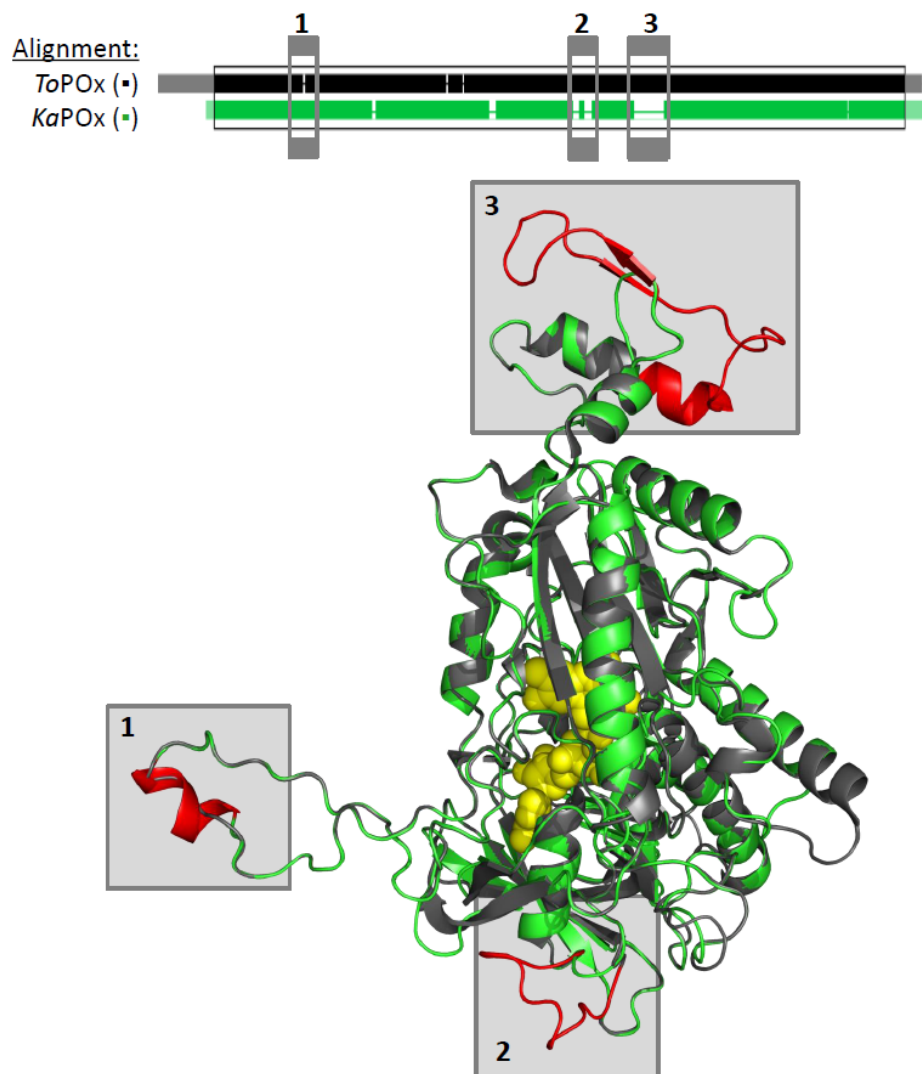
66

67

68 **SignalP, TatP prediction of N-terminal signal peptide cleavage sites in *KaPOx* and**
 69 ***ToPOx*.** The figure summarizes SignalP 4.1 signal peptide predictions from analyses of
 70 *POx* sequences: (A) *ToPOx* and (B) *KaPOx* with eukaryotic prediction; (C) *ToPOx* and
 71 (D) *KaPOx* with Gram-positive bacterial prediction. The TatP 1.0 online prediction tool

72 analyzed the first 70 residues of (E) *ToPOx* and (F) *KaPOx* to predict twin-arginine signal
73 peptide cleavage sites.
74

75 **Figure S4.**

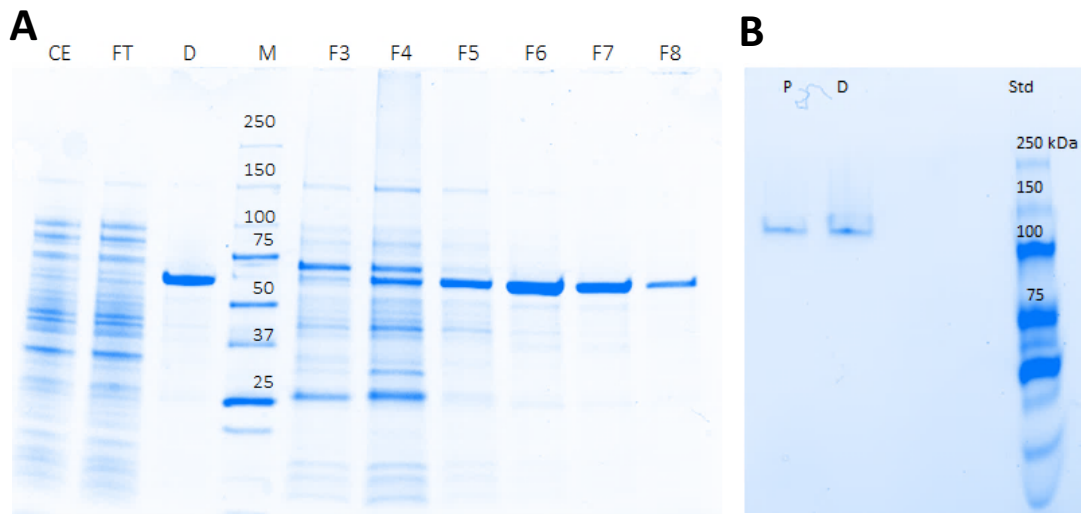


76

77 **Alignment sketch and structural overlap of *ToPOx* and the *KaPOx* homology**
78 **model.** The alignment sketch (top) displays the difference of sequence length and gaps
79 in the alignment of *ToPOx* and *KaPOx*. Deviations between the calculated *KaPOx* model
80 and the *ToPOx* crystal structure (PDB 1TT0) are highlighted in red for both structures.
81 The active-site FAD is displayed with a yellow sphere model. (1) An insertion in the
82 *KaPOx* sequence with respect to *ToPOx* translates into a short alpha-helix in the model.

83 (2) Two gapped stretches in the *KaPOx* sequence translate to a shortened-surface
84 exposed loop compared to *ToPOx*. (3) Another gap in the *KaPOx* sequence leaves a
85 truncated head domain in the homology model.

86 **Figure S5.**

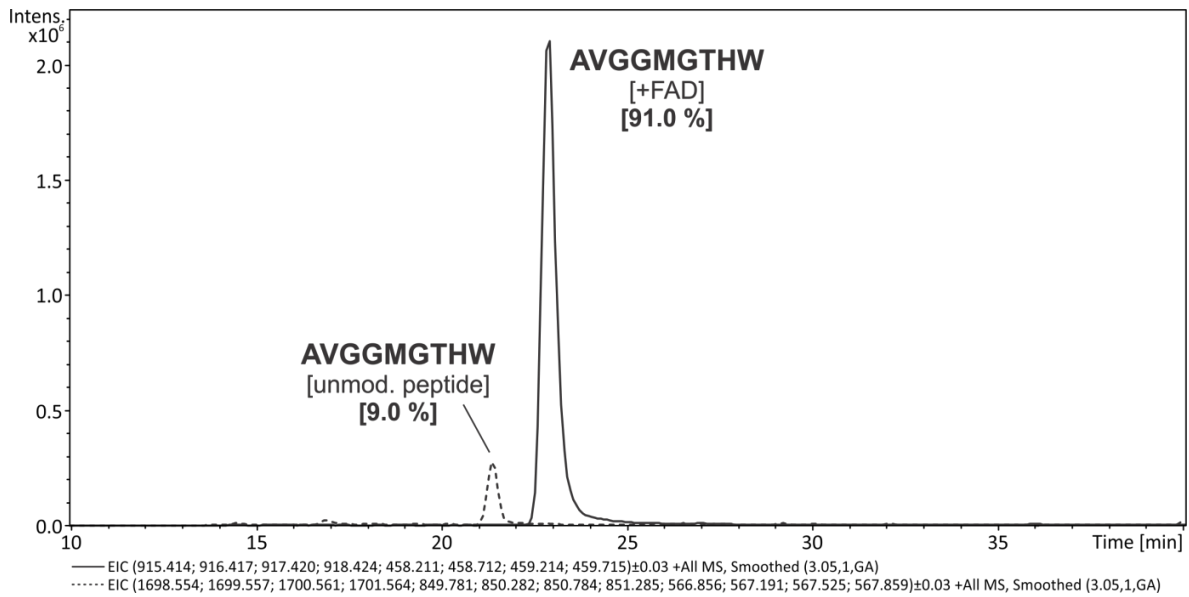


87

88 **SDS-PAGE and native PAGE of *KaPOx* purification samples.** (A) SDS-PAGE of IMAC
89 purification fractions. (CE) Crude extract, (FT) flow through, (M) mass standard, (F3-F8)
90 elution fractions, (D) dialyzed pool of fractions F6, F7, F8. (B) PAGE under non-
91 denaturing conditions. Here, (P) represents pooled sample, (D) represents pooled and
92 dialyzed (aggregated) sample. The numbers represent the molecular mass of the
93 respective standard bands in kDa.

94

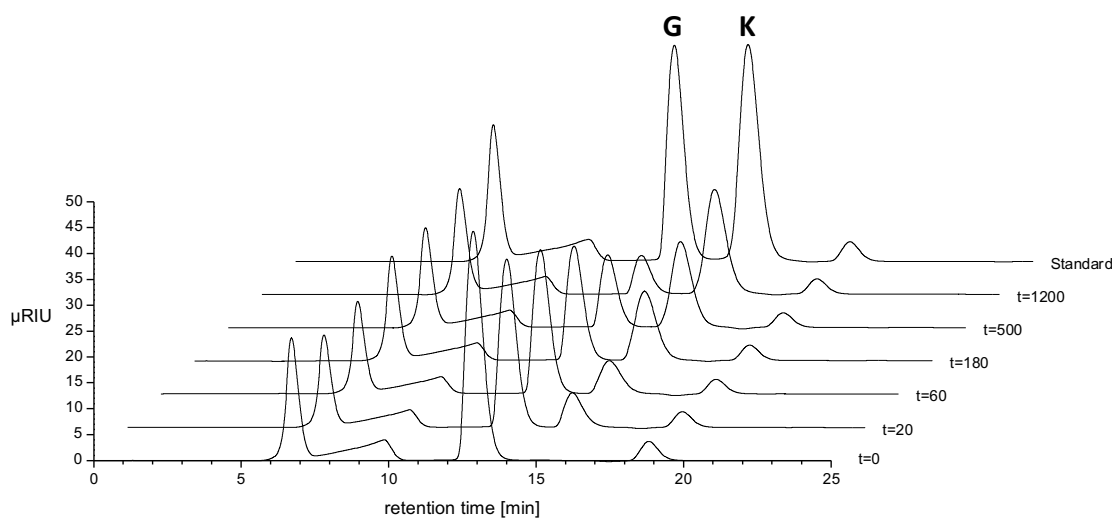
95 **Figure S6.**



97 **LC-ESI-MS analysis of covalent FAD attachment.** Mass spectrometry resolved two
98 different peptide masses for the 121AVGGMGTHW129 fragment after chymotryptic
99 digest of purified *KaPOx* sample. The FAD modified peptide (black) was identified by its
100 accurate theoretical mass and specific MS2 fragmentation profile (not shown).
101 Additionally, a small fraction of the unmodified fragment was detected too (dashed).

102

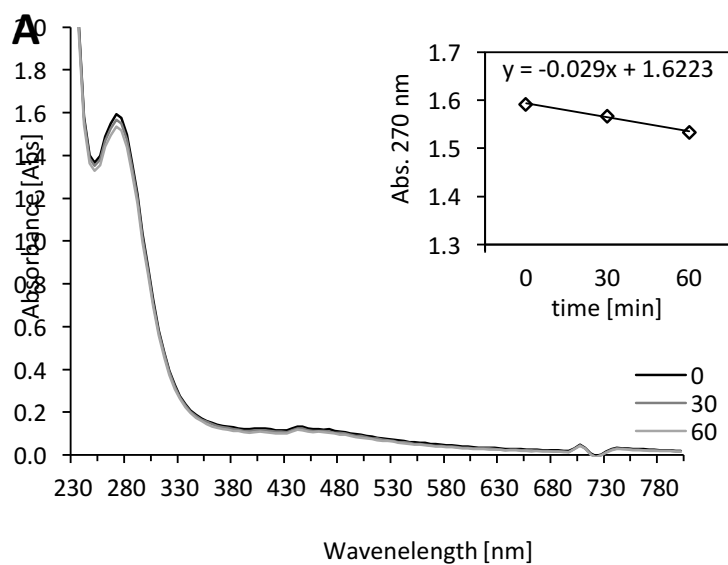
103 **Figure S7.**



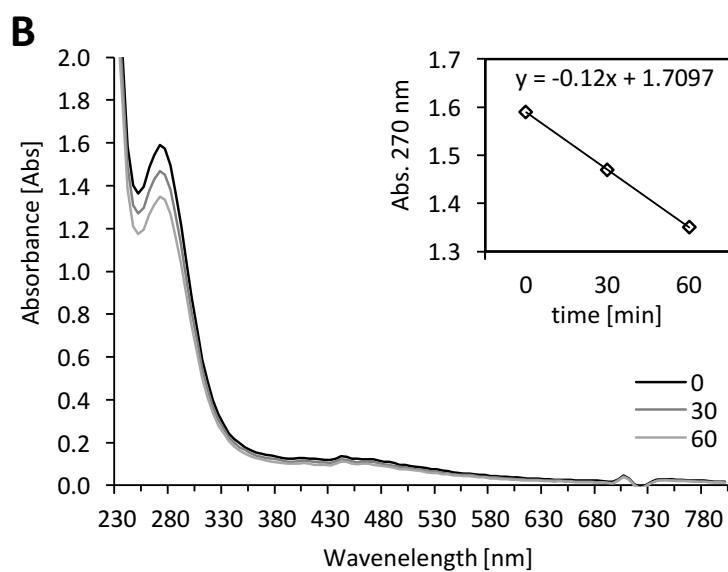
104

105 **Confirmation of C2-Glucose oxidation via HPLC.** Batch conversion experiments were
106 analyzed with HPLC. D-Glucose peaks elute after a retention time of approximately 13
107 minutes (G), the formed C2-oxidized 2-Keto-D-glucose (K) after 15 minutes. 2-Keto-D-
108 glucose is absent right at the reaction start ($t=0$) but accumulates in the reaction mix with
109 proceeding reaction time.

110 **Figure S8.**

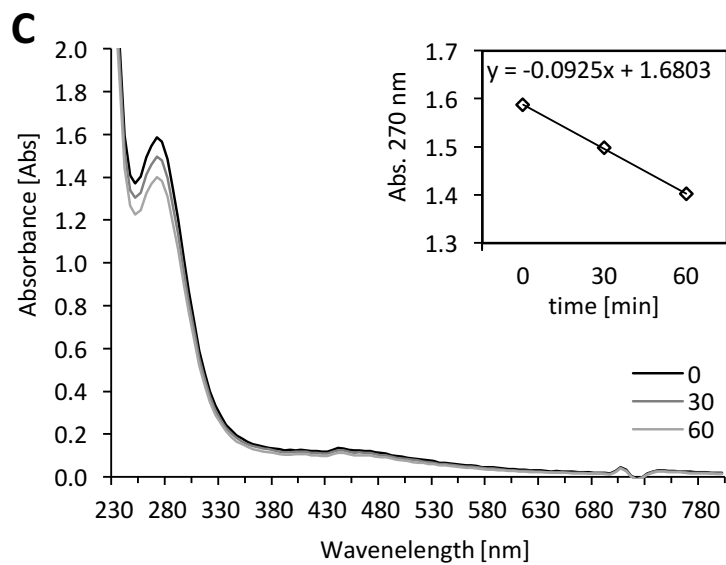


111

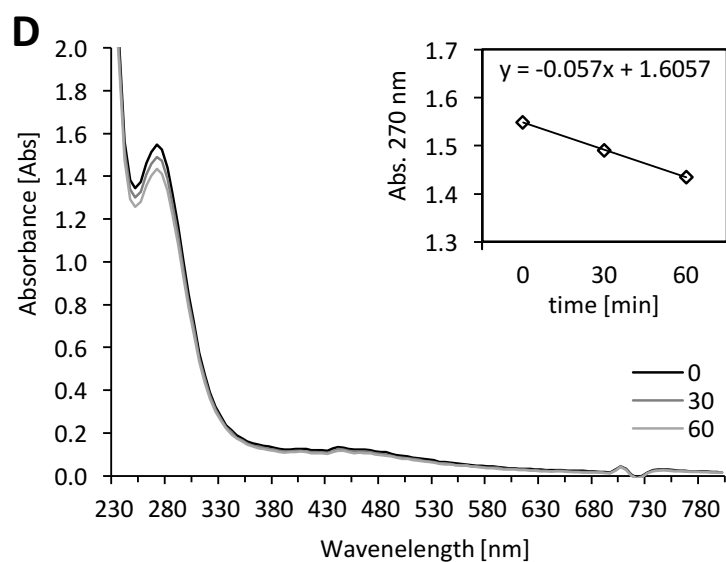


112

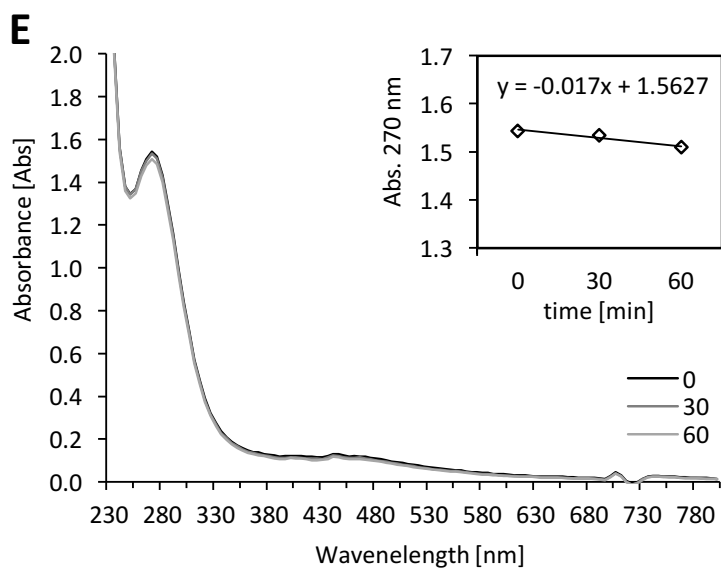
113



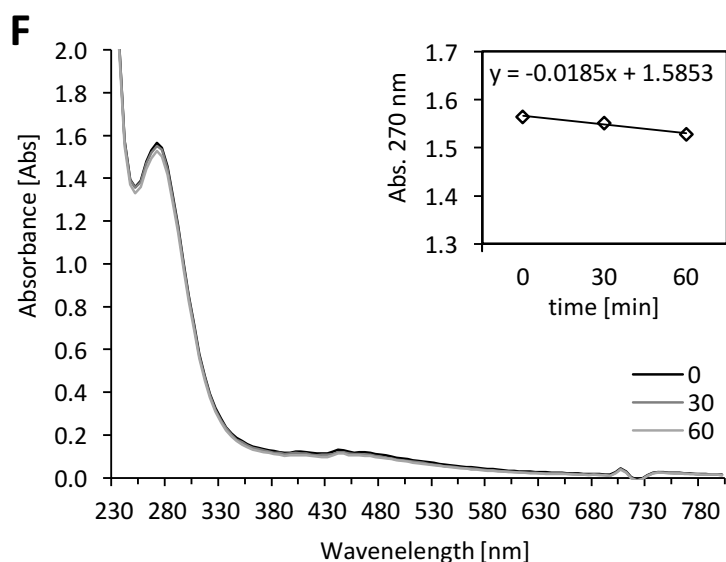
114



115



116



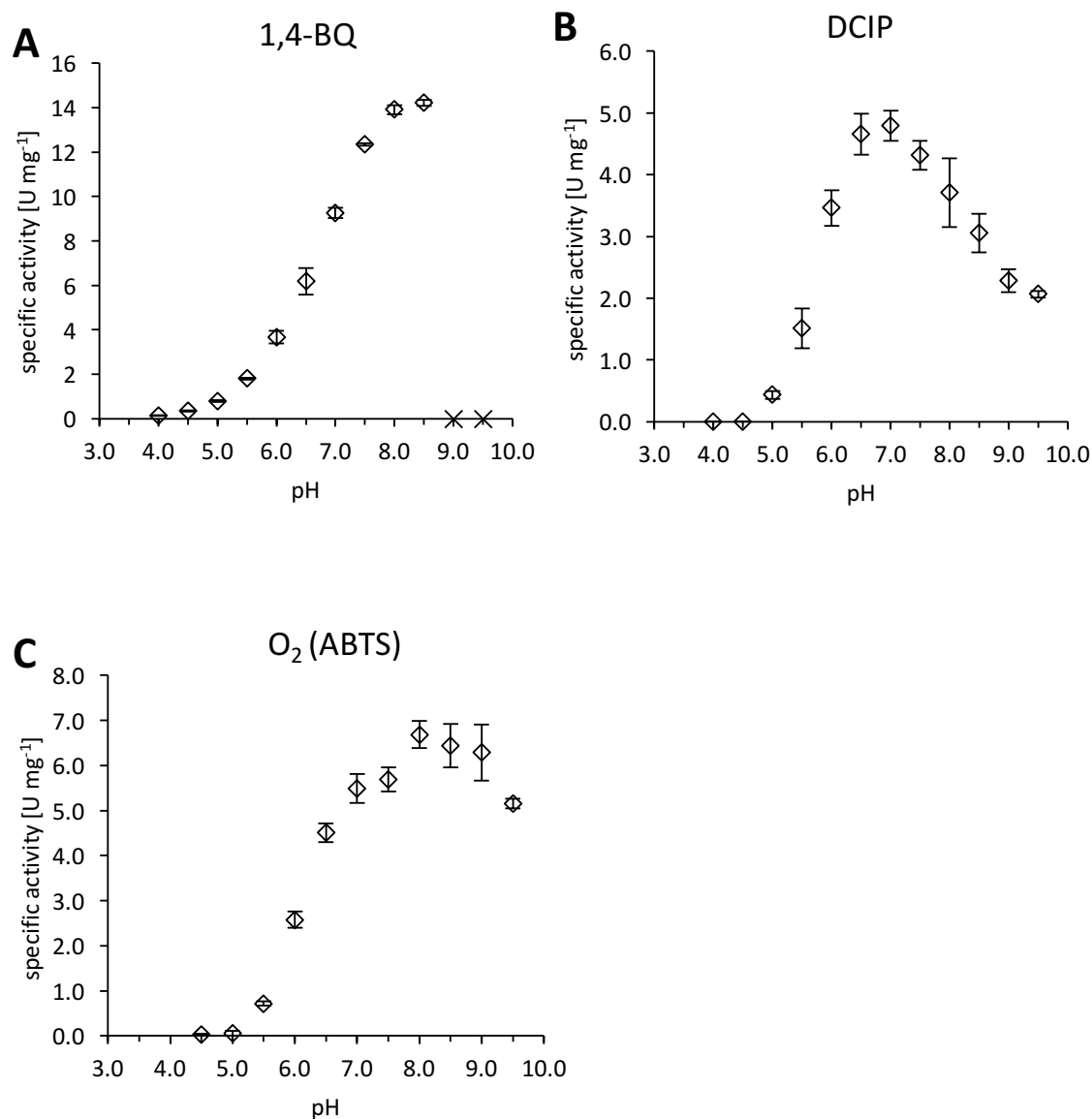
117

118 **KaPOx dehydrogenase activity of reducing complexed Mn(III).** A 5.0 μM solution of
 119 KaPOx was incubated with 1.0 mM Mn(III) acetate, varying concentrations of D-glucose
 120 and 50 mM, 50 U catalase in sodium malonate buffer pH 5.5 at 18 °C. The Mn(III)
 121 malonate complexation was allowed to equilibrate for 30 min before use. Absorbance
 122 spectra were recorded (230 – 800nm) before and 20, 40 minutes into the reaction. The
 123 absorbance change at 270 nm with proceeding reaction time is observable as an insert,

124 with slope and intercept of data fitting indicated. (A) Instead of *KaPOx*, 5.0 μM *A. niger*
125 glucose oxidase (Sigma) was present. (B, C. D) Concentrations of 30, 15, 8 mM D-
126 glucose (in Buffer) were added to start the reaction, respectively. (E) Instead of D-
127 glucose, buffer was added. (F) No *KaPOx* was present, 8 mM D-glucose were added.

128

129 **Figure S9.**



130

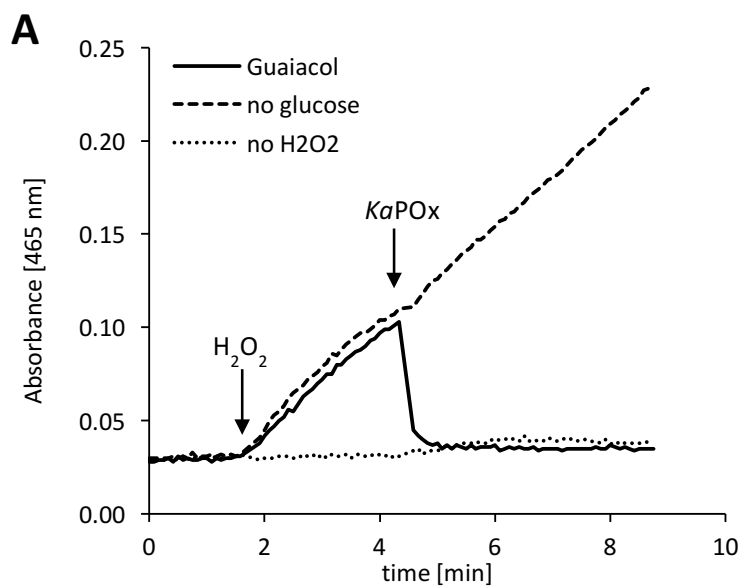
131

132 **The effect of pH on the activity of *KaPOx*.** Specific activities at different pHs were
133 determined for different electron acceptors. Each value represents the average value ±
134 standard deviation of technical triplicates. (A) 0.5 mM 1,4-benzoquinone (1,4-BQ) was
135 used in the colorimetric assay. Reactions at pH 9.0 and 9.5 (x) were fast initially but could

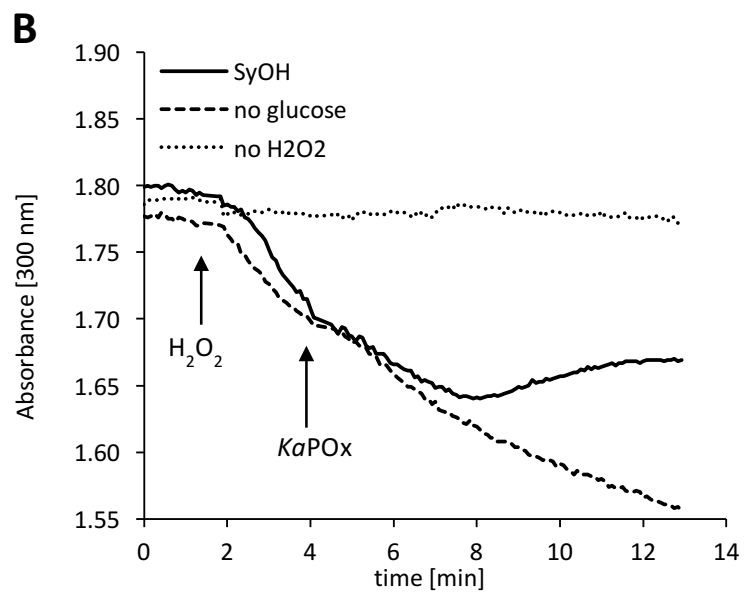
136 not be maintained longer than 150 seconds. (B) 0.3 mM dichloroindophenol (DCIP) were
137 used as electron acceptor. (C) Oxygen reduction was assayed with H₂O₂ production in
138 the standard ABTS assay.

139

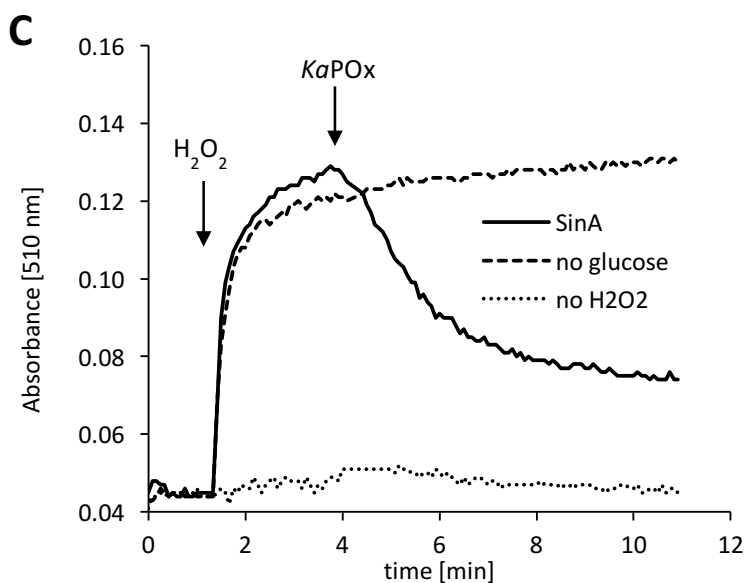
140 **Figure S10.**



141



142



143

144 **Additional redox cycling reactions of substituted phenols between *KaPOx* and**
 145 ***MnP***. Photometric assays display oxidation reactions of various substituted phenols.
 146 Assay mixtures contained manganese peroxidase (*MnP*), D-Glucose and the respective
 147 electron acceptor: (A) guaiacol, (B) acetosyringone (SyOH) and (C) sinapic acid (SinA).
 148 Reactions were started by the addition of H₂O₂. At approximately 4 minutes into the
 149 reaction *KaPOx* was added. Dashed line (---): no D-glucose was present. Dotted line (···):
 150 no H₂O₂ was added.

Chapter 3 – Introducing Enzyme Engineering

With the advent of recombinant DNA technologies in the early 1970s (Jackson, Symons, and Berg 1972; Mertz and Davis 1972; Cohen et al. 1973), dawn broke for the first design of proteins that was not governed by nature's dogma of evolution but rather by rational considerations of scientists. These milestones en route to the establishment of modern biotechnology were honored with the Nobel prize on two occasions (1978 and 1980) and paved the way for the technologies that transformed a multihued palette of industries: from the chemical industry, to biotechnology, the food and beverage industry, pharmaceutical industry, and many others. It has been estimated in 2015, that the global market for protein engineering as a service, not-including the products that go hand-in-hand with it, is valued at 168 billion dollars and projected to grow tremendously in the years coming (Liszewski 2015).

Enzymes endowed with the ability to operate at mild conditions and an unprecedented enantio- and regioselectivity frequently present themselves as assets to replace small molecules as catalysts in conventional processes. The urge to open up new resources for novel enzyme-supported processes and to meet the constant demand for adapting biocatalysts to match the needs of industrial applications prompted a variety of enzyme engineering techniques (Renata, Wang, and Arnold 2015).

A) Enzyme engineering

The adaptation of enzymatic function can be desirable on many occasions but is generally aimed at improving an enzymes stability or activity. Still, alterations in the protein sequence can also be dedicated for gaining an improved understanding of certain structural features or catalytic residues. For example, it is quite common to target basic amino acids in the active site of oxidoreductases to clarify their involvement in catalysis. If a loss of activity can be observed upon change to a different amino acid, the case is often clear (Rotsaert, Renganathan, and Gold 2003; Tsai et al. 2007).

Dependent on the degree of knowledge that is involved in engineering campaigns, one generally categorized approaches into:

Rational design: if a distinct set of substitutions or alterations has been proposed prior to engineering. Hence, detailed knowledge on the protein's structure and function is vital and needs to be available. This can be the case when the comparison of sequences of enzyme homologues identified a certain position that is not conserved in both homologues but can be attributed to a certain function in just one of them. Commonly, these sequence features are transferrable if template and target are similar enough (Felice et al. 2020). Aided by modern day computational methods, also the *de-novo* design of enzymatic functions – a design from scratch – is possible and represents as special case of rational design. Generally, the support from algorithms and machine learning in rational design campaigns boosted its success tremendously over the last decade. In the case of oxidoreductases for example, ambitious *de-novo* design projects involve small scaffolds that harbor metal cofactors as catalytic subunits. The introduction of certain amino acids in the surrounding of the cofactor then allows to establish substrate specificities or catalytic modes and is commonly supported by computational methods, as work pioneered by Donald Hilvert and colleagues highlights (Jiang et al. 2008; Siegel et al. 2010; Weitzner et al. 2019).

Seldomly, a detailed understanding of the enzyme's response to specific amino acid substitutions is attainable or can be predicted. More often, a likely position for interaction with a substrate or point for stabilization is projected but multiple options for replacement arise as reasonable. In an approach commonly referred to as "**semi-rational**" design this challenge is tackled. There, a small set of specific positions to be changed are selected based on profound understanding of the enzymes structure and function. These positions are then subject to mutation with either all possible substitutions or a biased set of mutations contained within a then "smart" library. This approach is often referred to as "focused mutagenesis". This helps minimizing the library size to a reasonable number and increases the chance to yield a positive outcome even if the enzyme is not fully understood (Chica, Doucet, and Pelletier 2005). One needs to keep in mind that, for every position, the theoretical library size increases by a factor of 20 and soon libraries grow from

the hundreds (2 pos., 400) into the thousands (4 pos., 16 000) and reach sizes that cannot be dealt with manually.

A different engineering technique harnesses the evolutionary principle of mutation and selection and is ideally employed if structural and functional information of the enzyme of interest is scarce: Directed Evolution.

B) Directed Evolution

The British naturalist Charles Darwin postulated his theorem “on the origin of species ...” in 1859 and constituted that the adaptation of species to their environment is sourced in genetic variation and driven by the process of natural selection (Darwin 1859). This scheme of phenotypic variation, differential fitness and heritability represent the foundation of evolutionary biology and equally applies to all biological entities, from species to proteins.

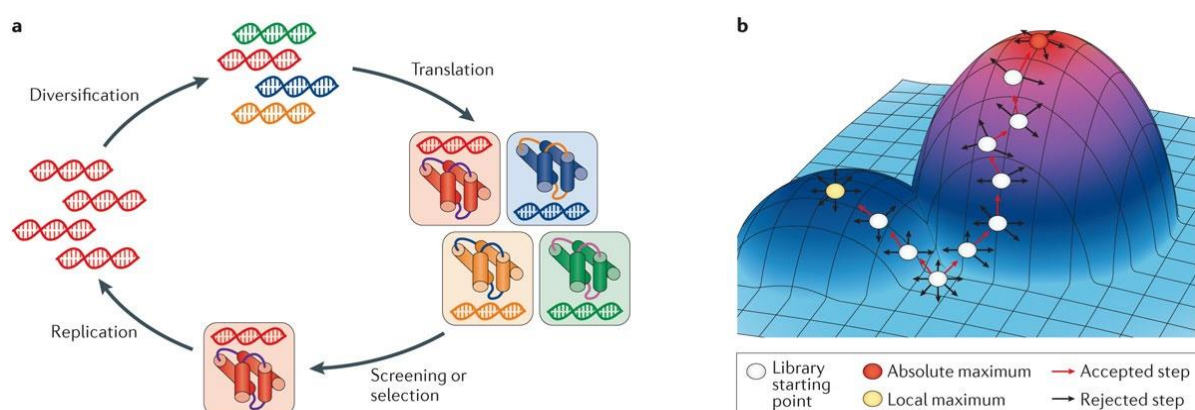


Figure 12 Directed Evolution schematic. The iterative process involves sequence diversification, selection or screening and replication (a). Repeated cycles of improvement can direct the enzyme functionality towards the desired properties but can be misdirected into dead ends (b). Figure by courtesy of Packer and Liu (Packer and Liu 2015)

Directed evolution mimics this biological algorithm in a laboratory setting and directs the adaptation of proteins towards externally imposed conditions, stressing their fitness. Parallel to natural evolution, this approach usually is an iterative practice that involves subsequent rounds of sequence diversification (or mutagenesis), exposition to selective pressure (selection, screening) and amplification (replication) of desired adaptations to it (Kuchner and Arnold 1997; K. Chen and Arnold 1991) as is highlighted in Figure 12-a.

The first visions of utilizing natural evolution for the redesign of an enzyme and its substrate were described by Spiegelman and colleagues for a bacteriophage RNA polymerase and its coding RNA template in 1967 (Mills, Peterson, and Spiegelman 1967). Half a century later, in 2018, the work on the development of enzymes by directed evolution was honored by the Royal Swedish Academy of Sciences awarding the Nobel Prize to Frances H Arnold for her pioneering work and substantial contributions to its advancement (Arnold, Smith, and Winter 2018; Arnold 2019).

During directed evolution campaigns, beneficial mutations that are identified after the screening and selection stage can serve as a new template and can be incorporated into libraries for ensuing rounds. It is often the case that multiple options arise when identifying the first improved variants and directed evolution can take different paths from there. The goal of directed evolution studies is to reach the anticipated peak in the fitness landscape by combining beneficial mutations over many generations on the way. Ultimately, early selections determine the route through the sequence space and every decision concomitantly limits the remaining degrees of freedom which can lead to dead-ends on the way to reaching maximal improvement as seen in **Figure 12-b** (Packer and Liu 2015). This phenomenon can be countered with an engineering approach called “neutral drift”. This tactic is based on the observation that improvement of enzymatic function, activity for instance, is commonly accompanied by a deleterious effect in a trade-off of functionality otherwise, stability potentially. Thus, detrimental impact on the enzyme accumulates in parallel to the desired gain in functionality and the final product is usually improved in one regard but not sufficiently fit anymore. Neutral drift libraries can be prepared as an optimized starting point for directed evolution or in between evolution rounds. These libraries are commonly prepared by random mutational methods and usually constitute substitutions to enhance protein solubility, stability or just increase sequence diversity whilst maintaining the original function. They thus support improvements in other regards and are also understood as a means to increasing the potential for additional changes, preventing dead-ends in directed evolution campaigns (Gupta and Tawfik 2008).

Enzyme engineering based on directed evolution allows circumventing the fundamental challenge of rationally devising enzymatic functionality. The prediction of an enzyme's catalytic capability from scratch is generally constrained by the inability to anticipate its protein structure and functionality from the protein sequence alone (Arnold 1997). Directed evolution has emerged as maybe the most versatile tool to create enzyme variants that are adjusted to non-native conditions or are equipped with an expanded catalytic repertoire.

11. Generation of genetic diversity

The generation of genetic diversity for the creation of mutational libraries is always tightly interconnected to statistical considerations, balancing theoretical and practical possibility. This adversity was nicely highlighted by Packer and Liu:

“It is impossible to cover the entire mutational space of a typical protein: complete randomization of a mere decapeptide would yield in 10^{13} unique combinations of amino acids, which exceeds the achievable library size of almost all known protein library creation methods.” (Packer and Liu 2015)

Since full systematic coverage of all substitutions is unfeasible, library creation methods focus on preparing screenable libraries of optimal composition or simply accept an underrepresented screening, just sampling limited fractions of the theoretical sequence space. Oftentimes, knowledge can feed into the diversification if for example the physicochemical properties of amino acid substitutions are limited to residues of a rather hydrophilic (core) or hydrophobic (surface) kind, or certain substitutions need to be avoided at all. Still, a higher degree of sophistication during library design often comes at the expense of practicability and is tightly connected to an established structure-function relationship.

Random mutagenesis

The non-rational creation of genetic diversity by these methods functions in the absence of structural information and can lead to the creation of gigantic libraries, following usually uncomplicated and quick protocols. It is also possible to combine these approaches with (semi-) rational design if relevant insights into the protein structure should be available. Commonly, directed evolution campaigns can ensue rational design if in the initial stage desirable variants were

identified but additional sequence space wants to be explored (Scheiblbrandner et al. 2017). *Vice versa*, a detailed look into the enzyme structure or the prediction of sequence hot spots by computational methods (molecular modeling and simulation, phylogenetic calculation and ancestral sequence reconstruction) can present a suitable starting point for directed evolution campaigns (Mateljak et al. 2019; Sun et al. 2019; Furukawa et al. 2020).

Historically, random mutagenesis methods relied on chemical methods to introduce alterations at random positions in the genes of interest. Prominent methodologies employ nucleotide analogues (Freese 1959), alkylating and deaminating reagents (Myers, Lerman, and Maniatis 1985; Lai et al. 2004) or UV irradiation (Bridges and Woodgate 1985) but were utilized more seldomly in the recent past given their biased substitutions patterns and lack of control. Another alternative for the introduction of genetic variation in a random manner is the utilization of mutator strains. Certain *E. coli* strains were developed that employ a compromised DNA replication and repair machinery. This allowed to increase error rates to 10^{-6} or more and could be used for plasmids containing the gene of interest (Cox 1976; Greener, Callahan, and Jerpseth 1997). With the advent of *in vitro* random mutagenesis approaches utilizing purified non-proof-reading polymerases, the mutator strain technology became less popular as it was recognized that concomitantly to introducing errors in the gene of interest, the host genome was similarly affected, and unsurmountable challenges arose from an increased genetic instability of the bacterial strains. These problems were later circumvented when the technology was transferred to *S. cerevisiae*, where a non-native polymerase and plasmid tandem from the closely related yeast *K. lactis* could be artificially introduced to establish an orthogonal mutagenesis system which was locally isolated. This allowed to concentrate elevated error rates to the gene of interest harbored on the *K. lactis* plasmid (cytosolic) and keep the genome of the eukaryotic host (nucleus) unaffected (Ravikumar, Arrieta, and Liu 2014).

As mentioned, *in vitro* methods experienced a boost with the rise of the directed evolution as a protein engineering strategy as they facilitated tunable mutation under controlled conditions and restriction to single genes, gene segments or even single positions. Some of the most prominent techniques will be explained in the following:

- *Error prone PCR (epPCR)*. The DNA replication capabilities of DNA polymerases can be exploited to introduce transitions (A > G, T > C) or transversion (A > C, T > G) at random positions into the genetic code during PCR reactions (Leung, Chen, and Goeddel 1989; Cadwell and Joyce 1992). For this purpose (engineered) non-proofreading polymerases, based on the prominent enzyme from *Thermus aquaticus* “*Taq*”, are used which are characterized by increased error rates (Chien, Edgar, and Trela 1976; Eckert and Kunkel 1990). These polymerases can be utilized under sub-optimal conditions (elevated manganese concentrations, nucleotide analogues) to further decrease replication fidelity, reaching mutation rates close to 1 in 1000. Commercial kits are available that employ these dedicated polymerases or even a combination of multiple ones to balance the enzymes preference for either transitions or transversions and hence allow to yield an unbiased mutational spectrum, where the error rate can be tuned with the amount of DNA template and number of PCR cycle.
- *Recombinatorial methods*. A set of methodologies is available that rely on the fragmentation of homologous genes and their subsequent randomized recombination. This can be utilized to shuffle and rearrange previously identified beneficial mutations or homologous wild-type genes with varying features (Cramer et al. 1998). This concept was first published by Stemmer and colleagues who digested gene variants with DNase I and reassembled them in an ensuing PCR reaction, employing the truncated DNA for priming (Stemmer 1994). It was reported that DNase concentration and incubation times provide means to control the degree of division, fragment sizes and crossover frequencies and thus allow tune variation. The group around Stemmer coined the term “gene shuffling” for this kind of approach but adaptations to this procedure soon arose that incorporated different strategies – chemical and enzymatic, homologous and non-homologous - to digest and ligate DNA and control the degree of diversification: ITCHY (Ostermeier, Shim, and Benkovic 1999), RACHITT (Coco et al. 2001) , NRR (Bittker et al. 2004) and NEXt (Müller et al. 2005) to name only a few. A special case of recombination is described as staggered extension PCR or “StEP”, where a heat denaturation step abruptly halts the polymerization reaction and creates truncated genes. These fragments reallocate between the templates at high temperatures and later randomly align in the

subsequent annealing step before being ligated into complete genes by the PCR reaction (Zhao et al. 1998)

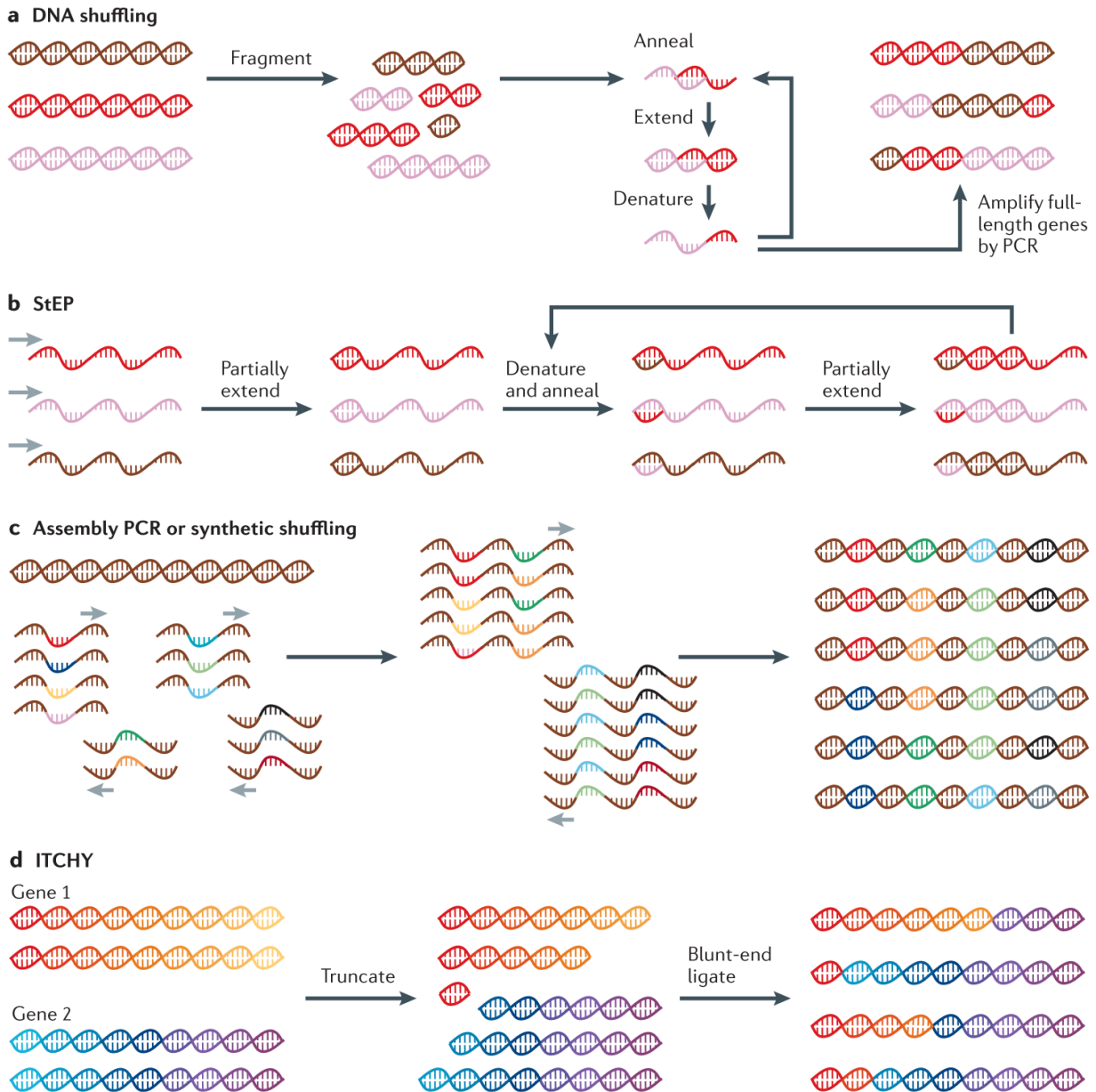


Figure 13 Sequence diversification by DNA recombination. DNA shuffling (a): Homologous genes are digested with DNase at random positions which creates truncated fragments of varying size. In a PCR step ensuing the fragmentation, these pieces anneal on a template and prime the PCR reaction in which they are ligated. Staggered extension PCR (b): The PCR extension step is repeatedly stopped by a denaturation step at elevated temperatures producing staggered gene fragments of different size. During denaturation, the fragments reallocate randomly onto the template and are resealed to create gene variants with multiple cross-overs. Assembly PCR or synthetic shuffling (c): Synthetic oligonucleotide primers are designed to overlap and create full-length genes in random PCR

recombination reactions. Incremental truncation for the creation of hybrid enzymes “ITCHY” (d): Depends on exonuclease activity to digest the gene templates from the termini. These fragments are then randomly interconnected by the activity of blunt-end ligases creating just single cross-over hybrids with varying composition of the parental gene variants. Figure by courtesy of Packer and Liu (Packer and Liu 2015).

Focused mutagenesis

At the beginning of 2021, more than 150 000 protein structure entries were available on the PDB database (<https://www.rcsb.org/stats/growth/growth-released-structures>) with annual release numbers on the rise again for the first time since 2016. These vast numbers highlight that structural information can be aplenty for certain classes of proteins and allows to implicate certain positions to biochemical properties of the enzyme. If that is the case, engineering can follow a straightforward route, especially if it is backed by conclusions from previous rounds of directed evolution or computational considerations on the sequence space, stemming from molecular modeling and simulations (Herman and Tawfik 2007; Cherny et al. 2013) or phylogenetic calculations (Lehmann et al. 2000; F. Chen et al. 2010). In that regard, focused mutagenesis allows to tune the degree of randomness and pinpoint it to a limited number of residues at the projected structural part. Research from Prof. Schwaneberg and his group from the last decade outlined how directed evolution (utilizing a randomized mutagenesis approach) and focused mutagenesis can synergistically act together and be employed in a stepwise engineering campaign, where the gained knowledge from each step is channeled into holistic considerations in an approach referred to as “KnowVolution”(Cheng, Zhu, and Schwaneberg 2015; Novoa et al. 2019; Islam et al. 2018) .

- The use of degenerate codons undoubtedly represents one of the most prominent and simple ways to introduce sequence variation to a certain target position of generally 1-2 amino acids. For this, synthetic oligonucleotide mixtures can be designed to code a desired amino acid substitution (site directed) or the complete set of 20 possible ones (site saturation). Many protocols exist that assemble these oligos into the gene libraries and usually depend on PCR reaction, restriction site digest and traditional ligation (Nour-Eldin, Geu-Flores, and Halkier 2010) or contemporary homology-based enzymatic DNA ligation (Gibson et al. 2009). With the smart design of oligos, strategies were developed that provide a more even representation of codons (Tang et al. 2012) biasing site saturation towards certain sets of amino acids while excluding others (Lorimer et al. 2009) or in the case of

“parsimonious mutagenesis” adjusting the probability between substitution and no substitution (Balint and Larrick 1993).

- The last years have seen an extraordinary drop in DNA synthesis costs that was supported by silicon chip technology, miniaturization, and automatization. Commercial suppliers nowadays offer DNA synthesis from oligos to entire genomes with unprecedented fidelity and progressively lower costs, starting at 0.07 \$ per base pair. These recent advancements allow to also incorporate library design directly into the manufacturing process and deliver focused mutagenesis libraries with a desired degree of sequence variation, harboring site-directed and saturated positions, as well as combinations of both, ready for cloning into labs.

12. A shift in the engineering paradigm

In enzyme engineering, we strive to discover a specific variant of the enzyme’s amino acid sequence that entails a desired improvement to the protein function. This process, as will be described later in this chapter, is an either highly sophisticated and delicate or simple yet arduously process of finding the needle in the haystack. Ultimately, the number of variants that can practically be evaluated is only a tiny fraction of the astronomical number of theoretically possible variations of the protein sequence and can only ineffectively be accessed by contemporary methods. Still, these obstacles are often accepted since the only alternative lies within designing protein structure and predicting the functionality from scratch which commonly represents an even bigger challenge (Baek et al. 2021). With the advent of self-improving algorithms in machine learning, many believe that one of the dogmas of protein chemistry, namely the prediction of structure (and function) from sequence is at the brink of being broken. As of today, the number of known sequences lies within the billions and is opposed by roughly 100 000 structurally resolved unique proteins (www.rcsb.org). The possibility to streamline the process of structure determination utilizing accurate computational methods could for the first time unveil this abundance in biological information and close the knowledge gap between protein sequence and function. This would undoubtedly have colossal impact on biotechnology and life sciences (Jumper et al. 2021).

The Critical Assessment of Structural Prediction (CASP) is a biannual contest for protein bioinformaticians in which a set of previously resolved but unpublished protein sequences are subject to structural prediction by bioinformatic algorithms. At its 14th repetition, Alphabet/Google's AlphaFold2 outscored the competition and its models resembled the actual structures with just minor deviations in most cases (36 % of models RMSF < 2 Å, 86 % of models RMSF < 5 Å). These predictions do not rely on homologous sequences being structurally elucidated and still come close to classical structure determination methods such as X-ray crystallography but allow to cut the time frame to just several days (Oxford Protein Informatics Group 2021).

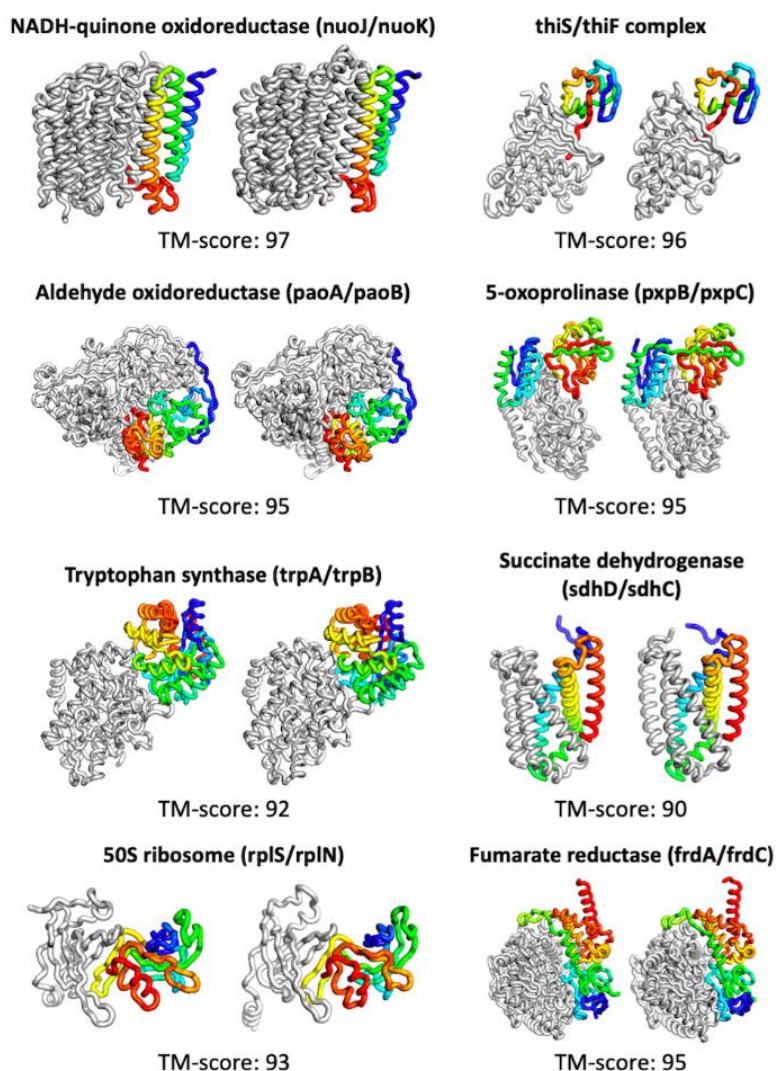


Figure 14 Examples of predicted structures from RoseTTAFold. Structurally resolved proteins and protein complexes *E. coli* (left) versus calculated RoseTTAFold models (right). TM-score values indicate the goodness of the fit and degree of structural similarity. A score of > 90 is regarded as accurate prediction.

In essence, the underlying principle for the success of AlphaFold2 or is sourced in a novel machine learning (ML) approach that integrates the general biophysical constraints of atomic interactions as well as multiple sequence alignment data. To simplify, modern ML algorithms automatize the identification of patterns in structural and sequence data to predict protein structures and forecast sequence alterations to improve protein properties. These programs learn from reiterating and refining their code and comparing the calculated models to available data, resolved protein structures for example (Mazurenko, Prokop, and Damborsky 2019). By running billions of these prepare-and-compare cycles they self-implement improvements to their code that are not necessarily guided by rational considerations but ultimately lead to improved predictive power and model quality. As was shown, it can help to guide this process by feeding biochemical constraints into this self-evolving algorithm and thus direct the development towards a more realistic and natural state, which is made possible by the neural network design of deep learning systems like Google's DeepMind or trRosetta (Baek et al. 2021).

It was hypothesized that the recent breakthroughs in applying deep-learning algorithms for biotechnology and structural bioinformatic could play an essential role in enzyme engineering in the future. A comprehensive review on the detailed mechanistic and practical challenges of ML in computational enzyme engineering was recently published by *Mazurenko* and colleagues (Mazurenko, Prokop, and Damborsky 2019). ML algorithms have already found success in enzyme engineering, predicting activities and substrate specificities (Robinson et al. 2020) temperature dependence (Foroozandeh Shahraki et al. 2021), stability and solubility (Hon et al. 2021) enzymatic mechanisms (De Ferrari and Mitchell 2014) or by designing smart libraries for directed evolution (Li, Dong, and Reetz 2019). It is currently foreseen that ML with aid to explore even more difficult tasks in the near future and likely advance the field to build a new domain of enzyme engineering (Feehan, Montezano, and Slusky 2021; Siedhoff, Schwaneberg, and Davari 2020). Its combination with other state-of-the-art technologies, such as next-generation sequencing, high-throughput screening, microfluidics could synergistically boost developments, potentially faster than expected. Likely, one major hurdle to overcome lies in harmonizing big database entries (sequences, structures, functional parameters) to make it more accessible for ML training (Mazurenko, Prokop, and Damborsky 2019).

C) Screening

Enzyme engineering can involve random approaches to alter enzymatic functions. In order to introduce these alterations on a genetic level, methods like site saturation mutagenesis, recombination methods or error-prone PCR are commonly applied to create genetic diversity, as was outlined. In practice, so established libraries can easily exceed 10^7 individuals (Packer and Liu 2015; Porter, Rusli, and Ollis 2016). This allows to aimlessly cover larger fractions of the sequence space but introduces a large fraction of deleterious or neutral variants alongside.

Thus, sequence diversification methods need to be met with elaborate methods to reliably assess the fitness of all relevant variants and to successfully isolate the best performers among them, while confidently excluding compromised variants. This process is commonly referred to as “screening” and its accurate operation is essential to assist directed evolution campaigns (Porter, Rusli, and Ollis 2016). As the step of library generation can be quite accelerated and straightforward, the stage of screening traditionally involves exhaustive manual handling and can span multiple months or rarely years - even if partially assisted by automatization. It is therefore of utmost importance that screening rounds are well-designed, maintain the true connection of genotype and phenotype, allow to confidently discriminate between desired and undesired performance (Fischlechner et al. 2014) whilst providing enough throughput to pace engineering (Truppo 2017). Throughput has been in the focus of attention in recent screening developments and multiple reports describe the utilization of microfluidic methods (flow cytometry with it) to drastically minimize screening times and efforts (Bunzel et al. 2018) with the scope of further untying enzyme engineering from methodological restraints.

In any case, the role of screening technology to enable effective enzyme engineering by directed evolution should not be underestimated as the infamous dogma and first law of directed evolution prevails: “You get what you screen for” (Schmidt-Dannert and Arnold 1999).

13. Methodology

Colorimetric screening methods for enzymes rely on the consumption of substrate or the formation of primary or secondary reaction products by the enzymes which is accompanied by the

concomitant change of color, fluorescence, luminescence, or turbidity either directly or indirectly by subsequent processing of the formed reaction products. In the case of oxidoreductases, utilization of those surrogate compounds facilitating a color reaction is common, practical, and often easily achieved. Still, in certain cases direct quantification of substrate consumption or product accumulation is inevitable and can be met with parallelized analysis of enzyme variant reactions via nuclear magnetic resonance (NMR), high-performance liquid chromatography (HPLC) or mass spectrometry (MS) (Packer and Liu 2015). A prominent example for the application of these techniques are reports on the directed evolution of the heme-dependent enzyme cytochrome P450 for novel enzymatic function (Coelho et al. 2013; R. K. Zhang et al. 2019)

One can categorize the methodology underlying enzyme screenings by the way in which isolation of the enzymatic reaction is achieved. It is clear that enzymatic reactions of different variants must proceed isolated from each other to exclude interfering influence and judge performances accordingly. In addition, isolation is needed to maintain the steady connection of an enzyme variant and its encoding gene, in order to allow retrieving the sequence of desired clones for a gain in knowledge (i.e. genotype-phenotype bond). In the simplest formats, this segregation is accomplished by cultivation and screening spatially separated on solid media plates or microtiter plates (MTP). But extensive miniaturization discovered the individual cell as a suitable reaction compartment and led to the development of entrapment and emulsification techniques that isolate enzymatic reactions of a single variant on a single cell in droplets, separated from neighboring variants.

14. Solid phase plates

The screening of oxidoreductase activity parallel to the cultivation of expressing cells is easily achieved when screenings are carried out directly on solid-phase media plates, containing an additional indicator for enzyme activity. With this, the stages of cultivation, induction, and screening can practically be united into a single location and hence screening regimes simplified. Dependent on the expression host, these plates can harbor clone numbers in the thousands and process library sizes of 10^5 in reasonable time frames with just macroscopic observation (Leemhuis, Kelly, and Dijkhuizen 2009).

A popular and well-established example for colorimetric screenings was developed for cloning purposes, to assess successful recombination of a gene of interest into a suitable vector, the “blue-white screen”. This system relies on a process referred to as α -complementation, where the functionality of a truncated and inactive β -galactosidase variant (ω -peptide) is reinstated when the small α -peptide is successfully co-expressed (Ullmann, Jacob, and Monod 1967; Langley et al. 1975). Upon association of the α - and ω -subunit, the β -galactosidase structurally reorganizes and forms active tetramers, which can then hydrolyze the synthetic lactose analogue X-gal (5-bromo-4-chloro-3-indolyl- β -D-galactopyranoside) and cause an intense blue color formation. This system can be exploited for cloning purposes when a suitable *E. coli* strain, harboring the gene for the inactive β -galactosidase ω -peptide (*LacZ- ω*) receives the complementing α -peptide coding sequence (*LacZ- α*) from a transformed plasmid. Bacterial colonies growing on solid media supplemented with X-gal will turn blue due to the α -complementation unless the α -peptide coding sequence is disrupted with a gene of interest – in these designs, multiple cloning sites were introduced into the *LacZ- α* sequence – and bacterial colonies with successful integration will appear white (Vieira and Messing 1982). This system establishes a fast and simple identification of successful transformation events as it allows to circumvent the tedious and cumbersome confirmation of gene integration via molecular biology techniques

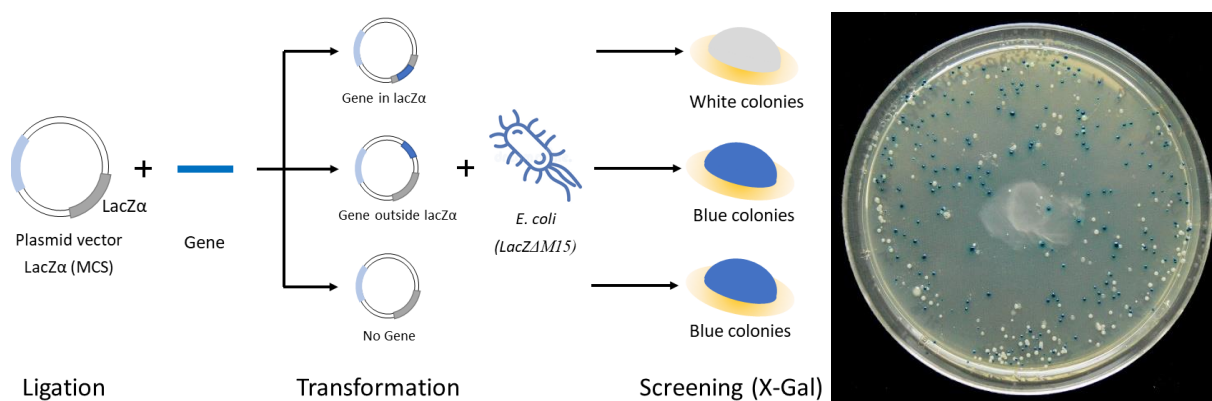


Figure 15 Blue-white screening of *E. coli* transformants on solid LB medium. Successful integration of the gene of interest into the multiple cloning site disrupts the coding sequence of the *LacZ α* gene and prevents the α -complementation to restore β -galactosidase activity in *E. coli* cells expressing a truncated and inactive variant of the enzyme (left). Where transformants harbor the gene of interest at the proper position, colonies appear white since the supplemented X-Gal compound in the medium cannot be enzymatically cleaved to release the blue indole (right). Photograph kindly provided by Stefan Walkowski.

In the framework of employing the directed evolution strategy for enzyme development, one of the first documented examples that needs mentioning involves a clearing halo assay for the engineering of the protease subtilisin E. To increase the enzymes fitness in nonaqueous solvents, the group around Frances Arnold utilized random mutagenesis methodologies to create enzyme libraries and subjected them to increasing concentrations of the organic solvent dimethylformamide (DMF), to stress their fitness in multiple rounds of directed evolution. In their setup, solid media screening plates for *E. coli* expression contained DMF and skim milk powder. In cases where the enzyme variant evolved to tolerate the organic solvent, enzyme activity led to the proteolytic digest of milk protein and a concurrent clearing of the opaque media around the active colonies in the form of halos. Directed evolution of subtilisin E supported by this screening setup resulted in the development of improved variants active in concentrations of up to 85 % DMF (K. Chen and Arnold 1991; You and Arnold 1996).

A prominent example for a colorimetric compound that is frequently utilized in the screening of oxidoreductase activity is 2,2'-Azino-bis 3-ethylbenzothiazoline-6-sulfonic acid (ABTS), which develops a characteristic green color upon oxidation to its cationic radical species. The utilization of ABTS in screenings is quite versatile, as it presents a suitable substrate for multiple oxidoreductases. It functions as a colorimetric indicator for laccase activity when oxygen is available as co-substrate, but similarly for peroxidase when H_2O_2 is present. In addition, screenings based on ABTS can be expanded to oxidase activity and H_2O_2 formation when working in conjunction with peroxidases. Furthermore, this tandem of oxidase and peroxidase activity can be used as a reporter itself when the enzymatic activity of an enzyme of interest forms a suitable substrate for the oxidase (Figure 16). This has been reported in the case of screening transaminases where glycine was formed from glyoxylate, and was detected by the action of a glycine oxidase and horseradish peroxidase couple (Weiß et al. 2014). Similarly, the enzymatic activity of alanine racemase on L-alanine to form the D-enantiomer was assayed by the cascading reaction of combining D-amino acid oxidase and horseradish peroxidase (Willies, White, and Turner 2012).

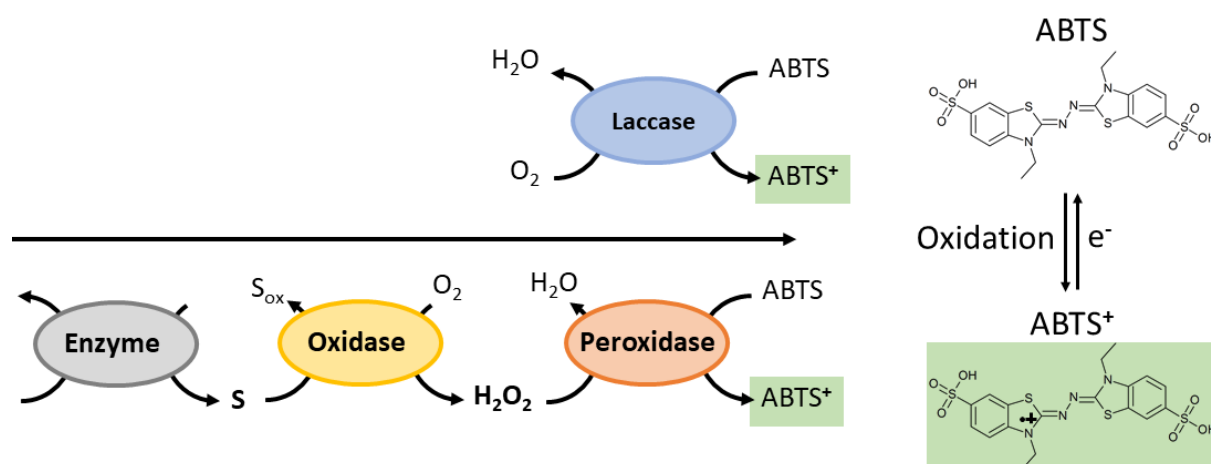


Figure 16 Enzymatic screening cascade. The oxidation of ABTS is a commonly employed assay reaction in solid-phase screenings and can be catalyzed by enzymes such as laccases (multicopper oxidases in general) and peroxidases, that are also present in the screening media. The necessity for its co-substrate peroxide, allows to couple the peroxidase reaction to a preceding oxidase activity, providing H₂O₂. This cascade reaction can even be expanded when another enzyme forms a substrate for the oxidase/peroxidase tandem prior (Weiß et al. 2014; Willies, White, and Turner 2012).

Instead of assaying enzyme activity in the growth and induction medium directly, these steps can be uncoupled using a top-agar layer containing most assay components to minimize interference from media components. Recent literature contains multiple reports that describe the detection of glucose oxidase activity after secretion or display. For this purpose, glucose, mediating peroxidase, and a suitable colorimetric indicator compound like ABTS are provided in the overlaid agar coating (Valdivieso-Ugarte et al. 2006; Ostafe et al. 2014). Notably, *Ostafe et al.* used this technique to assess the enrichment ability of their FACS-based screening by identifying glucose oxidase (GOx) displaying *S. cerevisiae* cells. In this case, glucose is required for the screening of GOx activity but needs to be absent in the growth medium to avoid its inhibitory effect on galactose dependent induction of protein expression in the utilized *S. cerevisiae* host. Hence, an overlaid screening agar allowed to combine cultivation of the host and screening locally united but temporally separated.

As these examples underline, screening on solid phases almost exclusively yields qualitative data to evaluate the functionality of enzymes and is not used to deliver quantitative comparison of variants. Still, the usefulness of solid-phase screening setups should not be underestimated. Their simplicity is of special value for the screening of environmental samples where information on the

biochemical properties of enzymes is scarce and at the beginning of engineering campaigns, where it can contribute immensely to reducing the screening effort. At this stage, plate screenings are commonly introduced as a pre-screening step to eliminate non-functional variants prior to the labor intensive, quantitative assessment under controlled conditions in different formats (You and Arnold 1996; Maté et al. 2010; Scheiblbrandner et al. 2017). Dependent on the mutational load and the engineering scope, a large fraction of the library - up to 98 % - can be left rendered inactive and should be eliminated from subsequent screening steps to save resources, time most of all (Zumarraga et al. 2008). Plate screening assays can provide qualitative statements on a variant's catalytic properties, but subsequent steps of quantitative assessments in a different format, usually the microtiter plate, are necessary.

15. Microtiter plates

Microtiter plates (MTP), synonymously also referred to as “multiwell plate” or “microwell plate”, represent a simple way of compartmentalizing a library throughout enzyme engineering campaigns. The separation into dedicated wells allows to maintain a steady connection between genotype (gene, expression host) and phenotype (enzyme activity) and simplifies handling. Commonly, the cultivation and screening stage are carried out in the same format to allow seamless parallelization from one stage to the next. Still, technological solutions such as colony picker robots can facilitate fully automatized transfer of microbial colonies from the solid to liquid phase, for virtually any available format. Dependent partially on the expression system and the ensuing screening platform, 96 well plates (around 200 μL) represent the most established format. But increasing miniaturization is regarded as one of the triumphs in screening technology and was accelerated by advancements in automated liquid handling and robotic automatization until the 2000s. It led to the development of high-density formats such as 384 well (50 μL), 1536 well (10 μL) and even 3456 well (5 μL) plates which found relevant applications in the pharmaceutical industry but are rare in academia (A. Smith 2002). The increase in well density allows to manage up to 100 000 variants per day but needs to be met with more elaborate methods for liquid transfer, assaying, data interpretation, storage and especially quality control, and efforts for maintaining these supporting processes should not be underestimated (Willey et al. 2017). In the grand scheme of things, the utilization of MTPs for screening in solutions can contribute to a drastic increase in throughput but needs to be tamed carefully, oftentimes rendering the processes static, only partially adaptable and vitally reliant on expensive equipment. Concomitantly, the decision to scale-down well sizes in practice is often not a matter of throughput but rather of costs, considering expensive fluorescent substrates or cell lines.

In the case of oxidases, standard activity assays for detection and characterization are often based on the quantification of the byproduct hydrogen peroxide, which has to be converted by a secondary enzyme (a peroxidase) with concurrent conversion of a suitable secondary product, such as ABTS, which can be quantified spectrophotometrically. For many dehydrogenases, a more direct spectrophotometric quantification is possible, as a number of suitable electron acceptors,

such as 1,4-benzoquinone, 2,6-dichlorophenol-indophenol (DCIP or DCPIP) or ferrocenium hexafluorophosphate allow direct spectrophotometric detection. Many of these assays are also suitable for enzymes with oxidase activity, as these are usually also highly active dehydrogenases, often using quinone or metal ion acceptors with higher affinity than molecular oxygen (Sützl et al. 2018). These reactions are generally characterized by the solubility of all components, enzyme, substrate, product, and byproduct (in contrast to, e.g., many hydrolases, where a product is released from an insoluble substrate). The enzymes are often secretory and are released into the supernatant, or are expressed intracellularly in *E. coli*, which requires cell lysis to release enzymes or accumulated substrates and byproducts for performance of the assay. Earlier efforts of engineering and evolution of such enzymes were mostly based on slightly modified standard assays, and compartmentalization in microtiter plate format was required in order to maintain the connection of gene, enzyme and quantifiable product.

Exemplary for early work in enzyme engineering relying on such a setup is the directed evolution of the fungal *Aspergillus niger* glucose oxidase. The enzyme was expressed as secretory enzyme in yeast and assayed using the electron acceptor ferrocene methanol as a reporter for its dehydrogenase activity. Two epPCR-generated libraries of 2000 colonies each were screened using a liquid handling workstation for 96-well-microtiter plates (Zhu et al. 2007). In a follow-up using results from this study as a starting point, similar assays employing ABTS/HRP for oxidase and quinone diimine for dehydrogenase activity were used in order to identify variants with decreased oxygen activity, still depending on a relatively small library size of 2200 clones using saturation mutagenesis and epPCR (Arango Gutierrez et al. 2013). Engineering attempts of the catalytically related *Trametes ochracea* (formerly *Trametes muticolor*) pyranose oxidase utilized the same setup as described before, but introduced an additional cell lysis step as the enzyme is readily expressed in *E. coli*. Enzyme activity is assayed after chemical disruption in the cell lysate with horseradish peroxidase and ABTS assessing oxygen reactivity. In various cases, library designs were limited to repeated saturation mutagenesis in multiple positions (Salaheddin et al. 2009; Spadiut et al. 2009; Brugger et al. 2014), as were approaches using cellobiose dehydrogenase from *Crassiparpon hotsonii* (from (Sygmund et al. 2013) and pyranose dehydrogenase from *Leucoagaricus meleagris* (Krondorfer et al. 2014).

The group around Miguel Alcalde pioneered the development of high-throughput screening systems for oxidoreductases: peroxidases and high-redox potential laccases (HRPL) in particular, using *S. cerevisiae* as expression host. Early work from 2010 describes directed evolution campaigns improving basidiomycetous laccases and Versatile Peroxidase (VP). *Garcia-Ruiz et al.* used combinations of StEP with *in vivo* DNA shuffling and screened two libraries of approximately 2,000 colonies each in microtiter plate format using an ABTS dependent assay (García-Ruiz et al. 2010). A similar approach was used by Mate et al. (Maté et al. 2010) to evolve a basidiomycete HRPL for improved secretion, stability and activity using multiple rounds of error-prone PCR combined with *in vivo* DNA shuffling. Ultimately, also site-directed mutagenesis was employed for the combination of beneficial mutations that did not happen by shuffling, or to recreate revertants. In this work altogether over 50,000 clones were screened over eight rounds and screening also relied on the ABTS-based assays which were subjected cell-free expression supernatants in microtiter plate format. The thus evolved laccase was further adapted to conditions prevalent in human blood: an above-neutral pH and high chloride concentration by using essentially the same methodology and screening procedure as is outlined in **Figure 17** (Mate et al. 2013).

Recently, *Zhang et al.* reported enzyme engineering campaigns on a bacterial copper export oxidase (CueO) which is responsible for copper homeostasis in its host *E. coli*. The researchers aimed at evolving the CueO enzyme towards improved electrochemical performance and increased electron transfer (L. Zhang et al. 2020). In their work, a variation of error-prone PCR with a high mutational load (seven mutations per kb) was used but a high population of active clones (75%) in a library of approximately 1,500 clones could be maintained, which was verified by colorimetric prescreening with ABTS. The actual screening was carried out in an 8-channel-electrochemical platform of immobilized enzymes on carbon nanotube-modified glassy carbon electrodes with an 8-channel potentiostat that enabled the screening of one microtiter plate in approximately 20 min. Positions where positive clones could be identified were subjected to site-saturation mutagenesis, in order to avoid the limitations of epPCR in covering all possible amino acids, and the best single mutants were combined in one variant with considerable reduction in electrochemical overpotential of 0.14 V.

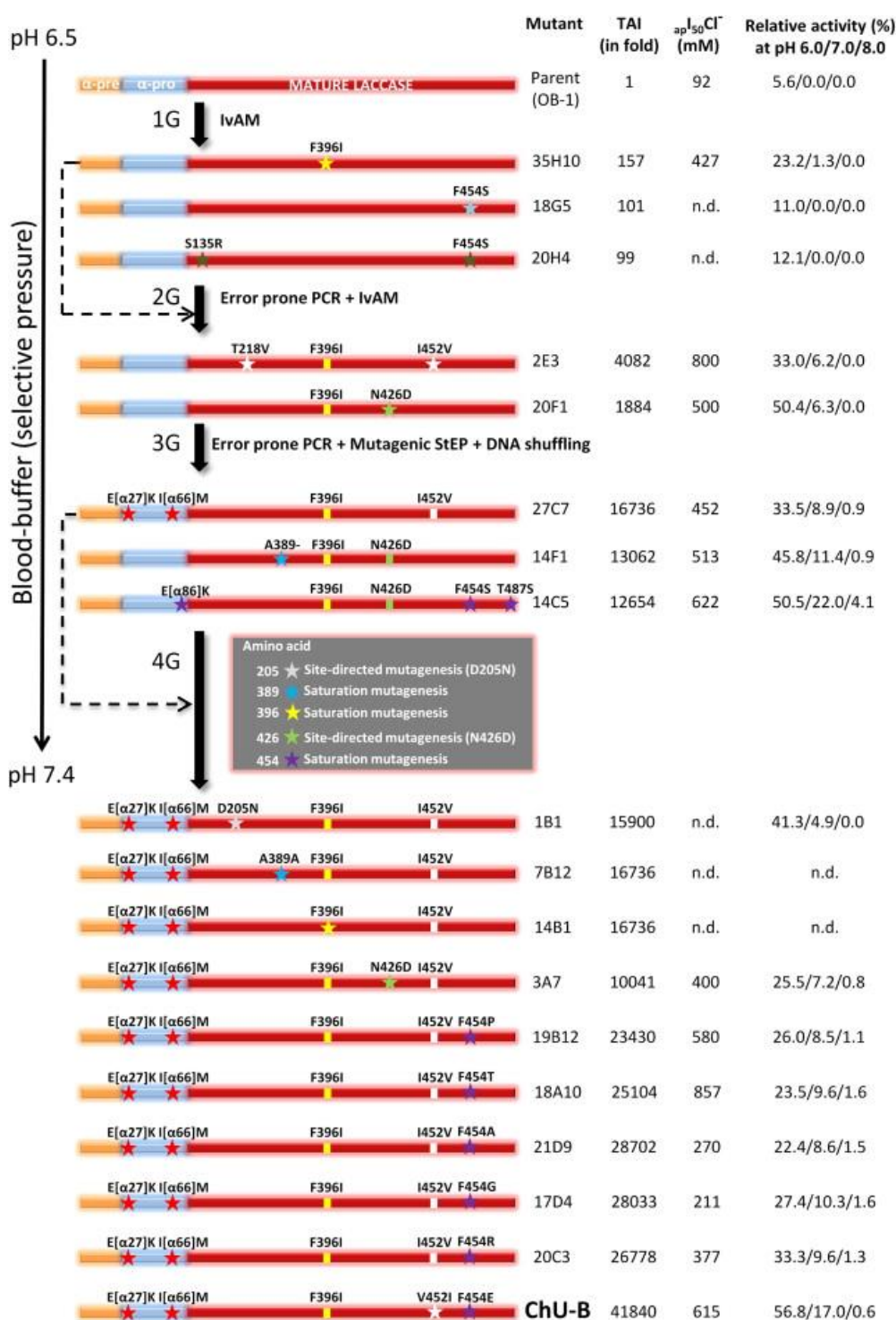


Figure 17 Exemplary overview over a directed evolution campaign for laccase. A basidiomycetous laccase gene was equipped with an α -factor secretion signal for *S. cerevisiae* expression and subjected to *in vivo* assembly, error-prone PCR, StEP, DNA shuffling and site saturation over 4 generations. Variant libraries were assessed under selective conditions with elevated pH and increased chloride concentrations and desirable mutations accumulated in variant “ChU-B”. Schematic by courtesy of D. Mate (Mate et al. 2013).

This approach further highlights the difficulties when screening for specific properties: the screening system has to be as close as possible to the actual application, for which an improvement is sought, and screening with soluble mediators will not mimic the situation of electrochemical oxidations on an electrode.

A common theme of all those campaigns is that the screening assays were adapted for microtiter plate format from the standard activity assays used in kinetic characterizations, and that multichannel pipettors or liquid handling workstations were employed. In any case, library sizes were generally in the range of 1,000 - 3,000 clones, and the total number of screened variants did not exceed 50,000 clones after multiple rounds of mutagenesis and screening. While it is not stated explicitly in these publications, it is reasonably clear that even with robotic assistance, the simultaneous handling of 20 - 50 cultivation plates and around 100 assay plates is a major limiting factor for the screenable sequence space, rather than methods of comprehensive diversity generation.

16. Display technology

Markel et al. have recently reviewed some trends in ultrahigh-throughput screening systems for enzymes utilizing diverse methodologies, mimicking biological systems and employing physicochemical approaches, involving cell surface display, microfluidics, next-generation compartments and *in vitro* compartmentalization in emulsions (Markel et al. 2020).

Surface display gained increased attention with the advent of affinity engineering for binders, where pioneering work on phage display from George P. Smith was awarded with the Nobel Prize in 2018 (G. P. Smith 1985; Arnold, Smith, and Winter 2018). Surface display systems can facilitate the anchoring of secretory enzymes on the surface of the expressing entity, thereby linking it to the encoding gene. This essentially leaves substrate and detectable product (or byproduct) as the only soluble component which needs to be isolated from neighboring reactions and interference. *In vitro* compartmentalization usually offers a solution to this problem, if the preparation of emulsions, the conversion of substrate to product and the detection of the product in a FACS or droplet sorter can be optimized - however, if the detectable product can be somehow associated with the cell as well, this steps are obsolete and setups can be simplified as was highlighted in recent examples (Pitzler et al. 2014; Vanella, Ta, and Nash 2019).

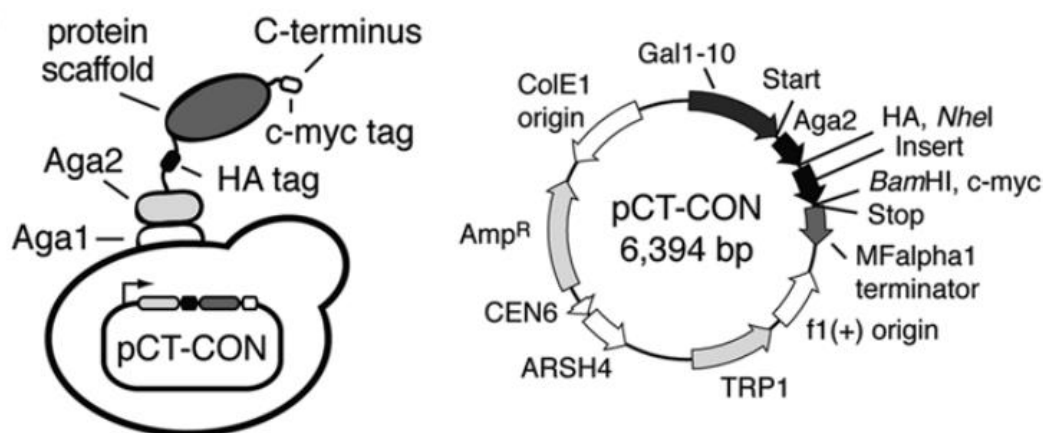


Figure 18 The *S. cerevisiae* Yeast Surface Display system. Schematic of the protein scaffolds involved in the decoration of the *S. cerevisiae* cell wall with a fusion construct of the protein of interest. With the help of the pCT-CON expression vector system (right), the protein of interest is expressed as an in-frame fusion construct with Aga2 and harbors tags for detection and normalization. This fusion protein is secreted and associates naturally to the native Aga1 cell wall protein via cysteine bridges. Schematics by courtesy of M. W. Traxlmayr and A. Angelini (Angelini et al. 2015).

The yeast surface display (YSD) system by Boder & Wittrup was developed for *S. cerevisiae* (Boder and Wittrup 1997) and needs mentioning as one of the key technologies to back the rise of display-based high-throughput screenings in recent times. This display system exploits the natural occurrence of a duo of α -agglutinin proteins (Aga1, Aga2) that take part in the yeasts mating process. Proteins of interest can be effortlessly cloned to the Aga2 moiety as a fusion construct using a variety of established plasmids, and once expressed, will covalently tether to the cell-wall integrated Aga1 partner via disulfide bridges. The use of a eukaryotic expression host conveys a handful of advantages and can alleviate some of the biases of protein expression since it relies on the eukaryotic post-translational machinery (Angelini et al. 2015). This is of particular interest when fungal enzymes are desired to be displayed, where the close phylogenetic relation to the *S. cerevisiae* host represents a clear advantage in terms of expressibility and posttranslational processing. The popularity of this system in enzyme engineering can - at least partially - also be ascribed to the wealth of reports and the availability of detailed protocols (Gai and Wittrup 2007; Traxlmayr and Obinger 2012; T. F. Chen et al. 2013; Angelini et al. 2015). Yeast display, in different forms, is predominantly employed for the engineering of pharmaceutically relevant binding

proteins but has seen emerging adaptation for the display of enzymes. Alongside oxidoreductases, this technology was successfully used for the cellular immobilization of proteases, sortases, lipases glucosidases and even peroxidases and oxidases as was reviewed by *Mei et al.* (Mei et al. 2017).

Parallel to the various yeast surface display systems, a multihued palette of systems and methodologies for the immobilization and tethering of enzymes has been developed but is unequally well established for the different fields of application. Uniformly, these methods rely on maintaining a steady connection of gene sequence (genotype) and enzyme function (phenotype) and include phage display (G. P. Smith 1985), ribosome and mRNA display (Hanes and Plückthun 1997), bacterial surface display (van Bloois et al. 2011), mammalian cell display (Bowers et al. 2014) spore display (Isticato et al. 2001). Still, most of these methods focus on affinity interaction with proteins, peptides or small molecules. For the purpose of evolving enzymes, bacterial display systems represent the most prominent alternative to yeast display and include multiple strategies for *E. coli* alongside many for gram-positive expression platforms (Becker et al. 2005; Yang and Withers 2009; van Bloois et al. 2011).

Flow cytometry and microfluidics

The advancements in the development of microfluidic systems, flow cytometers and cell sorters have unlocked the possibility to screen enzyme variants by the single cells within a suspension of millions of cells or more. The urge to discover pharmaceutically relevant binders (often antibodies) for clinical application surely was the main driver in these developments and was boosted by research of established companies with substantial financial effort. At the status quo, the combination of surface display technologies and flow cytometers allows to process variant libraries of sizes of 10^6 per hour (Markel et al. 2020), each cell being individually assessed for a wide array of biochemical properties within milliseconds by means of fluorescence. Every cell within a suspension can represent a single, unique variant with its gene encoded inside the cell and connected to a distinct enzymatic property (stability, activity, specificity) that is screened for and desirably unaffected by other variants.

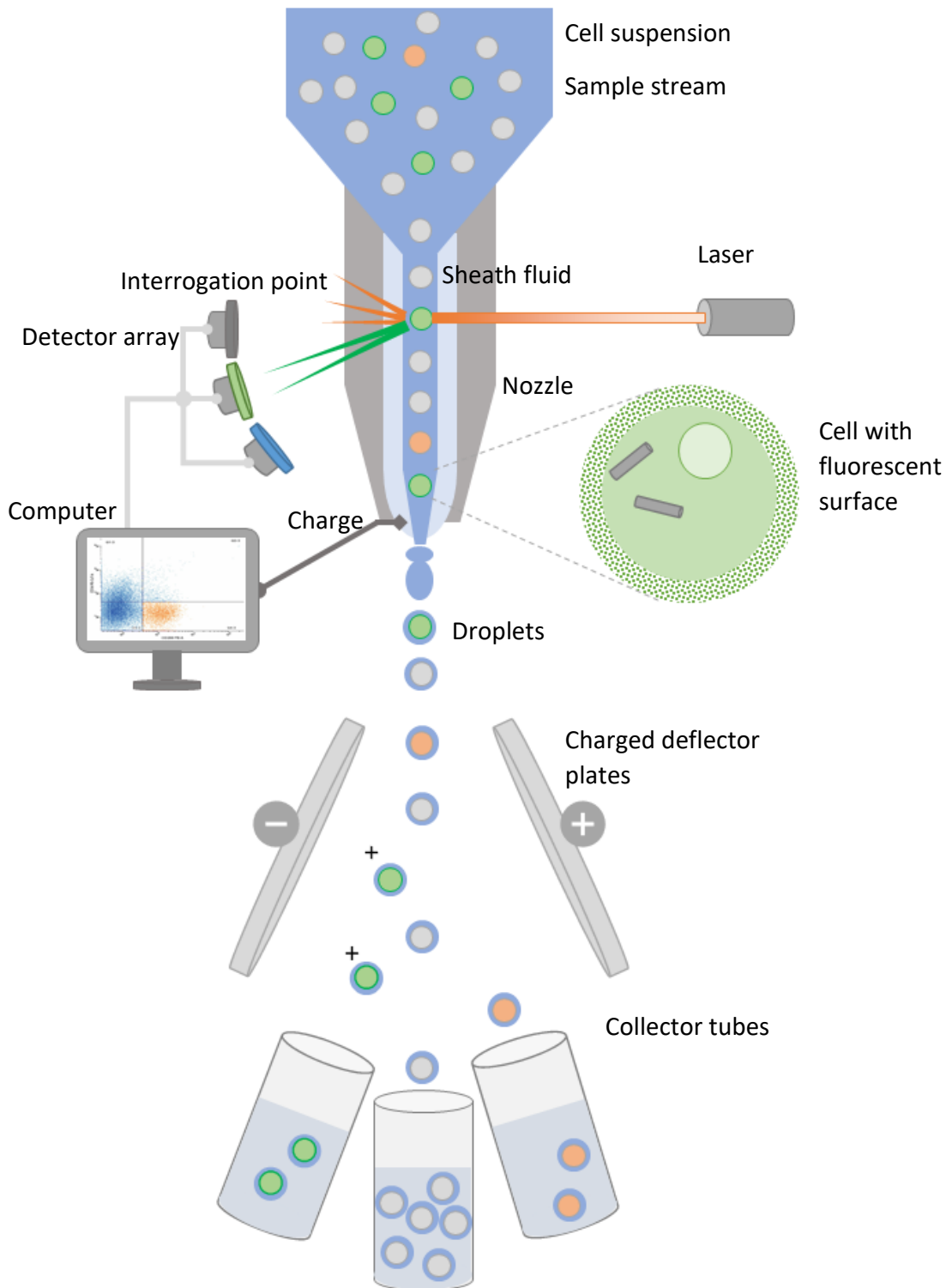


Figure 19 Principles of flow cytometers and cell sorters. The sample stream leaves the container and carries the cells in suspension before being united with the sheath fluid for fluidic focusing. The cells align in a single file and pass the interrogation point where their fluorescent properties are evaluated by a laser and a detector array. Information from this assessment triggers a charging of droplets that are formed by the nozzle. These polarized droplets are then deflected by dedicated plates which results in a slight change in trajectory for collection into separate tubes.

The screening of enzyme activity can similarly be realized as long as it can be converted to a fluorescent signal, for example the formation or attachment of a fluorescent reaction product at the cell surface.

The general functionality of microfluidic systems can be explained by exemplarily describing flow cytometers and cell sorters (FACS, fluorescence activated cell sorting), which are common in academic environments. In these devices, the entire transport of cells through the machine relies on microfluidic liquid transfer. The beginning marks a sample container which holds the assayed, fluorescently stained cell suspension and is usually pressurized to facilitate a flow of volume towards the flow cell, where the sample stream is surrounded by the sheath fluid. An elevated pressure in the enringing sheath fluid causes the sample stream to condense and drastically narrow in diameter, ultimately leading to a perfectly laminar flow of strung-out, single file cells in a process termed hydrodynamic focusing. The stream then continues till the interrogation point is reached where the cells are hit by an array of lasers, exciting the fluorescence of the reporter dyes on the cell surface. The so obtained fluorescence signals and scattered beams are further split by optical filters (dichroic mirrors) and processed by a detector unit one-by-one. In the case of flow cytometers, the resulting signals are the desired output and can provide information on the relative amount of fluorescent signal on the cell surface. Cell sorters function likewise up to that point but make use of the gathered signal data to isolate cells into separate collector tubes. Fluorescence data is processed in line and compared to a deliberately set threshold of values and ratios, by computer guided gating. In cell sorters, the sample stream continues to the nozzle, where harmonic oscillation of the tip causes the stream to partition and form droplets engulfing, ideally, a single cell per droplet. These droplets are charged according to their signals with respect to the gating limits shortly after they leave the interrogation point. When finally the differently charged droplets pass the deflector plates, they are exposed to an electromagnetic field and are redirected slightly, which is subject to the level of charge applied. This ultimately allows to collect them in separate tubes, depending on whether they fulfilled the gating criteria or not.

Standard cell sorters can achieve validated sorting rates of 10 000 events per second while maintaining practicable accuracy rates. For certain flagship instruments higher rates up to 50 000 events per second and sorting into usually multiple (5 or more) receiver slots is possible. It needs

to be stated that usually multiple rounds of sorting are required, and the common strategy entails initial enrichment of likely positive events at high rates and subsequent increase in accuracy at the cost of sorting speed. Thus, higher sorting rates do not necessarily cut analysis times and smart techniques to remove negative cells prior to cell sorting, magnetic bead sorting or size selection (Vanella et al. 2019) can contribute more substantially to speeding up the overall process.

Parallel to cell sorters, lab-on-a-chip solutions for cell sorting and enzyme screening developed rapidly in the past decade and pioneering work by the group around David A. Weitz stood in the scientific spotlight repeatedly (Utada et al. 2005; Baret et al. 2009; Agresti et al. 2010). The screening of cells displaying enzymes can be carried out using small microfluidic chips that are commercially available, customizable and commonly represent an affordable screening system. In certain applications, microfluidic chips made from silicon or various synthetic polymers, allow to create a stream of (displaying) cells and are united with the assay components and emulsified utilizing a micro-capillary setup. Upon mixing, the assay reaction is started, extended and analyzed shortly after in a fluorescence detector before being sorted, as can be performed in different setups as a recent review comprehensively outlined (Chiu and Stavrakis 2019).

Displayed Oxidoreductases

Lipovsek et al. (2007) have first evolved yeast-surface-displayed horse radish peroxidase (HRP) with two different enantiomers of a fluorescently labelled HRP substrate, the chiral phenol tyrosinol. Oxidation of these conjugates leads to the formation of radicals that are captured at the cell surface via reaction with exposed tyrosine residues, and the yeast cells can be sorted by FACS based on the ratio of the two dyes bound to the surface - which corresponds to the enantioselectivity of the HRP (Lipovšek et al. 2007). In this approach the reaction products are soluble and diffusible at first, and while they are subsequently captured on the cell, cross-labeling by radicals produced from neighboring cells is possible. Initially, directed evolution of the peroxidase yielded a positive outcome only in the case of a semi-rational approach, where a comparably small site-directed enzyme library was screened. In follow-up work, improved variants were also isolated from a random mutagenesis library and were characterized to be almost completely enantioselective. Obtained results could also be rationalized with computational

docking and strong influence on the enzymes enantioselectivity later attributed to a single amino acid in the active site (E. Antipov et al. 2008; Eugene Antipov, Cho, and Klivanov 2009).

Prodanovic and colleagues (2012) adapted this system for the evolution of H₂O₂-producing GOx, with the radical forming HRP as the secondary enzyme added in soluble form and found that under these conditions cross-labeling is prevalent. Therefore, the reactions (of 10⁷ cells) were performed in an emulsion of Tris buffer containing fluorescein-tyramide, glucose and HRP in oil and ascorbic acid for quenching of side reactions, after which the cells were recovered and sorted by FACS (Prodanovic et al. 2012). The performance of this screening system was, however, considered unsatisfactory. As the number of tyrosine residues on the cell surface that are available for labeling is limited, only a narrow window of activity increase can be used reliably. The system was subsequently adapted to double emulsions (water-in-oil-in-water), which works without tyramide-immobilization of the fluorescent products on the cells, and therefore requires constant compartmentalization during detection and sorting, and a number of fluorescent dyes was tested for HRP-dependent hydrogen peroxide detection. Ultimately, vanadium bromoperoxidase (from the macro alga *Corallina officinalis*) was employed for peroxide detection instead of HRP, in order to avoid the issue of unspecific oxidation of fluorescent phenolic compounds by HRP (leading to a drop in fluorescence) in the presence of an excess of peroxide (Ostafe et al. 2014). This assay allowed the sorting of 100,000 clones with an enrichment of up to 200-fold in one hour. In a further modification, the Prodanovic group used GOx-fusions with a modified yGFP variant in order to quantify GOx displayed on the yeast surface for the purpose of normalizing enzyme expression levels to activity for individual cells. GOx activity was measured as in the above systems by HRP-mediated DyLight650-tyramide labeling of the yeast cells, and FACS gating was set for a high ratio of activity-related DyLight650-fluorescence (red) vs yGFP-fluorescence (presence on the cell surface). Enrichment of cells expressing GOx with increased activity was achieved in a single round of screening and individual clones displayed up to 2.3-fold activity (Kovačević et al. 2019). Shortly after, similar campaigns aimed at improving the expression level and capabilities to neutralize harmful azo-dyes of versatile peroxidase and lignin peroxidase in a surface display setting in conjunction with fluorescent substrates (Ilić Đurđić et al. 2020).

Another publication reported the use of enzymatic radical-based polymerization to establish an ultra-high-throughput screening for oxidoreductases in one-pot reactions (Vanella R. et al., 2019a). In their work, *Vanella et al.* documented the formation of a fluorescent hydrogel to encapsulate yeast cells expressing active glucose oxidase and subsequent analysis of a mutational library via FACS (Vanella R. et al, 2019b). The described approach is based on a cascade reaction polymerizing chemically modified alginate, where alginate monomers contain covalently attached fluorescein and tyramine moieties for radical chemistry. *A. niger* GOx was displayed on *S. cerevisiae* cells utilizing the established yeast surface display system (Boder and Wittrup 1997). Glucose, horseradish peroxidase, and modified alginate were added in a soluble form and a fluorescent shell formed around cells harboring active enzyme. With this system, it could be shown that glucose oxidase activity can be successfully screened for in a selective approach: the alginate shell conveys immunity to enzymatic lysis and shell formation from polymerization increases particle diameter and facilitates enrichment by filtration. Additionally, this system could successfully be used in a quantitative approach via FACS as was described in the examples before. Using FACS *Vanella et al.* could isolate variants that were both catalytically improved and more stable from a library of $> 10^6$ variants within hours.

Similarly, a bio-encapsulation based on glucose oxidase-mediated H_2O_2 release was employed for the screening of hydrolase activity. In their work, *Pitzler et al.* realized a screening system for the directed evolution of a bacterial phytase that was recombinantly expressed in *E. coli* (Pitzler et al. 2014). Phosphatase activity causes the release of phosphate groups from glucose which then becomes a suitable substrate to fuel added glucose oxidase. H_2O_2 produced from this reaction triggers the polymerization of a fluorescent PEG-based shell around the cells. Instead of using a peroxidase to mediate radical formation, this system is based on bivalent cations to support radical Fenton-chemistry. Work from the same group also described adaptation of this system for hydrolases (Lülsdorf et al. 2015).

The micro-compartmentalization of enzyme displaying cells in emulsions has greatly attributed to the recent development of FACS-based screening technologies and is often adopted for screenings

in microfluidic chip setups, too. Still, the use of emulsions often accompanies certain limitations that restrict the generalizability of the approach and complicate its application.

One of the major hurdles to overcome is to achieve a definite distribution of the number of cells within the droplets and ideally guarantee the presence of just single cells within them. This aspect is often challenging and a matter of combating an unfavorable statistical distribution with optimal emulsification settings - which usually demands profound experience and sufficient testing. Once proper emulsions are established, they not only present a microfluidic container but also a boundary for diffusive in- and efflux. As is desired, the diffusivity of reaction products is curbed by the water-oil interface which concomitantly also restricts influx of substrate for the enzymatic reaction. This problem was elegantly tackled by the Prodanovic group using the detergent-like beta-octyl glucoside as a substrate for the screening of glucose oxidase (GOx): the glucose moiety accumulates in the aqueous side of the droplet and can be cleaved from the hydrophobic octanol moiety (by beta-glucosidase) and hence made available for GOx (Ostafe et al. 2014). As this approach aids to circumvent the challenge of supplying substrate for the enzymatic reaction, it also restricts the variety of substrates that can be used. If in a similar setting alternative GOx substrates were to be screened for, other - potentially not commercially available - beta-octyl sugars would be needed. Another fundamental puzzle of emulsified one-pot systems is how to realize a synchronous reaction start for all cells in the droplets. If mass transfer through the water-oil interface is biased, due to unequal droplet widths for example, differences in apparent reaction times and substrate concentrations will lead to false positive results. This bias can hardly ever be evaded and should always be accounted for in multi-phase systems.

17. Future directions

Recent years have seen significant progress in the development and refinement of compartmentalization in smaller volumetric units, detection and quantification of reactions in cells representing a minimal compartment and even cell-free expression and screening approaches using cell display, emulsions, microcapillaries and microfluidics technologies (see, e.g. Colin et al. 2015; Longwell, Labanieh, and Cochran 2017; Bunzel et al. 2018; Markel et al. 2020 for reviews). The latter technologies appear highly promising, but also entail a requirement for sophisticated technical equipment for the manufacturing of, e.g., microchambers or microcapillaries.

The naturally smallest compartment is the cell, and cell sorting is a comparably simple and established technology. Enzymes that are naturally active in the cytoplasm can be screened using the cell as compartment, provided that a suitable substrate or substrate analogue can be provided that can be taken up by the cell and be converted to a detectable product that remains in the cell. Aharoni et al. (2005) described such systems for glycosyl transferases, where a fluorescently labelled acceptor molecule can traffic in and out of the cell, but is unable to do so once an additional sugar residue is transferred to it by the transferase, thus enlarging the molecule (Aharoni et al. 2005). Accumulation of fluorescent product is then a measure for enzymatic activity. Enzymes as discussed above, however, are active outside the cell, and while anchoring on the cell is often feasible, it is the capturing or immobilization of a detectable product that is the major challenge, particularly when a secondary enzymatic reaction is required, as is the case for the detection of the co-product hydrogen peroxide. In that respect, approaches without *in vitro* compartmentalization in emulsion droplets have thus far not reached practical relevance, mostly due to problems with cross-labeling by the generated radicals, particularly when enzymatic cascades were employed, or to a limited capacity to capture the generated detectable radicals before saturation (Prodanovic et al. 2012). Gutscher et al. (2009) have used a modified roGFP, that can be oxidized by the hydrogen peroxide-scavenging yeast peroxiredoxin Orp1, leading to a measurable fluorescent signal. Such redox sensors could be co-immobilized with peroxide-producing enzymes offering direct detectability on the cell without the need for *in vitro* compartmentalization. A comparable protein-based peroxide sensor was already employed intracellularly when working in conjunction with cytochrome P450 BM3 and made lysis reactions obsolete (Lim and Sikes 2015). Similar approaches are conceivable for peroxidases or laccases, if they are capable of catalyzing comparable oxidations of reporter proteins. Alternatively, enzymes whose reactions result in the formation of radicals (peroxidases, laccases, etc.) could be assayed if capturing of the produced radicals on the cell surface could be facilitated via a different mechanism than tyramide-fluorescein, which was considered (Prodanovic et al. 2012).

Seemingly, scientific literature of the past decade highlighted a focus on radical-based methods to immobilize fluorescent output on the cell surface as is outlined above. Given the unspecific nature of such chemistry, the combination with compartmentalization methods such as emulsification can be deemed necessary and often represent the bottleneck of applicability. Novel methods to

decrease cross-talk between neighboring cells (and variants), limiting diffusion while simultaneously guaranteeing a tight connection of fluorescent readout to the enzyme variant and its gene promise improvement. Likely, non-diffusive protein based reporters (Gutscher et al. 2009) that are tightly tethered to the cells or partially diffusive polymers such as the recently introduced fluorescent alginate reporter (Vanella, Ta, and Nash 2019) attract the most attention in the upcoming years. The establishment of more widely applicable systems will additionally help to boost screening success as enzymes other than the notorious *A. niger* glucose oxidase are employed. Potentially, one of these enzymes in the spotlight is lactate oxidase, an enzyme so far unbeknownst to high-throughput screenings but unproportionally relevant in industry (Kucherenko, Topolnikova, and Soldatkin 2018).

D) References

- Agresti, Jeremy J., Eugene Antipov, Adam R. Abate, Keunho Ahn, Amy C. Rowat, Jean-Christophe Baret, Manuel Marquez, Alexander M. Klibanov, Andrew D. Griffiths, and David A. Weitz. 2010. "Ultra-high-Throughput Screening in Drop-Based Microfluidics for Directed Evolution." *Proceedings of the National Academy of Sciences of the United States of America* 107 (9): 4004. <https://doi.org/10.1073/PNAS.0910781107>.
- Aharoni, Amir, Gil Amitai, Kalia Bernath, Shlomo Magdassi, and Dan S. Tawfik. 2005. "High-Throughput Screening of Enzyme Libraries: Thiolactonases Evolved by Fluorescence-Activated Sorting of Single Cells in Emulsion Compartments." *Chemistry & Biology* 12 (12): 1281–89. <https://doi.org/10.1016/J.CHEMBIOL.2005.09.012>.
- Angelini, Alessandro, Tiffany F. Chen, Seymour de Picciotto, Nicole J. Yang, Alice Tzeng, Michael S. Santos, James A. Van Deventer, Michael W. Traxlmayr, and K. Dane Wittrup. 2015. "Protein Engineering and Selection Using Yeast Surface Display." In *Methods in Molecular Biology (Clifton, N.J.)*, 1319:3–36. https://doi.org/10.1007/978-1-4939-2748-7_1.
- Antipov, E., A. E. Cho, K. D. Wittrup, and A. M. Klibanov. 2008. "Highly L and D Enantioselective Variants of Horseradish Peroxidase Discovered by an Ultra-high-Throughput Selection Method." *Proceedings of the National Academy of Sciences* 105 (46): 17694–99. <https://doi.org/10.1073/pnas.0809851105>.
- Antipov, Eugene, Art E. Cho, and Alexander M. Klibanov. 2009. "How a Single-Point Mutation in Horseradish Peroxidase Markedly Enhances Enantioselectivity." *Journal of the American Chemical Society* 131 (31): 11155–60. <https://doi.org/10.1021/ja903482u>.
- Arango Gutierrez, Erik, Hemanshu Mundhada, Thomas Meier, Hartmut Duefel, Marco Bocola, and Ulrich Schwaneberg. 2013. "Reengineered Glucose Oxidase for Amperometric Glucose Determination in Diabetes Analytics." *Biosensors and Bioelectronics* 50 (December): 84–90. <https://doi.org/10.1016/j.bios.2013.06.029>.
- Arnold, Frances H. 1997. "Design by Directed Evolution." *FASEB Journal* 11 (9). <https://doi.org/10.1021/ar960017f>.
- Arnold, Frances H. 2019. "Innovation by Evolution: Bringing New Chemistry to Life (Nobel Lecture)." *Angewandte Chemie - International Edition*. Wiley-VCH Verlag. <https://doi.org/10.1002/anie.201907729>.
- Arnold, Frances H, George P Smith, and Gregory Winter. 2018. "The Nobel Prize in Chemistry 2018," 50005. <https://www.nobelprize.org/prizes/chemistry/2018/summary/>.
- Baek, Minkyung, Frank DiMaio, Ivan Anishchenko, Justas Dauparas, Sergey Ovchinnikov, Gyu Rie Lee, Jue Wang, et al. 2021. "Accurate Prediction of Protein Structures and Interactions Using a Three-Track Neural Network." *Science* 10 (11): eabj8754. <https://doi.org/10.1126/SCIENCE.ABJ8754>.
- Balint, Robert F., and James W. Larrick. 1993. "Antibody Engineering by Parsimonious Mutagenesis." *Gene* 137 (1): 109–18. [https://doi.org/10.1016/0378-1119\(93\)90258-5](https://doi.org/10.1016/0378-1119(93)90258-5).
- Baret, Jean Christophe, Oliver J. Miller, Valerie Taly, Michaël Ryckelynck, Abdeslam El-Harrak, Lucas Frenz, Christian Rick, et al. 2009. "Fluorescence-Activated Droplet Sorting (FADS): Efficient Microfluidic Cell Sorting Based on Enzymatic Activity." *Lab on a Chip* 9 (13): 1850–58. <https://doi.org/10.1039/b902504a>.
- Becker, Stefan, Sebastian Theile, Nele Heppeler, Anja Michalczyk, Alexander Wentzel, Susanne Wilhelm,

- Karl Erich Jaeger, and Harald Kolmar. 2005. "A Generic System for the Escherichia Coli Cell-Surface Display of Lipolytic Enzymes." *FEBS Letters* 579 (5): 1177–82. <https://doi.org/10.1016/j.febslet.2004.12.087>.
- Bittker, Joshua A., Brian V. Le, Jane M. Liu, and David R. Liu. 2004. "Directed Evolution of Protein Enzymes Using Nonhomologous Random Recombination." *Proceedings of the National Academy of Sciences of the United States of America* 101 (18): 7011–16. <https://doi.org/10.1073/pnas.0402202101>.
- Bloois, Edwin van, Remko T. Winter, Harald Kolmar, and Marco W. Fraaije. 2011. "Decorating Microbes: Surface Display of Proteins on Escherichia Coli." *Trends in Biotechnology*. Trends Biotechnol. <https://doi.org/10.1016/j.tibtech.2010.11.003>.
- Boder, Eric T., and K. Dane Wittrup. 1997. "Yeast Surface Display for Screening Combinatorial Polypeptide Libraries." *Nature Biotechnology* 15 (6): 553–57. <https://doi.org/10.1038/nbt0697-553>.
- Bowers, Peter M., Robert A. Horlick, Marilyn R. Kehry, Tamlyn Y. Neben, Geoffery L. Tomlinson, Larry Altobelli, Xue Zhang, et al. 2014. "Mammalian Cell Display for the Discovery and Optimization of Antibody Therapeutics." *Methods* 65 (1): 44–56. <https://doi.org/10.1016/j.ymeth.2013.06.010>.
- Bridges, B. A., and R. Woodgate. 1985. "Mutagenic Repair in Escherichia Coli: Products of the RecA Gene and of the UmuD and UmuC Genes Act at Different Steps in UV-Induced Mutagenesis." *Proceedings of the National Academy of Sciences of the United States of America* 82 (12): 4193–97. <https://doi.org/10.1073/pnas.82.12.4193>.
- Brugger, Dagmar, Iris Krondorfer, Kawah Zahma, Thomas Stoisser, Juan M. Bolivar, Bernd Nidetzky, Clemens K. Peterbauer, and Dietmar Haltrich. 2014. "Convenient Microtiter Plate-Based, Oxygen-Independent Activity Assays for Flavin-Dependent Oxidoreductases Based on Different Redox Dyes." *Biotechnology Journal* 9 (4): 474–82. <https://doi.org/10.1002/biot.201300336>.
- Bunzel, Hans Adrian, Xavier Garrabou, Moritz Pott, and Donald Hilvert. 2018. "Speeding up Enzyme Discovery and Engineering with Ultrahigh-Throughput Methods." *Current Opinion in Structural Biology*. Elsevier Ltd. <https://doi.org/10.1016/j.sbi.2017.12.010>.
- Cadwell, R. Craig, and Gerald F. Joyce. 1992. "Randomization of Genes by PCR Mutagenesis." *Genome Research* 2 (1): 28–33. <https://doi.org/10.1101/gr.2.1.28>.
- Chen, Fei, Eric A. Gauchera, Nicole A. Leal, Daniel Hutter, Stephanie A. Havemann, Sridhar Govindarajan, Eric A. Ortlund, and Steven A. Benner. 2010. "Reconstructed Evolutionary Adaptive Paths Give Polymerases Accepting Reversible Terminators for Sequencing and SNP Detection." *Proceedings of the National Academy of Sciences of the United States of America* 107 (5): 1948–53. <https://doi.org/10.1073/pnas.0908463107>.
- Chen, Keqin, and Frances H. Arnold. 1991. "Enzyme Engineering for Nonaqueous Solvents: Random Mutagenesis to Enhance Activity of Subtilisin E in Polar Organic Media." *Bio/Technology* 9 (11): 1073–77. <https://doi.org/10.1038/nbt1191-1073>.
- Chen, Tiffany F., Seymour de Picciotto, Benjamin J. Hackel, and K. Dane Wittrup. 2013. "Chapter Fourteen – Engineering Fibronectin-Based Binding Proteins by Yeast Surface Display." *Methods in Enzymology* 523: 303–26. <https://doi.org/10.1016/B978-0-12-394292-0.00014-X>.
- Cheng, Feng, Leilei Zhu, and Ulrich Schwaneberg. 2015. "Directed Evolution 2.0: Improving and Deciphering Enzyme Properties." *Chemical Communications* 51: 9760. <https://doi.org/10.1039/c5cc01594d>.
- Cherny, Izhack, Per Greisen, Yacov Ashani, Sagar D. Khare, Gustav Oberdorfer, Haim Leader, David Baker,

- and Dan S. Tawfik. 2013. "Engineering V-Type Nerve Agents Detoxifying Enzymes Using Computationally Focused Libraries." *ACS Chemical Biology* 8 (11): 2394–2403. <https://doi.org/10.1021/cb4004892>.
- Chica, Roberto A., Nicolas Doucet, and Joelle N. Pelletier. 2005. "Semi-Rational Approaches to Engineering Enzyme Activity: Combining the Benefits of Directed Evolution and Rational Design." *Current Opinion in Biotechnology*. *Curr Opin Biotechnol*. <https://doi.org/10.1016/j.copbio.2005.06.004>.
- Chien, Alice, David B Edgar, and John M Trela. 1976. "Deoxyribonucleic Acid Polymerase from the Extreme Thermophile *Thermus Aquaticus*." Vol. 127. <http://jb.asm.org/>.
- Chiu, Flora W.Y., and Stavros Stavrakis. 2019. "High-Throughput Droplet-Based Microfluidics for Directed Evolution of Enzymes." *Electrophoresis*. Wiley-VCH Verlag. <https://doi.org/10.1002/elps.201900222>.
- Coco, Wayne M., William E. Levinson, Michael J. Crist, Harm J. Hektor, Aldis Darzins, Philip T. Pienkos, Charles H. Squires, and Daniel J. Monticello. 2001. "DNA Shuffling Method for Generating Highly Recombined Genes and Evolved Enzymes." *Nature Biotechnology* 19 (4): 354–59. <https://doi.org/10.1038/86744>.
- Coelho, Pedro S., Z. Jane Wang, Maraia E. Ener, Stefanie A. Baril, Arvind Kannan, Frances H. Arnold, and Eric M. Brustad. 2013. "A Serine-Substituted P450 Catalyzes Highly Efficient Carbene Transfer to Olefins in Vivo." *Nature Chemical Biology* 9 (8): 485–87. <https://doi.org/10.1038/nchembio.1278>.
- Cohen, S. N., A. C.Y. Chang, H. W. Boyer, and R. B. Helling. 1973. "Construction of Biologically Functional Bacterial Plasmids in Vitro." *Proceedings of the National Academy of Sciences of the United States of America* 70 (11): 3240–44. <https://doi.org/10.1073/pnas.70.11.3240>.
- Colin, Pierre Yves, Balint Kintses, Fabrice Gielen, Charlotte M. Miton, Gerhard Fischer, Mark F. Mohamed, Marko Hyvönen, Diego P. Morgavi, Dick B. Janssen, and Florian Hoffelder. 2015. "Ultra-high-Throughput Discovery of Promiscuous Enzymes by Picodroplet Functional Metagenomics." *Nature Communications* 6 (1): 1–12. <https://doi.org/10.1038/ncomms10008>.
- Cox, E. C. 1976. "Bacterial Mutator Genes and the Control of Spontaneous Mutation." *Annual Review of Genetics*. *Annu Rev Genet*. <https://doi.org/10.1146/annurev.ge.10.120176.001031>.
- Cramer, Andreas, Sun Ai Raillard, Ericka Bermudez, and Willem P.C. Stemmer. 1998. "DNA Shuffling of a Family of Genes from Diverse Species Accelerates Directed Evolution." *Nature* 391 (6664): 288–91. <https://doi.org/10.1038/34663>.
- Darwin, Charles. 1859. *On the Origin of Species by Means of Natural Selection Or the Preservation of Favoured Races in the Struggle for Life*. H. Milford; Oxford University Press.
- Eckert, Kristin A., and Thomas A. Kunkel. 1990. "High Fidelity DNA Synthesis by the *Thermus Aquaticus* DNA Polymerase." *Nucleic Acids Research* 18 (13): 3739–44. <https://doi.org/10.1093/nar/18.13.3739>.
- Feehan, Ryan, Daniel Montezano, and Joanna S G Slusky. 2021. "Machine Learning for Enzyme Engineering, Selection and Design." *Protein Engineering, Design and Selection* 34 (February): 1–10. <https://doi.org/10.1093/PROTEIN/GZAB019>.
- Felice, Alfons K. G., Christian Schuster, Alan Kadek, Frantisek Filandr, Christophe V. F. P. Laurent, Stefan Scheiblbrandner, Lorenz Schwaiger, et al. 2020. "Chimeric Cellobiose Dehydrogenases Reveal the Function of Cytochrome Domain Mobility for the Electron Transfer to Lytic Polysaccharide Monooxygenase." *ACS Catalysis* 28: 517–32. <https://doi.org/10.1021/acscatal.0c05294>.
- Ferrari, Luna De, and John B.O. Mitchell. 2014. "From Sequence to Enzyme Mechanism Using Multi-Label Machine Learning." *BMC Bioinformatics* 15 (1). <https://doi.org/10.1186/1471-2105-15-150>.

- Fischlechner, Martin, Yolanda Schaerli, Mark F. Mohamed, Santosh Patil, Chris Abell, and Florian Hollfelder. 2014. "Evolution of Enzyme Catalysts Caged in Biomimetic Gel-Shell Beads." *Nature Chemistry* 2014 6:9 6 (9): 791. <https://doi.org/10.1038/nchem.1996>.
- Foroozandeh Shahraki, Mehdi, Kiana Farhadyar, Kaveh Kavousi, Mohammad H. Azarabad, Amin Boroomand, Shohreh Ariaeenejad, and Ghasem Hosseini Salekdeh. 2021. "A Generalized Machine-Learning Aided Method for Targeted Identification of Industrial Enzymes from Metagenome: A Xylanase Temperature Dependence Case Study." *Biotechnology and Bioengineering* 118 (2): 759–69. <https://doi.org/10.1002/bit.27608>.
- Freese, Ernst. 1959. "The Specific Mutagenic Effect of Base Analogues on Phage T4." *Journal of Molecular Biology* 1 (2): 87–105. [https://doi.org/10.1016/S0022-2836\(59\)80038-3](https://doi.org/10.1016/S0022-2836(59)80038-3).
- Furukawa, Ryutaro, Wakako Toma, Koji Yamazaki, and Satoshi Akanuma. 2020. "Ancestral Sequence Reconstruction Produces Thermally Stable Enzymes with Mesophilic Enzyme-like Catalytic Properties." *Scientific Reports* 10 (1): 1–13. <https://doi.org/10.1038/s41598-020-72418-4>.
- Gai, S. Annie, and K. Dane Wittrup. 2007. "Yeast Surface Display for Protein Engineering and Characterization." *Current Opinion in Structural Biology*. *Curr Opin Struct Biol*. <https://doi.org/10.1016/j.sbi.2007.08.012>.
- García-Ruiz, Eva, Diana Maté, Antonio Ballesteros, Angel T. Martinez, and Miguel Alcalde. 2010. "Evolving Thermostability in Mutant Libraries of Lignolytic Oxidoreductases Expressed in Yeast." *Microbial Cell Factories* 9 (1): 1–13. <https://doi.org/10.1186/1475-2859-9-17>.
- Gibson, Daniel G., Lei Young, Ray Yuan Chuang, J. Craig Venter, Clyde A. Hutchison, and Hamilton O. Smith. 2009. "Enzymatic Assembly of DNA Molecules up to Several Hundred Kilobases." *Nature Methods* 6 (5): 343–45. <https://doi.org/10.1038/nmeth.1318>.
- Greener, Alan, Marie Callahan, and Bruce Jerpseth. 1997. "An Efficient Random Mutagenesis Technique Using an E. Coli Mutator Strain." *Applied Biochemistry and Biotechnology - Part B Molecular Biotechnology* 7 (2): 189–95. <https://doi.org/10.1007/BF02761755>.
- Gupta, Rinkoo D., and Dan S. Tawfik. 2008. "Directed Enzyme Evolution via Small and Effective Neutral Drift Libraries." *Nature Methods* 5 (11): 939–42. <https://doi.org/10.1038/nmeth.1262>.
- Gutscher, Marcus, Mirko C. Sobotta, Guido H. Wabnitz, Seda Ballikaya, Andreas J. Meyer, Yvonne Samstag, and Tobias P. Dick. 2009. "Proximity-Based Protein Thiol Oxidation by H₂O₂-Scavenging Peroxidases." *Journal of Biological Chemistry* 284 (46): 31532–40. <https://doi.org/10.1074/jbc.M109.059246>.
- Hanes, Jozef, and Andreas Plückthun. 1997. "In Vitro Selection and Evolution of Functional Proteins by Using Ribosome Display." *Proceedings of the National Academy of Sciences of the United States of America* 94 (10): 4937–42. <https://doi.org/10.1073/pnas.94.10.4937>.
- Herman, Asael, and Dan S. Tawfik. 2007. "Incorporating Synthetic Oligonucleotides via Gene Reassembly (ISOR): A Versatile Tool for Generating Targeted Libraries." *Protein Engineering, Design and Selection* 20 (5): 219–26. <https://doi.org/10.1093/protein/gzm014>.
- Hon, Jiri, Simeon Borko, Jan Stourac, Zbynek Prokop, Jaroslav Zendulka, David Bednar, Tomas Martinek, and Jiri Damborsky. 2021. "EnzymeMiner: Automated Mining of Soluble Enzymes with Diverse Structures, Catalytic Properties and Stabilities." *Nucleic Acids Research* 48 (W1): W104–9. <https://doi.org/10.1093/NAR/GKAA372>.
- Ilić Đurđić, Karla, Raluca Ostafe, Aleksandra Đurđević Đelmaš, Nikolina Popović, Stefan Schillberg, Rainer

- Fischer, and Radivoje Prodanović. 2020. "Saturation Mutagenesis to Improve the Degradation of Azo Dyes by Versatile Peroxidase and Application in Form of VP-Coated Yeast Cell Walls." *Enzyme and Microbial Technology* 136 (January): 109509. <https://doi.org/10.1016/j.enzmictec.2020.109509>.
- Islam, Shohana, Dominic Laaf, Belén Infanzón, Helena Pelantová, Mehdi D. Davari, Felix Jakob, Vladimír Křen, Lothar Elling, and Ulrich Schwaneberg. 2018. "KnowVolution Campaign of an Aryl Sulfotransferase Increases Activity toward Cellobiose." *Chemistry – A European Journal* 24 (64): 17117–24. <https://doi.org/10.1002/chem.201803729>.
- Isticato, Rachele, Giuseppina Cangiano, Hao T. Tran, Annalisa Ciabattini, Donata Medagliani, Marco R. Oggioni, Maurilio De Felice, Gianni Pozzi, and Ezio Ricca. 2001. "Surface Display of Recombinant Proteins on *Bacillus Subtilis* Spores." *Journal of Bacteriology* 183 (21): 6294–6301. <https://doi.org/10.1128/JB.183.21.6294-6301.2001>.
- Jackson, D. A., R. H. Symons, and P. Berg. 1972. "Biochemical Method for Inserting New Genetic Information into DNA of Simian Virus 40: Circular SV40 DNA Molecules Containing Lambda Phage Genes and the Galactose Operon of *Escherichia Coli*." *Proceedings of the National Academy of Sciences of the United States of America* 69 (10): 2904–9. <https://doi.org/10.1073/pnas.69.10.2904>.
- Jiang, Lin, Eric A. Althoff, Fernando R. Clemente, Lindsey Doyle, Daniela Röthlisberger, Alexandre Zanghellini, Jasmine L. Gallaher, et al. 2008. "De Novo Computational Design of Retro-Aldol Enzymes." *Science* 319 (5868): 1387–91. <https://doi.org/10.1126/science.1152692>.
- Jumper, John, Richard Evans, Alexander Pritzel, Tim Green, Michael Figurnov, Olaf Ronneberger, Kathryn Tunyasuvunakool, et al. 2021. "Highly Accurate Protein Structure Prediction with AlphaFold." *Nature* 2021, July, 1–11. <https://doi.org/10.1038/s41586-021-03819-2>.
- Kovačević, Gordana, Raluca Ostafe, Ana Marija Balaž, Rainer Fischer, and Radivoje Prodanović. 2019. "Development of GFP-Based High-Throughput Screening System for Directed Evolution of Glucose Oxidase." *Journal of Bioscience and Bioengineering* 127 (1): 30–37. <https://doi.org/10.1016/j.jbiosc.2018.07.002>.
- Krondorfer, Iris, Katharina Lipp, Dagmar Brugger, Petra Staudigl, Christoph Sygmund, Dietmar Haltrich, and Clemens K. Peterbauer. 2014. "Engineering of Pyranose Dehydrogenase for Increased Oxygen Reactivity." *PLoS ONE* 9 (3): 1–9. <https://doi.org/10.1371/journal.pone.0091145>.
- Kucherenko, I.S., Ya.V. Topolnikova, and O.O. Soldatkin. 2018. "Advances in the Biosensors for Lactate and Pyruvate Detection for Medical Applications: A Review." *TrAC Trends in Analytical Chemistry*, November. <https://doi.org/10.1016/J.TRAC.2018.11.004>.
- Kuchner, Olga, and Frances H. Arnold. 1997. "Directed Evolution of Enzyme Catalysts." *Trends in Biotechnology* 15 (12): 523–30. [https://doi.org/10.1016/S0167-7799\(97\)01138-4](https://doi.org/10.1016/S0167-7799(97)01138-4).
- Lai, Yu Ping, Jing Huang, Lin Fa Wang, Jun Li, and Zi Rong Wu. 2004. "A New Approach to Random Mutagenesis in Vitro." *Biotechnology and Bioengineering* 86 (6): 622–27. <https://doi.org/10.1002/bit.20066>.
- Langley, K. E., M. R. Villarejo, A. V. Fowler, P. J. Zamenhof, and I. Zabin. 1975. "Molecular Basis of β Galactosidase α Complementation." *Proceedings of the National Academy of Sciences of the United States of America* 72 (4): 1254–57. <https://doi.org/10.1073/pnas.72.4.1254>.
- Leemhuis, Hans, Ronan M. Kelly, and Lubbert Dijkhuizen. 2009. "Directed Evolution of Enzymes: Library Screening Strategies." *IUBMB Life* 61 (3): 222–28. <https://doi.org/10.1002/iub.165>.

- Lehmann, M., L. Pasamontes, S. F. Lassen, and M. Wyss. 2000. "The Consensus Concept for Thermostability Engineering of Proteins." *Biochimica et Biophysica Acta - Protein Structure and Molecular Enzymology*. Biochim Biophys Acta. [https://doi.org/10.1016/S0167-4838\(00\)00238-7](https://doi.org/10.1016/S0167-4838(00)00238-7).
- Leung, David W., Ellson Chen, and David V. Goeddel. 1989. "A Method for Random Mutagenesis of a Defined DNA Segment Using a Modified Polymerase Chain Reaction." *Technique* 1: 11–15. <https://www.scienceopen.com/document?vid=29520c8d-cd63-4f44-9e42-4ff0df4097d5>.
- Li, Guangyue, Yijie Dong, and Manfred T. Reetz. 2019. "Can Machine Learning Revolutionize Directed Evolution of Selective Enzymes?" *Advanced Synthesis and Catalysis*. John Wiley & Sons, Ltd. <https://doi.org/10.1002/adsc.201900149>.
- Lim, Joseph B., and Hadley D. Sikes. 2015. "Use of a Genetically Encoded Hydrogen Peroxide Sensor for Whole Cell Screening of Enzyme Activity." *Protein Engineering, Design and Selection* 28 (3): 79–83. <https://doi.org/10.1093/protein/gzv003>.
- Lipovšek, Daša, Eugene Antipov, Kathryn A. Armstrong, Mark J. Olsen, Alexander M. Klibanov, Bruce Tidor, and K. Dane Wittrup. 2007. "Selection of Horseradish Peroxidase Variants with Enhanced Enantioselectivity by Yeast Surface Display." *Chemistry and Biology* 14 (10): 1176–85. <https://doi.org/10.1016/j.chembiol.2007.09.008>.
- Liszewski, Kathy. 2015. "Speeding up the Protein Assembly Line." *Genetic Engineering and Biotechnology News* 35 (4). <https://doi.org/10.1089/gen.35.04.02>.
- Longwell, Chelsea K., Louai Labanieh, and Jennifer R. Cochran. 2017. "High-Throughput Screening Technologies for Enzyme Engineering." *Current Opinion in Biotechnology*. Elsevier Ltd. <https://doi.org/10.1016/j.copbio.2017.05.012>.
- Lorimer, Don, Amy Raymond, John Walchli, Mark Mixon, Adrienne Barrow, Ellen Wallace, Rena Grice, Alex Burgin, and Lance Stewart. 2009. "Gene Composer: Database Software for Protein Construct Design, Codon Engineering, and Gene Synthesis." *BMC Biotechnology* 9 (April): 36. <https://doi.org/10.1186/1472-6750-9-36>.
- Lülsdorf, Nina, Christian Pitzler, Michael Biggel, Ronny Martinez, Ljubica Vojcic, and Ulrich Schwaneberg. 2015. "A Flow Cytometer-Based Whole Cell Screening Toolbox for Directed Hydrolase Evolution through Fluorescent Hydrogels." *Chemical Communications* 51 (41): 8679–82. <https://doi.org/10.1039/c5cc01791b>.
- Markel, Ulrich, Khalil D. Essani, Volkan Besirlioglu, Johannes Schiffels, Wolfgang R. Streit, and Ulrich Schwaneberg. 2020. "Advances in Ultrahigh-Throughput Screening for Directed Enzyme Evolution." *Chemical Society Reviews*. <https://doi.org/10.1039/c8cs00981c>.
- Maté, Diana, Carlos García-Burgos, Eva García-Ruiz, Antonio O. Ballesteros, Susana Camarero, and Miguel Alcalde. 2010. "Laboratory Evolution of High-Redox Potential Laccases." *Chemistry and Biology* 17 (9): 1030–41. <https://doi.org/10.1016/j.chembiol.2010.07.010>.
- Mate, Diana M., David Gonzalez-Perez, Magnus Falk, Roman Kittl, Marcos Pita, Antonio L. De Lacey, Roland Ludwig, Sergey Shleev, and Miguel Alcalde. 2013. "Blood Tolerant Laccase by Directed Evolution." *Chemistry and Biology* 20 (2): 223–31. <https://doi.org/10.1016/j.chembiol.2013.01.001>.
- Mateljak, Ivan, Emanuele Monza, Maria Fatima Lucas, Victor Guallar, Olga Aleksejeva, Roland Ludwig, Donal Leech, Sergey Shleev, and Miguel Alcalde. 2019. "Increasing Redox Potential, Redox Mediator Activity, and Stability in a Fungal Laccase by Computer-Guided Mutagenesis and Directed Evolution." *ACS Catalysis* 9 (5): 4561–72. <https://doi.org/10.1021/acscatal.9b00531>.

- Mazurenko, Stanislav, Zbynek Prokop, and Jiri Damborsky. 2019. "Machine Learning in Enzyme Engineering." *ACS Catalysis* 10 (2): 1210–23. <https://doi.org/10.1021/ACSCATAL.9B04321>.
- Mei, Meng, Yu Zhou, Wenfang Peng, Chan Yu, Lixin Ma, Guimin Zhang, and Li Yi. 2017. "Application of Modified Yeast Surface Display Technologies for Non-Antibody Protein Engineering." *Microbiological Research*. Elsevier GmbH. <https://doi.org/10.1016/j.micres.2016.12.002>.
- Mertz, J. E., and R. W. Davis. 1972. "Cleavage of DNA by R 1 Restriction Endonuclease Generates Cohesive Ends." *Proceedings of the National Academy of Sciences of the United States of America* 69 (11): 3370–74. <https://doi.org/10.1073/pnas.69.11.3370>.
- Mills, D. R., R. L. Peterson, and S. Spiegelman. 1967. "An Extracellular Darwinian Experiment with a Self-Duplicating Nucleic Acid Molecule." *Proceedings of the National Academy of Sciences of the United States of America* 58 (1): 217–24. <https://doi.org/10.1073/pnas.58.1.217>.
- Müller, Kristian M., Sabine C. Stebel, Susanne Knall, Gregor Zipf, Hubert S. Bernauer, and Katja M. Arndt. 2005. "Nucleotide Exchange and Excision Technology (NExT) DNA Shuffling: A Robust Method for DNA Fragmentation and Directed Evolution." *Nucleic Acids Research* 33 (13): 1–9. <https://doi.org/10.1093/nar/gni116>.
- Myers, Richard M., Leonard S. Lerman, and Tom Maniatis. 1985. "A General Method for Saturation Mutagenesis of Cloned DNA Fragments." *Science* 229 (4710): 242–47. <https://doi.org/10.1126/science.2990046>.
- Nour-Eldin, Hussam H., Fernando Geu-Flores, and Barbara A. Halkier. 2010. "USER Cloning and USER Fusion: The Ideal Cloning Techniques for Small and Big Laboratories." *Methods in Molecular Biology* 643: 185–200. https://doi.org/10.1007/978-1-60761-723-5_13.
- Novoa, Catalina, Gaurao V. Dhoke, Diana M. Mate, Ronny Martínez, Thomas Haarmann, Martina Schreiter, Jasmin Eidner, et al. 2019. "KnowVolution of a Fungal Laccase toward Alkaline PH." *ChemBioChem* 20 (11): 1458–66. <https://doi.org/10.1002/cbic.201800807>.
- Ostafe, Raluca, Radivoje Prodanovic, Jovana Nazor, and Rainer Fischer. 2014. "Ultra-High-Throughput Screening Method for the Directed Evolution of Glucose Oxidase." *Chemistry and Biology* 21 (3): 414–21. <https://doi.org/10.1016/j.chembiol.2014.01.010>.
- Ostermeier, Marc, Jae Hoon Shim, and Stephen J. Benkovic. 1999. "A Combinatorial Approach to Hybrid Enzymes Independent of DNA Homology." *Nature Biotechnology* 17 (12): 1205–9. <https://doi.org/10.1038/70754>.
- Oxford Protein Informatics Group. 2021. "CASP14: What Google DeepMind's AlphaFold 2 Really Achieved, and What It Means for Protein Folding, Biology and Bioinformatics." 2021. <https://www.bloig.com/blog/2020/12/casp14-what-google-deepminds-alphafold-2-really-achieved-and-what-it-means-for-protein-folding-biology-and-bioinformatics/>.
- Packer, Michael S., and David R. Liu. 2015. "Methods for the Directed Evolution of Proteins." *Nature Reviews Genetics* 16 (7): 379–94. <https://doi.org/10.1038/nrg3927>.
- Pitzler, Christian, Georgette Wirtz, Ljubica Vojcic, Stephanie Hiltl, Alexander Böker, Ronny Martinez, and Ulrich Schwaneberg. 2014. "A Fluorescent Hydrogel-Based Flow Cytometry High-Throughput Screening Platform for Hydrolytic Enzymes." *Chemistry and Biology* 21 (12): 1733–42. <https://doi.org/10.1016/j.chembiol.2014.10.018>.
- Porter, Joanne L., Rukhairul A. Rusli, and David L. Ollis. 2016. "Directed Evolution of Enzymes for Industrial

- Biocatalysis." *ChemBioChem* 17 (3): 197–203. <https://doi.org/10.1002/cbic.201500280>.
- Prodanovic, Radivoje, Raluca Ostafe, Andreea Scacioc, and Ulrich Schwaneberg. 2012. "Ultrahigh Throughput Screening System for Directed Glucose Oxidase Evolution in Yeast Cells." *Combinatorial Chemistry & High Throughput Screening* 14 (1): 55–60. <https://doi.org/10.2174/1386207311107010055>.
- Ravikumar, Arjun, Adrian Arrieta, and Chang C. Liu. 2014. "An Orthogonal DNA Replication System in Yeast." *Nature Chemical Biology* 10 (3): 175–77. <https://doi.org/10.1038/nchembio.1439>.
- Renata, Hans, Z. Jane Wang, and Frances H. Arnold. 2015. "Expanding the Enzyme Universe: Accessing Non-Natural Reactions by Mechanism-Guided Directed Evolution." *Angewandte Chemie International Edition* 54 (11): 3351–67. <https://doi.org/10.1002/anie.201409470>.
- Robinson, Serina L, Megan D Smith, Jack E Richman, Kelly G Aukema, and Lawrence P Wackett. 2020. "Machine Learning-Based Prediction of Activity and Substrate Specificity for OleA Enzymes in the Thiolase Superfamily." *Synthetic Biology* 5 (1). <https://doi.org/10.1093/SYNBIO/YSAA004>.
- Rotsaert, Frederik A.J., V. Renganathan, and Michael H. Gold. 2003. "Role of the Flavin Domain Residues, His689 and Asn732, in the Catalytic Mechanism of Cellobiose Dehydrogenase from *Phanerochaete Chrysosporium*." *Biochemistry* 42 (14): 4049–56. <https://doi.org/10.1021/bi027092k>.
- Salaheddin, Clara, Oliver Spadiut, Roland Ludwig, Tien Chye Tan, Christina Divne, Dietmar Haltrich, and Clemens Peterbauer. 2009. "Probing Active-Site Residues of Pyranose 2-Oxidase from *Trametes Multicolor* by Semi-Rational Protein Design." *Biotechnology Journal* 4 (4): 535–43. <https://doi.org/10.1002/biot.200800265>.
- Scheiblbrandner, Stefan, Erik Breslmayr, Florian Csarman, Regina Paukner, Johannes Führer, Peter L. Herzog, Sergey V. Shleev, et al. 2017. "Evolving Stability and PH-Dependent Activity of the High Redox Potential *Botrytis Aclada* Laccase for Enzymatic Fuel Cells." *Scientific Reports* 7 (1): 13688. <https://doi.org/10.1038/s41598-017-13734-0>.
- Schmidt-Dannert, Claudia, and Frances H. Arnold. 1999. "Directed Evolution of Industrial Enzymes." In *Trends in Biotechnology*, 17:135–36. [https://doi.org/10.1016/S0167-7799\(98\)01283-9](https://doi.org/10.1016/S0167-7799(98)01283-9).
- Siedhoff, Niklas E., Ulrich Schwaneberg, and Mehdi D. Davari. 2020. "Machine Learning-Assisted Enzyme Engineering." *Methods in Enzymology* 643 (January): 281–315. <https://doi.org/10.1016/BS.MIE.2020.05.005>.
- Siegel, Justin B., Alexandre Zanghellini, Helena M. Lovick, Gert Kiss, Abigail R. Lambert, Jennifer L. St.Clair, Jasmine L. Gallaher, et al. 2010. "Computational Design of an Enzyme Catalyst for a Stereoselective Bimolecular Diels-Alder Reaction." *Science* 329 (5989): 309–13. <https://doi.org/10.1126/science.1190239>.
- Smith, Adam. 2002. "How Small Should You Go?" *Nature* 418 (6896): 457. <https://doi.org/10.1038/418457a>.
- Smith, George P. 1985. "Filamentous Fusion Phage: Novel Expression Vectors That Display Cloned Antigens on the Virion Surface." *Science* 228 (4705): 1315–17. <https://doi.org/10.1126/science.4001944>.
- Spadiut, Oliver, Katrin Radakovits, Ines Pisanelli, Clara Salaheddin, Montarop Yamabhai, Tien-Chye Tan, Christina Divne, and Dietmar Haltrich. 2009. "A Thermostable Triple Mutant of Pyranose 2-Oxidase from *Trametes Multicolor* with Improved Properties for Biotechnological Applications." *Biotechnology Journal* 4 (4): 525–34. <https://doi.org/10.1002/biot.200800260>.

- Stemmer, Willem P.C. 1994. "Rapid Evolution of a Protein in Vitro by DNA Shuffling." *Nature* 370 (6488): 389–91. <https://doi.org/10.1038/370389a0>.
- Sun, Zhoutong, Qian Liu, Ge Qu, Yan Feng, and Manfred T. Reetz. 2019. "Utility of B-Factors in Protein Science: Interpreting Rigidity, Flexibility, and Internal Motion and Engineering Thermostability." *Chemical Reviews*. <https://doi.org/10.1021/acs.chemrev.8b00290>.
- Sützl, Leander, Christophe V.F.P. Laurent, Annabelle T. Abrera, Georg Schütz, Roland Ludwig, and Dietmar Haltrich. 2018. "Multiplicity of Enzymatic Functions in the CAZy AA3 Family." *Applied Microbiology and Biotechnology* 102 (6): 2477–92. <https://doi.org/10.1007/s00253-018-8784-0>.
- Sygmund, Christoph, Paul Santner, Iris Krondorfer, Clemens K Peterbauer, Miguel Alcalde, Gibson S Nyanhongo, Georg M Guebitz, and Roland Ludwig. 2013. "Semi-Rational Engineering of Cellobiose Dehydrogenase for Improved Hydrogen Peroxide Production." *Microbial Cell Factories* 12 (April): 38. <https://doi.org/10.1186/1475-2859-12-38>.
- Tang, Lixia, Hui Gao, Xuechen Zhu, Xiong Wang, Ming Zhou, and Rongxiang Jiang. 2012. "Construction of 'Small-Intelligent' Focused Mutagenesis Libraries Using Well-Designed Combinatorial Degenerate Primers." *BioTechniques* 52 (3): 149–58. <https://doi.org/10.2144/000113820>.
- Traxlmayr, Michael W., and Christian Obinger. 2012. "Directed Evolution of Proteins for Increased Stability and Expression Using Yeast Display." *Archives of Biochemistry and Biophysics* 526 (2): 174–80. <https://doi.org/10.1016/J.ABB.2012.04.022>.
- Truppo, Matthew D. 2017. "Biocatalysis in the Pharmaceutical Industry: The Need for Speed." *ACS Medicinal Chemistry Letters* 8 (5): 476–80. <https://doi.org/10.1021/acsmedchemlett.7b00114>.
- Tsai, Chi Lin, Kuppan Gokulan, Pablo Sobrado, James C. Sacchettini, and Paul F. Fitzpatrick. 2007. "Mechanistic and Structural Studies of H373Q Flavocytochrome B2: Effects of Mutating the Active Site Base." *Biochemistry* 46 (26): 7844–51. <https://doi.org/10.1021/bi7005543>.
- Ullmann, Agnes, François Jacob, and Jacques Monod. 1967. "Characterization by in Vitro Complementation of a Peptide Corresponding to an Operator-Proximal Segment of the β -Galactosidase Structural Gene of Escherichia Coli." *Journal of Molecular Biology* 24 (2): 339–43. [https://doi.org/10.1016/0022-2836\(67\)90341-5](https://doi.org/10.1016/0022-2836(67)90341-5).
- Utada, A. S., E. Lorenceau, D. R. Link, P. D. Kaplan, H. A. Stone, and D. A. Weitz. 2005. "Monodisperse Double Emulsions Generated from a Microcapillary Device." *Science* 308 (5721): 537–41. <https://doi.org/10.1126/science.1109164>.
- Valdivieso-Ugarte, Magdalena, Carmen Ronchel, Oscar Bañuelos, Javier Velasco, and José L. Adrio. 2006. "Expression of an Aspergillus Niger Glucose Oxidase in Saccharomyces Cerevisiae and Its Use to Optimize Fructo-Oligosaccharides Synthesis." *Biotechnology Progress* 22 (4): 1096–1101. <https://doi.org/10.1021/bp060076k>.
- Vanella, Rosario, Alfred Bazin, Duy Tien Ta, and Michael A. Nash. 2019. "Genetically Encoded Stimuli-Responsive Cytoprotective Hydrogel Capsules for Single Cells Provide Novel Genotype–Phenotype Linkage." *Chemistry of Materials* 31 (6): 1899–1907. <https://doi.org/10.1021/acs.chemmater.8b04348>.
- Vanella, Rosario, Duy Tien Ta, and Michael A. Nash. 2019. "Enzyme-Mediated Hydrogel Encapsulation of Single Cells for High-Throughput Screening and Directed Evolution of Oxidoreductases." *Biotechnology and Bioengineering* 116 (8): 1878–86. <https://doi.org/10.1002/bit.27002>.

- Vieira, Jeffrey, and Joachim Messing. 1982. "The PUC Plasmids, an M13mp7-Derived System for Insertion Mutagenesis and Sequencing with Synthetic Universal Primers." *Gene* 19 (3): 259–68. [https://doi.org/10.1016/0378-1119\(82\)90015-4](https://doi.org/10.1016/0378-1119(82)90015-4).
- Wei, Martin S., Ioannis V. Pavlidis, Clare Vickers, Matthias Hohne, and Uwe T. Bornscheuer. 2014. "Glycine Oxidase Based High-Throughput Solid-Phase Assay for Substrate Profiling and Directed Evolution of (R)- and (S)-Selective Amine Transaminases." *Analytical Chemistry* 86 (23): 11847–53. <https://doi.org/10.1021/ac503445y>.
- Weitzner, Brian D., Yakov Kipnis, A. Gerard Daniel, Donald Hilvert, and David Baker. 2019. "A Computational Method for Design of Connected Catalytic Networks in Proteins." *Protein Science* 28 (12): 2036–41. <https://doi.org/10.1002/pro.3757>.
- Wildey, Mary Jo, Anders Haunso, Matthew Tudor, Maria Webb, and Jonathan H. Connick. 2017. "High-Throughput Screening." In *Annual Reports in Medicinal Chemistry*, 50:149–95. Academic Press Inc. <https://doi.org/10.1016/bs.armc.2017.08.004>.
- Willies, Simon C., Jemma L. White, and Nicholas J. Turner. 2012. "Development of a High-Throughput Screening Method for Racemase Activity and Its Application to the Identification of Alanine Racemase Variants with Activity towards L-Arginine." In *Tetrahedron*, 68:7564–67. Elsevier BV. <https://doi.org/10.1016/j.tet.2012.06.062>.
- Yang, Guangyu, and Stephen G. Withers. 2009. "Ultrahigh-Throughput FACS-Based Screening for Directed Enzyme Evolution." *ChemBioChem*. Chembiochem. <https://doi.org/10.1002/cbic.200900384>.
- You, L., and F. H. Arnold. 1996. "Directed Evolution of Subtilisin E in *Bacillus Subtilis* to Enhance Total Activity in Aqueous Dimethylformamide." *Protein Engineering* 9 (1): 77–83. <https://doi.org/10.1093/protein/9.1.77>.
- Zhang, Lingling, Haiyang Cui, Gaurao V. Dhoke, Zhi Zou, Daniel F. Sauer, Mehdi D. Davari, and Ulrich Schwaneberg. 2020. "Engineering of Laccase CueO for Improved Electron Transfer in Bioelectrocatalysis by Semi-Rational Design." *Chemistry - A European Journal*. Wiley-VCH Verlag. <https://doi.org/10.1002/chem.202001027>.
- Zhang, Ruijie K., Kai Chen, Xiongyi Huang, Lena Wohlschlager, Hans Renata, and Frances H. Arnold. 2019. "Enzymatic Assembly of Carbon–Carbon Bonds via Iron-Catalysed Sp³ C–H Functionalization." *Nature* 565 (7737): 67–72. <https://doi.org/10.1038/s41586-018-0808-5>.
- Zhao, Huimin, Lori Giver, Zhixin Shao, Joseph A. Affholter, and Frances H. Arnold. 1998. "Molecular Evolution by Staggered Extension Process (StEP) in Vitro Recombination." *Nature Biotechnology* 16 (3): 258–61. <https://doi.org/10.1038/nbt0398-258>.
- Zhu, Ziwei, Mian Wang, Amit Gautam, Jovana Nazor, Carmen Momeu, Radivoje Prodanovic, and Ulrich Schwaneberg. 2007. "Directed Evolution of Glucose Oxidase from *Aspergillus Niger* for Ferrocenemethanol-Mediated Electron Transfer." *Biotechnology Journal* 2 (2): 241–48. <https://doi.org/10.1002/biot.200600185>.
- Zumarraga, Miren, Cristina Dominguez, Susana Camarero, Sergey Shleev, Julio Polaina, Arturo Martinez-Arias, Manuel Ferrer, et al. 2008. "Combinatorial Saturation Mutagenesis of the *Myceliophthora Thermophila* Laccase T2 Mutant: The Connection between the C-Terminal Plug and the Conserved VSG Tripeptide." *Combinatorial Chemistry & High Throughput Screening* 11 (10): 807–16. <https://doi.org/10.2174/138620708786734235>.

Chapter 4 – Developing new Enzymes

Developing a cell-bound detection system for the screening of oxidase activity using the fluorescent peroxide sensor roGFP2-Orp1

P L Herzog, E Borghi, M W Traxlmayr, C Obinger, H D Sikes, C K Peterbauer

Protein Engineering, Design and Selection, Volume 33, 2020, gzaa019,

<https://doi.org/10.1093/protein/gzaa019>

Published: 14 September 2020 Article history

Abstract

*Accurate yet efficient high-throughput screenings have emerged as essential technology for enzyme engineering via directed evolution. Modern high-throughput screening platforms for oxidoreductases are commonly assisted by technologies such as surface display and rely on emulsification techniques to facilitate single-cell analysis via fluorescence-activated cell sorting. Empowered by the dramatically increased throughput, the screening of significantly larger sequence spaces in acceptable time frames is achieved but usually comes at the cost of restricted applicability. In this work, we tackle this problem by utilizing roGFP2-Orp1 as a fluorescent one-component detection system for enzymatic H₂O₂ formation. We determined the kinetic parameters of the roGFP2-Orp1 reaction with H₂O₂ and established an efficient immobilization technique for the sensor on *Saccharomyces cerevisiae* cells employing the lectin Concanavalin A. This allowed to realize a peroxide-sensing shell on enzyme-displaying cells, a system that was successfully employed to screen for H₂O₂ formation of enzyme variants in a whole-cell setting.*

Original Article

Developing a cell-bound detection system for the screening of oxidase activity using the fluorescent peroxide sensor roGFP2-Orp1

P.L. Herzog¹, E. Borghi², M.W. Traxlmayr³, C. Obinger³, H.D. Sikes⁴, and C.K. Peterbauer^{1,*}

¹Food Biotechnology Laboratory, Department of Food Science and Technology, BOKU – University of Natural Resources and Life Sciences, Muthgasse 11, 1190 Vienna, Austria, ²Department of Life Sciences, University of Modena and Reggio Emilia, Via Giuseppe Campi 287, 41124 Modena, Italy, ³Institute of Biochemistry, Department of Chemistry, BOKU – University of Natural Resources and Life Sciences, Muthgasse 18, 1190 Vienna, Austria, and ⁴Department of Chemical Engineering, MIT – Massachusetts Institute of Technology, 77 Massachusetts Avenue, Cambridge 02139, MA, USA

*To whom correspondence should be addressed. E-mail: clemens.peterbauer@boku.ac.at

Received 19 February 2020; Revised 2 June 2020; Accepted 8 July 2020

Abstract

Accurate yet efficient high-throughput screenings have emerged as essential technology for enzyme engineering via directed evolution. Modern high-throughput screening platforms for oxidoreductases are commonly assisted by technologies such as surface display and rely on emulsification techniques to facilitate single-cell analysis via fluorescence-activated cell sorting. Empowered by the dramatically increased throughput, the screening of significantly larger sequence spaces in acceptable time frames is achieved but usually comes at the cost of restricted applicability. In this work, we tackle this problem by utilizing roGFP2-Orp1 as a fluorescent one-component detection system for enzymatic H₂O₂ formation. We determined the kinetic parameters of the roGFP2-Orp1 reaction with H₂O₂ and established an efficient immobilization technique for the sensor on *Saccharomyces cerevisiae* cells employing the lectin Concanavalin A. This allowed to realize a peroxide-sensing shell on enzyme-displaying cells, a system that was successfully employed to screen for H₂O₂ formation of enzyme variants in a whole-cell setting.

Key words: enzyme, flow cytometry, H₂O₂, screening, surface display

Introduction

During the past decades, many enzymes have emerged to complement conventional chemical processes in various industries. Their utilization as highly specific and tunable biocatalysts has accelerated the expansion of novel biocatalytic processes and technology. The demand for improved catalytic properties, increased stability under process conditions and for non-native reactions has led to the establishment of a wide array of enzyme engineering techniques, including directed evolution (Chen and Arnold, 1991; Kuchner and Arnold, 1997; Renata *et al.*, 2015). Directed evolution experiments generally require a balanced and sufficiently large library of variants accompanied by a screening method that reliably maintains the connection

of genotype and phenotype (Fischlechner *et al.*, 2014) and allows sufficient throughput (Porter *et al.*, 2016; Truppo, 2017). Display methods immobilizing proteins on the surface of phage particles (Smith and Petrenko, 1997) and yeast cells (Boder and Wittrup, 1997) have greatly boosted the development of screening technologies for the engineering and evolution of, e.g. antibodies, where the assay simply involves binding to a labeled antigen.

Catalytic screening assays for enzymes, oxidoreductases in particular, are a different proposition due to the diffusible nature of enzyme substrates, cofactors and products. This generally demands some form of compartmentalization, e.g. in microtiter plates, which in turn limits throughput due to the practical demands of handling large

numbers of plates: bench space, manipulation, reagent distribution, readout, time. Practically, the screening of 10^4 – 10^5 variants per month appears to be a limit, even when using automated handling stations, as described in literature (Dörr *et al.*, 2016). One approach to overcome this problem is through further miniaturization, by distributing enzyme variant producing cells and reaction components in emulsion droplets (water-in-oil, water-in-oil-in-water) or hydrogels to create microcompartments (Aharoni *et al.*, 2005; Ostafe *et al.*, 2014; Pitzler *et al.*, 2014; Blažič *et al.*, 2019; Vanella *et al.* 2019a; Markel *et al.*, 2020). These droplets establish a reaction chamber for—statistically—single enzyme variants and can be analyzed via fluorescence activated cell sorting (FACS). This allows the screening of dramatically larger libraries and provides access to a larger sequence space with reasonable effort in shorter times, with throughputs in the range of 10^5 library variants within days reported for different oxidoreductases (Ostafe *et al.*, 2014; Zhu *et al.*, 2015; Ilić Đurđić *et al.*, 2020). Several limitations remain: the water–oil interface maintains the reactants within the droplets and prevents influx into the system, therefore all assay components (substrate, secondary enzyme, fluorescent signal molecules) have to be supplied together with the enzyme-producing cells at emulsification. Appropriate distribution of cells into droplets needs to be optimized, and enzyme production and reaction start may vary across droplet populations. Increasing efforts are therefore directed toward systems that make artificial compartmentalization obsolete by physically linking a detectable readout of enzyme activity to the enzyme-producing cell harboring the respective variant gene. Most examples utilize a secondary enzyme like a peroxidase and some form of radical-mediated polymerization of a detectable (fluorescent) signal molecule to the cell (Lipovšek *et al.*, 2007; Ostafe *et al.*, 2014; Pitzler *et al.*, 2014; Blažič *et al.*, 2019; Ilić Đurđić *et al.*, 2020). With the exception of the hydrogel-polymerization-based approach by Vanella *et al.* (Vanella *et al.*, 2019b; Vanella *et al.* 2019a), none of these approaches, while successful in principle, could entirely obviate artificial compartmentalization. roGFP2-Orp1 is an artificial combination of a redox sensitive GFP variant (roGFP2) fused to the H_2O_2 sensing peroxidase Orp1—synonymously Gpx3 or Hyr1 (Ma *et al.*, 2007)—and has been established as a genetically encoded fluorescent peroxide sensor by T. Dick *et al.* in 2009 (Gutscher *et al.*, 2009). The mode of action of roGFP2-Orp1 is governed by a catalytic cysteine in Orp1. Upon contact with H_2O_2 , Orp1 mediates the formation of a disulfide bridge on the adjoining roGFP2 moiety which results in a modified fluorescence spectrum of the fluorescent protein. These changes are most prominent at around 400 nm and 490 nm excitation and hence a fluorescence intensity ratio of 400/490 nm excitation at 520 nm emission (or similar) is commonly used to indicate the redox change in roGFP2-based sensors. In 2017, a comprehensive analysis of the roGFP2-Orp1 reactivities with relevant oxidant species was carried out and concluded that the sensor does not exclusively respond to H_2O_2 (Müller *et al.*, 2017). Although roGFP2-Orp1 is robustly specific in a physiological (*in vivo*) setting, a pronounced unspecific reactivity in the presence of ambient oxygen concentrations was highlighted in this *in vitro* study.

In this work, we aimed to adapt roGFP2-Orp1 as a screening tool for H_2O_2 -producing oxidases and dehydrogenases fit for whole-cell high-throughput screenings. We defined the performance parameters of roGFP2-Orp1 as a fluorescent sensor to (relatively) quantify enzymatic H_2O_2 production. We were able to apply this concept to distinguish between varying H_2O_2 formation rates using roGFP2-Orp1 in combination with soluble pyranose 2-oxidase or surface-displayed cellobiose dehydrogenase (CDH) variants. We then explored the

coimmobilization of recombinantly produced roGFP2-Orp1 on the surface of yeast cells displaying a H_2O_2 -producing enzyme, thus providing an artificial shell for local H_2O_2 detection that can be employed for whole-cell screening of cells producing enzyme variants in a high-throughput setting without artificial compartmentalization.

Results

Production and purification of roGFP2-Orp1

Escherichia coli (*E. coli*) NEB Express 1^r cells, harboring the His-tagged roGFP2-Orp1 gene downstream of a T5 promoter, were cultivated in a shaking flask fermentation of 1.5 L. With this, 22 g of intensely green-colored *E. coli* cell pellet could be produced. After cell disruption and immobilized metal affinity chromatography (IMAC), the presence of the roGFP2-Orp1 protein was visible in various fractions by its characteristic fluorescence and a band at ~50 kDa in SDS PAGE (Fig. S1), conforming to the protein's 49.1 kDa theoretical size. An additional purification step with size exclusion chromatography (SEC) yielded 164 mg of apparently pure protein. The identity of the purified full-length roGFP2-Orp1 was confirmed by peptide mapping via mass spectrometry.

Determination of kinetic parameters for the reaction of soluble roGFP2-Orp1 with H_2O_2

In order to quantify the formation of oxidized roGFP2-Orp1 during the sensor's reaction with H_2O_2 by means of fluorescence, it was necessary to determine the absolute change in fluorescence signals between the reduced and oxidized state and relate it to a molar amount of roGFP2-Orp1. This we accomplished by assessing fluorescence signals between a reduced (dithiothreitol, DTT incubation) and an oxidized (H_2O_2 incubation) reference state at 400 versus 490 nm excitation and 520 nm emission, respectively. The calculations allowed to estimate differential molar fluorescence extinction coefficients (ϵ_{ox}) for the oxidation reaction and yielded $\epsilon_{ox,490} = -93\,209$ arbitrary units (a.u.) μM^{-1} at 490 nm and $\epsilon_{ox,400} = 25\,449$ a.u. μM^{-1} at 400 nm (Fig. S2). It should be noted that these fluorescence coefficients only apply for the given experimental setup and detection settings. This is due to the fact that the detection of fluorescence signals, contrary to absorbance, depends on laser and detector gain settings and is not an absolute measurement. Aided by the estimated $\epsilon_{ox,490}$ at 490 nm excitation, which was preferred for calculations due to the comparably higher signal, reactions of purified roGFP2-Orp1 with H_2O_2 allowed to estimate apparent kinetic parameters: a K_m of 0.30 ± 0.04 μM , V_{max} of 0.09 ± 0.01 $\mu M \text{ min}^{-1}$ was determined and yields a k_{cat} of $0.11 \pm 0.01 \text{ min}^{-1}$ at 0.9 μM sensor concentration (Fig. S3). As these kinetic parameters reflect the reaction cascade of the whole entirety of roGFP2-Orp1 they are not representative for the potentially much faster reaction rates of the Orp1 moiety with H_2O_2 .

Reactions of roGFP2-Orp1 with soluble pyranose 2-oxidase

Purified roGFP2-Orp1 was utilized in combination with pyranose 2-oxidase (POx), a pronounced oxidase, to resolve varying peroxide production rates by the enzyme. In this experimental setup, POx and roGFP2-Orp1 were present at a stoichiometric ratio of 1:100 and the POx oxygen-to-peroxide turnover was fueled with varying concentrations of D-glucose, the preferred substrate for the enzyme. This resulted in substrate-dependent rates of H_2O_2 formation that were

traced via the roGFP2-Orp1 fluorescence until all sensor molecules were oxidized. The apparent slopes (Fig. 2A) display a saturation of reaction rates at a D-glucose concentration of $\sim 250 \mu\text{M}$. These results are in accordance with published kinetic data on POx which, dependent on the testing conditions, reports a D-glucose concentration at half maximal reaction rate (K_m) in the triple digit μM range as was previously reported (Leitner, Volc and Haltrich, 2001; Tasca *et al.*, 2007; Salaheddin *et al.*, 2009; Spadiut *et al.*, 2009; Brugger *et al.*, 2014a; Halada *et al.*, 2016).

A similar differentiation of hydrogen peroxide production rates was obtained when different sugar substrates, to which POx has varying substrate specificity, were used at constant concentrations. In these reactions, D-glucose and D-xylose are preferred over D-galactose and D-maltose as substrates and yield steeper signal increases. No reaction was observed for D-fructose, D-glucose-1-phosphate and D-mannose (Fig. S4), in agreement with data from literature (Leitner *et al.*, 2001).

To simulate the behavior of roGFP2-Orp1 in a screening of oxidase variants, we repeated the experimental setup employing a constant D-glucose concentration in combination with established POx variants, all exhibiting an altered kinetic profile for oxygen and thus varying in their hydrogen peroxide formation rate (Brugger *et al.*, 2014b). As is observable in Fig. 2B, variants with a reportedly diminished oxidase activity: L547R, Q448H, N593C and the combined variant T166R/N593C could be discriminated from the *wt* due to their decreased H_2O_2 formation rate. Variant T166R expectedly aligns with the *wt* whereas also L545C display a reaction curve similar to the *wt* despite its decreased turnover rate for oxygen. To back literature-derived data, we assessed the variants different H_2O_2 formation rates utilizing the Amplex Red/peroxidase assay under the same experimental conditions as in the roGFP2-Orp1 setup: relative activities are given in brackets in the graph.

The saturation effect observed for the *wt* and variants T166R, L545C could be due to a limitation in the resolving power of the roGFP2-Orp1 sensor, that—present at a molar excess of 100:1—operates above a certain threshold of H_2O_2 production it is not able to process. As can be seen in Figs 2 and 3, negative controls (blank) without substrate also show a distinct increase in the fluorescence ratio, most likely from unspecific oxidation of the roGFP2-Orp1 sensor in the presence of ambient oxygen, as was described previously (Müller *et al.*, 2017). As was examined, this degree of unspecific oxidation of the roGFP2-Orp1 sensor disproportionally increases with lower concentrations (Fig. S5).

Reactions of soluble roGFP2-Orp1 with displayed CDH

We efficiently displayed *Myriococcum thermophilum* (synonymously *Crassicarpon hotsonii*) CDH flavin domain *wt* (CDH-F) and the oxygen reactive variant N748G (Kracher *et al.*, 2019) (CDH-F+) on the surface of *Saccharomyces cerevisiae* (*S. cerevisiae*) cells using the established Aga2 yeast surface display system (Boder and Wittrup, 1997; Angelini *et al.*, 2015). Display levels and enzyme activity were well-correlated and highest specific activities were obtained between 24 and 38 hours induction at 20°C. For CDH-F+ apparent oxidase activities of 1.7–2.8 mU ODml⁻¹ were reached, where 1 mU ODml⁻¹ is defined as the formation of 1 nmol of H_2O_2 per minute per milliliter of cell suspension of an OD₆₀₀ 1.0. For CDH-F and the empty vector control (EVC), no peroxide formation above the background was detected. Both CDH variants are displayed at near identical levels (Fig. S6).

Freshly induced, washed cells were incubated with purified roGFP2-Orp1 and equilibrated for 100 seconds before cellobiose was added (Fig. 3). As was expected, a H_2O_2 -mediated increase in the roGFP2-Orp1 fluorescence ratio was only detected for the displayed oxygen reactive CDH-F+ variant; CDH-F did not show any substrate specific H_2O_2 production above the background (EVC), which was also confirmed using the Amplex Red/peroxidase assay (Fig. S7). After the reaction had proceeded for another 420 seconds, iodoacetamide (IAA)—a well-established alkylating reagent for cysteines—was added to arrest the remaining unreacted roGFP2-Orp1 in the reduced state. Presumably, IAA derivatizes the cysteine thiol form and hence can prevent the formation of the cysteine disulfide bond and the concomitant shift in the fluorescent signatures in the roGFP2 moiety. For the untreated samples, the reactions proceeded as projected. Again, an increase in the fluorescence ratio was observed for the control reactions. Strikingly, this background reaction was also stopped by IAA. IAA thus functions as a potent stop reagent for the assay reaction and could be used in the format of a whole-cell assay in a one-pot screening reaction to stop the parallel unspecific reactions prior to analysis via flow cytometry and cell sorting.

Biotinylation and immobilization of roGFP2-Orp1 via the “ConAct” system

A sequence encoding an N-terminal 15 amino acid AviTag was added to the roGFP2-Orp1 gene to facilitate *in vivo* biotinylation during expression in *E. coli*. Repeating the previously used production procedure for native roGFP2-Orp1, we could produce mg amounts of pure biotinylated roGFP2-Orp1. Analysis of the purified protein via mass spectrometry confirmed the presence of the full sequence and complete biotinylation, and assessment of purified biotin-roGFP2-Orp1 confirmed reaction kinetics comparable to the unbiotinylated protein (Fig. S8).

Concanavalin A (ConA) is a plant-derived lectin which specifically binds to high-mannose type glycosyl moieties, characterized by a single digit μM dissociation constant K_d (Coulbaly and Youan, 2014). Effective and specific immobilization of biotinylated roGFP2-Orp1 on the yeast cell wall was accomplished by binding biotinylated ConA on the yeast cell wall and combining it with streptavidin (which is a tetramer) to bridge the two biotinylated moieties (ConAct). As could be shown by flow cytometry (Fig. S9), only the mixture containing all components could facilitate efficient immobilization of biotin-roGFP2-Orp1. The ConAct system was preferred over click chemistry-based technology to capture proteins on the cell surface (Rhiel *et al.*, 2014) due to the exceptionally high binding capacity, reliability and ease of handling.

Trials of a whole-cell assay combining surface display of CDH with immobilized roGFP2-Orp1

ConA-biotin, streptavidin and reduced biotin-roGFP2-Orp1 were added sequentially to induced and washed cells displaying CDH-F or CDH-F+ to generate a space-proximity detection system (Fig. 1). Soluble roGFP2-Orp1 was added in excess to the reaction mix to buffer unspecific oxidation at the cell surface. We then assessed whether this system is capable of differentiating the peroxide production of displayed CDH-F+ in comparison to CDH-F (negative) when the assay reactions were started with the native CDH substrate cellobiose (Fig. 4). With proceeding reaction time, differences in the ratio of fluorescence intensities were detectable as CDH-F+ fluorescence

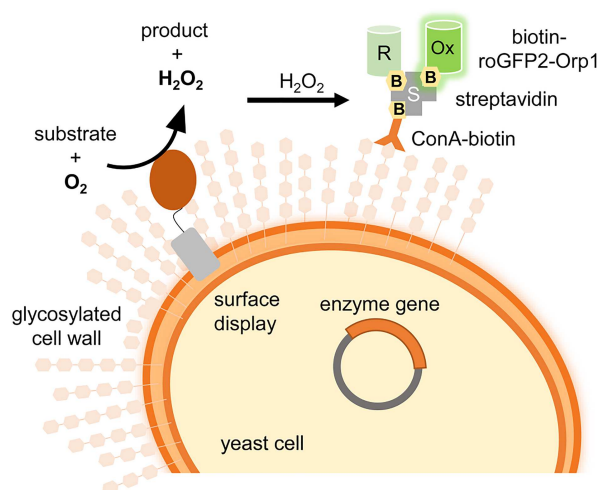


Fig. 1 Whole cell screening assay for peroxide formation with immobilized roGFP2-Orp1. Scheme depicting the designed whole cell screening assay where the displayed enzyme oxidizes its substrate and concomitantly reduces oxygen to H_2O_2 . The formed H_2O_2 causes oxidation of neighboring biotin-roGFP2-Orp1 from the reduced (R) to the oxidized (Ox) state and is connected to a change in the fluorescence. roGFP2-Orp1 is in close proximity since it is also immobilized on the surface of the cell via the ConA-biotin, streptavidin ConAct system.

signals at 405 nm excitation increased while the prospected negative reaction of CDH-F maintained a reduced state with predominant 488 nm excitation. For CDH-F, gated events reached a level of not <4.54% of the overall population (20 min) whereas for CDH-F+ the gated event count increased from 6.90% (1 min) to 41.08% (20 min), 9-fold of the respective CDH-F sample at stopping time and clear sign for specific roGFP2-Orp1 oxidation. To confirm specific enzymatic activities after the immobilization procedure we evaluated the prepared cultures with the established Amplex Red/Peroxidase assay and detected minor impact of washing and staining steps on the activity (65% remaining activity) of the displayed CDH variants and no unspecific H_2O_2 production. The immobilized biotin-roGFP2-Orp1 virtual concentration used is $\sim 0.08 \mu\text{M}$ and thus around 8% of the previously used soluble roGFP2-Orp1 concentration in the assays.

Discussion

With this report, we provide a mechanistic analysis of roGFP2-Orp1 as a fluorescent H_2O_2 resolving reporter and propose potential applications for screening of hydrogen peroxide producing enzymes. The characterization of its fundamental kinetic parameters and reactivities are valuable in all fields of application, for the improved understanding of this and other fluorescent probes and for the development of novel screening technologies.

roGFP2-Orp1 is a sensitive H_2O_2 reporter with a relatively low reaction rate

With the assessment of fluorescent intensities of roGFP2-Orp1 at the fully reduced and oxidized endpoint we were able to correlate the change in fluorescence signals to the roGFP2-Orp1 concentration and use it for the estimation of kinetic parameters K_m and V_{\max} (Fig. S3). With the given experimental setup, we could estimate a K_m of $0.3 \mu\text{M}$, suggesting a pronounced specificity for the interaction

of roGFP2-Orp1 with H_2O_2 . The estimation of V_{\max} allowed to calculate a catalytic rate constant k_{cat} of 0.11 min^{-1} , a comparably slow turnover of hydrogen peroxide when compared to the reactions of thiol peroxidases homologous to Orp1 (Parsonage *et al.*, 2005; Tanaka, Izawa and Inoue, 2005). Most likely, the rate limiting step in its fluorescent response to H_2O_2 is the non-native interdomain thiol-disulfide exchange from the Orp1 to the roGFP2 moiety, a mechanism that is likely defined by the probability for close contact of this non-native couple of domains.

The roGFP2-Orp1 resolving power depends on its stoichiometric excess

When combining the roGFP2-Orp1 peroxide sensor with H_2O_2 producing enzymes, one needs to acknowledge the sensor's relatively low turnover number of around 0.1 min^{-1} . This is of importance when hydrogen peroxide is produced at substantially higher rates as was observed in our experiments when H_2O_2 formation by POx was detected with roGFP2-Orp1 at a molar excess of a 100-fold (Fig. 2A and B). POx *wt* and variants T166R, L545C are pronounced oxidases with reported catalytic constants k_{cat} for H_2O_2 formation of 42 s^{-1} , 11 s^{-1} and 2.7 s^{-1} , respectively (Brugger *et al.*, 2014a). At the given conditions, the roGFP2-Orp1 sensor could not resolve these large differences in hydrogen peroxide formation since its turnover rates could not keep pace with elevated production. However, the fluorescent probe was successfully used to identify H_2O_2 formation from variant N593C (Brugger *et al.*, 2016), a rather strict dehydrogenase with substantially reduced oxygen reactivity (0.18 s^{-1}), which underlines the exceptional sensitivity of roGFP2-Orp1.

roGFP2-Orp1 is susceptible to unspecific oxidation reactions

The reactivity of roGFP2-Orp1 with molecular oxygen and various radical species has been extensively analyzed by Müller *et al.*, who concluded the Orp1 moiety to be more susceptible to unspecific thiol oxidation under aerobic conditions. Whether this is a direct effect of molecular oxygen or a radical-mediated oxidation, potentially from Fenton-like chemistry by transition metals in the buffer, was not resolved in their work (Müller *et al.*, 2017). Our experiments with roGFP2-Orp1 *in vitro* confirmed that specific reactions of the probe with H_2O_2 can only be achieved in the presence of ion-complexing EDTA (Fig. S10). In our experiments at ambient oxygen concentrations (Figs 2, 3, S4, S5), a certain degree of unspecific oxidation is detected in negative controls and blank measurements even though freshly degassed buffers were used. Especially the data summarized in Fig. S5 points toward a more unfavorable ratio of ambient oxygen to roGFP2-Orp1 with lower sensor concentrations.

Utilization of roGFP2-Orp1 in whole-cell assays

The first report on the employment of a fluorescent H_2O_2 probe for the screening of enzyme activity describes an intracellular system. The synthetic fluorescent H_2O_2 sensor HyPer was used for the detection of H_2O_2 formed by the uncoupling reaction of cytochrome P450 (Lim and Sikes, 2015) in the *E. coli* cytosol. In our setup, the enzyme (CDH variants) is displayed on the cell surface since this simplifies the addition of substrates and allows quantification of expression levels and normalization of activities via staining of a suitable tag with fluorescently labeled antitag antibodies if desired. Immobilization of roGFP2-Orp1—mediated by the ConAct system—in close spatial

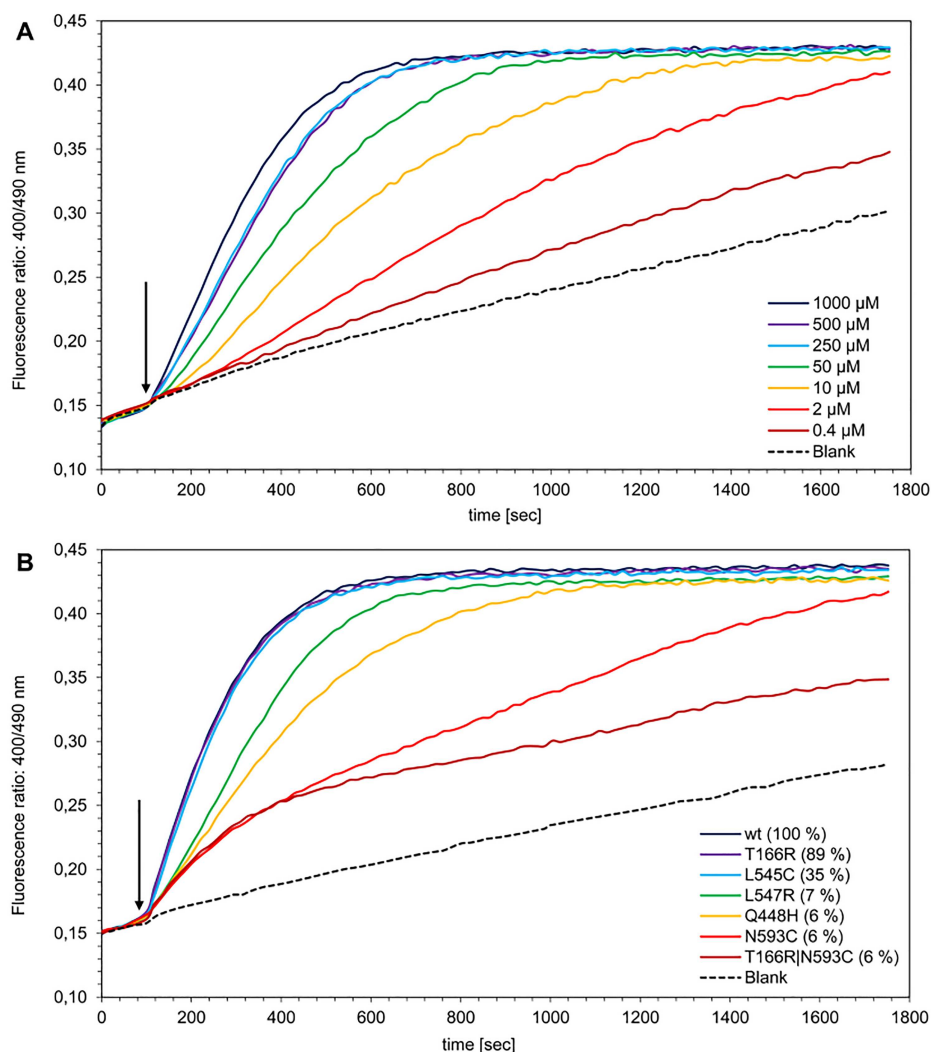


Fig. 2 Detection of pyranose 2-oxidase (soluble) dependent H_2O_2 formation with roGFP2-Orp1 (soluble). About $1.0 \mu\text{M}$ roGFP2-Orp1 was mixed with $0.01 \mu\text{M}$ recombinant POx from *T. ochracea* and let equilibrate for 100 seconds before substrate was added to start H_2O_2 formation (arrow). (A) POx wt was fueled with d-glucose at concentrations of $0.4 \mu\text{M}$, $2 \mu\text{M}$, $10 \mu\text{M}$, $50 \mu\text{M}$, $250 \mu\text{M}$, $500 \mu\text{M}$, $1000 \mu\text{M}$ and buffer only (dotted). (B) POx variants: wt, T166R, L545C, L547R, Q448H, N593C and the combinational variant T166R/N593C were fueled with d-glucose at a concentration of $500 \mu\text{M}$. Numbers in brackets reflect relative activities that were determined with the established Amplex Red/peroxidase assay under identical experimental conditions. Fluorescent intensities were tracked for 1800 seconds.

proximity to the place of H_2O_2 formation (the oxidase) (Fig. 1) minimizes crosstalk between neighboring cells in a reaction mix without compartmentalization in emulsions (Aharoni *et al.*, 2005; Ostafe *et al.*, 2014). The reactions can be stopped with IAA (Fig. 3) before cells are analyzed for their 400/490 nm fluorescence ratio and separated using FACS.

We used this system to successfully differentiate between CDH variants with differing oxidase activities. As enzymatic reactions progressed, cell populations shifted in their 405 versus 488 nm fluorescence excitation ratio due to H_2O_2 -mediated roGFP2-Orp1 oxidation and could be gated against the negative control (Fig. 4). It is still observable though, that populations are not strictly homogeneous and especially scattered for CDH-F+ in early reactions which could stem from a small portion of false-positives or an unsynchronized reaction start.

In our trials, differentiation of variants could only be accomplished when soluble roGFP2-Orp1 was added in excess to the assay reactions to buffer unspecific oxidation of the immobilized biotin-roGFP2-Orp1 by ambient oxygen. As was pointed out, higher roGFP2-Orp1 concentrations were less susceptible to unspecific oxidation (Fig. S5). Consequently, reactions could only be resolved via flow cytometry after cells and immobilized sensor were separated from the reaction mix via centrifugation. In the absence of excess roGFP2-Orp1, positive and negative reactions were indistinguishable since the unspecific oxidation left little margin for the contribution of peroxide-mediated oxidation (Fig. S11).

Although the screening assay employing roGFP2-Orp1 could benefit from an air-free environment to minimize disturbances—reactions could be performed in a ‘glove box’—the formation of H_2O_2 by the screened enzyme is dependent on (low concentrations

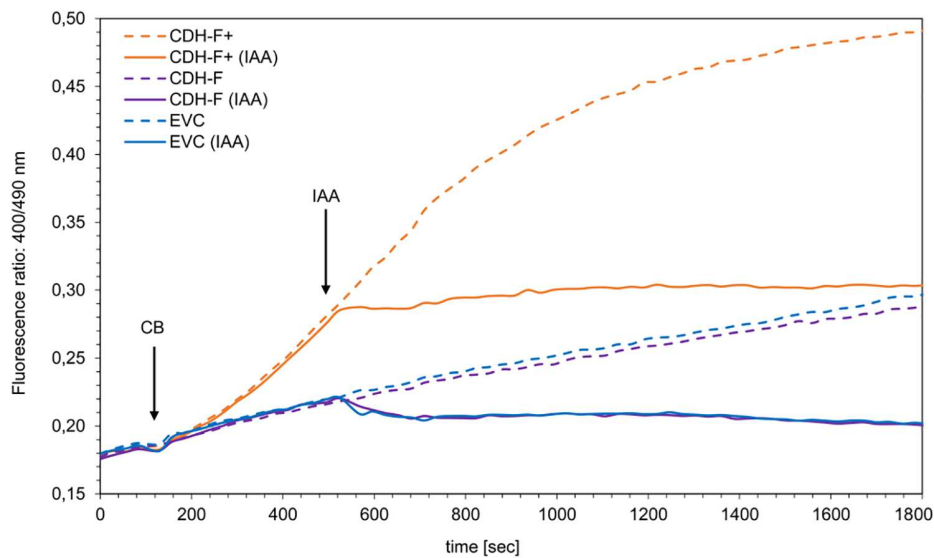


Fig. 3 Detection of cellobiose dehydrogenase-dependent (yeast-displayed) H_2O_2 formation with soluble roGFP2-Orp1 in a whole cell format. About $1.0 \mu M$ roGFP2-Orp1 was mixed with CDH-displaying *S. cerevisiae* cells present at an optical density OD600 of 1.0 and let equilibrate for 100 seconds before cellobiose was added to start the reaction (CB, arrow). Fluorescence ratios were tracked for the oxygen-reactive CDH-F+ variant (orange), the CDH-F wild type (violet) and an empty vector control (EVC) (blue). Four hundred and twenty seconds into the reaction, 50 mM IAA was added (IAA, arrow) to the samples (full lines). Negative controls (dashed lines) was added CB but buffer instead of IAA.

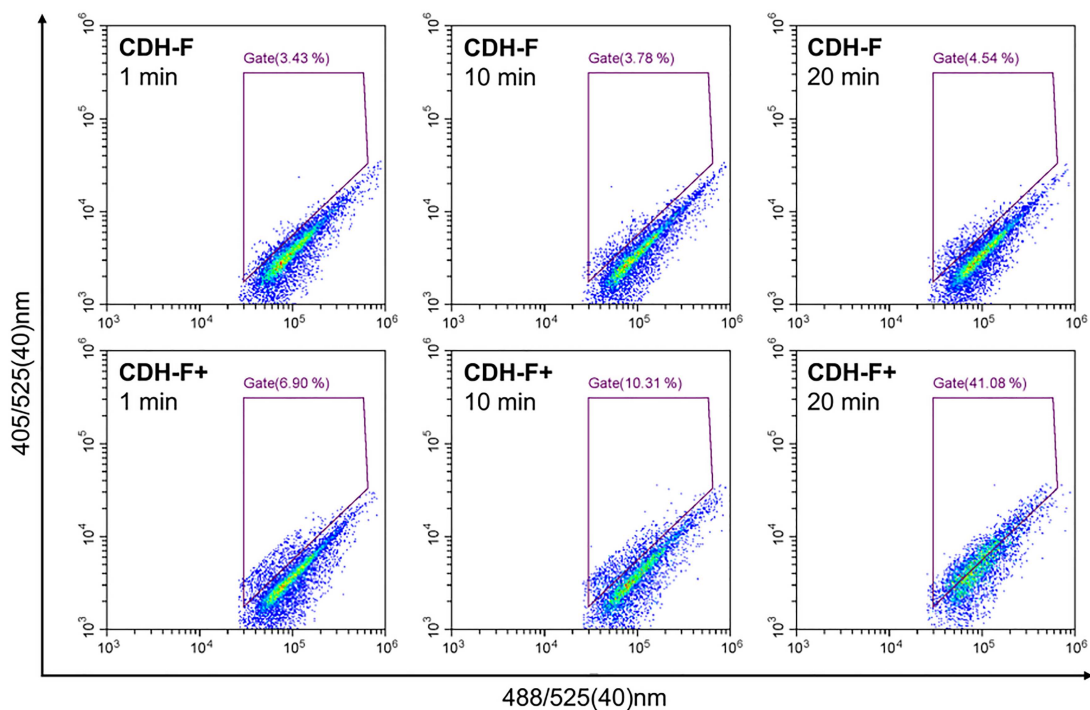


Fig. 4 Whole cell assay for the detection of displayed CDH-F+ activity with immobilized roGFP2-Orp1. *S. cerevisiae* cells displaying CDH-F or CDH-F+, respectively, were stained with ConA-biotin, streptavidin and biotin-roGFP2-Orp1 to immobilize the biotinylated sensor protein on the surface of the yeast cells. With the addition of the cellobiose substrate the formation of H_2O_2 was initiated in the case of CDH-F+. Accumulation of peroxide then led to oxidation of the roGFP2-Orp1 on the surface of individual cells which could be tracked by the fluorescence ratio. Reactions were stopped with IAA after 1, 10 and 20 minutes. Cells were washed and analyzed in the flow cytometer at 405/525(40) nm and 488/525(40) nm. About 10 000 events were recorded and the gate placed according to the CDH-F negative control. Numbers in brackets represent the proportion of gated events.

of) oxygen, and total exclusion of oxygen is not an option. Decreased O₂ concentrations may also be beneficial, but the required equipment and handling procedures run counter to the idea of a user-friendly and simple high-throughput screening system.

Conclusion

In this report, we describe the development of a screening platform for oxidase activity employing roGFP2-Orp1 as a fluorescent peroxide sensor that does not require artificial compartmentalization. Analysis of its catalytic properties and insights from trials in soluble format allowed us to successfully employ this system in combination with cells displaying CDH variants. The major obstacle, unspecific reactivity of the sensor with molecular oxygen, could be overcome by applying an excess of soluble sensor.

For full adaptation to ultra-high-throughput screenings, a modified sensor performing faster with hydrogen peroxide is desirable. Ideally, a hydrogen peroxide-specific oxidation outperforming the unspecific oxidation to a significantly higher degree would widen the detectable activity ranges of enzymes of interest and make handling of the system more user-friendly. Future studies will evaluate the performance of this platform with large libraries of oxidase variants.

Material and Methods

Materials

Unless otherwise stated, all chemicals and reagents used in this study were of highest available purity and purchased from Sigma–Aldrich (Germany).

Recombinant expression and purification of roGFP2-Orp1

The pQE-60 roGFP2-Orp1 expression plasmid (Gutscher *et al.*, 2009), containing a C-terminal His-tag was kindly provided by Tobias Dick (Addgene plasmid #64976, RRID:Addgene_64976). After isolation, the purified plasmid was transformed into NEB Express I^q competent *E. coli* cells (New England Biolabs, Germany), its presence and identity were confirmed via sequencing (Microsynth AG, Austria). For recombinant protein production, *E. coli* cultures were routinely grown in TB medium, supplemented with 1.0 g L⁻¹ glucose monohydrate and 100 µg ml⁻¹ ampicillin. Expression and IMAC purification were carried according to a previously published protocol (Brugger *et al.*, 2014a) with the adaptation of inducing cultures at 20°C for 20 hours and using Tris HCl-based buffers at pH 8.0 for all cell disruption and purification steps. As a polishing step, active fractions were pooled and subjected to SEC using a 180 ml HiPrep Sephacryl SEC column (GE Life Sciences, Germany) with 50 mM Tris HCl, 500 mM NaCl pH 7.5. Clean and fluorescent chromatography fractions, as judged by SDS-PAGE and their fluorescence signal (isosbestic fluorescence Ex. 423 nm, Em. 520 nm) were pooled, desalted and concentrated with centrifugal filters before being stored at -80°C in freshly prepared storage buffer (10 mM Tris HCl, 5 mM EDTA, 1 mM DTT, 10% *whw* glycerol, pH 7.5).

Protein analysis

The estimation of protein concentration was generally carried out by determination of the protein's absorbance at 280 nm wavelength. For His-tagged roGFP2-Orp1 an extinction coefficient of

$\epsilon_{280} = 39\,685\text{ M}^{-1}\text{ cm}^{-1}$ was used. The presence of the full-length protein was confirmed via peptide mapping by LC–ESI–MS. The purity of purification fractions and pooled solutions was evaluated by SDS PAGE and carried out using precast stain-free gels (Bio-Rad, Austria) that were visualized spectroscopically.

Preparation of roGFP2-Orp1 for fluorescent measurements

Frozen stock solutions of roGFP2-Orp1 at about 200 µM were diluted to 9.0 µM in GFP buffer (100 mM potassium phosphate buffer, 5 mM EDTA, pH 7.25, degassed and saturated with nitrogen). To facilitate work with the redox probe, roGFP2-Orp1 solutions were initially reduced on ice for 20 minutes in GFP buffer containing 20 mM DTT. DTT concentration in the solution was gradually decreased to <10 µM by repeated rebuffing against GFP buffer in 0.5 ml, 50 kDa cut-off spin filters (Merck Millipore, Germany) (Gutscher *et al.*, 2009) before the solution was diluted to ~1 µM and stored air-sealed for immediate use.

Unless otherwise stated, all measurements were carried out as 200 µl reactions in 96-well plate format. Fluorescent measurements were generally recorded at 400 nm, 490 nm excitation and 520 nm emission using an EnSpire alpha platreader (PerkinElmer, Austria). The resulting changes in fluorescence intensities at 520 nm, given in a.u., were commonly displayed as a ratio of 400 nm by 490 nm excitation, respectively and plotted against time.

Estimation of differential molar fluorescence extinction coefficients ϵ_{ox}

To quantify the correlation of roGFP2-Orp1 fluorescence and redox state, a dilution series (0.1–1.4 µM) of the fusion protein was equilibrated for 20 minutes in GFP buffer containing either 20 mM DTT or 0.1 mM H₂O₂. This yielded roGFP2-Orp1 in the reduced and oxidized state, respectively. Subsequently, fluorescence emission intensities (*IF*) at 400 nm, 490 nm excitation and 520 nm emission were recorded in 200 µl quintuplicates in a fluorescent plate reader and plotted against the roGFP2-Orp1 concentration. Obtained correlations, as linear least square fitted slopes (*m*), were used to calculate the change in fluorescence emission intensity per µM roGFP2-Orp1 (ϵ_{ox}) between the reduced and the oxidized state (oxidation reaction) at a certain wavelength (λ) for the given concentrations and experimental setup according to:

$$\epsilon_{ox,\lambda} = m_{ox,\lambda} - m_{red,\lambda} = \frac{d(IF_{ox,\lambda}) - d(IF_{red,\lambda})}{d([roGFP2 - Orp1])} \quad (1)$$

Based on the premise that every molecule of roGFP2-Orp1 can be present at only one of two distinct redox states, reduced or oxidized, the change in emission intensity for one molecule is proportional to the change in emission intensity of µM concentrations of roGFP2-Orp1. This principle was similarly described for the determination of roGFP redox potentials before (Aller, Rouhier and Meyer, 2013).

Determination of kinetic parameters of the H₂O₂-dependent roGFP2-Orp1 reaction

In order to estimate the kinetic parameters of the roGFP2-Orp1 reaction with H₂O₂, aliquots of the roGFP2-Orp1 fusion protein were prepared as described above and diluted to 1 µM in a 200 µl reaction mix. After an initial equilibration phase, H₂O₂ was added

in varying amounts to final concentrations of 0.05–10.0 μM . GFP buffer served as a blank measurement as described before (Gutscher et al., 2009; Müller et al., 2017). Resulting changes in the fluorescent signals were tracked for 1800 seconds and slopes obtained from four independent sets of measurements were calculated into catalytic rates using ε_{ox} . Apparent kinetic constants were estimated by nonlinear least-square regression fitting using the Microsoft Excel solver plugin.

Resolving enzymatic H_2O_2 formation with roGFP2-Orp1 *in vitro*

Initially, roGFP2-Orp1 was prepared as described before and diluted to 1 μM before being incubated with 10 nM of purified pyranose 2-oxidase (POx) from *Trametes ochracea* (formerly *Trametes multicolor*). To start the enzymatic formation of H_2O_2 by POx, D-glucose or alternative sugar substrates such as D-xylose, D-galactose, maltose were added after equilibration. For discrimination of activities of different POx variants, 10 nM of purified enzyme were used. Purified POx *wt* and variants were kindly gifted by Leander Sützl from BOKU University, Austria.

Display of CDH on the surface of *S. cerevisiae*

CDH from *Myriococcum thermophilum* (Zámocký et al., 2008; Tan et al., 2015), UniProtKB A9XK88 was expressed in a display format using the established yeast surface display format for *S. cerevisiae* (Boder and Wittrup, 1997; Angelini et al., 2015). The gene sequence encoding the wild type flavin domain of CDH (CDH-F) and an engineered flavin domain with increased oxygen reactivity (CDH-F+) which was kindly provided by Prof. Roland Ludwig from BOKU University, Austria (Kracher et al., 2019). The genes were cloned in frame into the pCTCON2 display plasmid, omitting the sequence encoding the 247 N-terminal residues comprising the signal peptide, cytochrome domain and linker. The recombinant constructs CDH-F, CDH-F+ and an EVC were transformed into competent *S. cerevisiae* EBY100 using the Frozen-EZ Yeast Transformation II Kit (Zymo Research, Germany). Vector and expression strain were kindly gifted by Dane Wittrup from MIT, USA.

Transformed cells were plated on SD-CAA selection plates and positive clones were expressed in SD-CAA liquid culture for 20 hours at 30°C prior to media change and induction in SG(R)-CAA medium supplemented with 1% *w/w* raffinose at 20°C for 30 hours (Puri et al., 2013; Angelini et al., 2015).

Assessment of display efficiency and enzyme activities

Assessment of display levels was carried out based on the fluorescent staining of a C-terminal myc-tag and detection by flow cytometry. The procedure consisted of binding of the myc-tag with an anti-myc (9B11) primary mouse antibody (Cell Signaling Technology, USA) and labeling of the primary antibody with an antimouse secondary antibody conjugated with fluorescent Alexa Fluor 647 dye (Cell Signaling Technology). In parallel, enzyme activities were evaluated by determining cellobiose dependent H_2O_2 formation by CDH-F+ using the established Amplex Red/peroxidase assay (10).

Use of roGFP2-Orp1 in combination with cell-displayed CDH

The CDH constructs were expressed as described. Cell suspensions were washed twice with phosphate buffered saline (PBS) at pH 7.4 to remove media components and diluted to an optical density (OD_{600})

of 5.0 in 100 mM potassium phosphate buffer, 5 mM EDTA at pH 6.0 (PPB, pH 6). In parallel, aliquots of roGFP2-Orp1 were prepared as described and diluted in GFP buffer. Aliquots of induced *S. cerevisiae* cultures displaying CDH-F, CDH-F+ and an EVC were transferred to a 96-well plate before roGFP2-Orp1 solution was added. After an initial equilibration phase of 100 seconds, enzymatic reactions were started with the addition of cellobiose to yield reaction mixtures of 1.0 μM roGFP2-Orp1, cells of $\text{OD}_{600} = 1.0$ and 10 mM cellobiose in 100 mM PPB pH 6.0. Another 420 seconds into the reaction IAA was added to a concentration of 50 mM. Fluorescent signals were tracked for 1800 seconds.

Immobilization of biotinylated roGFP2-Orp1 on yeast cells

We used a commercial *in vivo* biotinylation system, acquired from Avidity (USA), to equip roGFP2-Orp1 with an N-terminal AviTag. In this system, coexpression of the biotin ligase BirA mediates the enzymatic biotinylation at the AviTag during recombinant expression in *E. coli*. The roGFP2-Orp1 coding sequence was introduced in frame into the pAN4 expression vector (Avidity) using the NEBuilder HiFi Assembly Kit (New England Biolabs). The correct assembly of the pAN4 biotin-roGFP2-Orp1 expression plasmid was confirmed by sequencing before the construct was transformed into competent *E. coli* EVB101 cells for expression. The production of N-terminally biotinylated roGFP2-Orp1 was carried out as recommended by the supplier with the difference of inducing protein expression at 20°C for 18 hours. Purification of biotin-roGFP2-Orp1 was carried out as described above.

For plant lectin ConA mediated immobilization of biotinylated roGFP2-Orp1 on *S. cerevisiae*, EBY100 cells were cultivated in SD-CAA medium, harvested and washed in PBS twice as described. Immobilization was done after incubating 1.0 ml cells of $\text{OD}_{600} = 1.0$ in blocking buffer (PBS + 2% bovine serum albumin BSA) by consecutive incubation with 10 μg biotinylated ConA (Vector laboratories, USA), 50 μg Streptavidin (New England Biolabs) and 250 μg biotin-roGFP2-Orp1, each for 30 minutes shaking at room temperature. Between all steps, cells were washed with PBS-A (PBS + 0.1% BSA) by centrifugation at 12 000 rcf for 2 minutes and gentle resuspension. PBS-A was also used as a diluent for the labeling reagents. Labeled cells were analyzed in a CytoFLEX S flow cytometer (Beckman Coulter, USA) using a 488 nm laser for excitation and detection in the FITC channel (525/40 nm).

Detection of displayed CDH activities with cell-tethered roGFP2-Orp1

Biotin-roGFP2-Orp1 was reduced and prepared for fluorescent measurement as described for the unbiotinylated protein. *S. cerevisiae* cells were induced to display CDH-F and CDH-F+. From each clone, 500 μl cells of OD 1.0 were harvested, washed and blocked in blocking buffer. Subsequently, immobilization was carried out while maintaining biotin-roGFP2-Orp1 in the degassed buffer prior to use. About 25 μg ConA-biotin, 50 μg Streptavidin and 250 μg biotin-roGFP2-Orp1 were used for the sequential immobilization. For the whole cell assay reaction, cells were maintained in 2 ml of 125 $\mu\text{g ml}^{-1}$ biotin-roGFP2-Orp1 during the course of the reaction to detect peroxide locally (immobilized sensor) but simultaneously buffer the oxygen dependent background reaction (soluble sensor). Reactions were started with 10 mM cellobiose and then sequentially stopped after 1, 5 and 20 minutes of reaction using 50 mM IAA.

The assay cell suspensions were then subjected to centrifugation at 12 000 rcf for 2 minutes and a subsequent washing step in PBS-A before being analyzed for fluorescent ratios in the flow cytometer with lasers operating at 405 and 488 nm in the FITC channel 525/40 nm.

Supplementary data

Supplementary data are available at PEDS online.

Acknowledgments

This work was supported by the Austrian Science Fund FWF through the Doctoral Program BioToP Biomolecular Technology of Proteins (FWF W 1224) and by the Erasmus+ EU program for education. Experimental analysis and data processing were supported by EQ-BOKU VIBT GmbH and the BOKU Core Facility for Biomolecular and Cellular Analysis.

We especially like to thank Dr Leander Sützl for providing purified pyranose 2-oxidase variants and Roland Ludwig for supplying us with an engineered cellobiose dehydrogenase variant.

Authors' Contribution

Dr Florian Hollfelder, PEDS Board Member edited the manuscript.

Conflict of Interest

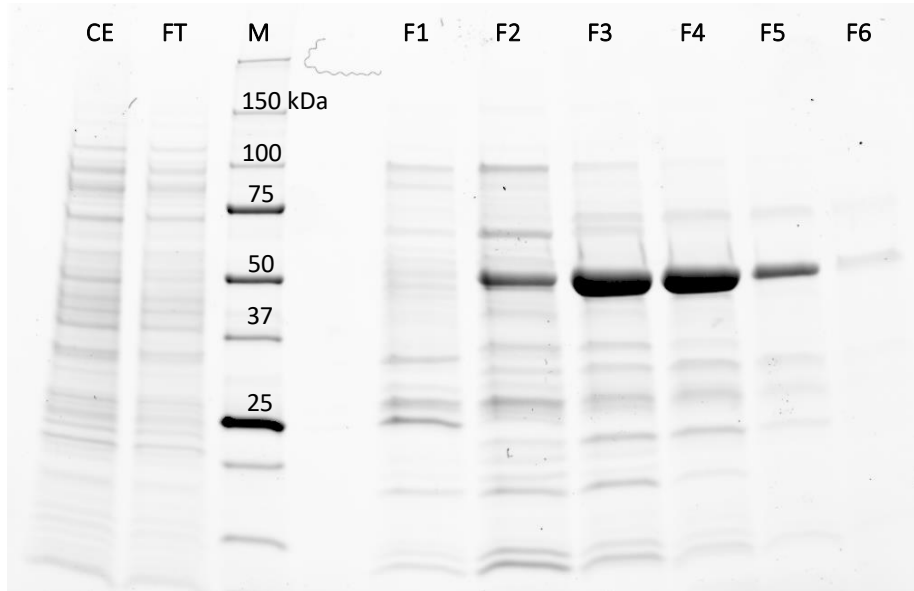
None declared.

References

- Aharoni, A., Amitai, G., Bernath, K. *et al.* (2005) *Chem. Biol. Cell Press*, **12**, 1281–1289. doi: [10.1016/J.CHEMBIOL.2005.09.012](https://doi.org/10.1016/J.CHEMBIOL.2005.09.012).
- Aller, I., Rouhier, N. and Meyer, A.J. (2013) *Front. Plant Sci.*, **4**, 1–12. doi: [10.3389/fpls.2013.00506](https://doi.org/10.3389/fpls.2013.00506).
- Angelini, A., Chen, T.F., de Picciotto, S. *et al.* (2015) Protein engineering and selection using yeast surface display. In *Yeast Surface Display*. Humana Press, New York, NY, pp. 3–36.
- Blažič, M., Balaž, A.M., Prodanovic, O. *et al.* (2019) *Appl. Sci.*, **9**, 1413. doi: [10.3390/app9071413](https://doi.org/10.3390/app9071413).
- Boder, E.T. and Wittrup, K.D. (1997) *Nat. Biotechnol.*, **15**, 553–557. doi: [10.1038/nbt0697-553](https://doi.org/10.1038/nbt0697-553).
- Brugger, D. *et al.* (2014a) *PLoS One*, **9**, e109242–e109242. doi: [10.1371/journal.pone.0109242](https://doi.org/10.1371/journal.pone.0109242).
- Brugger, D. *et al.* (2014b) *Biotechnol. J.*, **9**, 474–482. doi: [10.1002/biot.201300336](https://doi.org/10.1002/biot.201300336).
- Brugger, D., Sützl, L., Zahma, K. *et al.* (2016) *Phys. Chem. Chem. Phys.*, **18**, 32072–32077. doi: [10.1039/C6CP06009A](https://doi.org/10.1039/C6CP06009A).
- Chen, K. and Arnold, F.H. (1991) *Biotechnology*, **9**, 1073–1077. doi: [10.1038/nbt1191-1073](https://doi.org/10.1038/nbt1191-1073).
- Coulibaly, E.S. and Youan, B.B.C. (2014) *Biosens. Bioelectron.*, **59**, 404–411. doi: [10.1016/j.bios.2014.03.040](https://doi.org/10.1016/j.bios.2014.03.040).
- Dörr, M., Fibinger, M.P., Last, D. *et al.* (2016) *Biotechnol. Bioeng.*, **113**, 1421–1432. doi: [10.1002/bit.25925](https://doi.org/10.1002/bit.25925).
- Đurđić, K.I., Ece, S., Ostafe, R. *et al.* (2020) *J. Biosci. Bioeng.* doi: [10.1016/j.jbiosc.2019.12.009](https://doi.org/10.1016/j.jbiosc.2019.12.009).
- Fischlechner, M., Schaerli, Y., Mohamed, M. *et al.* (2014) *Nat. Chem.*, **6**, 791. doi: [10.1038/nchem.1996](https://doi.org/10.1038/nchem.1996).
- Gutscher, M., Sobotta, M.C., Wabnitz, G.H. *et al.* (2009) *J. Biol. Chem.*, **284**, 31532–31540. doi: [10.1074/jbc.M109.059246](https://doi.org/10.1074/jbc.M109.059246).
- Halada, P., Brugger, D., Volc, J. *et al.* (2016) *PLoS One*, **11**, e0148108. doi: [10.1371/journal.pone.0148108](https://doi.org/10.1371/journal.pone.0148108).
- Kracher, D., Forsberg, Z., Bissaro, B. *et al.* (2019) *FEBS J.*, febs.15067. doi: [10.1111/febs.15067](https://doi.org/10.1111/febs.15067).
- Kuchner, O. and Arnold, F.H. (1997) *Trends Biotechnol.*, **15**, 523–530. doi: [10.1016/S0167-7799\(97\)01138-4](https://doi.org/10.1016/S0167-7799(97)01138-4).
- Leitner, C., Volc, J. and Haltrich, D. (2001) *Appl. Environ. Microbiol.*, **67**, 3636–3644. doi: [10.1128/AEM.67.8.3636](https://doi.org/10.1128/AEM.67.8.3636).
- Lim, J.B. and Sikes, H.D. (2015) *Protein Eng. Des. Sel.*, **28**, 79–83. doi: [10.1093/protein/gzv003](https://doi.org/10.1093/protein/gzv003).
- Lipovšek, D., Antipov, E., Armstrong, K.A. *et al.* (2007) *Chem. Biol.*, **14**, 1176–1185. doi: [10.1016/j.chembiol.2007.09.008](https://doi.org/10.1016/j.chembiol.2007.09.008).
- Ma, L.H., Takamishi, C.L. and Wood, M.J. (2007) *J. Biol. Chem.*, **282**, 31429–31436. doi: [10.1074/jbc.M705953200](https://doi.org/10.1074/jbc.M705953200).
- Markel, U., Essani, K.D., Besirlioglu, V. *et al.* (2020) *Chem. Soc. Rev.*, **49**, 233–262. doi: [10.1039/C8CS00981C](https://doi.org/10.1039/C8CS00981C).
- Müller, A., Schneider, J.F., Degrossoli, A. *et al.* (2017) *Free Radic. Biol. Med.*, **106**, 329–338. doi: [10.1016/j.freeradbiomed.2017.02.044](https://doi.org/10.1016/j.freeradbiomed.2017.02.044).
- Ostafe, R., Prodanovic, R., Nazor, J. *et al.* (2014) *Chem. Biol.*, **21**, 414–421. doi: [10.1016/j.chembiol.2014.01.010](https://doi.org/10.1016/j.chembiol.2014.01.010).
- Parsonage, D., Youngblood, D.S., Sarma, G.N. *et al.* (2005) *Biochemistry*, **44**, 10583–10592. doi: [10.1021/bi050448i](https://doi.org/10.1021/bi050448i).
- Pitzler, C., Wirtz, G., Vojcic, L. *et al.* (2014) *Chem. Biol.*, **21**, 1733–1742. doi: [10.1016/j.chembiol.2014.10.018](https://doi.org/10.1016/j.chembiol.2014.10.018).
- Porter, J.L., Rusli, R.A. and Ollis, D.L. (2016) *Chembiochem*, **17**, 197–203. doi: [10.1002/cbic.201500280](https://doi.org/10.1002/cbic.201500280).
- Puri, V., Streaker, E., Prabakaran, P. *et al.* (2013) *MAbs*, **5**, 533–539. doi: [10.4161/mabs.25211](https://doi.org/10.4161/mabs.25211).
- Renata, H., Wang, Z.J. and Arnold, F.H. (2015) *Angew. Chem. Int. Ed.*, **54**, 3351–3367. doi: [10.1002/anie.201409470](https://doi.org/10.1002/anie.201409470).
- Rhiel, L., Krah, S., Günther, R. *et al.* (2014) *PLoS One*, **9**, e114887. doi: [10.1371/journal.pone.0114887](https://doi.org/10.1371/journal.pone.0114887).
- Salaheddin, C., Spadiut, O., Ludwig, R. *et al.* (2009) *Biotechnol. J.*, **4**, 535–543. doi: [10.1002/biot.200800265](https://doi.org/10.1002/biot.200800265).
- Smith, G.P. and Petrenko, V.A. (1997) *Chem. Rev.*, **97**, 391–410. doi: [10.1021/cr960065d](https://doi.org/10.1021/cr960065d).
- Spadiut, O., Radakovits, K., Pisanelli, I. *et al.* (2009) *Biotechnol. J.*, **4**, 525–534. doi: [10.1002/biot.200800260](https://doi.org/10.1002/biot.200800260).
- Tan, T.C., Kracher, D., Gandini, R. *et al.* (2015) *Nat. Commun.*, **6**, 7542. doi: [10.1038/ncomms8542](https://doi.org/10.1038/ncomms8542).
- Tanaka, T., Izawa, S. and Inoue, Y. (2005) *J. Biol. Chem.*, **280**, 42078–42087. doi: [10.1074/jbc.M508622200](https://doi.org/10.1074/jbc.M508622200).
- Tasca, F., Timur, S., Ludwig, R. *et al.* (2007) *Electroanalysis*, **19**, 294–302. doi: [10.1002/elan.200603740](https://doi.org/10.1002/elan.200603740).
- Truppo, M.D. (2017) *ACS Med. Chem. Lett.*, **8**, 476–480. doi: [10.1021/acsmmedchemlett.7b00114](https://doi.org/10.1021/acsmmedchemlett.7b00114).
- Vanella, R., Bazin, A., Ta, D.T. *et al.* (2019a) *Chem. Mater.*, **31**, 1899–1907. doi: [10.1021/acs.chemmater.8b04348](https://doi.org/10.1021/acs.chemmater.8b04348).
- Vanella, R., Ta, D.T. and Nash, M.A. (2019b) *Biotechnol. Bioeng.*, **116**, 1878–1886. doi: [10.1002/bit.27002](https://doi.org/10.1002/bit.27002).
- Zámocký, M., Schumann, C., Sygmund, C. *et al.* (2008) *Protein Expr. Purif.*, **59**, 258–265. doi: [10.1016/j.pep.2008.02.007](https://doi.org/10.1016/j.pep.2008.02.007).
- Zhu, B., Mizoguchi, T., Kojima, T. and Nakano, H. (2015) *PLoS One*, **10**. doi: [10.1371/journal.pone.0127479](https://doi.org/10.1371/journal.pone.0127479).

1 Supporting information

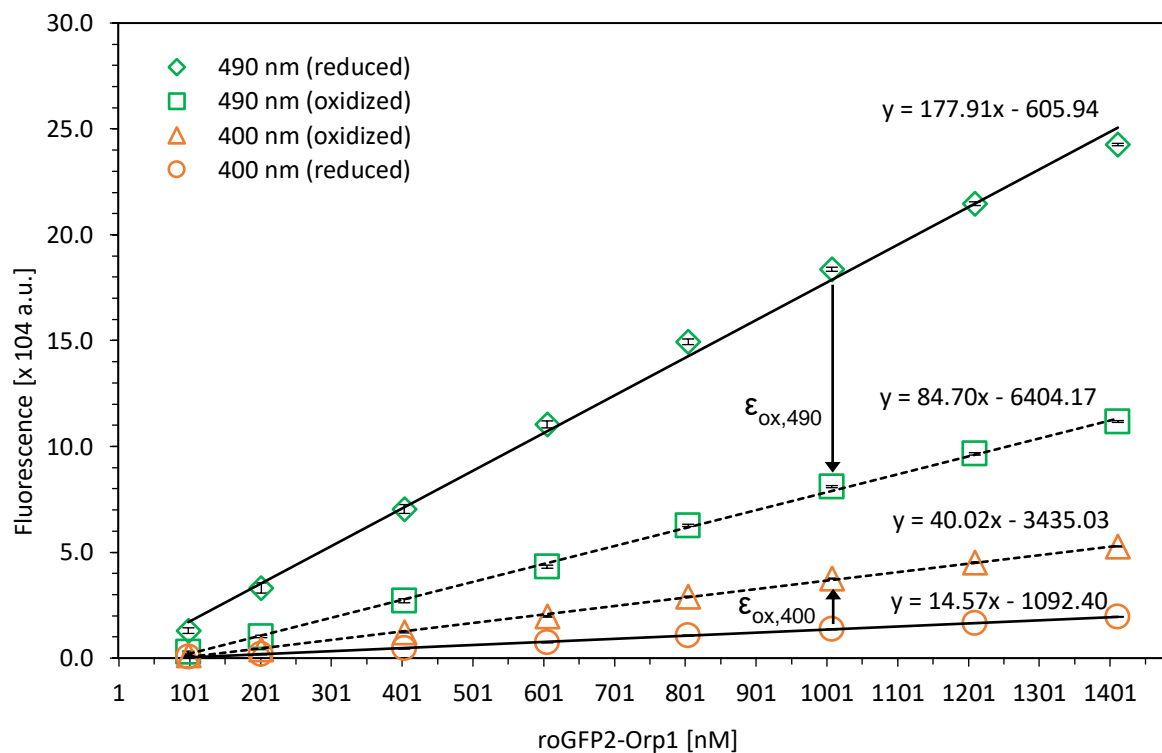
2 **Fig. S1: SDS PAGE of roGFP2-Orp1 IMAC purification fractions.** (CE) crude extract, (FT) flow
3 through, (M) mass standard and (F1-F6) elution fractions from the initial IMAC purification. The
4 respective molecular masses of the mass standard bands are given in kDa.



5

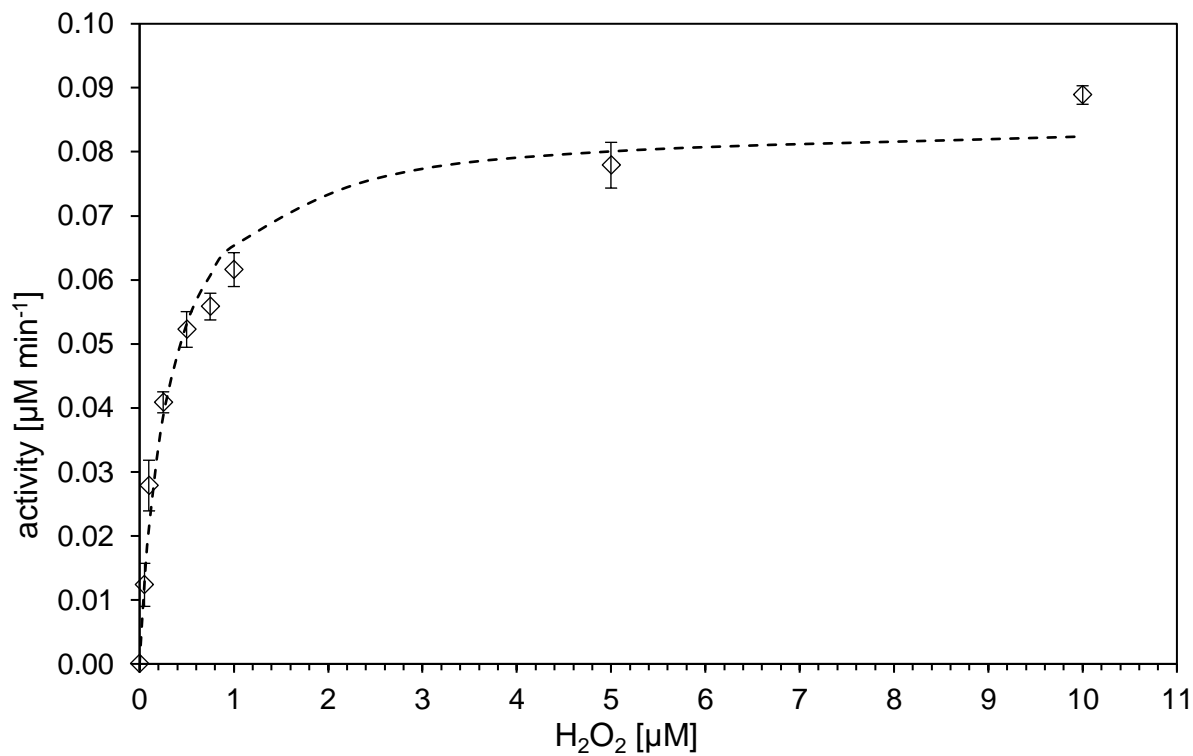
6

7 **Fig. S2. Correlation of roGFP2-Orp1 fluorescence and concentration in the reduced and**
 8 **oxidized state.** Fluorescence intensities of roGFP2-Orp1 samples at varying concentrations
 9 were measured in the reduced state (reduced, 20 mM DTT) and the oxidized state (oxidized,
 10 0.1 mM H₂O₂) in replicates of n=4. Measurements were performed at 520 nm emission and
 11 either 400 nm, or 490 nm excitation respectively where standard deviations are indicated with
 12 error bars. From the obtained data points, least square regression fits were prepared for the
 13 reduced (full line) as well as for the oxidized samples (dashed line), straight line equations (R^2
 14 > 0.99) are stated above. To yield differential molar fluorescence extinction coefficients (ϵ_{ox})
 15 slopes from the gained fits were subtracted to obtain an average over varying concentrations.
 16 ϵ_{ox} are indicated as arrows in the graph following the oxidation reaction from the reduced to
 17 the oxidized state.



18
 19

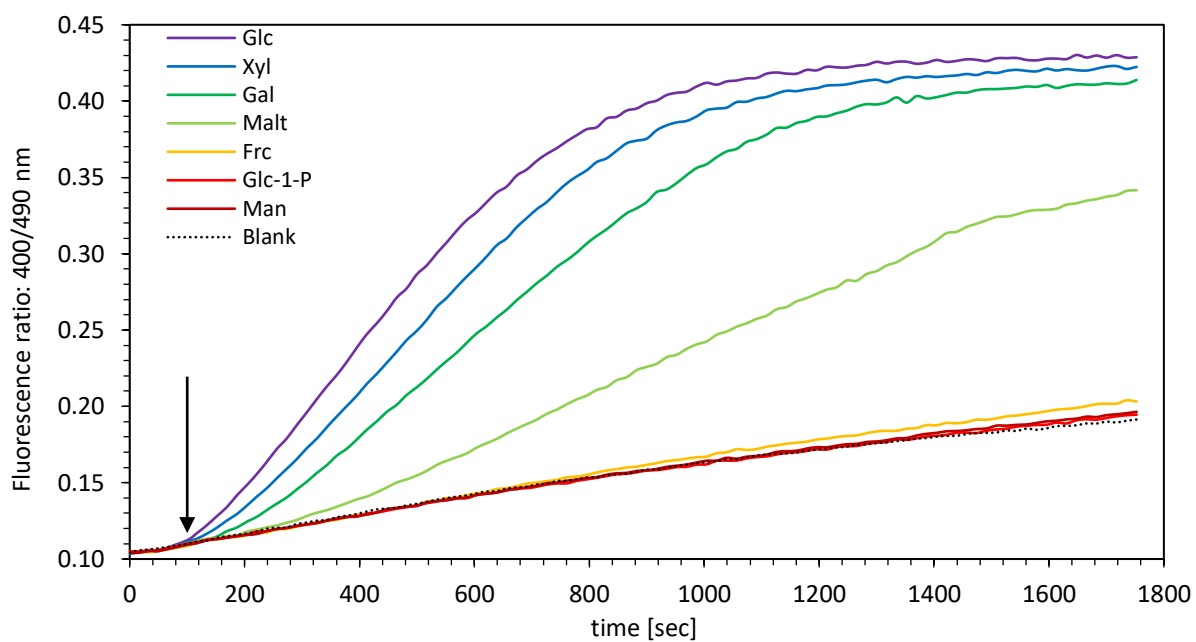
20 **Fig. S3. Michaelis Menten saturation curve describing the reaction of roGFP2-Orp1 with H₂O₂.**
21 0.9 μM roGFP2-Orp1 was prepared as described and incubated with 0.05, 0.10, 0.25, 0.50,
22 0.75, 1.0, 5.0, 10.0 μM H₂O₂ or buffer in triplicate measurements, standard deviations are
23 indicated by error bars. Reaction rates were calculated from the changes of fluorescence
24 intensities at 490 nm excitation, 520 nm emission and are given in μM of substrate turned
25 over per minute. Fitting the obtained data to the Michaelis Menten equation allowed to
26 estimate a K_m of 0.30 ± 0.04 μM and V_{max} of 0.09 ± 0.01 μM min⁻¹.



27

28

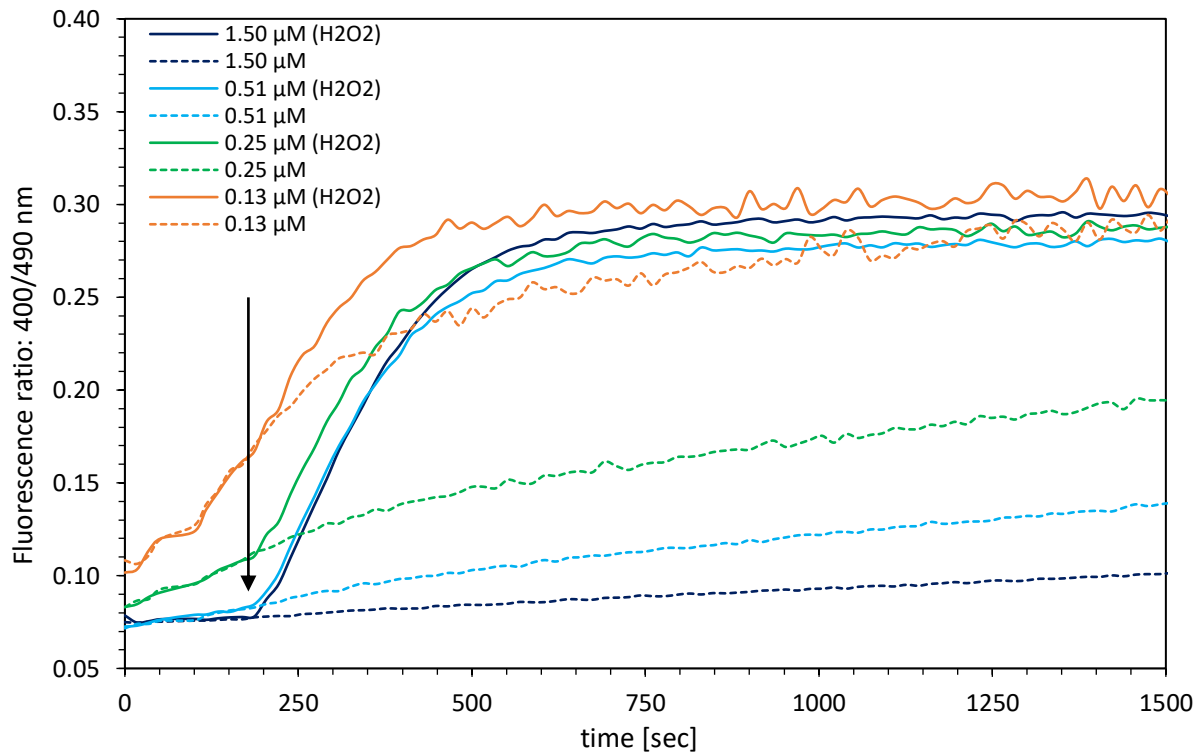
29 **Fig. S4. Detection of pyranose 2-oxidase (soluble) dependent H₂O₂ formation with roGFP2-Orp1**
30 **(soluble) – different sugars.** roGFP2-Orp1 was reduced (20 mM DTT) in the absence of oxygen
31 and filtered to remove DTT as is described in the material and method section. 1.0 μM roGFP2-
32 Orp1 was mixed with 0.01 μM recombinant POx from *T. ochracea* and let equilibrate for 100
33 seconds before its sugar substrate was added to start H₂O₂ formation (arrow). D-glucose (Glc),
34 D-xylose (Xyl), D-galactose (Gal), D-maltose (Malt), D-fructose (Frc), D-glucose-1-phosphate (Glc-
35 1-P) and D-mannose (Man) were tested at a concentration of 1.0 mM. Reactions were
36 performed in 200 μL reaction in a fluorescent plate reader and fluorescence intensities were
37 tracked as a ratio of 400 vs. 490 nm excitation at 520 nm emission.
38



39

40

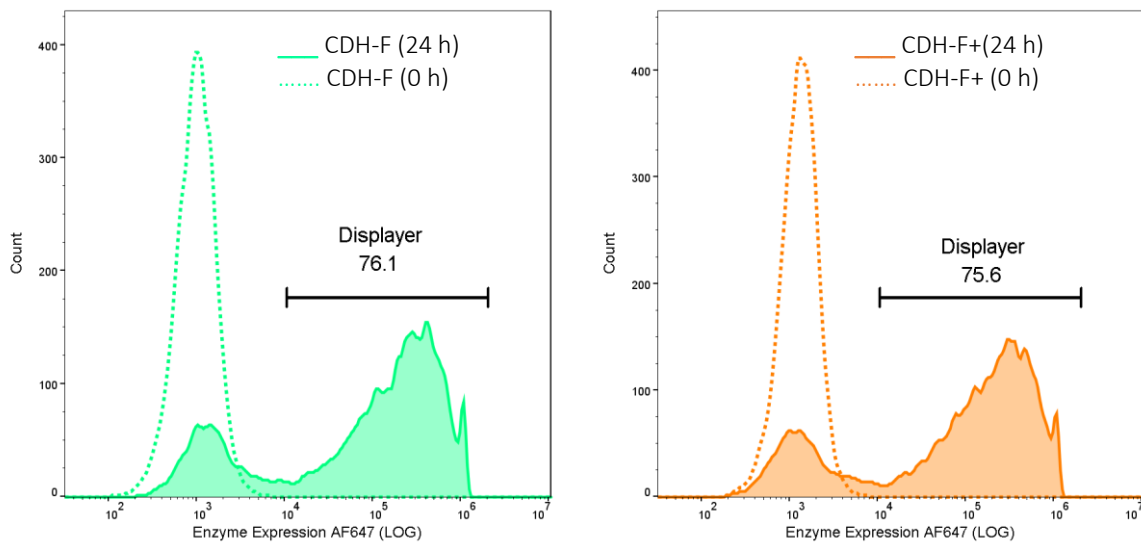
41 **Fig. S5. Dependence of the concentration of roGFP2-Orp1 for its unspecific reactivity.** A stock
42 solution of 9 μM roGFP2-Orp1 was reduced (20 mM DTT) in the absence of oxygen and filtered
43 to remove DTT as is described in the material and method section. This stock solution was then
44 diluted to 1.50, 0.51, 0.25, 0.13 μM in degassed GFP Buffer and let equilibrate for 200 seconds
45 before either 10 μM H_2O_2 (full lines) or buffer (dashed lines) was added. Reactions were
46 performed in 200 μL reaction in a fluorescent plate reader and fluorescence intensities were
47 tracked as a ratio of 400 vs. 490 nm excitation at 520 nm emission.



48

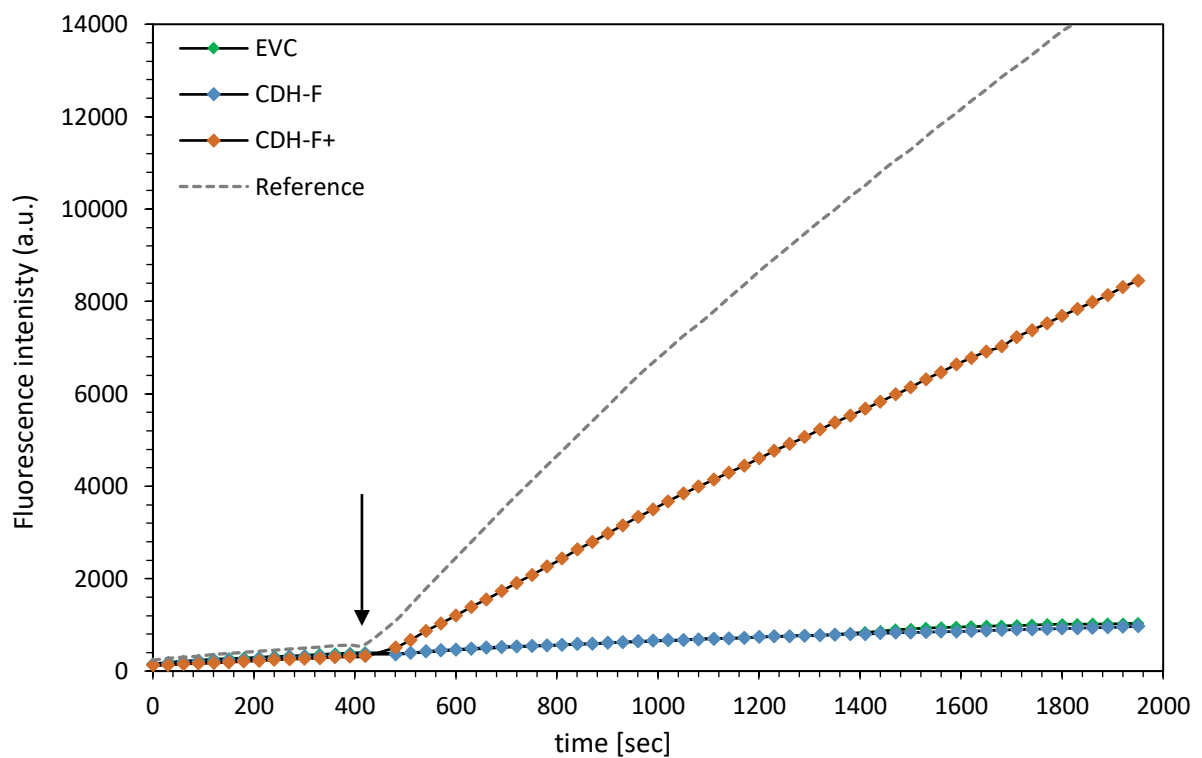
49

50 **Fig. S6. Flow cytometry histograms for the expression levels of CDH-F variants.** *S. cerevisiae* cells
51 carrying the pTCON2 plasmid containing either the CDH-F (left) or the peroxide producing
52 CDH-F+ construct (right) were induced in SG(R)-CAA medium at 20 °C for 24 h. Cells were
53 harvested before (dashed line) and 24 h into the induction (full line) and analyzed for their
54 expression level via fluorescent staining of the C-terminal myc-tag with fluorescent antibodies
55 (Alexa Fluor 647 dye) and analysis of 10 000 events via flow cytometry. A similar ratio of
56 displaying cells of around 76.1% and 75.6% and comparable fluorescent signals, median
57 fluorescence intensities of gated positives of $2.50 \cdot 10^5$ and $2.45 \cdot 10^5$, was estimated for CDH-F
58 and the CDH-F+ variant, respectively.
59



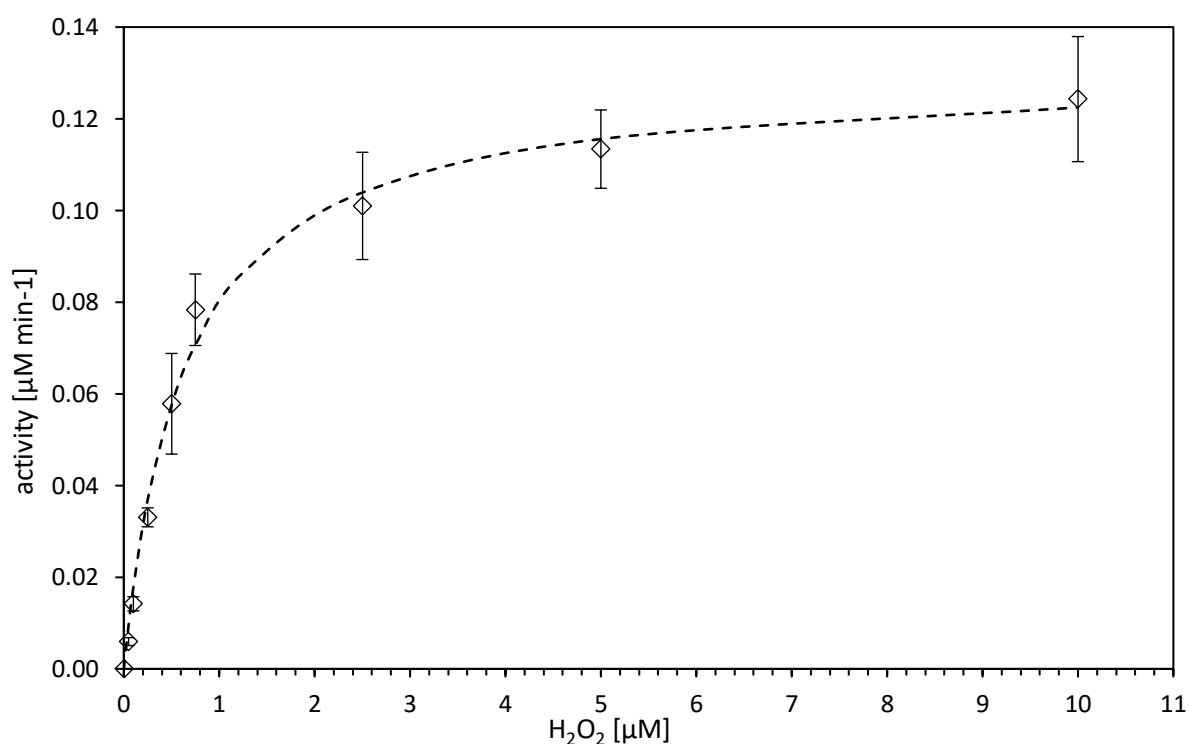
60

61 **Fig. S7. Detection of H₂O₂ formation from displaying *S. cerevisiae* cultures using the Amplex**
62 **Red/peroxidase assay.** 160 μL assay reagent containing 62.5 μM Amplex UltraRed, 10 U mL^{-1}
63 horseradish peroxidase in 50 mM potassium phosphate buffer (pH 6.0) were mixed with 60 μL
64 sample and 30 μL of 80 mM cellobiose to yield 250 μL assay reaction. *S. cerevisiae* cell cultures
65 (OD 5.0) displaying CDH-F, the peroxide producing variant CDH-F+ or an empty vector control
66 (EVC) were mixed with the assay reagent, let equilibrate for 420 seconds before 20 mM
67 cellobiose was added to start the reaction. Purified and soluble CDH-F+ at an activity of 1 mU
68 mL^{-1} (H₂O₂ formation, ABTS assay) was used as a reference. Fluorescence intensities were
69 tracked in a plate reader at 535 (9) nm excitation and 535 (20) nm emission every 25 seconds
70 and are given in arbitrary units (a.u.).



71
72

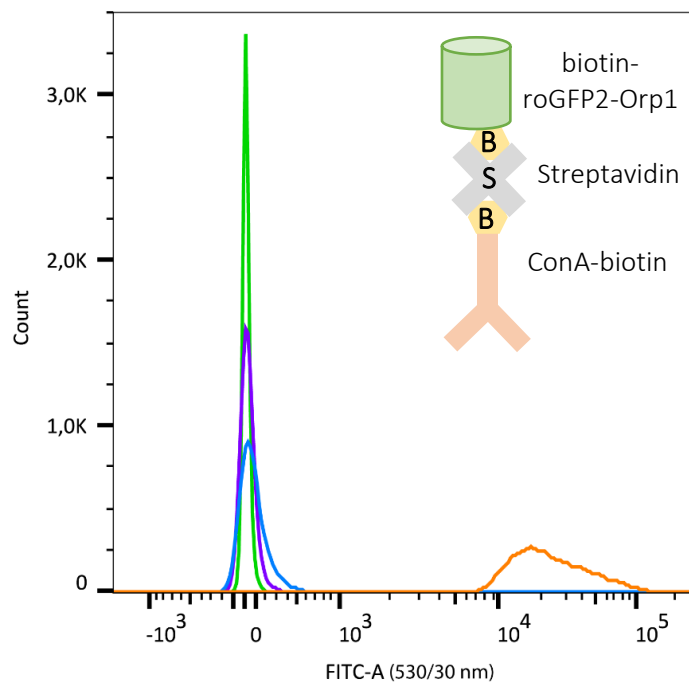
73 **Fig. S8. Michaelis Menten saturation curve for the reaction of biotinylated roGFP2-Orp1 with**
74 **H₂O₂.** 1.1 μM roGFP2-Orp1 was prepared as described and incubated with 0.05, 0.1, 0.25, 0.5,
75 0.75, 2.5, 5.0 ,10.0 μM H₂O₂ or buffer in triplicate measurements, standard deviations are
76 indicated by error bars. Reaction rates were calculated from the changes of fluorescence
77 intensities at 490 nm excitation, 520 nm emission and are given in μM of substrate turned over
78 per minute. Fitting the obtained data to the Michaelis Menten equation allowed to estimate a
79 K_m of $0.63 \pm 0.09 \mu\text{M}$ and V_{max} of $0.13 \pm 0.01 \mu\text{M min}^{-1}$. With roGFP2-Orp1 present at 1.1 μM in
80 the assay, a k_{cat} of 0.11 was calculated and aligned with the kinetic properties of unbiotinylated
81 roGFP2-Orp1.
82



83

84

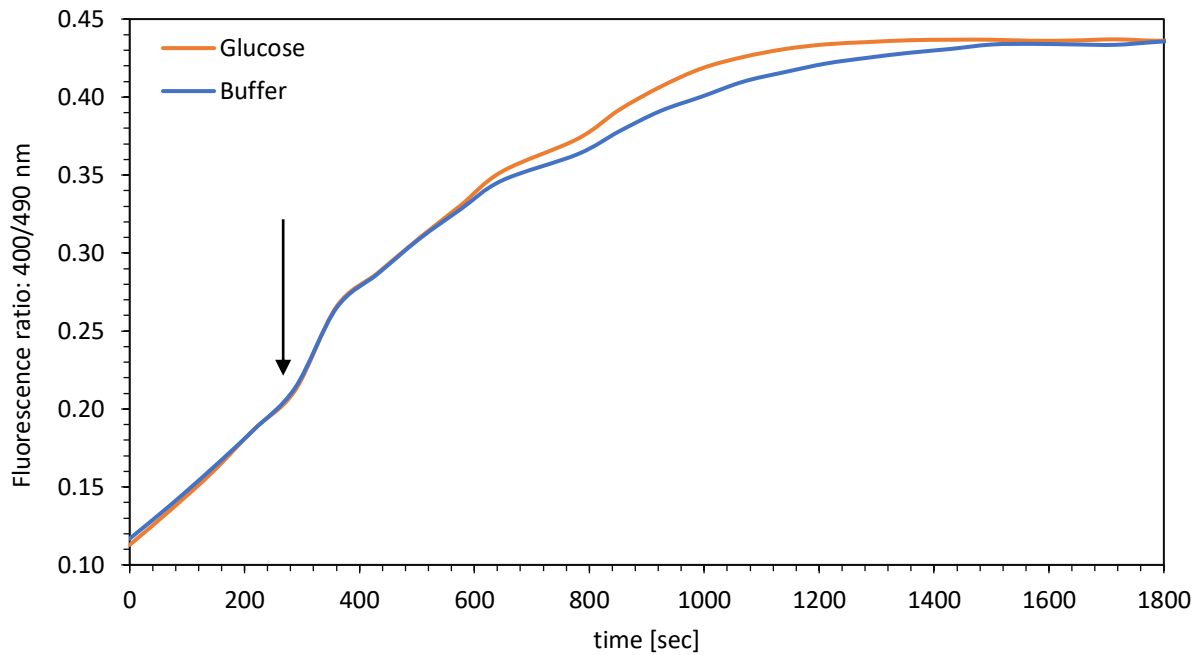
85 **Fig. S9. Flow cytometry histogram for the immobilization of biotin-roGFP2-Orp1 on yeast cells.**
86 *S. cerevisiae* EBY100 cells were mixed with ConA-biotin, streptavidin and biotin-roGFP2-Orp1
87 and 10 000 events were analyzed in a flow cytometer using the FITC channel (530/30 nm) for
88 detection of roGFP2 fluorescence. (Blue) A cells only sample served as negative control. A
89 sample containing all components (orange) was analyzed alongside a sample lacking ConA-
90 biotin (green) and a sample lacking streptavidin (violet). The binding mode of the various
91 components is schematically depicted (insert). The biotinylated lectin ConA binds to glycan
92 structures of the yeast cell wall and is in turn bound by free streptavidin. The tetrameric
93 streptavidin can bind three additional biotins and thus mediate association of biotin-roGFP2-
94 Orp1.



95

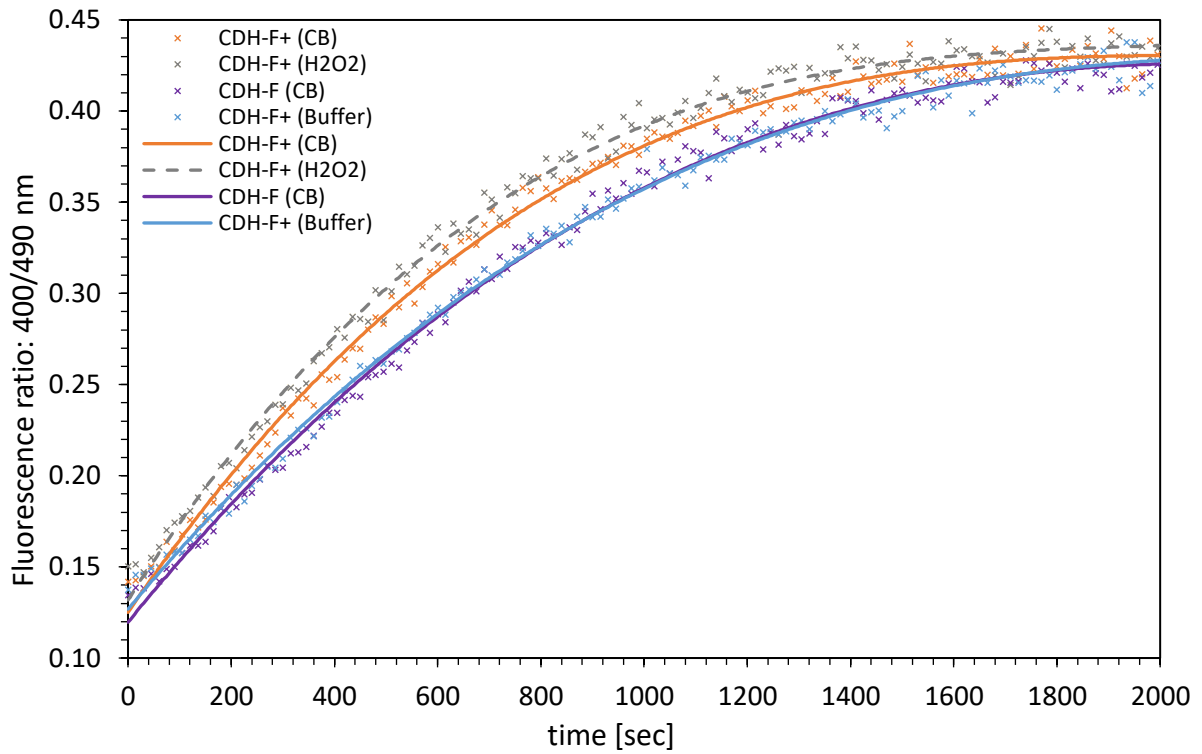
96

97 **Fig. S10. Detection of pyranose 2-oxidase (soluble) dependent H₂O₂ formation with roGFP2-**
98 **Orp1 (soluble) in the absence of EDTA.** Contrasting to previous measurements with GFP buffer,
99 the buffer formulation was changed to 100 mM degassed potassium phosphate buffer, pH 7.25
100 with no EDTA supplemented. 1.0 μM roGFP2-Orp1 was mixed with 0.01 μM recombinant POx
101 from *T. ochracea* before 500 μM D-glucose was added 300 seconds into the equilibration to
102 start H₂O₂ formation (arrow). As a negative control, buffer was added instead of D-glucose.
103



104

105 **Fig. S11. Whole cell assay for the detection of CDH-F+ display activity with immobilized roGFP2-**
106 **Orp1 but without scavenging soluble roGFP2-Orp1.** *S. cerevisiae* cells displaying CDH-F or CDH-
107 *F+*, respectively, were stained with ConA-biotin, streptavidin and biotin-roGFP2-Orp1. After the
108 immobilization procedure, cells were immediately mixed with cellobiose: CDH-F (CB), CDH-F+
109 (CB); buffer CDH-F+ (Buffer), or 10 μM H_2O_2 : CDH-F+(H2O2) to assess the impact of interfering
110 background reactions. Fluorescence intensities were recorded in a plate reader every 20 seconds
111 (colored x) and resulting curves smoothed (full lines).
112



Chapter 5 – Conclusion and Outlook

In the course of this PhD, research was conducted that aimed at incorporating novel approaches into the discovery and development of unknown enzymes or improved enzyme variants. The major revelations from these developments were published in two scientific publications.

As is summarized in **Chapter 2**, a comprehensive phylogenetic analysis revealed that fungal and newly discovered bacterial pyranose 2-oxidases (POx) are closely related and likely share a recent common ancestor. Further, it was shown that a wide variety of bacterial classes harbor putative POx genes, but sequences most closely related to fungal POx can uniformly be attributed to Actinobacteria. This class of bacteria is renowned for their decomposing lifestyle, fungal-like morphology and antibiotic production. Guidance by the phylogenetic calculations and a bioinformatic sequence analysis allowed to dissect these putative POx genes further and select a small set of sequences for expression trials.

The expression and ensuing characterization of one of these candidates, the POx from *Kitasatospora aureofaciens* (formerly *Streptomyces aureofaciens*) could successfully illustrate that the high degree of sequence similarity to fungal POx was also reflected in the similar enzymatic properties, most notably in terms of substrate preference and catalysis. In a series of *in vitro* experiments the bacterial *KaPOx* efficiently complement the activity of a manganese peroxidase and displayed astonishing synergistic catalysis. We resolved redox cycling of quinones and complexed manganese between the enzymes, facilitated by the versatile oxidase and dehydrogenase activity of the POx enzyme. Hence, we ascribed this tandem mechanism between POx and peroxidases a potential relevance in lignin attack, where processes involving these enzymes could be similar in specialized fungi and bacteria.

Currently, the scientific community lacks a holistic view of the intricate processes that facilitate bacterial lignocellulose decomposition. For only a few organisms (*Bacillus spp.*, *Streptomyces spp.*), parts of the enzymatic cascades are resolved and knowledge on bacterial lignocellulose decomposition oftentimes focuses on polysaccharide attack while ligninolytic activities are underrepresented. This gap in knowledge might best be tackled by gathering *in vivo* data from

bacterial model organisms during lignin attack in the future, to bring biochemical data into a biological perspective. Secretome studies could further help to elucidate the interplay of laccases, peroxidases, and auxiliary activity enzymes such as POx in a timely fashion. Still, such organisms are not quite established yet but could originate from the class of Actinobacteria, where several enzymes have been characterized to date.

The presence of POx and specialized peroxidase genes in the respective genomes could aid to predict ligninolytic activities to identify suitable bacteria. In comparison to fungal genomes, that often harbor multiple enzymes from the CAZy auxiliary activity family AA3 to support lignocellulose disintegration, knowhow is scarce on bacterial enzyme systems. As was reported in our publication, we found putative AA3 genes in the bacterial *K. aureofaciens* genome as well and identified them as cholesterol oxidase and choline dehydrogenase. Going forward, it would be of value to assess, whether these enzymes contribute to the ligninolytic machinery of bacteria and what the minimal set of enzymes required for efficient lignin depolymerization is. Such findings would greatly benefit biotechnological applications for lignin valorization, as nature's second most abundant biopolymer is still rendered predominantly inaccessible and renewable sources of fuels and chemicals are urgently demanded.

The proof-of-principle studies on deploying roGFP2-Orp1 for a novel high-throughput screening for oxidase activity in **Chapter 4** were a combination of a series of successful developments. It included the recombinant production and characterization of the roGFP2-Orp1 in terms of kinetic behavior with H₂O₂, as well as protein engineering to contain a biotin tag. Additionally, the yeast surface display system was adapted for the expression of cellobiose dehydrogenase (CDH) variants and protocols improved to facilitate high activity of the enzyme when displayed on the *S. cerevisiae* cell wall. To facilitate artificial compartmentalization by tethering the fluorescent roGFP2-Orp1 sensor proteins to the yeast cell wall, an efficient immobilization technique relying on biotin-streptavidin coupling and concanavalin association to the cell wall glycans was invented. Ultimately, the roGFP2-Orp1 side reactivity with ambient oxygen was identified as one of the major challenges for the application of the devised high throughput screening in enzyme engineering and could be overcome by implementing a simple oxygen scavenging system and stop-reagent into the

screening assay. These findings allowed to utilize roGFP2-Orp1 to differentiate between CDH variants with just marginally different H₂O₂ formation rates in a whole-cell flow cytometry platform.

Still, several steps are deemed necessary in order confirm that this system is indeed fit for the application in enzyme engineering campaigns. Most importantly, the described proof-of-principle experiments were performed with uniform cell populations, displaying the CDH variants in separate tubes in parallel, instead of in mixed populations. To guarantee actual variant libraries could be assayed in essentially a single tube, crosstalk between the individual variants (cells) needs to be avoided. Hence, the degree of this sort of interference needs to be evaluated in what is commonly referred to as a model-library recovery experiment. There, a series of cell suspensions containing different ratios of positive vs. negative variants (often 0.1 – 20 %) are assayed in the screening reaction, analyzed in a flow cytometer, before being sorted by FACS. The degree of positive variants in the sorted collection should come close to 100 % and cells should maintain high viability to justify real library sorts. Future research must address this evaluation and optimize assay conditions (cell densities, incubation times) to explore the borders of applicability. In any case, it should be noted the roGFP2-Orp1 screening managed to resolve slight differences in oxidase activity of a non-specialized enzyme, where comparable research commonly employed glucose oxidase, likely one of the best performing oxidase enzymes. It could thus be especially convenient in cases, where enzymes display just basal oxygen reactivity and enhancement is desired.

With these projects I hope to have highlighted how the discovery and development of novel enzymes can benefit from advanced technology. Clearly, I here want to emphasize that certain challenges in enzyme engineering and discovery, especially approaching other types of enzymes, might require different strategies and the described methodologies might not be tailored for all tasks. One of the major takeaways from this thesis could be that the recent advancements in bioinformatics are progressively changing the field of enzyme engineering. In my humble opinion, more and more tasks will rely on computer-guided predictions and certain reiterating trail-and-error approaches will greatly benefit from improved starting points. These revelations could, in some cases, be just around the corner.

Appendix

Figure Index

Figure 1 Structures of flavin coenzymes	7
Figure 2 PyMOL protein model of cellobiose dehydrogenase (CDH) from <i>Crassicarpon hotsonii</i>	8
Figure 3 Catalytic pathways of the FAD cofactor with O ₂ .	12
Figure 4 Scheme of the plant cell wall composition.	15
Figure 5 The lignin building blocks.	16
Figure 6 Lignin attack by mediated peroxidase catalysis.	19
Figure 7 Phylogenetic tree of characterized enzymes from the AA3 family.	23
Figure 8 3D structure model of the POx from <i>T. ochracea</i>	26
Figure 9 Phylogenetic tree of putative and characterized CDH sequences	31
Figure 10 Weblogo illustration of a multiple sequence alignment of putative basidiomycetous CDH	34
Figure 11 Graphical abstract summarizing bio-electrochemical applications of CDH	37
Figure 12 Directed Evolution schematic.	93
Figure 13 Sequence diversification by DNA recombination.	98
Figure 14 Examples of predicted structures from RoseTTAFold.	101
Figure 15 Blue-white screening of <i>E. coli</i> transformants on solid LB	105
Figure 16 Enzymatic screening cascade.	107
Figure 17 Exemplary overview over a directed evolution campaign for laccase.	112
Figure 18 The <i>S. cerevisiae</i> Yeast Surface Display system.	114
Figure 19 Principles of flow cytometers and cell sorters.	116

List of publications

Publications

- Scheiblbrandner, S., Breslmayr, E., Csarman, F., Paukner, R., Führer, J., **Herzog, P. L.**, Shleev, S. V., Osipov, E. M., Tikhonova, T. V., Popov, V. O., Haltrich, D., Ludwig, R. & Kittl, R. (2017). Evolving stability and pH-dependent activity of the high redox potential *Botrytis aclada* laccase for enzymatic fuel cells. *Scientific reports*, 7(1), 1-13.
- **Herzog, P. L.**, Sützl, L., Eisenhut, B., Maresch, D., Haltrich, D., Obinger, C., & Peterbauer, C. K. (2019). Versatile oxidase and dehydrogenase activities of bacterial pyranose 2-oxidase facilitate redox cycling with manganese peroxidase in vitro. *Applied and environmental microbiology*, 85(13), e00390-19.
- **Herzog, P. L.**, Borghi, E., Traxlmayr, M. W., Obinger, C., Sikes, H. D., & Peterbauer, C. K. (2020). Developing a cell-bound detection system for the screening of oxidase activity using the fluorescent peroxide sensor roGFP2-Orp1. *Protein Engineering, Design and Selection*, 33.
- Geiss, A. F., Reichhart, T. M., Pejker, B., Plattner, E., **Herzog, P. L.**, Schulz, C., Ludwig, R., Felice, A. K. G. & Haltrich, D. (2021). Engineering the Turnover Stability of Cellobiose Dehydrogenase toward Long-Term Bioelectronic Applications. *ACS Sustainable Chemistry & Engineering*.

Patent applications

- **Herzog, P. L.**, Leitner C., Preims, M., Ludwig, R. & Kittl, R., (2020) Production of carbonyl compounds using cell surface display of oxidases
- **Herzog, P. L.**, Eisenhut, B., Felice, A. K. G. (2021) Novel production method of Flavocytochrome b2

Curriculum vitae

Peter L. HERZOG, Dipl. Ing.

25.02.1989

p.herzog.wodo@gmx.at

04/2019 -	DirectSens Biosensors GmbH, Head of enzyme development <i>ELSAH: Electronic smart patch system for wireless monitoring of molecular biomarkers for healthcare and well-being (EU Horizon 2020)</i>
01/2016 – 03/2019	University of Natural Resources and Life Sciences, BOKU Vienna PhD studies protein biochemistry BioToP program: <i>Thesis: “Development of high-throughput screening of Flavin- and heme dependent oxidoreductases using GFP-based redox sensors”</i> (Prof. C. K. Peterbauer, Prof. C. Obinger)
01/2019 - 03/2019	Massachusetts Institute of Technology (MIT) – Dpt. of Chemical Engineering <i>Project: Oxygen insensitive detection of H₂O₂ with cell-tethered roGFP2-Orp1</i> (Prof. H. D. Sikes)
03/2019 - 07/2019	RWTH Aachen – Chair of biotechnology <i>Project: Ultra-high throughput screening for low oxidase activity</i> (Prof. U. Schwaneberg)
10/2012 - 01/2016	University of Natural Resources and Life Sciences, BOKU Vienna Master of Science in Biotechnology Curriculum completed with distinction, focus on protein chemistry
08/2014 – 12/2014	<i>Thesis: “Production, Purification and electrochemical Characterization of engineered Botrytis aclada Laccase variants”</i> (Dpt. of Food Science and Technology: Prof. R. Ludwig, Dr. R. Kittl; Prof. S. Shleev)
01/2015 – 04/2015	Malmö University – Dpt. of biomedical science (Erasmus) <i>Project: Electrochemical characterization of B. aclada laccase variants</i> (Prof. Sergey Shleev)
10/2008 – 10/2012	Bachelor of Science in Food Science and Biotechnology Curriculum completed, focus on biotechnology <i>Thesis: “Cloning and Expression of an engineered Fab fragment”,</i> (Dpt. of Applied Microbiology, Prof. F. Rüker, Dr. G. Wozniak-Knopp)
09/1999 – 06/2007	Secondary school Wolkersdorf Graduation: Math, Biology, Chemistry, French, German Literature